



Universidad de Valladolid

**ESCUELA TÉCNICA SUPERIOR DE INGENIERÍAS
AGRARIAS**

**DEPARTAMENTO DE INGENIERÍA AGRÍCOLA Y
FORESTAL**

TESIS DOCTORAL:

**ANALYSIS OF THE INFLUENCE OF
ENVIRONMENTAL VARIABLES ON
CARBON CONTENT OF SUGAR BEET CROP
AND ESTIMATION OF NITROGEN CONTENT
IN LEAVES BY VEGETATION INDICES**

Presentada por **D. Luis Fernando Sánchez Sastre**
para optar al grado de doctor por la Universidad
de Valladolid

Dirigida por:
Dr. Luis Manuel Navas Gracia
Dr. Salvador Hernández Navarro

AGRADECIMIENTOS

AGRADECIMIENTOS

Quiero expresar mi agradecimiento a todas aquellas personas que han aportado su ayuda en algún momento durante estos cinco años de trabajo:

A mis directores, Dr. Luis Manuel Navas Gracia y Dr. Salvador Hernández Navarro por guiarme y aconsejarme hasta llegar a buen puerto.

Al Dr. Jesús Martín Gil, del que nunca se puede aprender bastante, por su apoyo ante las complicaciones.

Al Dr. José María Durán Altisent por sus sabios consejos y a la Dr. María Anunciación Pérez Bartolomé por su desinteresada ayuda que facilitaron el comienzo de este proyecto.

A todo el personal de AIMCRA, en especial a D. José Antonio Centeno y D. José Antonio Paramio por su ayuda y su inmejorable disposición en los ensayos de campo.

A Dña. Carmen Bravo Sánchez por su ayuda en el laboratorio y sus premeditados sustos.

Al Dr. Norlan Miguel Ruiz Postome por sus ánimos y consejos en todo momento durante estos años.

A D. Zacarías Clérigo Pérez y los demás miembros del equipo UVa del proyecto LIFE+ Operación CO2 por su apoyo y facilitación en el último sprint.

Al Dr. Santiago Martínez Rodríguez por su ayuda y por compartir momentos difíciles pero divertidos coronados con la “operación” San Isidro y nuestro récord de altura.

A Dña. Paula Carrión Prieto por su colaboración inestimable en la última fase, para que pronto sea ella quien escriba líneas como estas.

A D. Eliecer Herrero Llorente por su apoyo, su sentido común y su buen humor para simular lo que haga falta.

Al Dr. Francisco Campos Sánchez-Bordona por permitirme colaborar en interesantes nuevas vías de investigación.

A la Dra. María Jesús Rodríguez Triana y al Dr. Luis Pablo Prieto Santos por su generosidad para apuntalar y mejorar este trabajo.

Al Dr. Shigeto Kawashima, al Dr. Takehide Hama y a todas las personas del Laboratorio de Ingeniería Ambiental e Hidrológica en la División de Ciencia y Tecnología Ambiental, Escuela de Agricultura, Universidad de Kyoto (Japón) por permitirme ser uno más y poder crecer dentro y fuera del campus.

Sin embargo, ni la portada de esta Tesis Doctoral sería posible sin la ayuda, oportunidades y confianza ciega de mis padres Fernando y María Esther. Sin la ayuda y el cariño de mi hermana Elvira, mi tío Carmelo y mi abuela María Esther.

Este trabajo tampoco sería posible sin Míriam Cimas Valencia, y su apoyo incondicional a Del Piero. Sin los consejos, sentencias y clásicos intemporales de Raúl Pérez Palacios, sin esos wednesdays los jueves con David Torres Sousa y Jorge Pérez León, sin las historias inventadas desde el hotel PAL de Ignacio Valverde Merino, sin la exploración del cielo nocturno sobre montones de arena con Fernando Rey Illera, sin una dieta equilibrada diseñada por mi capitán Guillermo Guillén Cubino, sin los viajes de supervisión por el sur de Valladolid junto a Carlos Antonio Rodríguez Tejedro ni sin su imprescindible ayuda en la maquetación y puesta en orden de lo que era un caos. También sería imposible sin haber coincidido en el vórtice con Fernando Martínez Vargas, sabedor que la vida es abandono.

Gracias a Chus y Luis Pablo por ayudarme y meterse en obras cuando ellos ya tenían chocolate suizo suficiente.

Gracias a la acogida en Japón de todo el mundo de la Universidad de Kyoto, especialmente a los profesores Kawashima y Hama que hicieron de esa estancia una experiencia inolvidable.

川島先生と濱先生、本とに心からありがとうございました

Gracias a Koji Fujita y toda su familia por hacerme sentir como en casa.

Y finalmente pero ni mucho menos importante, gracias a mi otra familia, Sachi y Hiroko Takeuchi, por ser como son, únicas. Y a Pico Iyer, ese viajero incansable, con quien espero compartir pronto un otoño por los jardines y templos de Kyoto.

Flectere si nequeo superos Acheronta movebo.
Con dos pitos y un tambor no se toca Parsifal...pero se puede intentar.

八神社

3776

A mi abuelo Luis

ÍNDICE DE TABLAS	8
ÍNDICE DE FIGURAS.....	9
1. RESUMEN.....	12
2. INTRODUCCIÓN Y MARCO DE REFERENCIA.....	15
2.1.Estado de la cuestión:.....	16
2.2.Cambio Climático	18
2.2.1. Concepto	18
2.2.2. Modelos climáticos.	22
2.2.3. Hitos importantes y Quinto Informe de Evaluación del IPCC (AR5).....	24
2.3.CULTIVO DE LA REMOLACHA (ASPECTOS FISIOLÓGICOS)	28
2.4.ÁMBITO DE ESTUDIO	31
2.5.METODOLOGÍA	32
2.5.1. Metodología para la Identificación del Impacto de Variables Climáticas en el Contenido de Carbono en Raíz de Remolacha Azucarera.....	32
2.5.2. Metodología para la Evaluación del Uso de Índices de Vegetación RGB para Determinar el Contenido de Clorofila en Hojas de Remolacha Azucarera en Cosecha.....	35
2.5.3. Metodología para el Análisis Regional del Cultivo de Remolacha Azucarera Bajo Futuros Escenarios de Cambio Climático	38
2.6.ESQUEMA GENERAL.....	40
2.7.REFERENCIAS.....	41
3. OBJETIVOS DE LA TESIS	48
4. IMPACT OF CLIMATE VARIABLES ON CARBON CONTENT IN SUGAR BEET ROOT	52
4.1.INTRODUCTION	54
4.2.MATERIALS AND METHODS.....	57
4.2.1. Field trials.....	57
4.2.2. Analyses	60
4.2.3. Statistics	62
4.3.RESULTS	63
4.3.1. ANOVA analysis	63
4.3.2. Principal component analysis.....	69
4.3.3. Final Remarks	79
4.4.CONCLUSIONS.....	81
4.5.ACKNOWLEDGEMENTS	81
4.6.REFERENCES	82
5. ASSESSMENT OF THE USE OF RGB VEGETATION INDICES TO DETERMINATE CHLOROPHYLL CONTENT IN SUGAR BEET LEAVES AT FINAL CULTIVATION STAGE.....	89
5.1.INTRODUCTION	90

5.2.METHODOLOGY	93
5.2.1. Chlorophyll measurement:	95
5.2.2. Leaf data acquisition:	96
5.2.3. Colour indices calculation:.....	100
5.2.4. Statistics:	104
5.3.RESULTS AND DISCUSSION	104
5.3.1. Chlorophyll content measurements	104
5.3.2. Correlation of CCM-200 measurements and color indices	106
5.3.3. Validation of new indices:.....	119
5.3.4. Analysis of indices performance:	121
5.3.5. Analysis of Leaf data acquisition procedure	130
5.4.CONCLUSIONS.....	130
5.5.REFERENCES	131
5.6.PRACTICAL APPLICATION OF DEVELOPED METHODOLOGY TO OTHER CASE STUDIES	136
6. REGIONAL ANALYSIS OF SUGAR BEET CROP UNDER FUTURE SCENARIOS OF CLIMATE CHANGE	146
6.1.INTRODUCTION	147
6.2.METHODOLOGY	153
6.2.1. Area of study:.....	153
6.2.2. Meteorological Data:.....	153
6.2.3. Projected Meteorological Data for 2050 and 2070 (RCP4.5):	154
6.2.4. Calculated Reference Evapotranspiration (ET ₀):.....	155
6.2.5. Crop Evapotranspiration (ET _c):	156
6.2.6. AquaCrop:	156
6.3.RESULTS	160
6.3.1. Evapotranspirationn Baseline:.....	160
6.3.2. Worldclim data.....	163
6.3.3. Adjustment Crop Model Validation:.....	164
6.3.4. Interpolation validation:	164
6.3.5. ET ₀ y ET _c	165
6.3.6. Yield.....	168
6.3.7. Biomass and CO ₂	170
6.4.CONCLUSION.....	172
6.5.REFERENCES	173
7. RESUMEN DE RESULTADOS	180
7.1.REFERENCIAS.....	190
8. CONCLUSIONES	194

ÍNDICE DE TABLAS

Tabla 2.1. Centros de Investigación y modelos desarrollados para el CMIP5	23
Tabla 2.2. Principales hitos en la lucha contra el Cambio Climático.....	24
Table 4.1. Weather data for 2011 and 2012 supplied by nearby SIAR stations	58
Table 4.2. Calculated climatic variables.....	58
Table 4.3. Soil analyses and fertilization data in 2011 and 2012 at the different locations	59
Table 4.4 Parameters obtained from the fresh weights, dry weights, and carbon and nitrogen concentrations in leaves, root crowns and roots.....	61
Table 4.5. GDD and days in which emergence took place for each of the locations in 2012. ...	63
Table 4.6. ANOVA analysis for 2011 data.....	64
Table 4.7. ANOVA analysis for 2012 data.....	64
Table 4.8. Results of the calculated climatic variables for the cultivation periods in 2011 and 2012.....	69
Table 5.1. Meteorological conditions during the experiment period.....	93
Table 5.2. Dates and time of the eight shoots of the experiment.....	97
Table 5.3. List of the colour vegetation indices considered in study, including their equations and reference sources.	102
Table 5.4. Summary of descriptive statistics for CCM-200 measurements: minimum, maximum, mean, standard error and coefficient of variation (CV).	105
Table 5.5. Summary of descriptive statistics for some of the indices studied in this work using mean values from all shoots: minimum, maximum, mean, standard error and coefficient of variation.....	105
Table 5.6. Correlation coefficients for indices studied by Kawashima et al. 1998.	108
Table 5.7. Correlation coefficients for indices studied for different researchers.....	111
Table 5.8. Correlation coefficients for new indices obtained by PCA process.	114
Table 5.9. Correlation coefficients for new indices obtained by SLR process.....	117
Table 5.10. Summary of descriptive statistics for (R-B)/(R+G+B), I_{PCA} , I_1 and I_2 indices for daily values: minimum, maximum, mean, standard error and coefficient of variation.....	127
Table 6.1. Global mean surface temperature change relative to 1986-2005 for the mid and the late 21st century for all AR5 scenarios.	151
Table 6.2: Meteorological variables supplied by S.I.A.R stations from 2011 to 2014.....	154
Table 6.3. Canopy development phases of growing cycle (GDD), adjusted for sugar beet.....	158
Table 6.4. Comparison between observed and simulated yields (t ha ⁻¹ of dry biomass).....	164
Table 6.5. Comparison between observed and interpolated values for “leave one out” cross-validation.....	165

ÍNDICE DE FIGURAS

Figura 2.1. Emisiones antropogénicas anuales totales de GHGs desde 1970 a 2010.	18
Figura 2.2. (a) Emisiones antropogénicas anuales de CO ₂ según los escenarios RCP hasta 2100 del WGIII (Grupo de Trabajo III del IPCC). (b) Calentamiento en función de la acumulación de emisiones de CO ₂ . Fuente: IPCC 2014.....	27
Figura 2.3. Situación de Castilla y León dentro de la península ibérica y de las azucareras que operan actualmente.	31
Figura 2.4. Resumen esquemático de la metodología aplicada en el primer artículo científico.	34
Figura 2.5. Resumen esquemático de la metodología aplicada en el segundo artículo científico.	37
Figura 2.6. Resumen esquemático de la metodología aplicada en el tercer artículo científico.	39
Figura 2.7. Esquema general de la línea metodológica seguida en esta Tesis Doctoral	40
Figure 4.1. Overview map of experiment locations	57
Figure 4.2. 3D plot and summary table of the PCA analysis for 2011.....	70
Figure 4.3. 2D plots and summary tables for PCA1b and PCA1c analyses, year 2011.	71
Figure 4.4. 2D plots and summary tables for PCA1d and PCA1e analyses, year 2011.	72
Figure 4.5. 2D plots and summary tables for PCA1f and PCA1h analyses, year 2011.	73
Figure 4.6. 2D plots and summary tables for PCA1h and PCA1i analyses, year 2011.	74
Figure 4.7. Top: 3D plot and summary table of PCA analysis for 2011 and 2012.	76
Figure 4.8. 2D plots and summary tables for PCA2c and PCA2d analyses in 2012...	77
Figure 4.9. 2D plots and summary tables for PCA2e and PCA2f analyses in 2012 ...	78
Figure 5.1. Some of the 35 leaves used in the experiment	94
Figure 5.2. Optic chlorophyll meter CCM-200 [®] from Opti-Sciences	95
Figure 5.3. Left: optical absorbance in the two wavelengths measured by CCM-200. Right: spectral signature of sugar beet (blue) and creeping thistle	95
Figure 5.4. The 35 leaves vertically arranged in individual polyurethane sheets for the photo shooting	96
Figure 5.5. LCD (Liquid Crystal Display) Sony α55 camera view with the leaf image about to photograph.	97
Figure 5.6: Frequency plot of red wavelength for leaves on a clear day (A) and a cloudy day (B) (taken from Kawashima and Nakatani 1998).....	98
Figure 5.7. Left: image as was taken loaded in Adobe [®] Photoshop [®] 14.1. Histogram shows RGB levels of the entire photograph. Right: same image after background removal. The histogram only shows the leaf RGB levels	100
Figure 5.8. Some of the leaves in which measurements with CCM-200 resulted in an increment of chlorophyll content after 4 days.	106

Figure 5.9. Relationship between $(R-B)/(R+B)$ index and CC measured by CCM-200 for all days dataset	109
Figure 5.10. Relationship between $(R-B)/(R+G+B)$ index and CC measured by CCM-200 for all days dataset	109
Figure 5.11. Relationship between ExR index and CC measured by CCM-200 for all days dataset.....	112
Figure 5.12. Relationship between IPCA index and CC measured by CCM-200 for all days dataset.....	112
Figure 5.13. Relationship between PCA2 index and CC measured by CCM-200 for all days dataset.....	115
Figure 5.14. Relationship between I1 index and CC measured by CCM-200 for all days dataset	115
Figure 5.15. Relationship between SLR1 index and CC measured by CCM-200 for all days dataset.....	118
Figure 5.16. Relationship between SLR4 index and CC measured by CCM-200 for all days dataset.....	118
Figure 5.17. Relationship between I2 index and CC measured by CCM-200 for all days dataset	119
Figure 5.18. Measured CCI with CCM-200 vs. predicted with I_1 for validation subdataset	120
Figure 5.19. Measured CCI with CCM-200 vs. predicted with I_2 for validation subdataset	120
Figure 5.20. Relationship between $(R-B)/(R+G+B)$ index and CC measured by CCM-200 for three shoots on day 18th (left) and day 21st (right).	122
Figure 5.21. Relationship between IPCA index and CC measured by CCM-200 for three shoots on day 18th (left) and day 21st (right).....	123
Figure 5.22. Relationship between I1 index and CC measured by CCM-200 for three shoots on day 18th (left) and day 21st (right).....	124
Figure 5.23. Relationship between SLR6 index and CC measured by CCM-200 for three shoots on day 18th (left) and day 21st (right).....	125
Figure 5.24. Relationship between $(R-B)/(R+G+B)$ index (left), IPCA index (right) and CC measured by CCM-200 validation subdataset.....	128
Figure 5.25. Relationship between I1 index (left), I2 index (right) and CC measured by CCM-200 for validation subdataset.....	129
Figure 5.26. NIR and RGB cameras mounted in Mikrokopter Ufocam.....	138
Figure 5.27. RGB vs. NIR-R-G composition	140
Figure 5.28. RGB vs. NDVI	141
Figure 5.29. RGB vs. $(R-B)/(R+B)$	142
Figure 5.30. RGB vs. $(R-B)/(R+B+G)$	143
Figure 6.1. Globally averaged greenhouse gas concentration.	148
Figure 6.2. GHG emission pathways 2000-2100: All AR5 scenarios.....	150
Figure 6.3. Up: Atmospheric CO ₂ (ppm) for all AR5 scenarios.....	150

Figure 6.4. Left: situation of Castilla y León region in Spain.	153
Figure 6.5. AquaCrop flow chart showing the main components of the soil-plant-atmosphere continuous	157
Figure 6.6. Actual daily ET_0 from the 29 stations in the area of our study, from 2001 to 2014 (Baseline scenario).	161
Figure 6.7. Monthly ET_0 at the 29 weather stations, from 2001 to 2014 (baseline scenario).....	161
Figure 6.8. ET_0 values obtained from 29 weather stations within the concerned area from 2001 to 2014 against ET_0 values calculated through FAO-56 PM	162
Figure 6.9. Annual mean Temperature at the 29 weather stations.	163
Figure 6.10. Spatial distribution of annual ET_0 (mm) in the area of study for baseline, 2050 and 2070 scenarios.	166
Figure 6.11. Spatial distribution of differences in yearly ET_0 (mm) in the area of the study, for the 2050 and 2070 scenarios, compared to those of the baseline scenario. .	166
Figure 6.12. Spatial distribution of monthly differences of ET_c (mm) in the area of study for 2050 and 2070 scenarios, compared to the baseline scenario.....	167
Figure 6.13. Spatial distribution of Yield (mm) in the concerned area, for the baseline, 2050 and 2070 scenarios with usual growing season.....	168
Figure 6.14. Spatial distribution of Yield (mm) in the area of study for baseline, 2050 and 2070 scenarios with extended growing season	169
Figure 6.15. Spatial distribution of Biomass (t ha ⁻¹) and CO ₂ uptake (t ha ⁻¹) in the area of our study, for the baseline, 2050 and 2070 scenarios with usual growing season...	171
Figure 6.16. Spatial distribution of Biomass (t ha ⁻¹) and CO ₂ uptake (t ha ⁻¹) in the area of study for baseline, 2050 and 2070 scenarios with extended growing season.	171

1. RESUMEN

RESUMEN

Abstract

In the first article, entitled “**Impact of Climate Variables on Carbon Contents in Sugar Beet Root**” the impact of climate variables on the growth and carbon contents of spring-sown sugar beet (*Beta vulgaris saccharifera*) in Castilla y Leon region (north-western Spain) was assessed by analysing 34 beet crop parameters at different sites over two years. By resorting to ANOVA, Principal Component Analysis and Cluster Analysis, the impact of different factors such as climatic variables, site, beet variety or fertilization was evaluated.

In the second article entitled “*Assessment of The Use of RGB Vegetation Indices to Determinate Chlorophyll Content in Sugar Beet Leaves at Final Cultivation Stage*” introduce the fact that high nitrogen levels in sugar beet leaves detected in the growing final stage can be an indicator of late incorporations of nitrogen from organic matter from soils or fertilizers. These tardy uptakes are known to decrease sugar yields. Thus, Among the different ways to measure nitrogen status in crops, here chlorophyll content determination using vegetation indices is explored. In this study, pictures of sugar beet leaves taken with a commercial camera were used to calculate 25 RGB indices found in bibliographic review and to obtain two new indices. The performance of studied indices are examined to evaluate its ability to measure chlorophyll content and degradation for sugar beet leaves in different natural light conditions along 4 days at final cultivation stage.

In the short communication named “*Detection of Sinapis arvensis Weeds in Alfalfa Crop by Using RGB Indices*” based on the good correlations shown by R-B/R+B and R-B/R+B+G at leaf scale for sugar beet leaves, considering that the colour rank in that study was from dark green to yellow, it was proposed to use these indices for checking its possible utility in detection of yellow weeds in fields of green crops. So in the frame of European LIFE Project Operation CO₂ yellow weeds (*Sinapis arvensis*) infection occurred in alfalfa crop (*Medicago sativa*) plots sited in the experimental parcel of Soto de Cerrato (Palencia, Spain) which belongs to University of Valladolid. Thus images from UAV were used to make a mosaic from which were calculated R-B/R+B, R-B/R+B+G and NDVI index for visual comparison.

In the third article entitled “*Regional Analysis of Sugar Beet Crop under Future Scenarios of Climate Change*” Evapotranspiration (ET) is studied as a main factor affecting crop yields which is related to water requirements of the plants. Because of changes predicted in future global climate it is necessary to assess the effects of different environmental conditions in crops such as sugar beet, which depend on irrigation to obtain high yields, in order to foresee measurements of adaptation. In the study presented herein future conditions extracted from RCP4.5 scenario of IPCC for 2050 and 2070, in Spanish region of Castilla y León, were used as inputs of FAO crop simulation model (Aquacrop). Thus, a regional analysis of future trends in yields, biomass and CO₂ assimilation of sugar beet crop are carried out and adaptation measurements are also proposed.

Keywords: sugar beet; climatic factors; fertilization; location; plant parameters; sugar content; variety, vegetation indices, chlorophyll content, climate change, AR5, evapotranspiration, Aquacrop, CO₂.

2. INTRODUCCIÓN Y MARCO DE REFERENCIA

INTRODUCCIÓN Y MARCO DE REFERENCIA

El desarrollo y finalización de esta Tesis Doctoral ha sido posible gracias a la contratación del doctorando por la Universidad de Valladolid a través del programa de becas “Ayudas a la Contratación de Personal Investigador de Reciente Titulación (2009-2013)” cofinanciado por el Departamento de Educación de la Junta de Castilla y León y el Fondo Social Europeo.

El estudio “Detection of *Sinapis arvensis* Weeds in Alfafa Crop by Using RGB Indices” se desarrolló dentro del marco del proyecto europeo LIFE+ “Operation CO₂” (LIFE11 ENV/ES/535).

2.1. Estado de la cuestión:

La agricultura representa más del 31% del total de los gases de efecto invernadero (GHG) de origen antropogénico si se consideran los cambios de uso de la tierra (Smith et al, 2007). Además, la agricultura es el mayor contribuyente de las emisiones a la atmósfera de GHGs, tanto directa –a través de operaciones agrícolas y procesos bioquímicos que tienen lugar en suelos agrícolas- como indirectamente –debido a combustible fósil utilizado en operaciones agrícolas, en la producción de agroquímicos y en convertir tierras para la agricultura-. Algunas iniciativas relacionadas con Agricultura, Ingeniería Forestal y Otros Usos de las Tierras (AFOLU) (IPCC: Intergovernmental Panel on Climate Change, 2014) prefieren utilizar *balance de carbono* en vez de *huella de carbono*, dado que lo anterior tiene en cuenta no solo las emisiones sino también el carbono asimilado por los sistemas agroforestales (Victoria Jumilla et al, 2011).

Este es el caso de los cultivos que toman el carbono de la atmósfera por medio del proceso de la fotosíntesis. El dióxido de carbono secuestrado por las plantas es el resultado de la diferencia entre el CO₂ asimilado por la fotosíntesis y el CO₂ emitido durante la respiración (Taiz et al, 2015), y representa el 40-50% de la biomasa de la materia seca de la planta (McKendry, 2002). Consecuentemente, a medida que la tasa de crecimiento aumenta, los cultivos pueden considerarse como sumideros de carbono (Carvajal et al, 2009). Sin embargo, el hecho de que factores ambientales (duración del día, temperatura, precipitación, nutrientes del suelo, concentración de CO₂...) cambien

continuamente y que las plantas respondan desigualmente a los diferentes ambientes, también se ha tomado en consideración (Gardner et al, 1985).

Los resultados de los cálculos de balance o de huella de carbono, los cuales están basados en metodologías como el Análisis de Ciclo de Vida (ACV o LCA: Life Cycle Assessment) o las Metodologías de Huella Ambiental (EFM, Environmental Footprint Methodologies) dependen de la exactitud y del alcance de la base de datos, pero muchas veces sólo se dispone de valores generales o aproximaciones debido a la carencia de la investigación. Este es el caso de la remolacha, un importante cultivo industrial en la región de Castilla y León (España). A pesar del hecho de que hay numerosos estudios de Huella de Carbono para este cultivo y sus sub-productos (Klenk et al, 2012), cifras sobre el contenido de carbono en investigación experimental son escasas y se han usado aproximaciones en su lugar (Crutzen et al, 2008).

Por otra parte y paralelamente, la agricultura, como el resto de sistemas naturales, se enfrenta a cambios ambientales determinantes para el futuro cercano. Así, por ejemplo, la disponibilidad de agua para el riego de cultivos probablemente disminuirá en el futuro debido a un aumento en las demandas hídricas desde otros sectores y por los cambios ambientales (Santos et al., 2010). De hecho, estos cambios ambientales son la principal fuente de incertidumbre concerniente a los rendimientos futuros de los cultivos, especialmente teniendo en cuenta la influencia humana sobre el sistema climático, la cual parece ser clara y aceptada por la mayoría del mundo científico (IPCC 2001). El último informe del IPCC, esto es, el Quinto Informe de Evaluación (AR5 por sus siglas en inglés. IPCC, 2014) manifiesta que las emisiones antropogénicas de GHGs son las mayores de la historia (Figura 2.1) y sus efectos son la causa más probable del calentamiento observado desde la mitad del siglo XX.

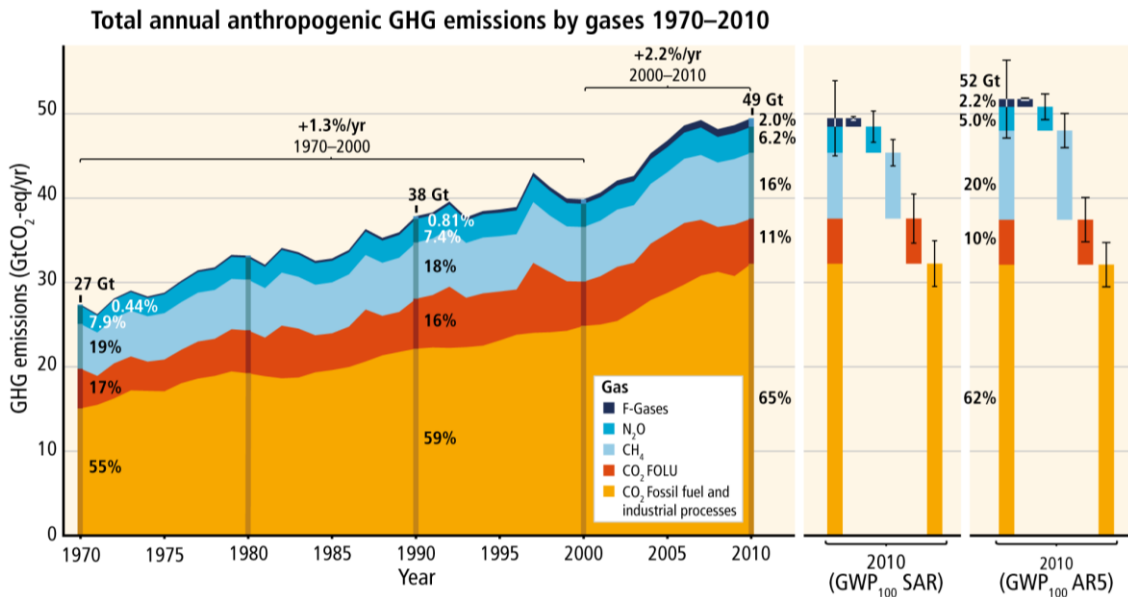


Figura 2.1. Emisiones antropogénicas anuales totales de GHGs desde 1970 a 2010. Fuente IPCC 2014

Por lo tanto, se plantea la necesidad de identificar y estudiar los parámetros que afectan a un cultivo agrícola, en este caso la remolacha azucarera, como sumidero temporal de CO₂ y su respuesta ante cambios ambientales previstos en el futuro cercano. En esta Tesis Doctoral, dicho planteamiento se desarrolla a través de tres estudios que tratan de, en primer lugar, identificar variables climáticas determinantes en el contenido de carbono del cultivo y cuantificar el porcentaje de carbono en la raíz de remolacha; en segundo lugar, desarrollar herramientas para la evaluación de cambios en el contenido de carbono mediante la estimación del nitrógeno en hojas; y en tercer lugar, analizando las tendencias en el cultivo en posibles escenarios futuros de cambio climático.

2.2. Cambio Climático

2.2.1. Concepto

Muchos trabajos basados en series climáticas históricas proporcionan cifras ilustrativas sobre cambios producidos en el clima durante las últimas décadas. Desde 1900, el calentamiento global ha sido de entre 0.3°C y 0.6°C, y en la mayoría de Europa, el incremento en la temperatura media actual durante el siglo XX ha sido de alrededor de 0.8°C (Ros, 1991). De hecho, varios estudios han confirmado un incremento en la ET₀ (Evapotranspiración de referencia) bajo condiciones de cambio climático, en el área

mediterránea en general (García-Garizabal et al., 2014), y especialmente en España (Espadafor et al., 2011 y Vicente-Serrano et al., 2014a). Por ejemplo, Vicente Serrano et al., (2014a) obtienen como resultado un cambio en la media anual de evapotranspiración a lo largo de España de 29.4 mm cada década desde 1961 hasta 2011. Además de este incremento en ET_0 , la precipitación observada en España entre 1961 y 2011 disminuyó 218.7 mm por década (Vicente-Serrano et al., 2014b). Además de esto cabe resaltar que la frecuencia y la intensidad de eventos de lluvias torrenciales se ha incrementado en Europa durante los últimos años (IPCC, 2014).

Existen varias definiciones academicistas tradicionales del concepto de clima, pudiendo decirse que el clima es la síntesis de las condiciones meteorológicas correspondientes a un área geográfica dada, elaborada en base a un período suficientemente largo como para establecer sus propiedades estadísticas de conjunto (valores medios, varianzas, probabilidades de fenómenos extremos, entre otras). Sin embargo, en la actualidad no hay una definición consensuada en la comunidad científica mundial de lo que es el clima. En realidad, a la hora de intentar establecer este consenso se habla más bien del *sistema climático del planeta*, dentro del cual se encuentra la atmósfera, la hidrosfera, la litosfera, la criosfera y la biosfera. Todos estos elementos del sistema están en equilibrio y es la mano del hombre el que lo rompe. Así, la superficie terrestre y su capacidad de absorber y/o reflejar la radiación solar ha sido objeto de fuertes modificaciones, fundamentalmente en el último siglo y medio, debido a actividades que, por otra parte, son importantes para el desarrollo de la vida diaria de la humanidad, como son la producción de energía procedente de combustibles fósiles, el transporte o la práctica agrícola y ganadera.

El sistema climático es dinámico y, en cualquier caso, hay siempre un estado inicial y final en la evolución del mismo. Si los estados inicial y final forman parte del mismo conjunto, es decir, tienen las mismas propiedades estadísticas, el sistema se denomina ergódico (situación que ocurre en los procesos cíclicos). En el caso de que las propiedades estadísticas sean diferentes el sistema se denomina intransitivo. Esta cuestión está relacionada con la irreversibilidad de los procesos, que por otra parte no es deseable para el sistema climático. Hoy en día no hay certeza clara de esta intransitividad del sistema climático, pero sí que hay evidencias de que la evolución se produce a un sistema cuasi-intransitivo, lo cual significa que se puede alcanzar un

estado final significativamente distinto del estado inicial, a través de una evolución larga pero finita.

El hombre se encuentra inmerso en la atmósfera terrestre, la cual se puede considerar como un sistema abierto que intercambia materia y energía con el resto del universo (suelo y espacio exterior). A lo largo de su historia la humanidad ha sido capaz de desarrollar una serie de instrumentos y técnica de medida que permiten conocer en cualquier instante el estado de la atmósfera y su evolución en un intervalo de tiempo relativamente corto. A este estado físico instantáneo del sistema atmosférico se le denomina *tiempo atmosférico*, el cual está en continuo cambio.

El clima de una zona determinada quedará determinado por una síntesis de los estados del tiempo atmosférico, y será la climatología la que estudiará la permanencia del tiempo atmosférico, es decir, los elementos invariantes del conjunto de estados del tiempo atmosférico, los cuales tienen un carácter eminentemente estadístico por los métodos empleados y por la hipótesis de que estos elementos invariantes tienen una naturaleza aleatoria. De esta manera se puede caracterizar el clima por la probabilidad estadística de ocurrencia de los distintos estados atmosféricos en una zona determinada durante un tiempo determinado.

De esta manera, se puede hacer una descripción del estado climático utilizando índices, los cuales son comparados con referencias tomadas como estándares por la Organización Meteorológica Mundial, estando estos valores referidos a periodos de 30 años (1960-1990).

Evidentemente, estos estadísticos permiten solamente describir un estado climático pero no permiten evaluar las variaciones del clima con precisión y, por otro lado, tampoco permiten calcular la probabilidad de que ocurra un estado atmosférico concreto en una zona determinada, cálculos que, por otra parte, son imprescindibles para valorar los distintos elementos climáticos. Esto significa que para determinar variaciones climáticas es necesario efectuar análisis de datos meteorológicos instrumentales que se han ido midiendo día a día en los diferentes centros de observación.

Además de los estadísticos utilizados en las descripciones climáticas, se utilizan otros índices para establecer los estados climáticos, los cuales son valores medios que se obtienen como combinación de diferentes elementos climáticos. Estos parámetros no son tampoco los más adecuados para realizar una clasificación climática ya que las clasificaciones que resultan mediante la utilización de estos índices tiene un objetivo muy determinado o bien se limitan a analizar el elemento climático que ejerce mayor

influencia en una actividad específica. Por ejemplo, la clasificación de Copen está realizada en base a precipitaciones y temperatura, que son los que mayor influencia tiene en el desarrollo de la vegetación; la clasificación de Thornthwaite busca las diferentes condiciones ambientales a través de la respuesta en el crecimiento de las plantas; el índice de Martonne resalta la aridez del clima; el índice de continentalidad marca las diferencias estacionales de la temperatura y de la precipitación; y los índices hídricos determinan la cantidad de agua dulce disponible.

Por otro lado, se habla de *variabilidad climática* como las fluctuaciones en las propiedades estadísticas sobre períodos de semanas, meses o años. De esta manera, se determinan límites dentro de los cuales los valores medios, desviaciones o frecuencias de valores entre los límites establecidos pueden ser aceptados como normales. Los eventos fuera de estos límites pueden ser vistos como anómalos a un cierto nivel de significación. De esta forma, se habla de *Cambio Climático* (CC) cuando las propiedades estadísticas de una secuencia de años difieren considerablemente respecto de otra secuencia de años de referencia. De acuerdo con el IPCC, por CC se debe entender “el cambio del clima atribuido directa o indirectamente a actividades humanas, que alteran la composición de la atmósfera del planeta y que vienen a añadirse a la variabilidad natural del clima observada durante periodos de tiempo comparables”.

En cualquier caso, todas las hipótesis de partida en el estudio del CC indican que el clima es algo estable y que las modificaciones que éste puede sufrir de forma natural son a escala geológica. Sin embargo, a partir de los años setenta, la comunidad científica toma conciencia de cierta crisis climática como consecuencia de la mayor aparición de fenómenos extremos (sequías y lluvias torrenciales fundamentalmente). Desde un punto de vista científico, el fenómeno extremo está integrado como algo asociado intrínsecamente al clima, pero siempre con una baja probabilidad de que ocurra. Esta variabilidad climática extrema es algo que la sociedad tiene que asumir y aceptar y, por tanto, estar preparada para cuando ocurra a pesar de la baja frecuencia. El problema acontece cuando esta frecuencia aumenta y dicha variabilidad deja de serlo para

Una observación continua del sistema climático permite, mediante aplicaciones técnicas y métodos climáticos, obtener resultados concretos y prácticos para como son la determinación de probabilidades de fenómenos meteorológicos extremos, determinación de épocas del año en las que las condiciones atmosféricas son o no favorables para el desarrollo de cierta actividad o estimar cambios de los patrones de

precipitación y temperatura, entre otros. Por su parte, en el sector agrario se realizan planificaciones que conducen a un aumento de la producción agrícola, como son los abonados, el drenaje adecuado o los tratamientos fitosanitario. Pero, sin embargo, la modificación del clima es imposible de prever, por lo menos a gran escala, y es algo con lo que hay que contar junto con su variabilidad en la planificación y explotación de recursos primarios.

2.2.2. Modelos climáticos.

Los modelos globales de circulación son modelos físico-matemáticos que reproducen la dinámica de los componentes del clima, principalmente la atmósfera y el océano, y permiten simular su tendencia futura en función de la actividad humana (Gutiérrez *et al.*, 2006). Los escenarios futuros de emisión son los forzamientos inducidos por actividades humanas (concentración de CO₂ en la atmósfera, etc.). Dichos escenarios representan la fuente principal de incertidumbre para la modelización del CC.

Puesto que la resolución espacial de los modelos es bastante limitada (entre 250 y 500 km) y que sólo permiten obtener resultados sobre tendencias promedio de las variables climáticas en regiones muy extensas de la Tierra, en los últimos años se han desarrollado distintas estrategias para la proyección regional del CC, que proporcionen mayor detalle en zonas para realizar estudios de impacto.

Para el estudio cualitativo de la respuesta global del clima ante diferentes hipótesis se pueden utilizar modelos simples (de una y dos dimensiones), pero para poder hacer proyecciones cuantitativas es necesario utilizar un modelo climático de circulación general, lo que requiere computadoras muy potentes para poder ejecutarlos, que sólo puede ser llevado a cabo por grandes centros de investigación que ponen sus resultados a disposición de la comunidad científica para su estudio, como son el Centro Hadley, o el Max Planck Institute. En la Tabla 1.1 se recogen todos los centros participantes y los modelos que han desarrollado dentro del CMIP5 (Coupled Model Intercomparison Project Phase 5) para el AR5. Las salidas globales de dichos modelos se utilizan en diferentes proyectos como entrada de los métodos de generación de escenarios regionales

Tabla 2.1. Centros de Investigación y modelos desarrollados para el CMIP5. (Fuente CMIP5)

Código del Centro	Modelo	Institución
BCC	BCC-CSM1.1 BCC-CSM1.1(m)	Beijing Climate Center, China Meteorological Administration
CCCma	CanAM4 CanCM4 CanESM2	Canadian Centre for Climate Modelling and Analysis
CMCC	CMCC-CESM CMCC-CM CMCC-CMS	Centro Euro-Mediterraneo per I Cambiamenti Climatici
CNRM-CERFACS	CNRM-CM5	Centre National de Recherches Meteorologiques / Centre Europeen de Recherche et Formation Avancees en Calcul Scientifique
CNRM-CERFACS	CNRM-CM5-2	Centre National de Recherches Meteorologiques / Centre Europeen de Recherche et Formation Avancees en Calcul Scientifique
COLA and NCEP	CFSv2-2011	Center for Ocean-Land-Atmosphere Studies and National Centers for Environmental Prediction
CSIRO-BOM	ACCESS1.0 ACCESS1.3	CSIRO (Commonwealth Scientific and Industrial Research Organisation, Australia), and BOM (Bureau of Meteorology, Australia)
CSIRO-QCCCE	CSIRO-Mk3.6.0	Commonwealth Scientific and Industrial Research Organisation in collaboration with the Queensland Climate Change Centre of Excellence
EC-EARTH	EC-EARTH	EC-EARTH consortium
FIO	FIO-ESM	The First Institute of Oceanography, SOA, China
GCESS	BNU-ESM	College of Global Change and Earth System Science, Beijing Normal University
INM	INM-CM4	Institute for Numerical Mathematics
IPSL	IPSL-CM5A-LR IPSL-CM5A-MR IPSL-CM5B-LR	Institut Pierre-Simon Laplace
LASG-CESS	FGOALS-g2	LASG, Institute of Atmospheric Physics, Chinese Academy of Sciences; and CESS, Tsinghua University
LASG-IAP	FGOALS-g1 FGOALS-s2	LASG, Institute of Atmospheric Physics, Chinese Academy of Sciences
MIROC	MIROC4h MIROC5	Atmosphere and Ocean Research Institute (The University of Tokyo), National Institute for Environmental Studies, and Japan Agency for Marine-Earth Science and Technology
MIROC	MIROC-ESM MIROC-ESM-CHEM	Japan Agency for Marine-Earth Science and Technology, Atmosphere and Ocean Research Institute (The University of Tokyo), and National Institute for Environmental Studies
MOHC (additional realizations by INPE)	HadCM3 HadCM3Q HadGEM2-A HadGEM2-CC HadGEM2-ES	Met Office Hadley Centre (additional HadGEM2-ES realizations contributed by Instituto Nacional de Pesquisas Espaciais)
MPI-M	MPI-ESM-LR MPI-ESM-MR MPI-ESM-P	Max Planck Institute for Meteorology (MPI-M)
MRI	MRI-AGCM3.2H MRI-AGCM3.2S MRI-CGCM3 MRI-ESM1	Meteorological Research Institute

Código del Centro	Modelo	Institución
NASA GISS	GISS-E2-H GISS-E2-H-CC GISS-E2-R GISS-E2-R-CC	NASA Goddard Institute for Space Studies
NASA GMAO	GEOS-5	NASA Global Modeling and Assimilation Office
NCAR	CCSM4	National Center for Atmospheric Research
NCC	NorESM1-M NorESM1-ME	Norwegian Climate Centre
NICAM	NICAM.09	Nonhydrostatic Icosahedral Atmospheric Model Group
NIMR/KMA	HadGEM2-AO	National Institute of Meteorological Research/Korea Meteorological Administration
NOAA GFDL	GFDL-CM2.1 GFDL-CM3 GFDL-ESM2G GFDL-ESM2M GFDL-HIRAM-C180 GFDL-HIRAM-C360	Geophysical Fluid Dynamics Laboratory
NSF-DOE-NCAR	CESM1(BGC) CESM1(CAM5) CESM1(CAM5.1,FV2) CESM1(FASTCHEM) CESM1(WACCM)	National Science Foundation, Department of Energy, National Center for Atmospheric Research

2.2.3. Hitos importantes y Quinto Informe de Evaluación del IPCC (AR5)

Durante las últimas décadas, ante la toma de consciencia sobre la realidad de un cambio climático provocado o acelerado por las actividades humanas, se han producido una serie de iniciativas políticas para responder a las evidencias científicas recogidas durante muchos años de estudio. A continuación, en la Tabla 2.2 se recogen las principales iniciativas hasta el año 2015.

Tabla 2.2. Principales hitos en la lucha contra el Cambio Climático.

AÑO	ACTUACIÓN
1898	Svante Arrhenius hace el primer análisis serio sobre las consecuencias climáticas derivadas de un aumento de la concentración de CO ₂ .
1979	Se celebra la Primera Conferencia Mundial sobre el clima. Se reconoce al Cambio Climático (CC) como un problema grave.
1988	Se crea el Panel Intergubernamental para el Cambio Climático (IPCC) con el objetivo de analizar la información científica sobre el cambio climático y sus consecuencias ambientales y socioeconómicas. El primer "Informe de Evaluación", publicado en 1990, genera alarma política y social. Los científicos alertan sobre la imperiosa necesidad de reducir los niveles de CO ₂ , el principal gas causante del efecto invernadero (GEI).
1992	En Río de Janeiro (Brasil) se celebra la Conferencia de las Naciones Unidas para el Ambiente y el Desarrollo y se crea la Convención Marco de las Naciones Unidas para el Cambio Climático (CMNUCC), con el fin de proteger el sistema climático mundial de los efectos de los GEI y sus implicancias sobre el calentamiento global. Para ello se establece como meta la estabilización atmosférica de las concentraciones de GEI en un nivel que no resulte peligroso y que permita el desarrollo económico de manera sostenible. La Convención clasifica a los países en dos grupos: Países del Anexo I (industrializados) y Países no incluidos en el Anexo I (en desarrollo).

AÑO	ACTUACIÓN
1995	La Conferencia de las Partes (COP) se transforma en la autoridad máxima de la Convención y a partir de aquí, se reúnen anualmente buscando alcanzar acuerdos entre los países miembros para mitigar los efectos del CC.
1997	A fin de cumplir con el objetivo planteado en la Convención de Río de Janeiro, los representantes de más de ciento cincuenta países firman en el marco la COP3 el Protocolo de Kyoto. Se trata de una declaración de voluntades en la que se proponen disminuciones obligatorias en las emisiones de GEI, por parte de treinta y nueve de los principales países industrializados. A partir de este momento, comienza una fase que comprende arduas negociaciones y compromisos internacionales, seguida por una serie de ratificaciones paulatinas del Protocolo.
2004	Con la ratificación de Rusia ¹ , entra en vigor el Protocolo de Kyoto. Esto marca el comienzo de la etapa en la que deben disminuirse las emisiones de los GEI, en un 5.2 % respecto de los valores de 1990. Esta meta debería ser alcanzada al finalizar el Primer Período del Compromiso (entre 2008 y 2012). Para esto, cada uno de los países del Anexo I acuerda el compromiso específico de reducción de emisiones que deberá alcanzar durante ese período.
2007	La Conferencia de las Naciones Unidas sobre el CC (Bali) finalizó con la adopción del Plan de Ruta de Bali, que intenta asegurar el clima futuro mediante decisiones que incluyan el planteamiento de su futura repercusión.
2007	Cuarto Informe del IPCC. Fourth Assessment Report (AR4)
2008	En las Negociaciones sobre CC de Bangkok se anuncia un calendario que responde a un acuerdo internacional a largo plazo en materia de CC, que deberá concluir dos años más tarde en Copenhagen.
2014	Quinto Informe del IPCC. Fifth Assessment Report (AR5)
2015	Vigésimo primera Conferencia de las Partes de la Convención Marco de Naciones Unidas sobre el Cambio Climático de 2015 (COP21/CMP11), también llamada «París 2015»

En 2007, los escenarios utilizados en el AR4 se conocen por las siglas SRES (*Special Reports on Emission Scenarios*), y fueron elaborados por un grupo de expertos mundiales dentro del IPCC con proyecciones hasta el año 2100. El IPCC propuso 40 hipótesis diferentes, agrupadas en 4 familias de escenarios: A1, A2, B1, B2. La descripción de cada escenario describe un futuro demográfico, político-social, económico y tecnológico con énfasis en las principales características y dinámica. Dentro de cada familia, uno o más escenarios consideran la energía global, la industria y otros desarrollos, y sus implicaciones para las emisiones de gases de efecto invernadero y otros contaminantes. Pese a que estas descripciones no indican en forma explícita políticas sobre el CC, hay algunos ejemplos de medidas de mitigación indirectas en algunos escenarios.

Posteriormente, en el año 2014, los cuatro escenarios SRES (*Special Reports on Emission Scenarios*) del Cuarto Informe de Evaluación del IPCC (AR4. IPCC, 2007) son reemplazados en el AR5 por cuatro nuevos escenarios de emisión conocidos como RCP (*Representative Concentration Pathways*) propuestos en van Vuuren et al. (2011).

¹ El Protocolo de Kyoto debía ser ratificado por al menos cincuenta y cinco países del Anexo I, los cuales debían representar al menos el 55 % del total de emisiones de GEI contabilizadas en 1990.

Estos nuevos escenarios (Figura 2.2) están definidos en base a su forzamiento radiactivo (2.6, 4.5, 6.0 y 8.5 W m^{-2} en 2100: RCP2.6, RCP4.5, RCP6.0 y RCP8.5 respectivamente). Los nuevos escenarios pueden tomar en consideración las políticas dirigidas a mitigar el cambio climático en el siglo XX. Cada uno de los escenarios RCP están basados en un conjunto de suposiciones socioeconómicas internamente consistentes que incluyen: un escenario en el cual los esfuerzos en la mitigación llevan a un muy bajo nivel de forzamiento que permitiría mantener el calentamiento global por debajo de 2°C sobre temperaturas preindustriales (RCP2.6); dos escenarios de estabilización (RCP4.5 y RCP6.0); y un escenario con un nivel elevado de emisiones de GHG (RCP8.5).

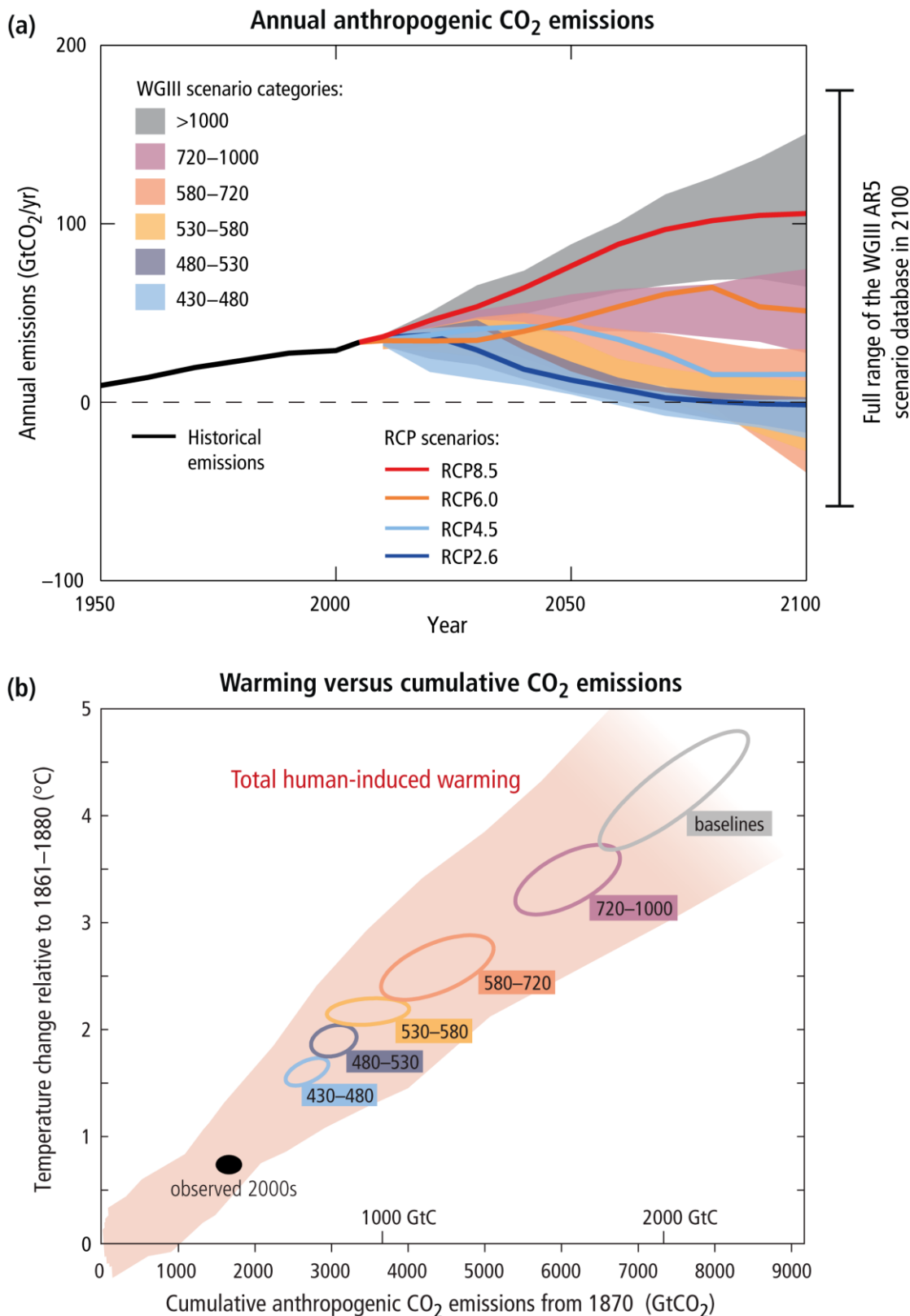


Figura 2.2. (a) Emisiones antropogénicas anuales de CO₂ según los escenarios RCP hasta 2100 del WGIII (Grupo de Trabajo III del IPCC). (b) Calentamiento en función de la acumulación de emisiones de CO₂. Fuente: IPCC 2014.

No obstante, como se ha visto anteriormente, hay que tener en cuenta que la deficiencia de los modelos globales para pronosticar diferencias y tendencias regionales, como por ejemplo los distintos climas dentro de un mismo país, hace necesario realizar un esfuerzo adicional para obtener proyecciones que estimen los efectos regionales del CC. Este ha sido el objetivo de algunos proyectos europeos, orientados a la generación de escenarios a escala regional (AEMET, 2009), con una gran variedad de métodos y modelos climáticos globales y regionales.

2.3. CULTIVO DE LA REMOLACHA (ASPECTOS FISIOLÓGICOS)

La mayor parte de las plantas verdes contienen azúcar en una u otra proporción pero industrialmente solo ofrecen interés la caña y la remolacha azucarera. Villarías-Moradillo, (2000) hace un recorrido por la historia del cultivo en el que se explica que las características de las cualidades azucaradas de la remolacha ya fue citada por Teofrasto, Galeno y Dioscorides en la antigüedad. En el siglo XVIII el químico alemán Margraff comenzó a estudiar la posibilidad de extraer azúcar de unas remolachas muy primitivas que solamente contenían un 6% de azúcar y obtuvo en 1747 por primera vez azúcar cristalizado. A partir de estos resultados Franz Carl Achard mejoró el cultivo y la extracción. En España el cultivo fue investigado por el conde Torres-Cabrera y el ingeniero agrónomo D. José Martí y Sánchez.

Ya en épocas más recientes, el cultivo de remolacha ha sufrido importantes cambios en las últimas décadas, como la mejora de las variedades (Jaggard et al, 1999) y mejores prácticas de cultivo: siembra precoz, mayor densidad de plantación, uso más eficiente de fertilizantes, control de plagas y enfermedades, etc. (Milford et al, 1999). La capacidad de producción de la remolacha proviene de su capacidad para captar la radiación para su proceso de fotosíntesis, es decir, de su capacidad para lograr la mayor cobertura de terreno tan rápido como sea posible y mantener esa cobertura el mayor tiempo posible, para así ser capaz de optimizar la captura de luz solar (Van Heemst, 1986). Se sabe que la cobertura del terreno de la remolacha alcanza su máximo cuando ya se ha alcanzado la máxima radiación del año, debido a la lenta formación de las hojas en primavera (Scott et al, 1993 and Kenter et al, 2006). La remolacha fija el CO₂ y

acumula azúcar (Echevarría et al, 2005) en forma de sacarosa. La sacarosa que se va sintetizando es utilizada por la planta para el ahorro de metabolismo, formación de hojas y raíces, y finalmente para la acumulación de azúcar en la raíz (Gordo-Ingelmo, 1994). Desde el punto de vista enzimático, la acumulación neta de sacarosa en la raíz ocurre durante los primeros estadios del crecimiento, con un aumento de la actividad de la enzima sacarosa-sintetasa y una gran contribución de sacarosa desde las hojas a la raíz. Posteriormente, se observa una disminución del aumento de la polarización (riqueza en azúcar), hasta que se detiene o se convierte en negativa inicio de la actividad de la sacarosa invertasa) (Jiménez et al, 2005).

Existen alguna controversia sobre si el crecimiento y la acumulación de azúcar en la remolacha están limitados por las condiciones externas (*source-limited*), el clima específico, la fertilización, el campo, etc... (Thomas, 2000 and Bell et al, 1996) o si dicha limitación es ontogénica (*sink-limited*) (Demmers-Derks et al, 1998, Hoffmann y Kluge-Severin, 2010). Milford et al (1985) afirman que la temperatura es el principal factor para el crecimiento de la remolacha y que la integral térmica (temperatura acumulada) explica el cambio en las diferentes etapas. Villarías-Moradillo et al. (1999) afirman que la suma total de calor para la germinación en Castilla y León (España) es de 120-130 °C·d (10-12 días). Hull et al. (1970), citado en Hoffmann y Kluge-Severin, (2010), indicaron que la duración de la época de crecimiento tiene un fuerte efecto positivo en la cosecha de remolacha.

Hay estudios que respaldan que la cosecha potencial de remolacha depende principalmente del lugar (terreno, clima e interacciones) y de los efectos del año (condiciones climáticas y periodo de vegetación), mientras que la influencia de la agronomía sería menor (Kenter et al, 2006). En esta línea, otros grupos han tratado de resolver la influencia de factores climáticos en el crecimiento de la remolacha, en ambas siembras de primavera y otoño, en relación con diferentes áreas geográficas, como Freckleton et al. (1999) y Clover et al. (2001) en Inglaterra, Gordo et al. (2005) en España para la siembra de otoño, Petkeviciene (2009) en Lituania, Hoffmann y Kluge-Severin (2010 y 2011) (siembra de primavera), y Loel y Hoffmann (2014) (siembra de otoño) en Alemania.

Otros factores importantes susceptibles de mayores estudios están relacionados con la precipitación, temperatura, demanda de evaporación y capacidad de retención del suelo (Jaggard et al, 1998), aunque Tanner et al. (1983), citado en Rinaldi y Vonella

(2006), afirman que la remolacha muestra un uso eficiente del agua. Es más, Fabeiro et al. (2003) concluye que la remolacha es una planta resistente a la sequía que puede producir una cosecha rentable incluso con disminución del riego. Es éste, el riego, un factor decisivo para conseguir una buena cosecha durante la época de germinación (AIMCRA: Asociación de Investigación para la Mejora del Cultivo de la Remolacha Azucarera 2015), y el contenido de humedad en un suelo óptimo en España se ha determinado que es 12-15% (Villarías-Moradillo et al, 1999).

Otro factor a considerar es el papel que juega el nitrógeno en la expansión de las hojas de remolacha para la captura de la luz (Manderscheid et al, 2010 y Malnou et al, 2008). La concentración de nitrógeno en las hojas, el órgano responsable de la fijación de CO₂, se considera el factor que modifica de manera significativa el grado de crecimiento tanto en hojas como en la raíz de almacenamiento (Grzebisz et al, 2012). Se sabe que la concentración de nitrógeno en las hojas aumenta durante los primeros 70 días y disminuye a medida que avanza el ciclo de crecimiento (Gordo-Ingelmo, 1994), y hay varios estudios sobre la óptima fertilización de la remolacha (Malnou et al, 2006 y Malnou et al, 2008), sobre la relación entre fertilización y riego (Kiyamaz et al, 2015) e incluso sobre los efectos de la fertilización de carbono en este cultivo (Burkart et al, 2009 and Manderscheid et al, 2010).

En cuanto a la composición de la raíz de la remolacha, los factores que pueden influenciarla también se han investigado, porque es un factor crítico para la calidad industrial de la raíz y particularmente para el proceso de extracción del azúcar (Jaggard et al, 1999, Kenter et al, 2006, Giaquinta, 1979 y Hoffmann, 2005). La composición de la raíz de la remolacha en cosecha es: 77% agua y 23% materia seca, con 70-76% de sacarosa, 18% de marco y 6% de otras sustancias como betaína (Gordo-Ingelmo, 1994 and Hoffmann et al, 2005). El marco es un parámetro de calidad y consiste en todos los componentes que persisten insolubles después de la extracción de agua caliente (a 80 °C), específicamente celulosa, hemicelulosa, sustancias de pectina, saponinas, lípidos, ligninas, etc. La concentración de marco depende del lugar y de la variedad (Hoffmann et al, 2005).

2.4. ÁMBITO DE ESTUDIO

La región de Castilla y León es particularmente representativa porque responde al 90% de la producción española de la siembra de primavera de remolacha con 26573 ha (MAGRAMA 2014). Además, el norte de España es el área de la Unión Europea donde se logran las mayores cosechas por hectárea, consiguiendo más de 120 toneladas por hectárea en el caso de 33.7% de los agricultores (AIMCRA 2015).

Existen cuatro azucareras funcionando en Castilla y León actualmente (Figura 1.2): Olmedo (Valladolid), Toro (Zamora), La Bañeza (León), y Miranda de Ebro (Burgos).



Figura 2.3. Situación de Castilla y León dentro de la península ibérica y de las azucareras que operan actualmente.

2.5. METODOLOGÍA

En cada uno de los artículos que conforman esta Tesis Doctoral se han seguido las metodologías descritas someramente a continuación:

2.5.1. Metodología para la Identificación del Impacto de Variables Climáticas en el Contenido de Carbono en Raíz de Remolacha Azucarera

El primer estudio presentado en esta Tesis Doctoral, se desarrolla para tratar de determinar si el contenido de carbono en la raíz de las remolacha azucarera, como órgano aprovechable del que se extrae el azúcar mediante procesos industriales, está influenciado por variables como la localización, suelo, clima, variedad, abonado o si bien está ontogénicamente determinado y no caben variaciones.

Para ello se hicieron estudios previos con el fin de diseñar un experimento que duraría dos campañas 2010-2011 y 2011-2012. Gracias a la colaboración de AIMCRA, se pudieron establecer parcelas de ensayo en 3 zonas distintas de Castilla y León la primera campaña y en cuatro zonas durante la segunda. Dichas parcelas pertenecen a agricultores particulares que manejan el cultivo bajo las recomendaciones técnicas de AIMCRA. En este trabajo se consideraron como factores de estudio, para analizar su influencia en el contenido de carbono, los siguientes: la localización, la variedad (una de alta riqueza en azúcar y menor producción y otra con mayor producción pero menor riqueza en azúcar), y el nivel de abonado (el óptimo recomendado y el doble de éste. Solo durante la primera campaña). Cada uno de los dos años, en la época de cosecha se procedía a recoger plantas aleatoriamente, se llevaban al laboratorio donde se procesaban: limpieza; separación por raíz, corona y hojas; pesaje en fresco; secado en estufa; peso seco; pulverización en molino de cuchillas; homogenización de muestras; pesaje de precisión de las muestras; y análisis de los niveles de C y N en analizador LECO. En total, cerca de 170 plantas y más de 500 muestras formaron la base de datos para el posterior estudio estadístico.

Para los 34 parámetros estudiados relativos al peso fresco, peso seco y contenido de carbono y nitrógeno, se llevó a cabo un análisis ANOVA junto a los pertinentes tests de

homogeneidad de varianzas, normalidad de la distribución e independencia. Los resultados se clasificaron en tres niveles de significatividad $p < 0.05$, $p < 0.01$ y $p < 0.001$. A esto se añadió un test post-hoc HSD (Honestly-significant-difference) de Tukey para la comparación de medias en los factores con más de dos niveles (localización)

Una vez se comprueba que existen diferencias significativas debidas a la localización y por lo tanto a las variables climáticas y edafológicas particulares de cada parcela (asumiendo que todas las necesidades hídricas y nutritivas del cultivo están cubiertas) se procedió a estudiar la influencia de esas variables climáticas mediante el uso del Análisis de Componentes Principales (ACP o PCA) y el Análisis de Agregados o Clusters (CA). ACP es una técnica estadística multivariante que se utiliza para encontrar patrones en un conjunto de datos mediante la reducción de las variables observadas a un número menor de variables artificiales (componentes principales) que acumulen la mayor parte de la varianza en las variables de observación (O'Rourke et al, 2013). El CA, por su parte se utiliza para detectar segregaciones (clusters) naturales en el conjunto de datos observados puesto que esto aporta una fuerte evidencia de diferencias estadísticamente significativas entre muestras del conjunto de datos (Harrigan and Goodacre, 2003).

Para llevar a cabo los análisis mediante ACP y CA, previamente, a partir de los datos obtenidos de la red SIAR (Sistema de Información Agroclimática para el Regadío) se calcularon 12 variables climáticas. Éstas se usaron junto a algunos de los 39 parámetros medidos en las plantas como entradas para los análisis.

En la figura 2.4 se muestra el resumen esquemático de la metodología aplicada



Figura 2.4. Resumen esquemático de la metodología aplicada en el primer artículo científico.

2.5.2. Metodología para la Evaluación del Uso de Índices de Vegetación RGB para Determinar el Contenido de Clorofila en Hojas de Remolacha Azucarera en Cosecha

La determinación de los niveles de nitrógeno en hojas de remolacha en la última fase del cultivo cobra especial relevancia ya que muchos autores han demostrado que incorporaciones tardías de abonado o liberaciones de nitrógeno desde la materia orgánica del suelo reduce el contenido de sacarosa (Pocock et al., 1990). Además, estudios como los de Draycott y Christenson (2003) y Malnou et al. (2008) afirman que una cantidad de nitrógeno por encima del nivel óptimo tiene un efecto negativo en el rendimiento de azúcar. En este segundo estudio se trató de validar una técnica de estimación de nitrógeno (indirectamente a través del contenido de clorofila), mediante el uso de índices de vegetación, basados en las bandas RGB (rojo-verde-azul) del espectro visible. Siguiendo la filosofía propuesta por Kawashima y Nakatani (1998), se propone un método de diagnóstico de bajo coste usando una cámara digital convencional para la toma de imágenes de hojas de las cuales se extraerán los valores RGB mediante un software de edición fotográfica de uso común. Para la toma de las imágenes se implementó una metodología que tuviera en cuenta los problemas y restricciones asociados al uso de luz natural descritos en la literatura científica: efectos perniciosos de reflectancia direccional debidos a radiación solar directa (Pinter et al., 1990); variaciones en las condiciones de iluminación; o modificaciones de los colores por el balance de blancos (Murphy et al., 2009). Para ello las hojas de remolacha utilizadas en el experimento fueron colocadas verticalmente en planchas de poliuretano. La cámara utilizada se montó en un trípode a una distancia y altura fija. Previamente a cada fotografía se utilizó una tarjeta de grises para calibrar tanto la temperatura de color (balance de blancos en manual) como la exposición (medición manual puntual). Durante cuatro días se tomaron fotografías de hojas a lo largo de varios momentos del día para comprobar el funcionamiento de este método. Paralelamente se medía el contenido de clorofila de las hojas con un medidor óptico. El siguiente paso consiste en extraer de las fotografías capturadas los valores RGB de las imágenes de las hojas. Con esos valores se calcularon 25 índices encontrados en revisión bibliográfica y se propusieron 2 nuevos obtenidos por ACP y regresión lineal paso a paso (SLR), que fueron validados mediante un grupo de control. Hecho esto, el objetivo era comprobar el funcionamiento de estos índices a la hora de estimar el contenido en clorofila en distintas condiciones lumínicas

y si con ellos se podía detectar la degradación de la misma a lo largo de los días de experimento.

Los resultados de este segundo trabajo motivaron un estudio paralelo sobre la utilidad de índices RGB para la detección de malas hierbas (*“Detection of Sinapis arvensis Weeds in Alfafa Crop by Using RGB Indices”*). Para ello, dentro del marco del proyecto LIFE+ Operación CO₂, se realizaron vuelos con un vehículo aéreo no tripulado o dron equipado con dos cámaras RGB comerciales (una de ellas modificada para capturar el infrarrojo cercano, NIR) sobre un cultivo de alfalfa (*Medicago sativa*), afectado por *Sinapis arvensis*. A partir de las fotografías tomadas se realizó un mosaico de la parcela estudiada y se generaron imágenes para el índice NDVI (Normalized Difference Vegetation Index) que utiliza el infrarrojo cercano, y los índices $R-B/R+B$ y $R-B/R+B+G$, que sólo utilizan el visible. Mediante una comparación visual se evalúa su comportamiento para la detección de las malas hierbas dentro del cultivo y su discriminación con respecto al suelo.

En la figura 2.5 se muestra el resumen esquemático de la metodología aplicada



Figura 2.5. Resumen esquemático de la metodología aplicada en el segundo artículo científico.

2.5.3. Metodología para el Análisis Regional del Cultivo de Remolacha Azucarera Bajo Futuros Escenarios de Cambio Climático

En el tercer estudio se plantea un análisis a escala regional, en la zona remolachera de Castilla y León, de posibles efectos del cambio climático en el cultivo de la remolacha. Para ello, en primer lugar se reúnen datos climáticos diarios de 29 estaciones de la red S.I.A.R distribuidas por la zona de trabajo, desde el año 2001 al 2014. A partir de estos datos se genera un año climático tipo para cada una de las estaciones que será tomado como línea base. Seguidamente, se obtienen las predicciones futuras de temperatura y precipitación anual para los años 2050 y 2070 generadas por el modelo MPI-ESM-LR desarrollado por el Instituto Max Planck de Meteorología (MPI-M) bajo el escenario RCP4.5 del AR5. Estos datos se extrajeron gracias a la herramienta Worldclim (Hijmans et al., 2005), y en base a ellos, se calculan los escenarios futuros de 2050 y 2070 teniendo en cuenta la variación predicha en temperatura y precipitación. Paralelamente con la fórmula FAO-56 PM, se calcula la evapotranspiración para esos dos escenarios futuros. Por lo tanto en esta primera fase se obtiene la caracterización climática de cada uno de los tres escenarios considerados en el estudio. A continuación, estos datos climáticos servirán de entrada al modelo de simulación de cultivos Aquacrop (Raes et al., 2009; Steduto et al., 2009), de la FAO (Organización de las Naciones Unidas para la Alimentación y la Agricultura), previamente ajustado y validado a las características del cultivo en Castilla y León. Finalmente, mediante herramientas SIG (Sistemas de Información Geográfica) de interpolación, se generan por una parte, los mapas de distribución espacial de evapotranspiración a partir de los resultados arrojados por la fórmula FAO-56 PM, y por otra, los mapas de distribución de rendimiento, biomasa total y captura de CO₂, a partir de los resultados de las simulaciones ejecutadas en Aquacrop. Todos ello, para cada uno de los escenarios considerados, esto es, escenario línea base (situación actual), escenario de 2050 y escenario de 2070.

En la figura 2.6 se muestra el resumen esquemático de la metodología aplicada.

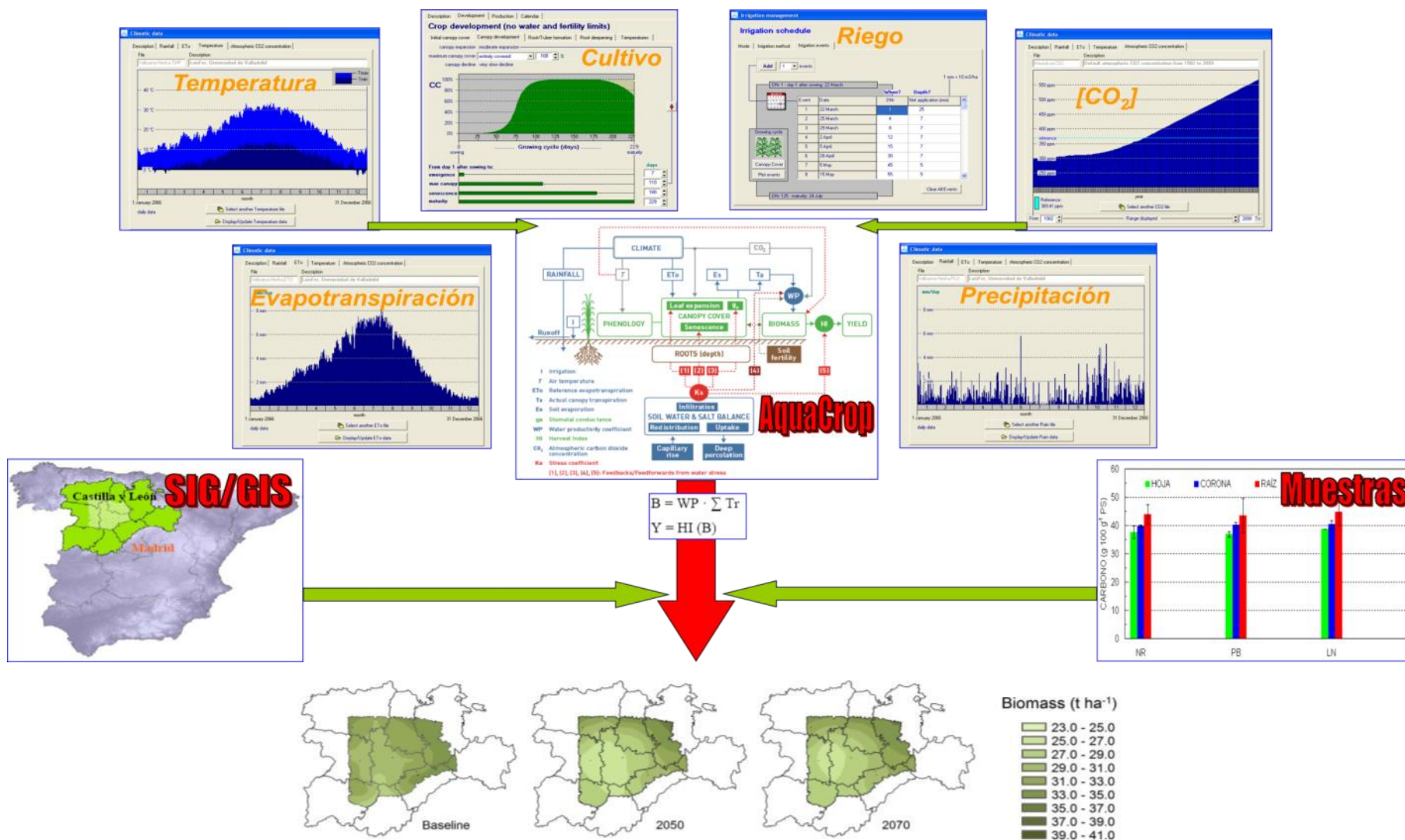


Figura 2.6. Resumen esquemático de la metodología aplicada en el tercer artículo científico.

2.7. REFERENCIAS

- AEMET, Agencia Estatal de Meteorología. (2009). Generación de escenarios regionalizados climáticos para España.
- AIMCRA. 2015. Memoria Campaña 2014/2015 (Siembra Primavera). Valladolid
- Bell, C.I., Milford, G.F.J., Leigh, R.A. (1996). Sugar beet, in: E. Zamski, A.A. Schaffer (Eds.) Photoassimilate distribution in Plants and crops: source-sink relationships, Marcel Dekker Inc., New York, 1996, pp. 691-707.
- Burkart, S., Manderscheid, R., Weigel, H.J. (2009). Canopy CO₂exchange of sugar beet under different CO₂concentrations and nitrogen supply: results from a free-air CO₂enrichment study, *Plant Biol.*, 11 (2009) 109-123.
- Carvajal, M., Mota, C., Alcaraz-López, C., Iglesias, M., Martínez-Ballesta, M.C. (2009) Investigación sobre la absorción de CO₂ por los cultivos más representativos, in, Consejo Superior de Investigaciones Científicas, Murcia, Spain, 2009.
- Clover, G.R.G., Jaggard, K.W., Smith, H.G., Azam-Ali, S.N. (2001). The use of radiation interception and transpiration to predict the yield of healthy, droughted and virus-infected sugar beet, *The Journal of Agricultural Science*, 136 (2001) 169-178.
- Crutzen, P.J., Mosier, A.R., Smith, K.A., Winiwarter, W. (2008). N₂O release from agro-biofuel production negates global warming reduction by replacing fossil fuels, *Atmospheric chemistry and physics*, 8 (2008) 389-395.
- Demmers-Derks, H., Mitchell, R.A.C., Mitchell, V.J., Lawlor, D.W. (1998). Response of sugar beet (*Beta vulgaris* L.) yield and biochemical composition to elevated CO₂ and temperature at two nitrogen applications, *Plant, Cell and Environment*, 21 (1998) 829-836.
- Draycott, A.P., Christenson, D.R., 2003. Nutrients for Sugar Beet Production: Soil-Plant Relationships. CAB International, Wallingford, 242 pp.
- Echevarría Ruiz de Vargas, C., Fera Bourrellier, A.B., Terencio Jiménez, E. (2005). Conceptos generales del metabolismo y del transporte de sacarosa, in: Aspectos fisiológicos de la remolacha de siembra otoñal, Junta de Andalucía, Consejería de Agricultura y Pesca, Sevilla, Spain, 2005, pp. 11-22.

- Espadafor, M., Lorite, I.J., Gavilan, P., Berengena, J., 2011. An analysis of the tendency of reference evapotranspiration estimates and other climate variables during the last 45 years in Southern Spain. *Agricultural Water Management* 98,1045–1061.
- Fabeiro, C., Martín de Santa Olalla, F., López, R., Domínguez, A. (2003). Production and quality of the sugar beet (*Beta vulgaris* L.) cultivated under controlled deficit irrigation conditions in a semi-arid climate, *Agric. Water Manage.*, 62 (2003) 215-227.
- Freckleton, R.P., Watkinson, A.R., Webb, D.J., Thomas, T.H. (1999). Yield of sugar beet in relation to weather and nutrients, *Agricultural and Forest Meteorology*, 93 (1999) 39-51.
- Garcia-Garizabal, I., Causape, J., Abrahao, R., Merchan, D., 2014. Impact of climate change on Mediterranean irrigation demand: historical dynamics of climate and future projections. *Water Resources Management* 28, 1449–1462.
- Gardner, F.P., Pearce, R.B., Mitchell, R.L., (1985) Carbon fixation by crop canopies, in: *Physiology of crop plants*, Iowa State University Press, Iowa, USA, 1985, pp. 31-57.
- Giaquinta, R.T. (1979). Sucrose Translocation and Storage in the Sugar Beet, *Plant Physiol.*, 63 (1979) 828-832.
- Gordo-Ingelmo, L.F. (1994). Composición química y control agrícola de los no-azúcares en la remolacha azucarera, Caja de Ahorros Municipal de Burgos, Burgos, Spain, 1994.
- Gordo, L.F., Morillo-Velarde, R., Martínez, J.J., S. García-Mauriño, E.C. (2005). Crecimiento y desarrollo de la remolacha azucarera de siembra otoñal, in: *Aspectos fisiológicos de la remolacha de siembra otoñal*, Junta de Andalucía, Consejería de Agricultura y Pesca, Sevilla, Spain, 2005, pp. 23-44.
- Grzebisz W., Pepliński K., Szczepaniak W., Barłóg P., Cyna K. (2012). Impact of nitrogen concentration variability in sugar beet plant organs throughout the growing season on dry matter accumulation patterns. *J. Elem.* 17(3): 389-407, DOI: 10.5601/jelem.2012.17.3.03.

- GUTIÉRREZ, J.M.; PONS, M.R. (2006). Modelización numérica del Cambio Climático: Bases científicas, incertidumbres y proyecciones para la península ibérica. *Revista de Cuaternario y Geomorfología*, 20 (3-4): 15-28.
- Harrigan, G.G., Goodacre, R. (2003). *Metabolic profiling: its role in biomarker discovery and gene function analysis*, Springer US, New York, USA, 2003.
- Hijmans, R.J., S.E. Cameron, J.L. Parra, P.G. Jones and A. Jarvis, 2005. Very high resolution interpolated climate surfaces for global land areas. *International Journal of Climatology* 25: 1965-1978.
- Hoffmann, C.M. (2005). Changes in N Composition of Sugar Beet Varieties in Response to Increasing N Supply, *Journal of Agronomy and Crop Science*, 191 (2005) 138-145.
- Hoffmann, C.M., Kenter, C., Bloch, D. (2005). Marc concentration of sugar beet (*Beta vulgaris* L) in relation to sucrose storage, *J. Sci. Food Agric.*, 85 (2005) 459-465.
- Hoffmann, C.M., Kluge-Severin, S. (2010). Light absorption and radiation use efficiency of autumn and spring sown sugar beets, *Field Crops Res.*, 119 (2010) 238-244.
- Hull, R., Webb, D.J. (1970). The effect of sowing date and harvesting date on the yield of sugar beet, *The Journal of Agricultural Science*, 75 (1970) 223.
- Intergovernmental Panel on Climate Change (IPCC), 2007. *Climate change: impacts, adaptation & vulnerability*. In: *Contribution of Working Group II to the Fourth Assessment Report of the Intergovernmental Panel on Climate Change*. Cambridge University Press.
- IPCC, 2001. *Climate Change 2001 — The Scientific Basis*. Cambridge University Press, Cambridge. 881 pp.
- IPCC, 2014: *Climate Change 2014: Synthesis Report*. Contribution of Working Groups I, II and III to the Fifth Assessment Report of the Intergovernmental Panel on Climate Change [Core Writing Team, R.K. Pachauri and L.A. Meyer (eds.)]. IPCC, Geneva, Switzerland, 151 pp.
- Jaggard, K.W., Clark, C.J.A., Draycott, A.P. (1999). The weight and processing quality of components of the storage roots of sugar beet (*Beta vulgaris* L), *J. Sci. Food Agric.*, 79 (1999) 1389-1398.

- Jaggard, K.W., Dewar, A.M., Pidgeon, J.D. (1998). The relative effects of drought stress and virus yellows on the yield of sugarbeet in the UK, 1980–95, *The Journal of Agricultural Science*, 130 (1998) 337-343.
- Jiménez, E.T., García-Mauriño, S., Morillo-Velarde, R., Echevarría, C. (2005). Actividades enzimáticas de degradación de la sacarosa producción de azúcares reductores en la remolacha de siembra otoñal, in: *Aspectos fisiológicos de la remolacha de siembra otoñal*, Junta de Andalucía, Consejería de Agricultura y Pesca, Sevilla, Spain, 2005, pp. 45-69.
- Kawashima, S. and Nakatani, M. (1998). An Algorithm for Estimating Chlorophyll Content in Leaves Using a Video Camera. *Annals of Botany* 81: 49-54, 1998
- Kenter C., Hoffmann C. M. , Märländer B., Effects of weather variables on sugar beet yield development (*Beta vulgaris* L.), *European Journal of Agronomy*, Volume 24, Issue 1, January 2006, Pages 62-69, ISSN 1161-0301.
- Kiyamaz, S., Ertek, A. (2015). Yield and quality of sugar beet (*Beta vulgaris* L.) at different water and nitrogen levels under the climatic conditions of Kırşehir, Turkey, *Agric. Water Manage.*, 158 (2015) 156-165.
- Klenk, I., Landquist, B., Ruiz de Imaña, O. (2012). The Product Carbon Footprint of EU Beet Sugar. Summary of Key Findings, *Sugar Industry Journal*, 137 (2012) 169-177.
- Loel, J., Hoffmann, C.M. (2014). Importance of growth stage and weather conditions for the winter hardiness of autumn sown sugar beet, *Field Crops Res.*, 162 (2014) 70-76.
- MAGRAMA, in, Ministry of Agriculture, Food and Environment of Spain, 2014.
- Malnou, C.S., Jaggard, K.W., Sparkes, D.L. (2006). A canopy approach to nitrogen fertilizer recommendations for the sugar beet crop, *European Journal of Agronomy*, 25 (2006) 254-263.
- Malnou, C.S., Jaggard, K.W., Sparkes, D.L. Nitrogen fertilizer and the efficiency of the sugar beet crop in late summer, *European Journal of Agronomy*, Volume 28, Issue 1, January 2008, Pages 47-56, ISSN 1161-0301.
- Manderscheid, R., Pacholski, A., Weigel, H.-J., 2010. Effect of free air carbon dioxide enrichment combined with two nitrogen levels on growth, yield and yield quality of

- sugar beet: evidence for a sink limitation of beet growth under elevated CO₂. *Eur. J. Agron.* 32, 228–239.
- McKendry, P. (2002) Energy production from biomass (part 1): overview of biomass, *Bioresour. Technol.*, 83 (2002) 37-46.
- Milford, G.F.J., Pocock, T.O., Riley, J. (1985). An analysis of leaf growth in sugar beet I. Leaf appearance and expansion in relation to temperature under controlled conditions, *Ann. Appl. Biol.*, 106 (1985) 163-172.
- Murphy, R.J., Underwood, A.J., Jackson, A.C. (2009) Field-based remote sensing of intertidal epilithic chlorophyll: Techniques using specialized and conventional digital cameras. *Journal of Experimental Marine Biology and Ecology* 380 (2009) 68–76.
- O'Rourke, N., & Hatcher, L. (2013). *A Step-by-Step Approach to Using SAS for Factor Analysis and Structural Equation Modeling* (2nd Ed.). Cary, NC: SAS Press. Edition: 2nd, Publisher: SAS Press, ISBN: 978-1-59994-230-8.
- Petkeviciene, B. (2009) The effects of climate factors on sugar beet early sowing timing, *Agron. Res*, 7 (2009) 436-443.
- Pinter PJ Jr, Jackson RD, Moran MS. 1990. Bidirectional reflectance factors of agricultural targets : A comparison of ground-, aircraft-, and satellite-based observations. *Remote Sensing of Environment* 32: 215-228.
- Pocock, T.O., Milford, G.F.J., Armstrong, M.J., 1990. Storage root quality in sugar-beet in relation to nitrogen uptake. *J. Agric. Sci., Camb.* 115, 355–362.
- Raes, D., Steduto, P., Hsiao, T.C., Fereres, E., 2009. AquaCrop—The FAO crop model to simulate yield response to water. II. Main algorithms and software description. *Agronomy J.* 101 (3), 438–477.
- Rinaldi, M., Vittorio Vonella, A. 2006. The response of autumn and spring sown sugar beet (*Beta vulgaris* L.) to irrigation in Southern Italy: Water and radiation use efficiency. *Field Crops Research.* 95: 103-114.
- Ros, J. (1991). *El Cambio Climático y la Subida del Nivel del Mar*. Centro de Estudios y Experimentación de Obras Públicas, Madrid. 74 p. ISBN: 84-7790-097-3.

- Santos, C., Lorite, I.J., Tasumi, M., Allen, R.G., Fereres, E., 2010. Performance assessment of an irrigation scheme using indicators determined with remote sensing techniques. *Irrigation Science* 28, issue 6, 461-477.
- Scott, R.K., Jaggard K.W., 1993. Crop physiology and agronomy. In: Cooke, D.A., Scott, R.K. (Eds.), *The Sugar Beet Crop: Science into Practice*. Chapman & Hall, pp. 179±237
- Smith P., Martino D., Cai Z., Gwary D., Janzen H., Kumar P., McCarl B., Ogle S., O'Mara F., Rice C., Scholes B., Sirotenko O., Howden M., McAllister T., Pan G., Romanenkov V., Schneider U. and Towprayoon S. (2007) .Policy and technological constraints to implementation of greenhouse gas mitigation options in agriculture. *Agriculture, Ecosystems and Environment* 118, 6-28.
- Steduto, P., Hsiao, T.C., Raes, D., Fereres, E., 2009. AquaCrop—The FAO crop model to simulate yield response to water. I. Concepts and underlying principles. *Agronomy J.* 101 (3), 426–437.
- Taiz, L., Zeiger, E., Moller, I.M., Murphy, A. (2015). *Plant Physiology*, 6 ed., Sinauer Associates Inc., Sunderland, MA, USA, 2015.
- Tanner, C.B., Sinclair, T.R. (1983). Efficient water use in crop production: research or re-search?, in: H.M. Taylor, W.R. Jordan, T.R. Sinclair (Eds.) *Limitations to efficient water use in crop production*, American Society of Agronomy Madison, WI, Madison, WI, USA, 1983, pp. 1-27.
- Thomas, T.H. (2000). Sugar beet, in: D.L. Smith, C. Hamel (Eds.) *Crop yield: physiology and processes*, Springer Verlag, Berlin, Germany, 2000, pp. 311–332.
- van Heemst, H.D.J. (1986). Physiological principles, in: H.v. Keulen, J. Wolf (Eds.) *Modelling of agricultural production: weather, soils and crops*, Pudoc, Wageningen, The Netherlands, 1986, pp. 13-26.
- van Vuuren et al (2011) *The Representative Concentration Pathways: An Overview*. *Climatic Change*, 109 (1-2), 5-31
- Vicente-Serrano, S. M., C. Azorin-Molina, A. Sanchez-Lorenzo, J. Revuelto, E. Morán-Tejeda, J. I. López-Moreno, and F. Espejo (2014a), Sensitivity of reference evapotranspiration to changes in meteorological parameters in Spain (1961–2011), *Water Resour. Res.*, 50, 8458–8480.

- Vicente-Serrano, S. M., C. Azorin-Molina, A. Sanchez-Lorenzo, J. Revuelto, J. I. López-Moreno, J. C. González-Hidalgo, and F. Espejo (2014b), Reference evapotranspiration variability and trends in Spain (1961–2011), *Clim. Dyn.*, 42, 2655–2674.
- Victoria Jumilla, F., Costa Gómez, I., Castro Corbalán, T., García Cárdenas, R., Romojaro Casado, M.C., Mesa del Castillo Navarro, M.L., Motos Alarcón, M.I. (2011). La Iniciativa de Ecorresponsabilidad Agricultura Murciana como Sumidero de CO₂. Marca LESSCO₂, in, Observatorio Regional de Cambio Climático. Región de Murcia, Murcia, Spain, 2011.
- Villarías-Moradillo, J.L. (2000). La Remolacha Azucarera. Consejería de Agricultura y Ganadería de la Junta de Castilla y León.
- Villarías-Moradillo, J.L. de Liñán y Vicente, C. (1999). La Remolacha Azucarera, Ediciones Agrotécnicas, Madrid, Spain, 1999.

3. OBJETIVOS DE LA TESIS

OBJETIVOS DE LA TESIS

En base a los antecedentes expuestos, se pretende identificar y estudiar los parámetros que afectan al cultivo de remolacha azucarera, como sumidero temporal de CO₂ y su respuesta ante cambios ambientales previstos en el futuro cercano. Para ello se ha estructurado la Tesis Doctoral en tres líneas investigación o estudios con sus respectivos objetivos específicos. Cada una de estos estudios se ha plasmado en formato de artículo científico para su publicación en revistas especializadas.

El objetivo de la primera parte de la Tesis, cuya consecución se persigue en el artículo científico *“Identificación del Impacto de Variables Climáticas en el Contenido de Carbono en Raíz de Remolacha Azucarera”* es tratar de comprobar si el contenido de carbono en la raíz de las remolacha azucarera, está influenciado por variables ambientales o si bien está ontogénicamente determinado y no caben variaciones. Como objetivos específicos se pueden enumerar los siguientes:

1.1 Determinar si el porcentaje de carbono en la raíz de remolacha está influenciado por factores ambientales o es independiente de las condiciones climáticas y edafológicas de cada zona de cultivo.

1.2 Analizar el papel del abonado nitrogenado y la variedad sobre parámetros medidos en cosecha relativo a peso fresco, peso seco y concentraciones de carbono y nitrógeno en raíz, corona y hojas.

1.3 Estudiar posibles relaciones entre el contenido de carbono de la raíz y otros parámetros relativos a la composición de la raíz

1.4 Detectar posibles interrelaciones entre el contenido en carbono de la raíz y otros parámetros estudiados.

1.5 Estudiar la influencia de variables climáticas a lo largo del periodo del cultivo sobre el desarrollo del mismo y la cantidad de carbono presente en la raíz al final del ciclo.

1.6 Cuantificar el porcentaje de carbono contenido en los órganos estudiados de la planta de remolacha, particularmente en la raíz, para permitir posteriores trabajos sobre estimaciones de CO₂ absorbido o estudios de huellas de carbono.

El objetivo de la segunda parte de la Tesis plasmado en el segundo artículo científico “**Evaluación del Uso de Índices de Vegetación RGB para Determinar el Contenido de Clorofila en Hojas de Remolacha Azucarera en Cosecha**” consiste en validar una técnica de estimación de clorofila mediante el uso de índices de vegetación, basados en las bandas RGB a través de fotografías tomadas con una cámara comercial. (Dentro de este estudio se incluye como anexo la aplicación práctica recogida en la comunicación “*Detección de malas hierbas (Sinapis arvensis) en un cultivo de alfalfa mediante el Uso de Índices RGB*”). Objetivos específicos:

2.1 Evaluar la viabilidad de estimar el contenido en clorofila de hojas de remolacha a través de fotografías tomadas con una cámara convencional bajo luz natural mediante el uso de índices de vegetación del espectro visible.

2.2 Proponer nuevos índices de vegetación que trabajen con las bandas RGB del espectro visible y alcancen altos coeficientes de correlación con los contenidos de clorofila en las hojas de remolacha.

2.3 Evaluar el comportamiento de los índices estudiados, bajo distintas condiciones de luz natural (haciendo varias tomas fotográficas en distintas horas del día y durante varios días), para reproducir la evolución del contenido en clorofila de las hojas.

2.4 Proponer un método de calibración y toma de las imágenes fotográficas que minimice los problemas ligados a las capturas bajo luz natural y permite comparar entre imágenes tomadas a distintas hojas y distintos días.

2.5 Evaluar la aplicabilidad de índices de vegetación RGB calculados a partir de imágenes obtenidas con una cámara convencional montada en un UAV (drone) para la detección de malas hierbas amarillas (Medicato sativa) en un cultivo de alfalfa.

El objetivo del tercer estudio plasmado en el artículo científico “**Análisis Regional del Cultivo de Remolacha Azucarera Bajo Futuros Escenarios de Cambio Climático**” es realizar un análisis a escala regional, en la zona remolachera de Castilla y León, de posibles efectos del cambio climático en el cultivo de la remolacha. Como objetivos específicos se encuentran:

3.1 Estudiar los efectos cuantitativos y en cuanto a distribución espacial sobre la evapotranspiración en la zona remolachera de Castilla y León a partir de los cambios

previstos de temperatura y precipitaciones para los años 2050 y 2070 según el escenario de emisiones RCP4.5 propuesto en el AR5 del IPCC.

3.2 Evaluar los efectos sobre el rendimiento de cosecha de la remolacha azucarera en Castilla y León en escenarios climáticos futuros de 2050 y 2070 a través del modelo de crecimiento Aquacrop en comparación con la situación actual.

3.3 Estimar los efectos sobre la cantidad de biomasa y CO₂ capturado por la remolacha azucarera en Castilla y León en escenarios climáticos futuros de 2050 y 2070 a través del modelo de crecimiento Aquacrop en comparación con la situación actual.

3.4 Detectar y examinar posibles tendencias en los parámetros estudiados.

4. IMPACT OF CLIMATE VARIABLES ON CARBON CONTENT IN SUGAR BEET ROOT

IMPACT OF CLIMATE VARIABLES ON CARBON CONTENT IN SUGAR BEET ROOT

Luis Fernando Sánchez Sastre¹, Pablo Martín Ramos², Luis Manuel Navas Gracia¹, Salvador Hernández Navarro¹ and Jesús Martín Gil¹

¹ Agriculture and Forestry Engineering Department, ETSIIAA, Universidad de Valladolid, Avenida de Madrid 44, 34004 Palencia, Spain.

² Department of Agricultural and Environmental Sciences, EPSH, University of Zaragoza, Carretera de Cuarte, s/n, 22071 Huesca, Spain.

Abstract

There is some controversy over whether the growth and accumulation of sugar in sugar beet is limited by external conditions (*source-limited*) or if such limitation is ontogenetic (*sink-limited*). In the study presented herein, the impact of climate variables on the growth and carbon contents of spring-sown sugar beet (*Beta vulgaris saccharifera*) in Castilla y Leon region (north-western Spain) was assessed by analysing 34 beet crop parameters at different sites over two years. By resorting to ANOVA, Principal Component Analysis and Cluster Analysis, the impact of different factors such as climatic variables, site, beet variety or fertilization has been evaluated.

Keywords: climatic factors; fertilization; location; plant parameters; sugar content; variety

Highlights:

- Root sugar content depends on location conditions (soil, climate and interactions)
- There is a positive relationship between sucrose content and dry matter content
- Carbon content at harvest is positively influenced by mean temperature in crop's 1st stage.
- Radiation accumulated in crop's 1st stage has positive influence on carbon content
- Radiation accumulated in final stage has a negative influence on carbon content

4.1. INTRODUCTION

Agriculture represents up to 31% of all global anthropogenic Green House Gases (GHG) if land use changes are considered (Smith et al, 2007). Therefore, agriculture is a major contributor of GHGs emissions to the atmosphere, both directly -throughout farming operations and biochemical processes that take place in agricultural soils- and indirectly -due to fossil fuel use in farm operations, the production of agrochemicals and the conversion of land to agriculture-. Some initiatives related to Agriculture, Forestry and Other Land Use (AFOLU) (IPCC, 2014) prefer to use *carbon balance* instead of *carbon footprint*, since the former takes into account not only emissions but also the carbon assimilated by agroforestry systems (Victoria Jumilla et al, 2011).

That is the case for crops which uptake carbon from the atmosphere by means of the photosynthesis process. Carbon dioxide sequestered by plants is the result of the difference between the CO₂ assimilated by photosynthesis and the CO₂ emitted during respiration (Taiz et al, 2015), and it represents 40-50% of plant biomass dry matter (McKendry, 2002). Consequently, as long as growth rates are high, crops can be deemed as carbon sinks (Carvajal et al, 2009). Nevertheless, the fact that environmental factors (day length, temperature, precipitation, soil nutrients, CO₂ concentration...) continuously change and that plants respond unequally to different environments also has to be taken into account (Gardner et al, 1985).

Life Cycle Assessment (LCA) or Environmental Footprint Methodologies (EFM) results depend on the accuracy and scope of their database, but many times only general values or approximations are available due to the lack of research. That is the case for sugar beet, an important industrial crop in Castilla y León region (Spain). In spite of the fact that there are numerous Carbon Footprint studies for this crop and its sub-products (Klenk et al, 2012), figures about carbon content from experimental research are scarce and approximations have been used instead (Crutzen et al, 2008).

Sugar beet crops have undergone important changes in the last decades, such as improved varieties (Jaggard et al, 1999) and better cultural practices: earlier sowing, higher planting densities, more efficient use of fertilizers, control of pests and diseases, etc. (Milford et al, 1999). The productive capacity of sugar beet stems from its ability to intercept radiation for its photosynthetic process, that is, on its ability to attain the highest ground coverage as quickly as possible and to maintain that cover for the maximum possible amount of time, thus being able to optimize sunlight capture (Van

Heemst, 1986). It is known that sugar beet crop canopy reaches its maximum when the maximum radiation of the year is already over, due to the slow formation of leaves in spring (Scott et al, 1993 and Kenter et al, 2006). Beet fixes CO₂ and accumulates sugar (Echevarría et al, 2005), and sucrose is used by the plant for metabolism conservation, sheet formation, root tissue formation and, finally, for the accumulation of sugar in the root (Gordo-Ingelmo, 1994). From the enzymatic point of view, net accumulation of sucrose in the root occurs during the first growth stages, with an increased activity of the sucrose-synthase enzyme and a greater contribution of sucrose from the leaves to the root. Subsequently, a decrease in the polarization increase rate is observed, till it stops or it even becomes negative (onset of sucrose invertase activity) (Jiménez et al, 2005).

There is some controversy over whether the growth and accumulation of sugar in sugar beet is limited by external conditions (*source-limited*), namely climate, fertilization, soil, etc. (Thomas et al, 2000 and Bell et al, 1996) or if such limitation is ontogenetic (*sink-limited*) (Demmers-Derks et al, 1998, Hoffman and Kluge-Severin (2010). Milford et al (1985) stated that temperature is the main factor for sugar beet growth and thermal time explains the shift in different stages. Villariás-Moradillo et al. (1999) explained that the heat summation for germination in Castilla y Leon (Spain) is 120-130 °C·d (10-12 days). Hull et al. (1970), cited in Hoffman and Kluge-Severin (2010), indicated that the length of the growing season have a strong positive effect on sugar beet yield.

There are studies which support that the potential yield of sugar beet mainly depends on the site (soil, climate and interactions) and year effects (weather conditions during vegetation period), while the influence of agronomy would be lower (Kenter et al, 2006). In this line, other groups have attempted to resolve the influence of climatic factors on beet growth, both for spring- and autumn-sowing, in connection to different geographical areas, such as Freckleton et al. (1999) and Clover et al. (2001) in England, Gordo et al. (2005) in Spain for autumn sowing; Petkeviciene (2009) in Lithuania; Hoffman and Kluge-Severin (2010 and 2011) (spring sowing) and Loel and Hoffman. (2014) (autumn sowing) in Germany.

Other important factors subject to further study are related to the crop's water needs, which in turn are related to precipitation, temperature, evaporative demand and soil retention capacity (Jaggard et al, 1998), although Tanner et al. (1983), cited in Rinaldi and Vonella (2006), stated that beet is an efficient user of water. What's more,

Fabeiro et al. (2003) reported that sugar beet is drought-resistant plant that can produce economic yield even with declined irrigation. A deciding factor for obtaining a good harvest is the irrigation during the sprouting season (AIMCRA 2015), and the moisture content in an optimum soil in Spain has been determined to be 12-15% (Villarías-Moradillo et al, 1999).

Another factor to consider is the role played by nitrogen in the expansion of beet leaves in order to capture light (Manderscheid et al, 2010 and Malnou et al, 2008)]. Nitrogen concentration in leaves, the plant organ responsible for CO₂ fixation, is considered as a factor which modifies the growth rate of both leaves and the storage root in a significant manner (Grzebisz et al, 2012). It is known that the nitrogen concentration in leaves increases during the first 70 days and then decreases as the growth cycle advances (Gordo-Ingelmo, 1994), and there are various studies on the optimal fertilization of beet (Malnou et al, 2006 and Malnou et al, 2008), on the interaction of fertilization and irrigation (Kiymaz et al, 2015) and even on the effects of carbon fertilization in this crop (Burkart et al, 2009 and Manderscheid et al, 2010).

As for the composition of the beet root, the factors that may influence it have also been investigated, because it is a critical factor for the industrial quality of the root and in particular for the sugar extraction process (Jaggard et al, 1999, Kenter et al, 2006, Giaquinta, 1979 and Hoffmann, 2005). The composition of the beet root at harvest is: 77% water and 23% dry matter, with 70-76% of sucrose, 18% of marc and 6% of other substances such as betaine (Gordo-Ingelmo, 1994 and Hoffmann et al, 2005). The marc is a quality parameter and consists of all the components that remain insoluble after a hot water extraction (at 80 °C), namely cellulose, hemicellulose, pectin substances, saponins, lipids, lignins, etc. The concentration of the marc depends on the site and the variety (Hoffmann et al, 2005).

The main goal of this research is to determine carbon content at harvest and, subsequently, the total amount of CO₂ absorbed by sugar beet at different locations of Castilla y León region, assessing the influence of weather/environmental conditions on the amount of carbon sequestered by the crop. The chosen region is particularly representative because it accounts for 90% of the Spanish production of spring-sown sugar beet with 26573 ha (MAGRAMA 2014). Moreover, the north of Spain is the area of the European Union in which the highest yields per hectare are attained, with 33.7% of the farmers getting more than 120 tonnes per hectare (AIMCRA 2015). Thus, this

study aims to discriminate -using ANOVA, factorial and cluster analysis- if significant differences occur in the carbon content in the plant as a consequence of different locations, soils and climates, in an attempt to deepen our understanding of the various factors that have an influence on the growth of this plant.

4.2. MATERIALS AND METHODS

4.2.1. Field trials

Field trials were conducted on commercial farm fields at 3 sites in 2011 and at 4 sites in 2012, all of them in spring-sown sugar beet cultivation areas in Castilla y León region, in north-western Spain (Figure 4.1).

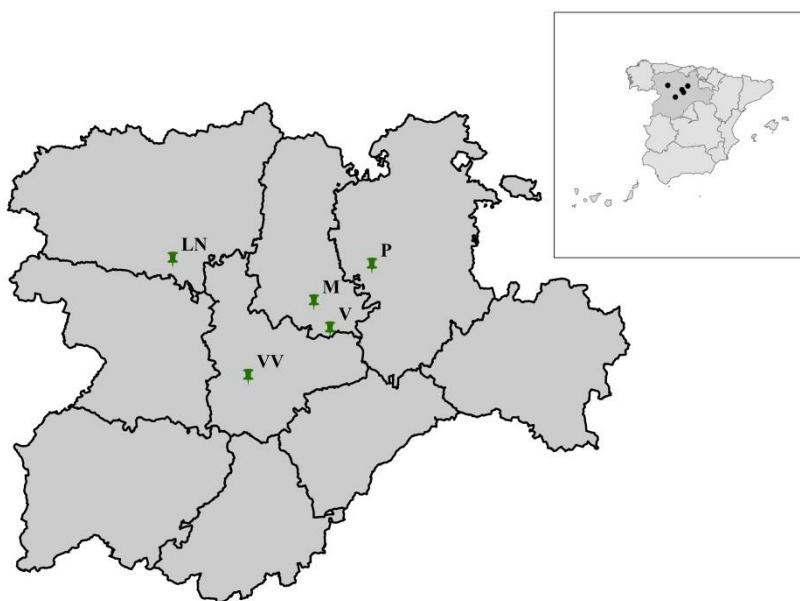


Figure 4.1. Overview map of experiment locations. *LN*: Laguna de Negrillos; *M*: Magaz de Pisuerga; *P*: Pampliega; *V*: Vertavillo; *VV*: Villavieja.

Daily weather data during the cultivation period (Table 4.1) were collected from six nearby automatic weather stations belonging to the SIAR network (Agroclimatic Information System for Irrigation) of the MAGRAMA (Ministry of Agriculture, Food and Environment of Spain). All stations were within a 20 km radius of the experiment locations.

Table 4.1. Weather data for 2011 and 2012 supplied by nearby SIAR stations. *T*: mean temperature (in °C); *P*: total precipitation (in mm); *ETo*: total evapotranspiration (in mm); *R*: total radiation (in MJ·m⁻²) of the cultivation period.

Site	Year	Coordinates			Meteorological data			
		Latitude	Longitude	Altitude	T	P	ETo	R
Magaz (M)		N 41° 59' 24''	W 04° 24' 36''	737	17.0	100	792	4125
Laguna de Negrillos-I (LN-I)	2011	N 42° 13' 56''	W 05° 37' 37''	782	16.8	182	805	4312
Villavieja-I (VV-I)		N 41° 29' 59''	W 05° 03' 53''	674	16.9	134	872	4679
Pampliega (P)		N 42° 12' 26''	W 04° 00' 02''	764	15.5	178	941	4662
Laguna de Negrillos-II (LN-II)	2012	N 42° 15' 47''	W 05° 07' 57''	778	15.5	199	898	4684
Vertavilo (V)		N 41° 50' 52''	W 04° 19' 23''	785	16.0	147	798	3949
Villavieja-II (VV-II)		N 41° 31' 39''	W 05° 01' 30''	710	15.8	100	908	4853

The weather data in Table 4.1, namely temperature (*T*), precipitation (*P*), evapotranspiration (*ETo*) and radiation (*R*), were used as an input in order to calculate 12 additional climate parameters, which are summarized in Table 4.2.

Table 4.2. Calculated climatic variables

Variable	Description	Units
R1	Accumulated radiation a.e.	MJ·m ⁻²
R2	Accumulated radiation until 1200 °C·d a.s.	MJ·m ⁻²
R3	Accumulated radiation from 1200° C·d a.s.	MJ·m ⁻²
R4	Accumulated radiation the first 65 days a.s.	MJ·m ⁻²
R5	Accumulated radiation the last 25 days	MJ·m ⁻²
R6	Accumulated radiation from the day 175 a.s.	MJ·m ⁻²
T1	Mean temperature during the first 65 days	°C
T2	Mean temperature during the first 1200 °C·d a.s.	°C
T3	Mean temperature deviation from 18 °C from 1200 °C·d a.s.	°C
GDD	Growth grades day a.s.	°C·d
GDD1	Growth grades day a.e.	°C·d
GDD2	Growing grades day from 1200°Cd	°C·d

a.e. stands for after emergence; *a.s.* stands for after sowing

According to Kenter et al. (2006), there is a positive correlation between the growth of roots and leaves and the average temperature during the first days of growth (0-65 days a.s.). In the final period (from 175 days a.s. onwards), the most significant impact on growth falls on solar radiation.

Consequently, bearing in mind that temperature and radiation are critical parameters in crop development, six cumulative radiation parameters (R1 to R6) and three average temperature parameters (T1 to T3) were calculated, taking as a reference the number of days after sowing. Thus, it was possible to distinguish between the accumulated radiation or temperature in the early stages of cultivation (R2, R4, T1, T2), since the end

of the first stages until harvest (R3) and in the final stages of the vegetative life (R5, R6).

In addition, 18 was taken as the ideal average temperature for root growth during the summer months (T3), considering that a loss of dry matter accumulation occurs if the crop deviates from that optimum temperature (Kenter et al, 2006).

Variables related to thermal time (GDD, growing degree days) were calculated daily and accumulated using a base temperature of 3 °C [25,47]. GDD is strongly related to phenological development and growth stage (Derscheid et al, 1981).

Previous works by Milford et al. (1985) suggested that ca. 750 °C·d are necessary for beet to form a close canopy, while Malnou et al. (2006) reported that 900 °C·d and 100 kg N/ha were required for the crop to reach 85% canopy. Kenter et al. (2006) concluded that the leaf dry matter increases linearly, while that of the root increases in an exponential way up to 1200 °C·d.

Soil characteristics and fertilization for the locations under study are shown in Table 4.3. Sowing and harvest dates, fertilization and irrigation were decided and carried out by farmers under AIMCRA (Research Association for Sugar Beet Crop Improvement) recommendations for optimum yield (aimcra 2015). Therefore, it was assumed that, as plots received the full recommended rate of nutrients and irrigation, the weather conditions were the main factor modifying the plants growth and final yields (Grzebisz et al, 2012).

Table 4.3. Soil analyses and fertilization data in 2011 and 2012 at the different locations. *LN*: Laguna de Negrillos; *M*: Magaz de Pisuerga; *P*: Pampliega; *V*: Vertavillo; *VV*: Villavieja.

Site	Soil Analysis										Fertilization		
	Type	Texture	pH	SOM (%)	P (ppm)	K (ppm)	Mg (ppm)	Ca (ppm)	Na (ppm)	CO ₃ ²⁻ (%)	N (kg ha ⁻¹)	P ₂ O ₅ (kg ha ⁻¹)	K ₂ O (kg ha ⁻¹)
<i>2011</i>													
M	Entisol	Clay-Loam	8.8	1.7	20	166	300	4570	71	24.3	140	125	100
LN-I	Inceptisol	Loam	6.7	1.1	25	137	80	950	35	1.1	180	75	0
VV-I	Entisol	Loam	8.5	1.2	19	162	590	2480	118	4.2	180	75	0
<i>2012</i>													
P	Entisol	Silty-Clay	7.9	3.6	55	410	520	3710	58	15	110	84	28
LN-II	Inceptisol	Sandy-Clay-Loam	7.0	0.8	15	111	220	1100	29	0.8	183	70	0
V	Inceptisol	Clay	8.1	2.2	23	633	290	5220	13	25.3	155	208	92
VV-II	Entisol	Sandy-Clay-Loam	8.5	1.0	10	195	320	3610	35	13.9	180	115	0

SOM: soil organic matter; P: phosphorus; K: potassium; Mg: magnesium; Ca: calcium; Na: sodium; CO₃²⁻: carbonates; N: nitrogen. *I* and *II* stand for 2011 and 2012, respectively.

Two commercial sugar beet varieties were sown: one with a high sucrose content and another with a high yield, in comparison to test varieties (AIMCRA 2015). The first type was represented by Dulzata Hilleshög-Syngenta in 2011 and by Amalia KWS in 2012, while Sandrina KWS was chosen for the second type. The population density was 125000 plants·ha⁻¹ in all the sites, in both years. Herbicides were applied following AIMCRA's recommendations and pesticides were also used when necessary. Nonetheless, damages by nematode were reported in Magaz or site M (in 2011). In 2012, leaves from Laguna de Negrillos (LN-II) plants could not be collected. In 2011 the experimental treatments were conducted at three sites, with two levels of fertilization (N1, which is the optimum recommended for each location, and 2N, which is twice the recommended dose) and for the two aforementioned varieties. In 2012 only the effect of location (four different sites) and the variety (two varieties) were assessed. In 2011, experiments were arranged in a split-plot design, in three randomized blocks of 12 plots with nitrogen as the main factor and three replications. In 2012, the trials were conducted in a completely randomized block design with two replications (8 plots). In both years each plot was 9.75 m² and consisted of 3 rows, out of which only the beets of the central row were harvested. Entire plants were manually harvested on the same date that farmers began to harvest their fields.

4.2.2. Analyses

The entire plants were divided into leaves, root crowns (that is, the part of the root system which sticks out of the ground and from stems arise, that represents 3-10% of the root) (Gordo-Ingelmo, 1994) and roots at the laboratory, where they were separately washed and weighted as fresh matter. Then each part was completely cut up and oven-dried at 105 °C until constant weight so as to determine the dry matter content. Afterwards, the oven-dried materials were milled and homogenized to obtain 1 mm sieve powder.

In order to measure carbon and nitrogen content, samples were analysed using a LECO CHN-2000 (LECO Corp., USA). Along with EDTA calibration samples, dry matter samples were placed into tin foil wrappers (100 to 150 mg) and loaded into the analyser, where they were combusted in a resistance furnace (950 °C) using pure oxygen. Combustion gas was collected and used for nitrogen determination via a thermal conductivity cell. Carbon was detected using infrared detection. Carbon and

nitrogen were measured concurrently with a total analysis time of 4 minutes. The final results are reported as weight percentages.

34 parameters were calculated out of the fresh weights (6 parameters), dry weights (9 parameters), and carbon (10 parameters) and nitrogen contents at harvest (9 parameters) (see Table 4.4). Thus, measurements relative to fresh weight and dry weight per organs (leaves, crown and root) and per plant were obtained. From these primary variables, percentages of dry matter in each of the organs were calculated. The product of these percentages and the concentrations of carbon and nitrogen obtained in the LECO equipment resulted in the total amount of these elements in each organ, in the whole plant and –since the sowing density was also known- per hectare. In this way, it was possible to estimate the total absorbed nitrogen or the captured CO₂. In addition, the carbon content in root to nitrogen content in leaves ratio (CNR) was also calculated, together with the ratio of root to leaves fresh weights (RTLr) (Kenter et al, 2006). Uptaken CO₂ was obtained by multiplying dry matter, C content and a C to CO₂ conversion factor (relation between molecular mass of CO₂ and atomic mass of C: 44/12).

Table 4.4 Parameters obtained from the fresh weights, dry weights, and carbon and nitrogen concentrations in leaves, root crowns and roots.

Fresh matter			Dry matter		
Variable	Description	Units	Variable	Description	Units
PFW	Plant fresh weight	g	RDW	Root dry weight	g
RFW	Root fresh weight	g	LDW	Leaves dry weight	g
LFW	Leaves fresh weight	g	CDW	Crown dry weight	g
CFW	Crown fresh weight	g	RDM	Root dry matter content	g/kg
RTLr	Root to leaves ratio	-	LDM	Leaves dry matter content	g/kg
Yield	Root fresh weight per ha	t/ha	RBio	Root dry weight per ha	t/ha
			LBio	Leaves dry weight per ha	t/ha
			CBio	Crown dry weight per ha	t/ha
			PBio	Plant dry weight per ha	t/ha

Carbon			Nitrogen		
Variable	Description	Units	Variable	Description	Units
RC	Root Carbon content	g/kg	RN	Root Nitrogen content	g/kg
LC	Leaves Carbon content	g/kg	LN	Leaves Nitrogen content	g/kg
CC	Crown Carbon content	g/kg	CN	Crown Nitrogen content	g/kg
RC/plant	Root Carbon weight per plant	g	RN/plant	Root Nitrogen weight per plant	g
LC/plant	Leaves carbon weight per plant	g	LN/plant	Leaves Nitrogen weight per plant	g
CC/plant	Crown carbon weight per plant	g	CN/plant	Crown Nitrogen weight per plant	g
C/plant	Total Carbon per plant	g	TN/plant	Total Nitrogen absorbed per plant	g
TC	Total Carbon per ha	t/ha	TN	Total Nitrogen absorbed per ha	kg/ha
CO ₂ /plant	CO ₂ per plant	g			
TCO ₂	CO ₂ per ha	t/ha	CNR	RC/LN	-

4.2.3. Statistics

The statistical analysis of the data was carried out using STATISTICA 8.0 (StatSoft Inc., 2007) for the analysis of variance (ANOVA) and for subsequent tests for homogeneity of variances, normal distribution and independence. Levels of significance are indicated as follows: * ($p < 0.05$), ** ($p < 0.01$) and *** ($p < 0.001$). Tukey's HSD was chosen as a comparison *post-hoc* test to compare means.

In addition to this, Principal Component Analysis (PCA) and Clustering Analysis (CA) multivariate techniques were also applied, using IBM SPSS Statistics 21 (IBM Corp., 2012). PCA was used to find patterns in the dataset by reducing the observed variables into a smaller number of principal components (artificial variables) that account for most of the variance in the observed variables (O'Rourke et al, 2013). For all the analyses, orthogonal rotation Varimax was used. Barlett's Test of Sphericity ($p < 0.050$) and Kaiser-Meier-Olkin (KMO) measure of sampling adequacy test ($MKO > 0.50$) were successfully passed (Pérez López, 2004) for the analyses shown in the results. The new variables (components) obtained accounted for more of the 68% of the accumulated variance in all the cases. Among all the different PCAs conducted with different combination of variables, only those which resulted in two components and which met the Barlett, KMO and variance criteria were selected.

2D plots were generated in order to allow a clearer interpretation of the correlation or influence between variables. The distance of a parameter from the centre (0,0) indicates its influence, which will increase for distant positions. The correlation between parameters is given by the angle to the centre, with an acute angle indicating a positive correlation and an obtuse angle indicating a negative correlation (Loel and Hoffmann, 2014).

CA is used for detecting natural segregation of data (subsets) since that provide strong evidence for statistically significant differences between samples of dataset (Harrigan and Goodacre, 2003). In this study, CA was carried out by plotting the datasets in 3D dispersion graphs in which the axes were the new variables calculated after PCA.

4.3. RESULTS

In order to conduct a rigorous analysis of whether the sugar beet growth of the composition of its root are influenced by location, crop variety and type of fertilization, and by the specific conditions of each campaign, an ANOVA analysis is first required, followed by a PCA so as to determine which are the environmental factors that influence most the crop in each area and in each campaign. Previously, it had been observed for emergence data in 2012 that there was a clear relationship between the GDD necessary for the emergence and the thermal gradient (maximum temperature minus minimum temperature from planting to emergence). In Table 4.5 it can be observed that in those sites in which the thermal gradient was larger, the crop needed less GDD to emerge.

Table 4.5. GDD and days in which emergence took place for each of the locations in 2012.

Site	Days	GDD (°C·day)	Temperature Gradient ($T_{\max}-T_{\min}$)
VV	22	152	18.1°
P	21	185	15.5°
LN	23	205	14.6°
V	25	210	14.1°

VV: Villavieja; P: Pampliega; LN: Laguna de Negrillos; V: Vertavillo.

4.3.1. ANOVA analysis

The results of the ANOVA analysis for 10 representative harvest parameters are summarized in Table 4.6 and Table 4.7 for each of the factors under study (location, variety and fertilization) and for the two campaigns: (i) fresh weight and yield (PWF, Yield, LWF and RTL); (ii) carbon content in the root, dry weight and CO₂ (RC, RDM and TCO₂) and (iii) nitrogen content in the leaves, total N absorption and carbon to nitrogen ratios (LN, TN and CNR). The factorials Site × Fertilization (2011) and Site × Variety (2012) were not included in this analysis of results, because when they showed statistical significance, it was due to the fact that some of the factors also showed it separately. The results for Tukey's HSD *post-hoc* test for the location factor are also discussed at the end of this subsection.

Table 4.6. ANOVA analysis for 2011 data. Significance levels are indicated as * ($p < 0.05$), ** ($p < 0.01$) and *** ($p < 0.001$). $S \times F$ is the combined effect of *Site* and *Fertilization*. Figures highlighted in bold indicate the main contributions to the significance, according to Tukey's HSD *post-hoc* test.

Var	Treatments							Effects			
	Site			Variety		Fertilisation		Site	Variety	Fertilisation	$S \times F$
	M	LN-I	VV-I	Dulzata	Sandrina	N	2N				
PWF	888.64	1377.69	1808.29	1288.21	1428.20	1252.67	1463.74	*** (87.54)	n.s.	* (71.48)	n.s.
YIELD	74.73	92.51	120.94	95.14	96.98	92.50	99.62	*** (6.72)	n.s.	n.s.	n.s.
LFW	182.24	499.19	524.29	351.69	452.12	343.41	460.40	*** (25.426)	* (20.76)	*** (20.76)	*** (35.95)
RTLRL	3.58	1.68	1.99	2.72	2.11	2.76	2.07	*** (0.14)	*** (0.121)	*** (0.121)	*** (0.209)
RC	42.32	44.97	42.93	43.43	43.38	42.66	42.88	*** (0.47)	n.s.	n.s.	n.s.
LN	2.24	1.96	2.19	2.06	2.20	2.00	2.26	*** (0.039)	** (0.032)	*** (0.032)	*** (0.056)
CNR	19.09	23.74	19.73	21.25	19.88	21.92	19.21	*** (0.45)	* (0.367)	*** (0.37)	*** (0.64)
RDM	19.87	25.13	22.04	22.00	22.68	22.50	22.19	*** (0.342)	n.s.	n.s.	n.s.
TN	195.43	386.09	500.14	345.15	375.95	325.46	395.64	*** (22.92)	n.s.	* (18.71)	* (32.41)
TCO ₂	31.53	52.53	63.84	46.65	51.09	46.35	51.40	*** (3.27)	n.s.	n.s.	n.s.

Table 4.7. ANOVA analysis for 2012 data. Significance levels are indicated as * ($p < 0.05$), ** ($p < 0.01$) and *** ($p < 0.001$). $S \times V$ is the combined effect of *Site* and *Variety*. Figures highlighted in bold indicate the main contributions to the significance, according to Tukey's HSD *post-hoc* test.

Var	Treatments						Effects		
	Site			Variety			Site	Variety	$S \times V$
	P	LN-II	V	VV-II	Amalia	Sandrina			
PWF	1789.46	-	1534.67	1754.70	1579.32	1806.58	n.s.	n.s.	n.s.
YIELD	110.03	96.41	119.69	124.38	104.45	120.80	* (7.47)	* (5.28)	n.s.
LFW	639.52	-	367.92	482.26	465.29	527.83	*** (31.27)	n.s.	*** (44.22)
RTLRL	1.43	-	2.83	2.23	2.11	2.22	*** (0.153)	n.s.	*** (0.216)
RC	42.35	44.63	44.10	43.91	43.68	43.75	* (0.559)	n.s.	n.s.
LN	2.25	-	1.92	2.04	2.00	2.14	*** (0.047)	* (0.038)	n.s.
CNR	19.02	-	23.34	21.97	22.01	20.73	*** (0.59)	* (0.48)	n.s.
RDM	22.94	24.36	23.04	23.11	23.62	23.11	* (0.385)	** (0.27)	* (0.54)
TN	494.02	-	370.72	362.79	381.71	436.64	*** (24.597)	n.s.	n.s.
TCO ₂	69.42	-	62.37	65.98	62.85	68.99	n.s.	n.s.	n.s.

4.3.1.1 Dry weight and yield

Regarding the location factor, the first step was to study the parameters of fresh weight and yield (PFW, LFW, Yield, RTLRL), finding that in both campaigns (2011 and 2012) the statistical results showed highly significant differences between the means of the fresh weight and yield parameters in the treatments at different locations, except in 2012 for plant fresh weight (PFW) (see Table 4.6 and Table 4.7). PFW presents statistical significance in 2011 due to the fact that Villavieja (VV-I) was the location with the highest root yield (yield = 120.94 t/ha), highest leaves weight (LFW = 524.29 g/plant) and highest total plant fresh weight (PFW = 1808.29 g/plant). In the second year (2012), Villavieja (VV-II) was again the location with the highest yield (yield = 124.38 t/ha), but the leaves fresh weight (LFW) was higher in Pampliega (639.52

g/plant vs. 482.26 g/plant) and the differences in the total plant fresh weight from one location to the other (PFW = 1789.46 g/plant vs. 1754.70 g/plant for P and V-II, respectively) were small, which accounts for the fact that no statistical significance was obtained. These results for the plots located in Villavieja and Pampliega corresponded to longer cultivation periods and, consequently, to a higher thermal integral or growth in °C·days (GGD) and to a larger cumulative radiation (R) (Table 4.8). This is in good agreement with several statements previously made by other authors, such as the fact that the length of the growing season is known to have a strong positive effect on sugar beet yield (hull and Webb, 1970) (cited in Hoffmann and Kluge-Severin, 2010), that there is a linear relationship between radiation interception and biomass (Martínez Quesada et al, 2003), that the total production of crop dry matter is strongly correlated with the intercepted radiation (Monteith and Moss, 1977) and that increasing nitrogen increases dry weight (Kiymaz and Ertek, 2015).

In 2011, the roots to leaves weight ratio (RTLr) achieved its highest value in Magaz (3.58) in comparison to Laguna de Negrillos (1.68) or Villavieja (1.99), which could be readily ascribed to the low weight exhibited by the leaves of the plants at that location due to the presence of nematodes. In 2012, the highest RTLr ratio was attained in Vertavillo (2.83), followed by Villavieja (2.23) and with a significantly lower value for Pampliega (1.43). From this results a positive relationship of RTLr with the carbon content in the root RC and with polarization (AIMCRA 2012), which is in agreement with the findings of Kenter et al. (2006). This positive relationship between RTLr and RC would also be valid for 2011 results with the optimum N fertilization, provided that Magaz results are excluded.

With regard to the variety factor, in 2011 (Dulzata or Sandrina varieties) significant differences in the leaves fresh weight (LFW) and in its ratio with the root fresh weight (RTLr) could be observed, while in the 2012 (Amalia or Sandrina varieties) the significance was reflected in the yield. This yield was higher for Sandrina variety, both in 2011 (96.98 t/ha vs. 95.14 t/ha for Dulzata) and in 2012 (120.80 t/ha vs. 104.45 t/ha for Amalia); and same applied to fresh weight (PFW) both in 2011 (1428.20 g/kg vs. 1288.21 g/kg for Dulzata) and in 2012 (1806.58 g/kg vs. 1579.32 g/kg of Amalia). The exception for RTLr in 2011, as noted above, was a consequence of the nematode infection. On the other hand, the populations which showed higher polarization or sugar/ha contents were always those which cultivated the Amalia variety in comparison

to the Sandrina variety (17.9% vs. 16.28%, respectively, in Vertavillo; 17.73% vs. 16.65% in Villavieja; 17.68% vs. 16.83% in Pampliega; and 18.78% vs. 17.48% in Laguna de Negrillos) (AIMCRA 2012).

In relation to the fertilization factor, in a similar fashion to the trend observed for the variety fashion, significant differences were observed in the leaves fresh weight (LFW), in the total plant fresh weight (PFW) and in the RTL ratio, but not for the yield. The leaf production growth rate is known to be directly dependent on the nitrogen availability for the crop and, furthermore, a clear relationship between the leaves dry weight and the nitrogen concentration in the plant could also be confirmed (Martínez Quesada et al, 2003).

In 2011 it could be observed that the fertilization with higher amounts of nitrogen (2N) led higher values for the parameters derived from fresh weight, except for the RTL, which is reasonable provided that a higher leaves fresh weight decreases the ratio of root to leaves weight. It should be borne in mind that as the nitrogen content increases, the green leaves biomass and the total biomass increase (Manderscheid et al, 2010) and in those situations in which concentrations higher than optimum rates of nitrogen fertilizers were applied, the extra N had little impact on yield (Allison et al, 1996).

4.3.1.2 Carbon content in the roots, dry weight and CO₂

As to the location factor effect on the C content in the root (RC), the highest concentrations were attained in Laguna de Negrillos both in 2011 and in 2012 (44.97 g/kg and 44.63 g/kg, respectively), as it also occurred for the root dry matter content (RDM = 25.13 g/kg in 2011 and 24.36 g/kg in 2012), These concentrations were higher than those obtained in other populations such as Magaz in 2011 or Pampliega in 2012. Therefore, there was a positive relationship between the C content in root (RC) and the dry matter content (RDM) and there was also a positive relationship between RC and the polarization or sucrose content (Kenter et al, 2006).

In 2011, Villavieja was the location in which the highest CO₂ capture took place (TCO₂ = 63.84 CO₂/ha), provided that the higher fresh weight of its plans implied that, in spite of its lower RDM and RC percentages in comparison to Laguna de Negrillos, the total amount of dry matter accumulated was larger and this was determining in the

absorbed CO₂ calculation (summation of the products of the amount of dry matter and the carbon content in each of the three parts of the plant). On the other hand, in 2012, the highest CO₂ assimilation occurred in Pampliega (TCO₂ = 69.42 CO₂/ha) since, as in the previous case, a higher total fresh weight in its plants was obtained due to the contribution of the larger biomass of their leaves.

With reference to the impact of the sugar beet variety, and as regards the amount of dry matter (RDM) in 2012, statistical significance was only verified for Amalia variety vs. Sandrina variety (23.62 vs. 23.11, respectively). In relation to the fertilization factor, no statistical significance was found for any of the parameters related to the root carbon content, dry matter content or CO₂ (RC, RDM and TCO₂).

4.3.1.3 Nitrogen content in the leaves, total nitrogen absorption and carbon to nitrogen ratio

Regarding the location factor and its effect on the nitrogen content in leaves, the total N absorption and the CNR ratio (LN, TN and CNR), the locations where more N absorption took place (i.e., Villavieja-I and Pampliega) led to an increased production in terms of fresh weight. With respect to the N content in leaves (LN), the lowest concentration was found in Laguna de Negrillos in 2011 (1.96 g/kg) and in Vertavillo in 2012 (1.92 g/kg), accompanied by the highest root carbon content in Laguna de Negrillos in 2011 (44.63 g/kg) and in Vertavillo in 2012 (44.10 g/kg). Hence an inverse relationship of the nitrogen content in the leaves (LN) with the root carbon content (RC) and -to some extent- with polarization could be observed. This would be in line with the results of Shock et al (2000), who found a negative relationship between nitrate concentration in petioles and polarization, albeit for only one of the two years of their study. The ratio of the percentage of carbon in root and nitrogen in leaves (CNR) showed a positive relationship with RC and a negative relationship with LN.

With regard to the variety factor, no significant differences in the absorption of nitrogen (TN) could be found, although it is higher for Sandrina variety, both in 2011 (375.95 kg/ha vs. 345.15 kg/ha for Dulzata) and in 2012 (436.64 kg/ha vs. 381.71 kg/ha for Amalia). Nonetheless, significant differences could be found for the leaves nitrogen concentration (LN), which was higher for Sandrina variety both in 2011 (2.20 g/plant vs. 2.16 g/plant for Dulzata) and in 2012 (2.14 g/plant vs. 2.00 g/plant for Amalia).

These results are in agreement with those reported by Hoffmann (2005), which showed a dependence of the leaves nitrogen composition (LN) with the variety. When the CNR ratio between the root carbon content (RC) and the leaves nitrogen content (LN) was studied, it was evinced that it was lower for Sandrina variety both in 2011 (19.88 vs. 21.25 for Dulzata) and in 2012 (20.73 vs. 22.01 for Amalia). Thus, it could be inferred that the varieties which had a lower leaves nitrogen concentration (LN) and a higher CNR ratio were Dulzata and Amalia, that is, the varieties with a higher polarization (sucrose content) according to data from the 2012 campaign (AIMCRA 2012). Therefore, it follows that the varieties with higher polarizations also have a higher carbon content in the root (RC) and higher values of the CNR ratio.

In relation to the fertilization factor, as with the variety factor, there were differences in the concentration of nitrogen in leaves (LN) and in the total amount of absorbed nitrogen (TN). It is known that beet has a high affinity for nitrogen and this makes that, for a greater availability of nitrogen, higher absorption occurs (Martínez Quesada et al, 2003). Both the concentration of nitrogen in leaves (LN) and the nitrogen absorption (TN) increased with higher N fertilizer concentrations (2N vs. N). The CNR coefficient was lower for the 2N fertilizing program, since at that fertilizer lever the denominator (LN) was larger. Again, it could be observed that there was an inverse relationship between the carbon content in the root (RC) and the concentration of nitrogen in the leaves (LN) and, for the optimum fertilization program (N), there was a direct relationship between RC and CNR and a positive relationship between RTLR and RC.

In short, the site factor was the most relevant factor (in comparison to variety or fertilization factors) and the one with the highest significance amongst the set of parameters under study.

4.3.1.4 Tukey's Test

The values in bold in the ANOVA analysis results (see Table 4.6 and Table 4.7) show the main contributions to the significance according to Tukey's HSD *post-hoc* test. It was evinced that in 2011 the significant differences were attributable to the yield parameter in Villavieja vs. Magaz and Laguna de Negrillos. Laguna de Negrillos would be the site that contributes most to the significant differences in the RC, LN and CNR parameters, while Magaz would contribute most to LFW, RTLR and TCO₂. In 2012,

Tukey's HSD test attributed the statistical significance to the differences between Laguna de Negrillos and Villavieja for the Yield parameter. In RC, LN, CNR, RDM and TN, Tukey's test parameters pointed at the differences between Pampliega (P) and Laguna de la Nava (LN-II) (when data was available) as the source of the statistical significance of the site factor.

4.3.2. Principal component analysis

The climatic variables derived from the data collected at the weather stations during the cultivation periods in 2011 and 2012 are shown in Table 4.8. It is worth noting that the length of cultivation period (CP) for the three locations in which the experiments were conducted in 2011 was 190 days on average, due to the fact that the planting date was somewhat late (13th April) in the case of Laguna de Negrillos-I (LN-I), and that differences in the climate variables can also be observed, such as the average temperature and radiation for LN-I during the first 65 days (T1/R4), which was 14.9 °C/1481 MJ·m⁻², higher than the 13.5 °C/1153 MJ·m⁻² registered in Magaz (M) and the 12.2 °C/1240 MJ·m⁻² registered in Villavieja (VV-I). The precipitation in LN-I (182 mm, Table 4.1) was also slightly higher than in Magaz (100 mm) or in Villavieja (134 mm). On the other hand, the cultivation period (CP) in 2012 for the four sites where the experience was repeated (P, LN-II, V and VV-I) was on average 209 days, i.e., slightly longer than in 2011. If the accumulated radiation (R1 to R6) for the different seasons in 2011 and in 2012 is compared, it was almost always higher in 2012, except for Vertavillo (because planting was delayed until late March).

Table 4.8. Results of the calculated climatic variables for the cultivation periods in 2011 and 2012. *LN*: Laguna de Negrillos; *M*: Magaz de Pisuerga; *P*: Pampliega; *V*: Vertavillo; *VV*: Villavieja.

Site	Sowing date (SD), Cultivation Period (CP) and Calculated Meteorological Data														
	SD	Emergence d (°C·d)	VP d	R1 MJ·m ⁻²	R2 MJ·m ⁻²	R3 MJ·m ⁻²	R4 MJ·m ⁻²	R5 MJ·m ⁻²	R6 MJ·m ⁻²	T1 °C	T2 °C	T3 °C	GDD °C·d	GDD1 °C·d	GDD2 °C·d
<i>2011</i>															
M	23.03	-	190	-	1595	2530	1153	506	285	13.49	13.97	1.5	3249	-	2049
LN-I	13.04	-	180	-	1853	2459	1481	457	84	14.85	15.7	-0.3	3048	-	1848
VV-I	10.03	-	201	-	1840	2839	1240	524	546	12.21	13.4	1.7	3412	-	2212
<i>2012</i>															
P	16.03	21 (185)	206	4297	2118	2544	1166	376	500	9.6	12.1	0.7	3207	3025	2007
LN-II	21.03	23 (205)	203	4286	2100	2584	1279	363	428	10.58	12.7	0.1	3160	2955	1960
V	26.03	25 (210)	191	3557	1873	2076	1183	447	207	10.49	12.9	1.2	2982	2772	1782
VV-II	05.03	22 (152)	226	4460	2082	2771	1056	312	835	8.38	12	1.2	3593	3430	2393

In subsections 0 and 0, the variables subject to PCA for each of the conducted assays are displayed together with the generated graphs and their rotated components loadings and commonalities, that is, the percentage of variance explained by the components (Loel and Hoffmann, 2014).

As a consistent research criterion, we have resorted to a 3D representation from the principal component analysis, through segregation in clusters. In the three graphs labelled as PCA1a (2011), PCA2a and PCA2b (2012), corresponding to Figure 4.2 and Figure 4.7, it is possible to observed the organization of the initial data, and the aggregates or clusters corresponding to an adequate sample selection of the sites chosen for the study in 2011 and 2012 can be easily identified. For a better understanding of the results, these have been reported separately for each year of study.

4.3.2.1. 2011

The 3D graph corresponding to PCA1a is shown in Figure 4.2. Component 1 is positively correlated with crop growth parameters (PFW, Yield, RDW and TNplant), the second component shows a strong relationship with cumulative radiation climatic variables R and R3 and the third component has the highest correlations for nitrogen content in the leaves (LN) –positive correlation- and for carbon content in roots (RC) – negative correlation-.

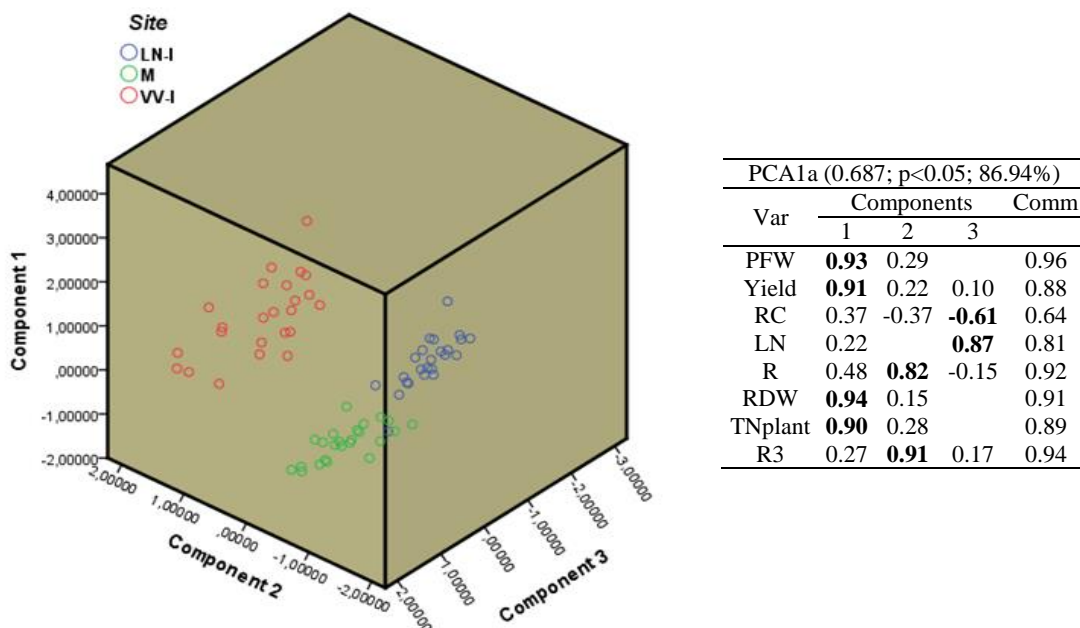


Figure 4.2. 3D plot (left) and summary table of the PCA analysis for 2011.

Eight bivariate plots in rotated space for 2011 (Figure 4.3, Figure 4, Figure 4.5 and Figure 4.6) show the relationship between components. PFW, Yield, RC, LN, R, RDW and TN were fixed and then calculated radiation variables (R2, R4, R5 and R6), temperature variables (T2 and T3) and thermal time (GGD and GGD2) were sequentially tested. For all the analyses, component 1 was correlated with PFW, Yield, R, RDW and TN (all of which have to do with the growing process of plants). Component 2 was influenced by RC, LN and the calculated climate variable chosen on each instance.

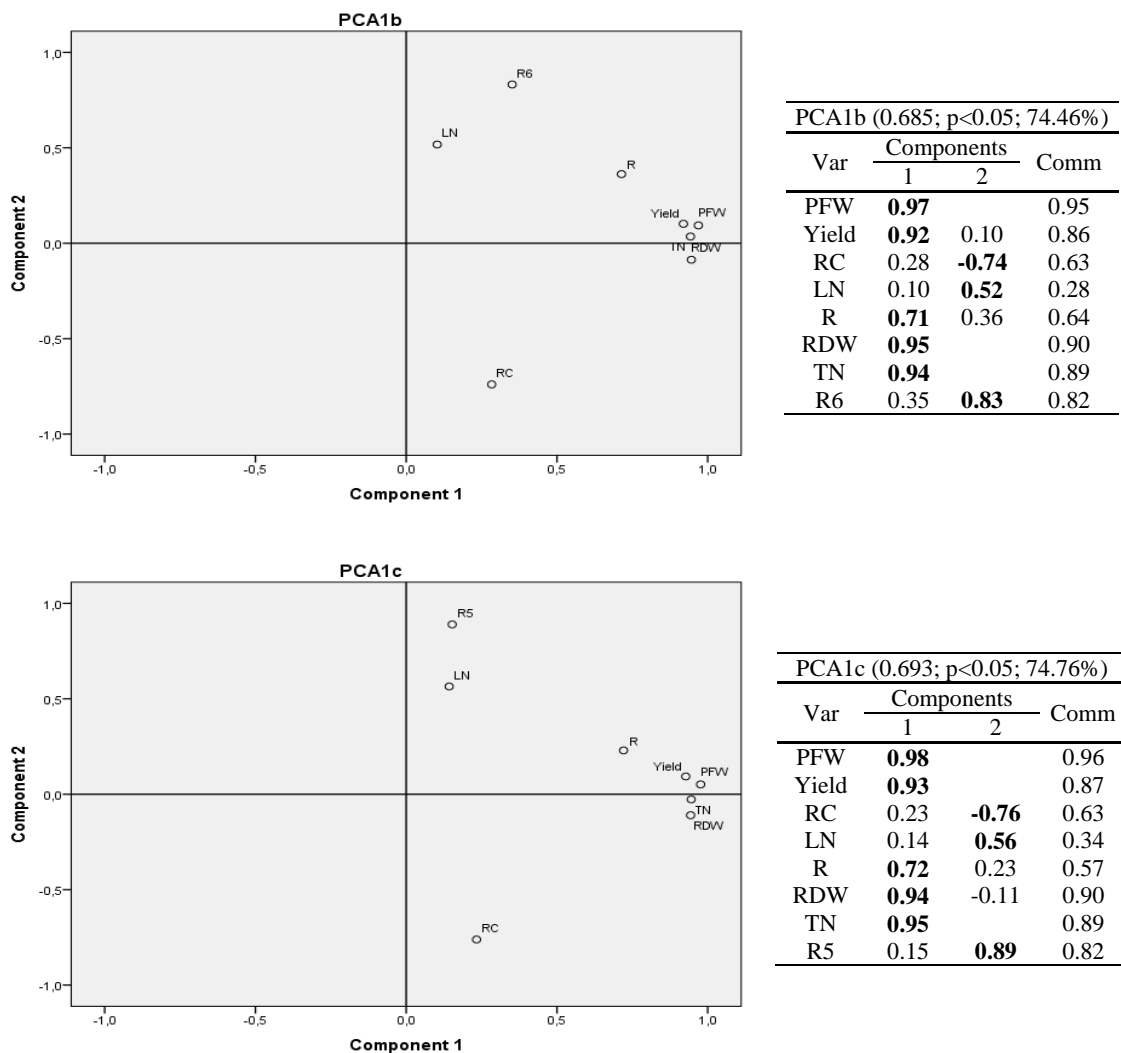


Figure 4.3. 2D plots and summary tables for PCA1b (top) and PCA1c (bottom) analyses, year 2011. *Var* stands for variables and *Comm* stands for commonalities.

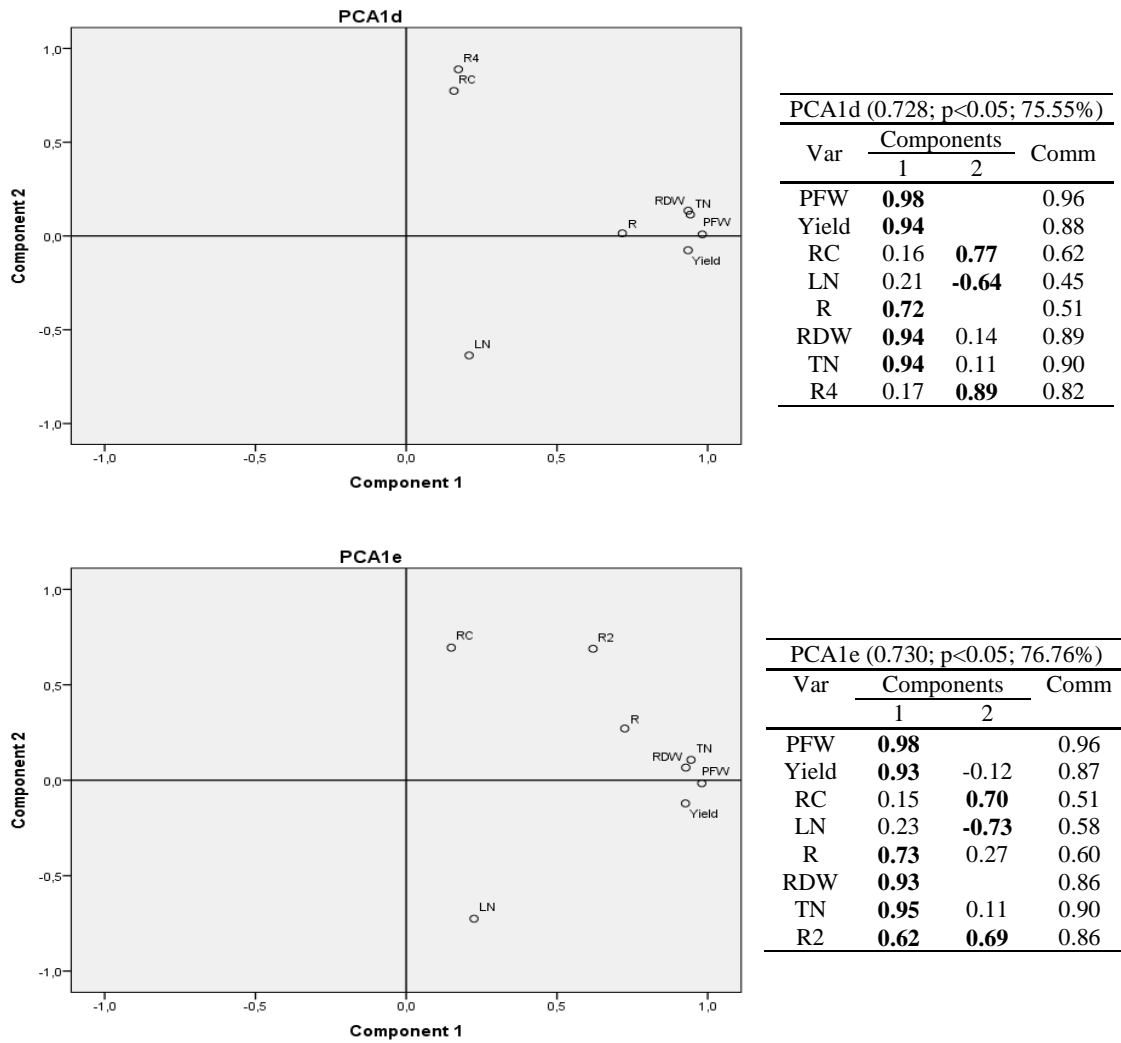


Figure 4.4. 2D plots and summary tables for PCA1d (*top*) and PCA1e (*bottom*) analyses, year 2011.

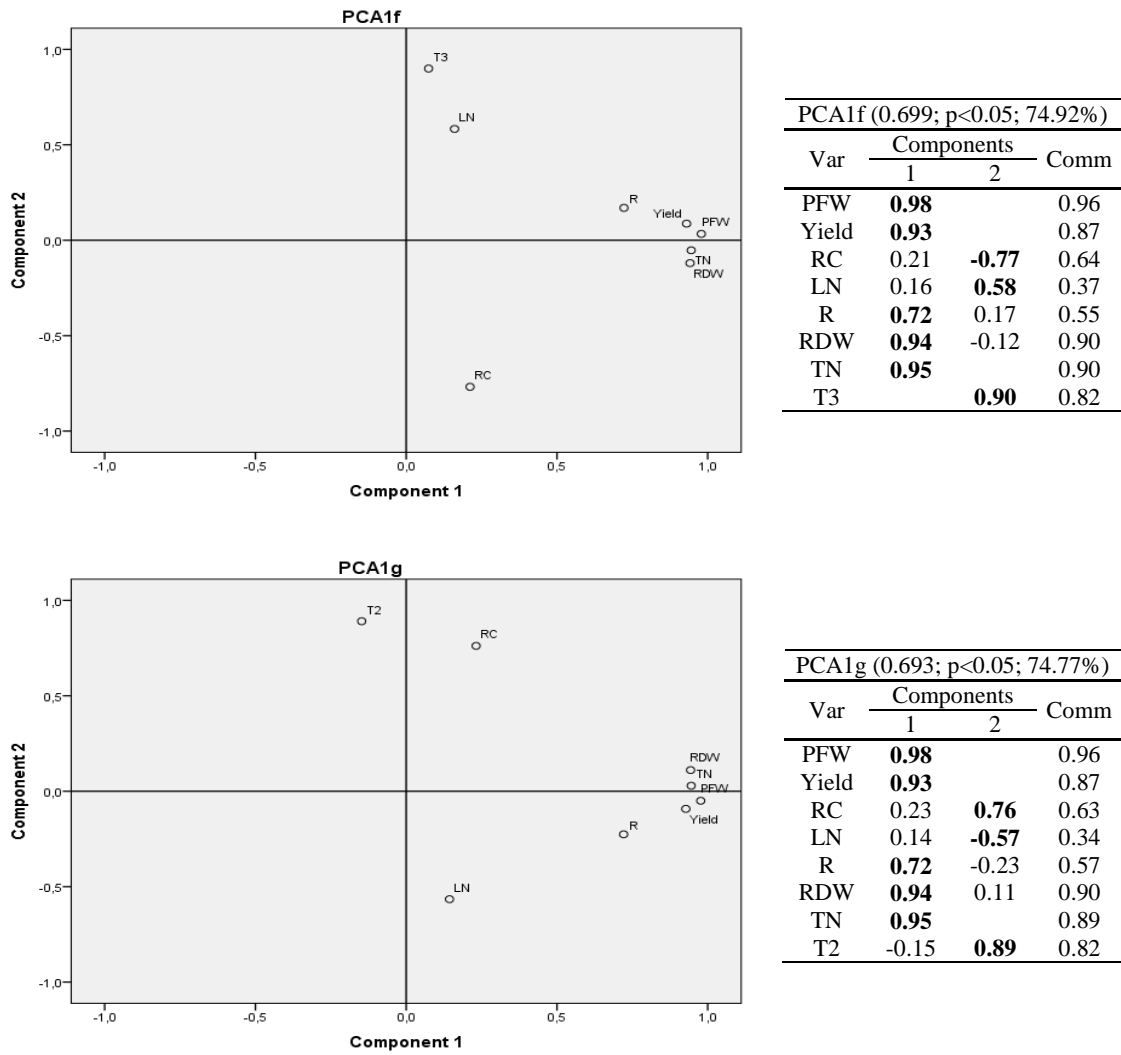


Figure 4.5. 2D plots and summary tables for PCA1f (*top*) and PCA1h (*bottom*) analyses, year 2011.

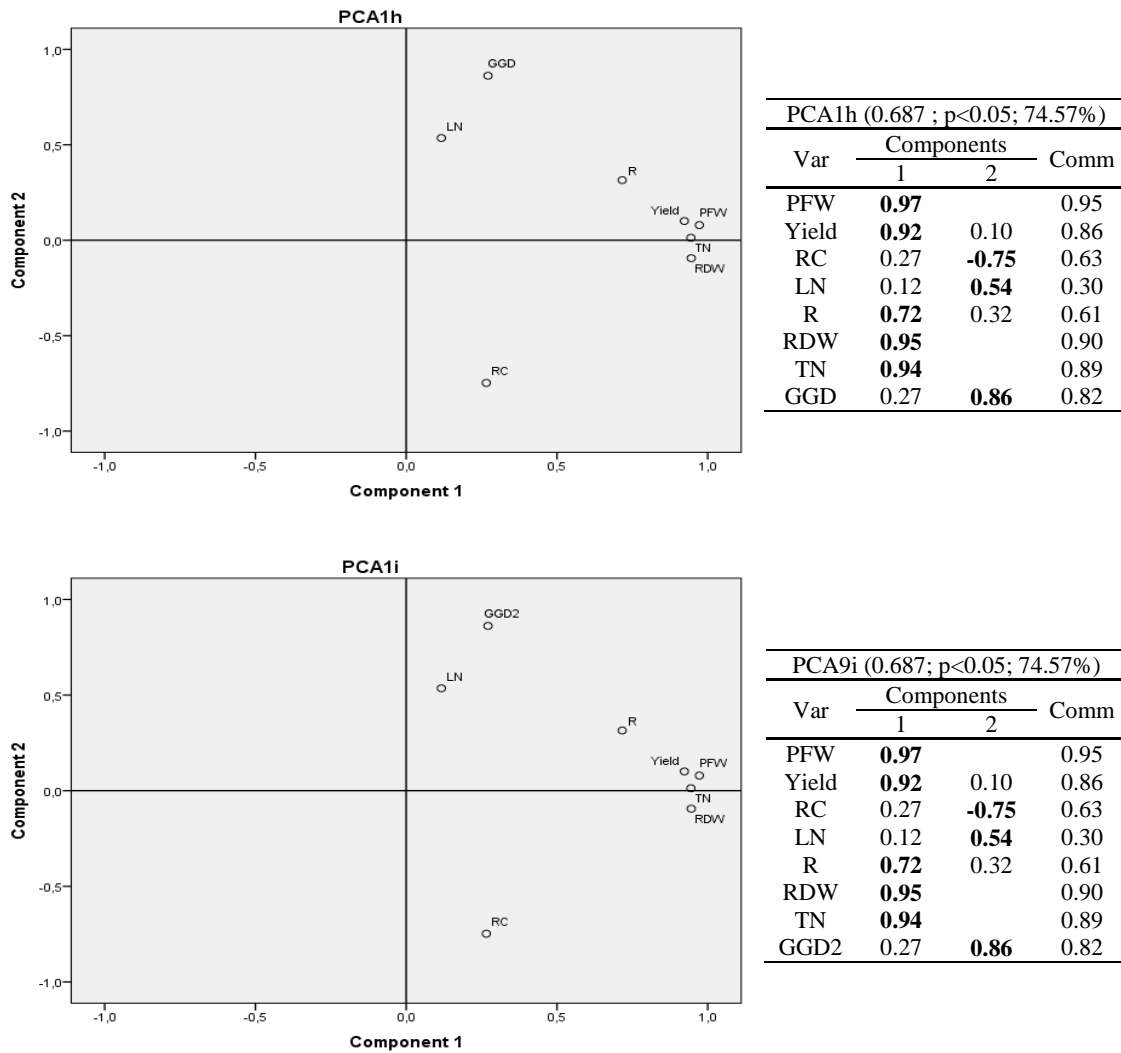


Figure 4.6. 2D plots and summary tables for PCA1h (*top*) and PCA1i (*bottom*) analyses, year 2011.

In brief, all the plots showed that the variables of component 1 were close together and hence very highly correlated. Again, it is noteworthy that there was an inverse relationship between LN and RC. RC had a positive correlation with R2, R4 and T2 (same for T1, not shown) and a negative correlation with R6, R5, T3, GGD and GGD2. Thus, the higher the average temperature in the first stage of growth up to 1200 °C·d (T2) and the radiation accumulated in the first 65 days (R4) were, the higher the percentage of carbon in the root was. We may also notice that R2, the accumulated radiation up to 1200 °C·d a.s. has virtually the same weight in the two components with a positive correlation with RC and crop parameters. However, it can be observed that the larger the accumulated radiation in the last phase of cultivation was, for example the

last 25 days or from the day 175 onwards, the lower the carbon concentration was. The same behavior occurred with T3, that is, the greater the deviation from the mean optimum temperature of 18 °C in the stage after 1200 °C·d was, the lower the carbon content in the root was.

GGD and GGD2 variables, i.e. the total thermal time after planting and the accumulated thermal time from 1200 °C·d till harvest, showed a positive relationship with the nitrogen content in leaves and a negative correlation with the carbon content in root. This may be related to a slight trade-off between production and polarization, in which increased levels of assimilable nitrogen in the soil increase performance in terms of root weight but decrease the richness of sugar (Gordo-Ingelmo, 1994) and increase the unusable compounds (Ouda, 2002).

4.3.2.2. 2012

A 3D graph corresponding to the 4 sites or PCA2a is shown in Figure 4.7(*top*). Since it includes Laguna de Negrillos (LN-II), no variables related to leaves could be used. Conversely, Figure 4.7(*bottom*) or PCA2b only includes 3 sites (LN-II was excluded), but variables related to leaves were considered.

In Figure 4.7(*top*), the first component again consisted of variables related to plant growth (RFW, RDW, Yield, RNplant and RCplant) and the other two components were determined by climatic variables (R1, R6, T3) together with the root carbon content (CR). When only three sites were considered (Figure 4.7 *bottom*), the first component consisted of variables related to plant growth (RFW, RDW, Yield and TN) the other two components were associated to climatic variables (T3, R6) and the nitrogen content in leaves (LN).

In comparison to the previous year, it could be observed that in 2012 the weight of RC and its commonality value in all analyses was lower, so the possible relationships with other variables of study were attenuated. Again, in PCA2a a negative relationship between RC and T3 was observed and, when data of the variables related to leaves were excluded in PCA2b, a positive relationship between LN and T3 also appeared.

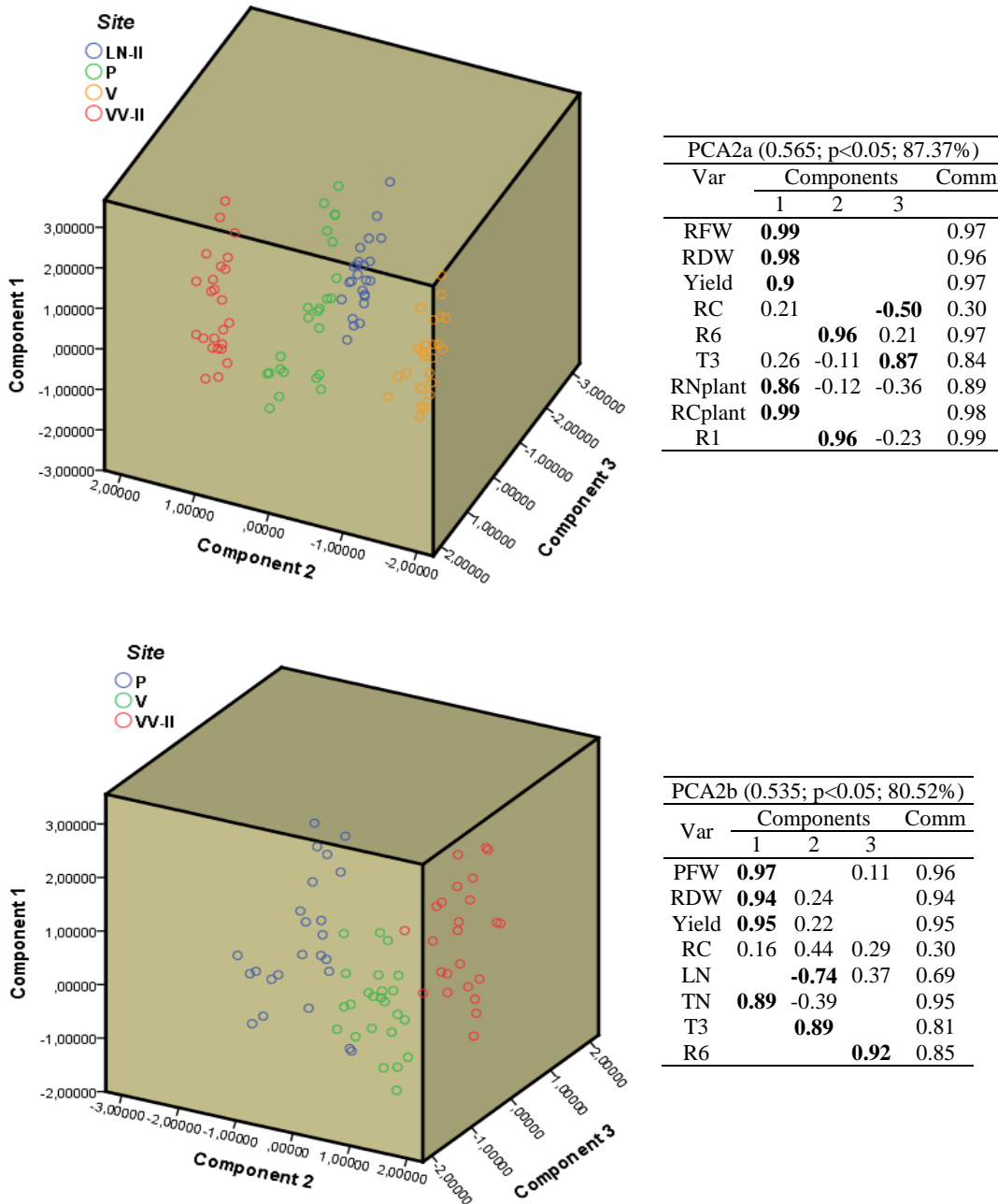


Figure 4.7. Top: 3D plot and summary table of PCA analysis for 2012 for all the sites. Parameters related to leaves have been excluded. Bottom: 3D plot and summary table of PCA analysis for 2011 and three sites (Laguna de Negrillos has been excluded). All parameters have been included.

When the 2D graphics shown below were analysed, it was possible to observe that in PCA2c and PCA2d (Figure 4.8), which include the four locations, a negative relationship of RC with T3 and a positive relationship with T2 (same for T1, not shown) appeared, as it also happened for 2011 data. In PCA2c the weight RC was lower than 50%, but it showed the same trend between RC and T3. Nonetheless, the low commonality of RC weakened this possible relationship between these parameters.

In PCA2e, in which all variables (for only three sites) were considered (Figure 4.9, *top*) a significant positive correlation between LN and R6 was again detected, and in PCA2f (Figure 4.9, *bottom*) a positive correlation between RC and T2 (T1) was once more found. In this case, LNplant contributes to the two components, since it is related to both crop parameters and nitrogen concentration; the latter is evinced as a negative correlation with T2 (T1) and RC. Consequently, the results were consistent with those obtained in the 2011 campaign.

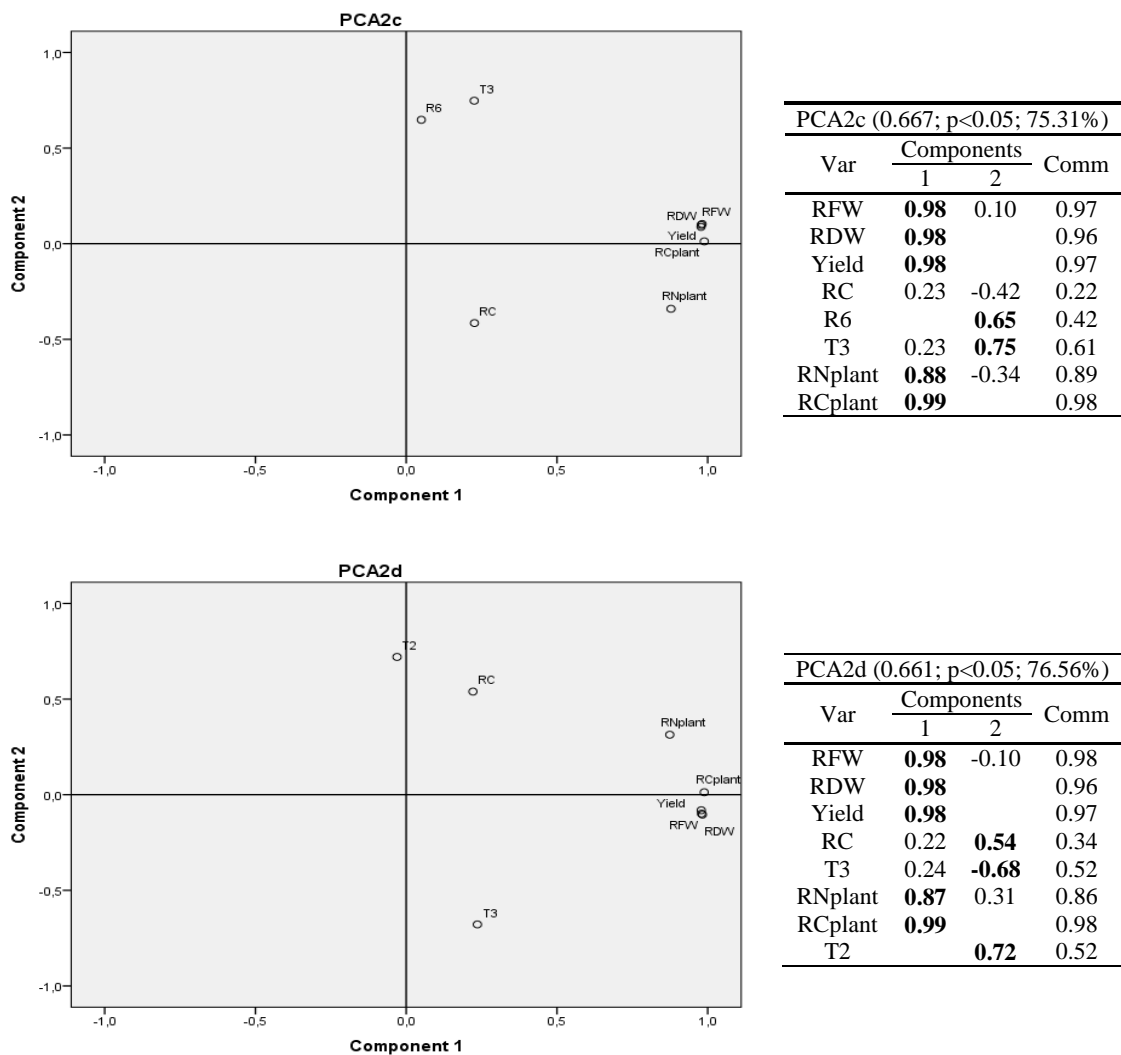


Figure 4.8. 2D plots and summary tables for PCA2c (top) and PCA2d (bottom) analyses in 2012. All parameters have been included. Laguna de Negrillos has been excluded.

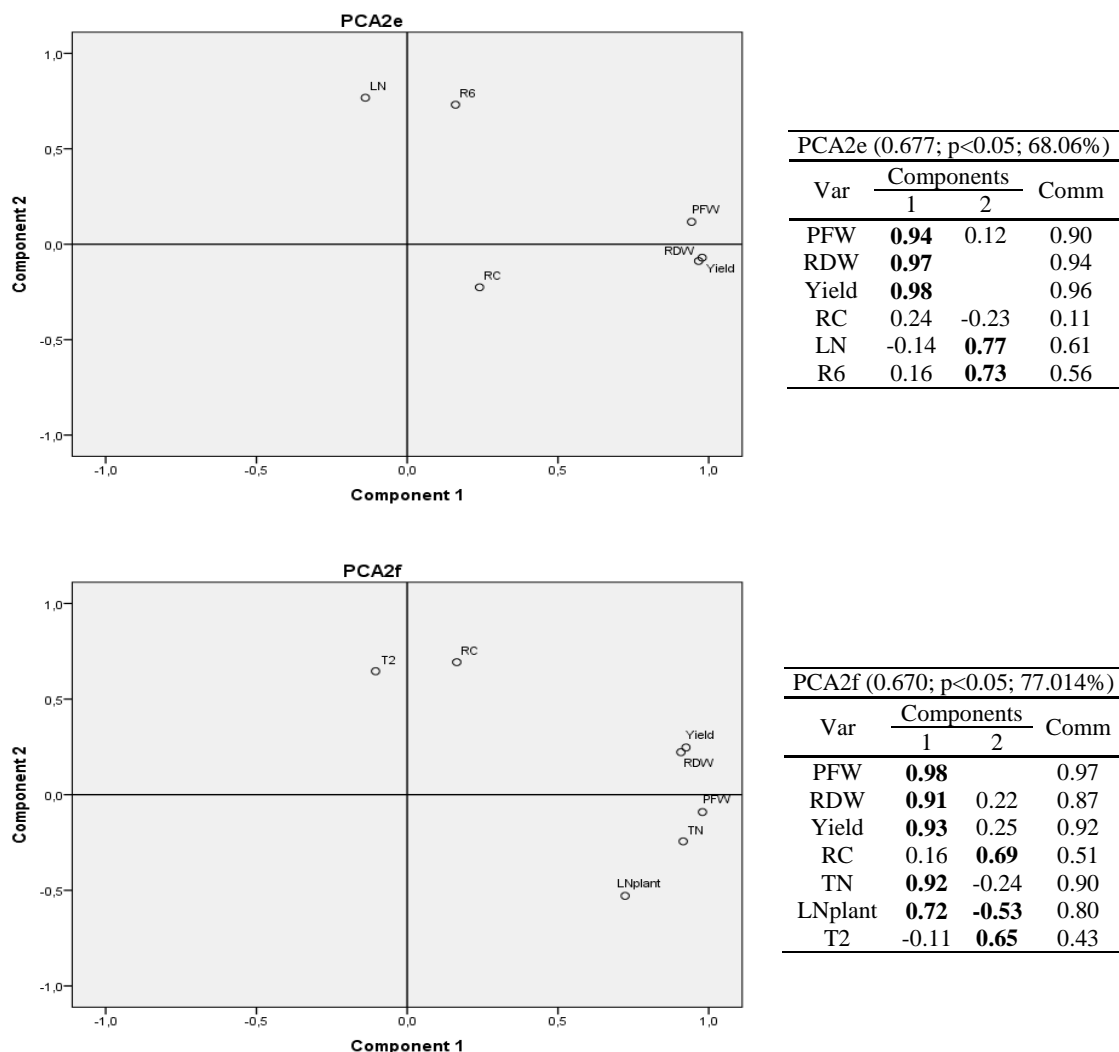


Figure 4.9. 2D plots and summary tables for PCA2e (top) and PCA2f (bottom) analyses in 2012. All parameters have been included. Laguna de Negrillos has been excluded.

In the two campaigns, in 2011 and 2012, there was a positive relationship between the carbon content in the root (RC) and T2 (T1), R2 and R4, and a negative relationship with R6 and T3. The former positive relationship between the root carbon content and the average temperature and the accumulated radiation in the first phase of cultivation is in agreement with the results of Hoffmann et al. (2005), who stated that the decisive time in the growing season for quality formation of sugar beet is the early growth until June. The later negative relationship between RC and the accumulated radiation in the last stage (175 a.s. onwards, R6) would be explained by the fact that a higher radiation dose would promote a maintenance of vegetative development with a greater leaf development Tabourel-Tayot et al. (1998).

4.3.3. Final Remarks

In the study presented herein it has been confirmed that, in agreement with Kenter et al. (2006), the growth of sugar beet, its root composition and its carbon content are influenced by the climatic and edaphological of each cultivation site and by the specific conditions of each campaign, concluding that the location factor would have more influence than the plant variety or fertilization, since it the factor that has the highest significant differences for the various treatments.

A comparative analysis of the carbon content in root (RC) and the dry matter content (RDM) evinced that there is a positive relationship between the two parameters, so that a higher carbon content leads to a higher percentage of dry matter, and that there is also a positive relationship between RC and the sucrose content or polarization.

The application of twice the recommended dose of N fertilizer had an influence on the parameters derived from the quantity of fresh matter, in particular for leaves, while the choice of the sugar beet variety led to significant differences in the concentration of nitrogen in leaves and in the carbon content in root to nitrogen content in leaves ratio.

It may also be inferred that that the percentage of root carbon is linked to the relative composition of sucrose, marc (cellulose, hemicellulose and lignin) and other components. The data over the two campaigns showed a higher root carbon content (RC) in those locations with higher polarization or sucrose content, higher dry matter percentage (RDM) and therefore higher amount of marc, and a positive relationship of the root to leaves ratio (RTL) with RC and the polarization ratio.

In this regard, Hoffmann et al. (2005) suggested that the positive correlation between sucrose concentration and marc could be explained by thicker cell walls, smaller cells and/or more cells, which may influence the proportion of carbon in root tissues. It is also worth noting that a compound with high carbon content, such as betaine, is related to sucrose storage, so that the higher the concentration of sucrose, the higher concentration of betaine and the higher carbon content (Kenter et al. (2006) and Hoffmann et al. (2005)).

The principal component analysis (PCA) of the various climatic variables calculated for the different areas and periods of cultivation and the parameters of the plant measured at harvest showed a clear segregation of the data in clusters, indicating the specificity of each area and the influence of climate factors on beet growth.

It can also be stated that there is a positive relationship between the carbon content in the root and the average temperature and accumulated radiation in the first phase of cultivation, since the decisive time for quality formation of sugar beet are the early growth stages (Hoffmann et al, 2005). A negative relationship between carbon content and the radiation accumulated in the last stages of cultivation was also detected. The explanation for this effect is linked to the fact that crop growth rate declines in autumn due to decreasing radiation or temperature with leaves senescence (Milford et al. (1973) and Martínez Quesada et al (2003)), which causes a movement of assimilates towards the root. In this process the availability of nitrogen for the plant also has an influence, because its shortage prevents further development of new tissues, with a subsequent increase in leaf senescence, allowing accumulation of assimilates in the root. Therefore, greater radiation and/or availability of nitrogen in the last stage of the cultivation can stop senescence and promote the birth of new leaves, consuming assimilates from the root.

In the same line, an inverse relationship between the nitrogen content in the leaves with the carbon content in root (and to some extent with the polarization) could also be observed, in agreement with Shock et al. (2000) previously mentioned, with Pocock et al. (2009), who reported that late additions or releases of nitrogen from soil organic matter reduce the sucrose content, and with Draycott et al. (2003) and Malnou et al. (2008), who indicated that an amount of nitrogen above the optimum has a negative effect on sugar yield. Gordo-Ingelmo (1994) explained that beet reacts to nitrogen fertilization increases with a greater development of the leaves and roots, which can cause excessive consumption of sucrose and an increase of non-sugars. This happens in particular for excessive organic fertilizer additions, in which some of the nitrogen is released belatedly, causing a stop on the maturity of the root. Consequently, the lower polarization and carbon content in root for the assays conducted in Pampliega in the second year, with the highest content of organic matter, would be associated to a delayed release of nitrogen, which would explain the fact that the crops had the highest leaves weight and the highest nitrogen absorbed per hectare.

The average carbon content in dry matter of root were 43.40 g/kg in the first year and 43.74 g/kg in the second campaign. However, the total amount of fixed CO₂ not only depends on the dry matter percentage and its carbon content, but mainly on the total amount of dry matter that the plant has formed, and it increases with increasing

fresh weight. Therefore, it can be inferred that –in general terms- the higher the fresh weight of the plant is, the higher CO₂ capture will be. In the first year, Villavieja was the location in which most CO₂ assimilation occurred due to its larger sugar beet harvest, whereas in the second year, the highest total leaves fresh weight and total biomass were attained in the town of Pampiega, in spite of the fact that the yield was not the highest.

4.4. CONCLUSIONS

The impact of climatic variables on the growth and carbon contents of spring sown sugar beet (*Beta vulgaris saccharifera*) in Castilla y Leon region (north-western Spain) was assessed by analysing 34 beet crop parameters at three sites in 2011 and at four sites in 2012. An ANOVA analysis allowed to discern the factors that were more influenced by location, crop variety and type of fertilization, and the specific conditions of each campaign, concluding that location was the most important factor. Fertilization treatments had a significantly impact on the parameters derived from the quantity of fresh material (leaves), while the beet variety choice influenced the amount of nitrogen in leaves and the carbon to nitrogen ratio. It could also be inferred that the root carbon content depended mostly on the location and that a higher root carbon content led to a higher content of dry matter, with a positive relationship with the sucrose content for the two types of varieties which were tested. Principal Component Analysis distinguished the climatic factors that influenced most each cultivation area in each campaign and provided a clear separation of the data in clusters, specifically showing the uniqueness of each site. It followed that in each area of study, the root carbon content was directly dependent on the average temperature in the first stage of growth up to 1200 °C·d and on the cumulative radiation in the first 65 days, while a higher the cumulative radiation during the last stage of cultivation led to a decrease in carbon concentration.

4.5. ACKNOWLEDGEMENTS

L.F. Sánchez-Sastre would like to acknowledge the financial support of Universidad de Valladolid through “Ayudas a la Contratación de Personal Investigador de Reciente Titulación (2009-2013)” scholarship program, co-funded by the Education Department of Junta de Castilla y León regional government and the European Social Fund.

4.6. REFERENCES

- AIMCRA, Memoria campaña 2012/2013 siembra primavera 2012, in, AIMCRA, Valladolid, Spain, 2012, pp. 124.
- AIMCRA, Plan 2020 para la sostenibilidad de la remolacha azucarera, Revista AIMCRA, 120 (2015) 29-31.
- AIMCRA, Recomendaciones de cultivo: zona norte, in, 2015.
- Allison, M.F., Armstrong, M.J., Jaggard, K.W., Todd, A.D., Milford, G.F.J. (1996). An analysis of the agronomic, economic and environmental effects of applying N fertilizer to sugarbeet (*Beta vulgaris*), *The Journal of Agricultural Science*, 127 (1996) 475.
- Bell, C.I., Milford, G.F.J., Leigh, R.A. (1996). Sugar beet, in: E. Zamski, A.A. Schaffer (Eds.) *Photoassimilate distribution in Plants and crops: source-sink relationships*, Marcel Dekker Inc., New York, 1996, pp. 691-707.
- Boiffin, J., Durr, C., Fleury, A., Marin-Laflèche, A., Maillet, I. (1992). Analysis of the variability of sugar beet (*Beta vulgaris* L) growth during the early stages. I. Influence of various conditions on crop establishment, *Agronomie*, 12 (1992) 515-525.
- Burkart, S., Manderscheid, R., Weigel, H.J. (2009). Canopy CO₂exchange of sugar beet under different CO₂concentrations and nitrogen supply: results from a free-air CO₂enrichment study, *Plant Biol.*, 11 (2009) 109-123.
- Carvajal, M., Mota, C., Alcaraz-López, C., Iglesias, M., Martínez-Ballesta, M.C. (2009) Investigación sobre la absorción de CO₂ por los cultivos más representativos, in, Consejo Superior de Investigaciones Científicas, Murcia, Spain, 2009.
- Clover, G.R.G., Jaggard, K.W., Smith, H.G., Azam-Ali, S.N. (2001). The use of radiation interception and transpiration to predict the yield of healthy, droughted and virus-infected sugar beet, *The Journal of Agricultural Science*, 136 (2001) 169-178.
- Crutzen, P.J., Mosier, A.R., Smith, K.A., Winiwarter, W. (2008). N₂O release from agro-biofuel production negates global warming reduction by replacing fossil fuels, *Atmospheric chemistry and physics*, 8 (2008) 389-395.

- Demmers-Derks, H., Mitchell, R.A.C., Mitchell, V.J., Lawlor, D.W. (1998). Response of sugar beet (*Beta vulgaris* L.) yield and biochemical composition to elevated CO₂ and temperature at two nitrogen applications, *Plant, Cell and Environment*, 21 (1998) 829-836.
- Derscheid, L.A., Lytle, W.F. (1981). Growing degree days (GDD), in, Cooperative Extension Service, South Dakota State University, South Dakota, USA, 1981, pp. 4.
- Draycott, A.P., Christenson, D.R. (2003). Nutrients for sugarbeet production: soil-plant relationships, CABI Publishing, Wallingford, Oxfordshire, England, 2003.
- Echevarría Ruiz de Vargas, C., Feria Bourrellier, A.B., Terencio Jiménez, E. (2005). Conceptos generales del metabolismo y del transporte de sacarosa, in: Aspectos fisiológicos de la remolacha de siembra otoñal, Junta de Andalucía, Consejería de Agricultura y Pesca, Sevilla, Spain, 2005, pp. 11-22.
- Fabeiro, C., Martín de Santa Olalla, F., López, R., Domínguez, A. (2003). Production and quality of the sugar beet (*Beta vulgaris* L.) cultivated under controlled deficit irrigation conditions in a semi-arid climate, *Agric. Water Manage.*, 62 (2003) 215-227.
- Freckleton, R.P., Watkinson, A.R., Webb, D.J., Thomas, T.H. (1999). Yield of sugar beet in relation to weather and nutrients, *Agricultural and Forest Meteorology*, 93 (1999) 39-51.
- Gardner, F.P., Pearce, R.B., Mitchell, R.L., (1985) Carbon fixation by crop canopies, in: *Physiology of crop plants*, Iowa State University Press, Iowa, USA, 1985, pp. 31-57.
- Giaquinta, R.T. (1979). Sucrose Translocation and Storage in the Sugar Beet, *Plant Physiol.*, 63 (1979) 828-832.
- Gordo-Ingelmo, L.F. (1994). Composición química y control agrícola de los no-azúcares en la remolacha azucarera, Caja de Ahorros Municipal de Burgos, Burgos, Spain, 1994.
- Gordo, L.F., Morillo-Velarde, R., Martínez, J.J., S. García-Mauriño, E.C. (2005). Crecimiento y desarrollo de la remolacha azucarera de siembra otoñal, in:

- Aspectos fisiológicos de la remolacha de siembra otoñal, Junta de Andalucía, Consejería de Agricultura y Pesca, Sevilla, Spain, 2005, pp. 23-44.
- Grzebisz, W., Szczepaniak, W., Pepliński, K., Barłóg, P., Cyna, K. (2012). Impact of nitrogen concentration variability in sugar beet plant organs throughout the growing season on dry matter accumulation patterns, *Journal of Elementology*, (2012).
- Harrigan, G.G., Goodacre, R. (2003). *Metabolic profiling: its role in biomarker discovery and gene function analysis*, Springer US, New York, USA, 2003.
- Hoffmann, C.M. (2005). Changes in N Composition of Sugar Beet Varieties in Response to Increasing N Supply, *Journal of Agronomy and Crop Science*, 191 (2005) 138-145.
- Hoffmann, C.M., Kenter, C., Bloch, D. (2005). Marc concentration of sugar beet (*Beta vulgaris* L) in relation to sucrose storage, *J. Sci. Food Agric.*, 85 (2005) 459-465.
- Hoffmann, C.M., Kluge-Severin, S. (2010). Light absorption and radiation use efficiency of autumn and spring sown sugar beets, *Field Crops Res.*, 119 (2010) 238-244.
- Hoffmann, C.M. (2011), Kluge-Severin, S. (2011). Growth analysis of autumn and spring sown sugar beet, *European Journal of Agronomy*, 34 (2011) 1-9.
- Hull, R., Webb, D.J. (1970). The effect of sowing date and harvesting date on the yield of sugar beet, *The Journal of Agricultural Science*, 75 (1970) 223.
- IPCC, *Climate Change 2014: Synthesis Report*, in: *Fifth Assessment Report of the Intergovernmental Panel on Climate Change*, IPCC, Geneva, Switzerland, 2014, pp. 151.
- Jaggard, K.W., Clark, C.J.A., Draycott, A.P. (1999). The weight and processing quality of components of the storage roots of sugar beet (*Beta vulgaris* L), *J. Sci. Food Agric.*, 79 (1999) 1389-1398.
- Jaggard, K.W., Dewar, A.M., Pidgeon, J.D. (1998). The relative effects of drought stress and virus yellows on the yield of sugarbeet in the UK, 1980–95, *The Journal of Agricultural Science*, 130 (1998) 337-343.
- Jiménez, E.T., García-Mauriño, S., Morillo-Velarde, R., Echevarría, C. (2005). *Actividades enzimáticas de degradación de la sacarosa producción de azúcares*

- reductores en la remolacha de siembra otoñal, in: Aspectos fisiológicos de la remolacha de siembra otoñal, Junta de Andalucía, Consejería de Agricultura y Pesca, Sevilla, Spain, 2005, pp. 45-69.
- Kenter, C., Hoffmann, C.M., Märlander, B. (2006). Effects of weather variables on sugar beet yield development (*Beta vulgaris* L.), *European Journal of Agronomy*, 24 (2006) 62-69.
- Kiyamaz, S., Ertek, A. (2015). Yield and quality of sugar beet (*Beta vulgaris* L.) at different water and nitrogen levels under the climatic conditions of Kırşehir, Turkey, *Agric. Water Manage.*, 158 (2015) 156-165.
- Klenk, I., Landquist, B., Ruiz de Imaña, O. (2012). The Product Carbon Footprint of EU Beet Sugar. Summary of Key Findings, *Sugar Industry Journal*, 137 (2012) 169-177.
- Loel, J., Hoffmann, C.M. (2014). Importance of growth stage and weather conditions for the winter hardiness of autumn sown sugar beet, *Field Crops Res.*, 162 (2014) 70-76.
- MAGRAMA, in, Ministry of Agriculture, Food and Environment of Spain, 2014.
- Malnou, C.S., Jaggard, K.W., Sparkes, D.L. (2006). A canopy approach to nitrogen fertilizer recommendations for the sugar beet crop, *European Journal of Agronomy*, 25 (2006) 254-263.
- Malnou, C.S., Jaggard, K.W., Sparkes, D.L. (2008). Nitrogen fertilizer and the efficiency of the sugar beet crop in late summer, *European Journal of Agronomy*, 28 (2008) 47-56.
- Manderscheid, R., Pacholski, A., Weigel, H.J. (2010). Effect of free air carbon dioxide enrichment combined with two nitrogen levels on growth, yield and yield quality of sugar beet: Evidence for a sink limitation of beet growth under elevated CO₂, *European Journal of Agronomy*, 32 (2010) 228-239.
- Martínez Quesada, J.J., Morillo Velarde, R., Aguilera García, Y., Infante Vázquez, J.M. (2003). Growth of Sugar Beet Under Limited Nitrogen Conditions, in: *Sugar Beet Growth and Growth Modelling. Advances in Sugar Beet Research*, Institut International de Recherches Betteravieres, Brussels, Belgium, 2003, pp. 33-45.

- McKendry, P. (2002) Energy production from biomass (part 1): overview of biomass, *Bioresour. Technol.*, 83 (2002) 37-46.
- Monteith, J.L., Moss, C.J. (1977). Climate and the Efficiency of Crop Production in Britain [and Discussion], *Philosophical Transactions of the Royal Society B: Biological Sciences*, 281 (1977) 277-294.
- Milford, G.F.J. (1973). The growth and development of the storage root of sugar beet, *Ann. Appl. Biol.*, 75 (1973) 427-438.
- Milford, G.F.J., Houghton, B.J. (1999) An analysis of the variation in crown size in sugar-beet (*Beta vulgaris*) grown in England, *Ann. Appl. Biol.*, 134 (1999) 225-232.
- Milford, G.F.J., Pocock, T.O., Jaggard, K.W., Biscoe, P.V., Armstrong, M.J., Last, P.J., Goodman, P.J. (1985). An analysis of leaf growth in sugar beet IV. The expansion of the leaf canopy in relation to temperature and nitrogen, *Ann. Appl. Biol.*, 107 (1985) 335-347.
- Milford, G.F.J., Pocock, T.O., Riley, J. (1985). An analysis of leaf growth in sugar beet I. Leaf appearance and expansion in relation to temperature under controlled conditions, *Ann. Appl. Biol.*, 106 (1985) 163-172.
- O'Rourke, N., Psych, R., Hatcher, L. (2013). A step-by-step approach to using SAS for factor analysis and structural equation modeling, 2 ed., SAS Institute, Cary, North Carolina, USA, 2013.
- Ouda, M.M.S (2002). Effect of nitrogen and sulphur fertilizers levels on sugar beet in newly cultivated sandy soil, *Zagazig J. Agric. Res.* , 29 (2002) 33-50.
- Pocock, T.O., Milford, G.F.J., Armstrong, M.J. (2009). Storage root quality in sugarbeet in relation to nitrogen uptake, *The Journal of Agricultural Science*, 115 (2009) 355.
- Pérez López, C. (2004). Técnicas de análisis multivariante de datos: aplicaciones con SPSS, Pearson Educación, Madrid, Spain, 2004.
- Petkeviciene, B. (2009) The effects of climate factors on sugar beet early sowing timing, *Agron. Res*, 7 (2009) 436-443.

- Rinaldi, M., Vonella, A.V. (2006). The response of autumn and spring sown sugar beet (*Beta vulgaris* L.) to irrigation in Southern Italy: Water and radiation use efficiency, *Field Crops Res.*, 95 (2006) 103-114.
- Scott, R., Jaggard, K. (1993). Crop physiology and agronomy, in: *The sugar beet crop*, Springer, The Netherlands, 1993, pp. 179-237.
- Shock, C.C., Seddigh, M., Saunders, L.D., Stieber, T.D. Miller, J.G. (2000). Sugarbeet nitrogen uptake and performance following heavily fertilized onion, *Agron. J.*, 92 (2000) 10-15.
- Smith, P., Martino, D., Cai, Z., Gwary, D., Janzen, H, Kumar, P., McCarl, B., Ogle, S., O'Mara, F., Rice, C., Scholes, B., Sirotenko, O. (2007) Agriculture, in: *Climate Change 2007, Mitigation of Climate Change WGIII - IPCC Fourth Assessment Report*, Intergovernmental Panel on Climate Change, Geneva, Switzerland, 2007, pp. 498-540.
- Tabourel-Tayot, F., Gastal, F. (1998). MecaNiCAL, a supply–demand model of carbon and nitrogen partitioning applied to defoliated grass: 2. Parameter estimation and model evaluation, *European journal of agronomy*, 9 (1998) 243-258.
- Taiz, L., Zeiger, E., Moller, I.M., Murphy, A. (2015). *Plant Physiology*, 6 ed., Sinauer Associates Inc., Sunderland, MA, USA, 2015.
- Tanner, C.B., Sinclair, T.R. (1983). Efficient water use in crop production: research or re-search?, in: H.M. Taylor, W.R. Jordan, T.R. Sinclair (Eds.) *Limitations to efficient water use in crop production*, American Society of Agronomy Madison, WI, Madison, WI, USA, 1983, pp. 1-27.
- Thomas, T.H. (2000). Sugar beet, in: D.L. Smith, C. Hamel (Eds.) *Crop yield: physiology and processes*, Springer Verlag, Berlin, Germany, 2000, pp. 311–332.
- van Heemst, H.D.J. (1986). Physiological principles, in: H.v. Keulen, J. Wolf (Eds.) *Modelling of agricultural production: weather, soils and crops*, Pudoc, Wageningen, The Netherlands, 1986, pp. 13-26.
- Victoria Jumilla, F., Costa Gómez, I., Castro Corbalán, T., García Cárdenas, R., Romojaro Casado, M.C., Mesa del Castillo Navarro, M.L., Motos Alarcón, M.I. (2011). *La Iniciativa de Ecorresponsabilidad Agricultura Murciana como Sumidero*

de CO₂. Marca LESSCO₂, in, Observatorio Regional de Cambio Climático. Región de Murcia, Murcia, Spain, 2011.

Villarías-Moradillo, J.L. de Liñán y Vicente, C. (1999). La Remolacha Azucarera, Ediciones Agrotécnicas, Madrid, Spain, 1999.

**5. ASSESSMENT OF THE USE OF RGB VEGETATION
INDICES TO DETERMINATE CHLOROPHYLL
CONTENT IN SUGAR BEET LEAVES AT FINAL
CULTIVATION STAGE**

ASSESSMENT OF THE USE OF RGB VEGETATION INDICES TO DETERMINATE CHLOROPHYLL CONTENT IN SUGAR BEET LEAVES AT FINAL CULTIVATION STAGE

Luis Fernando Sánchez Sastre

Agriculture and Forestry Engineering Department, ETSIIAA, Universidad de Valladolid, Avenida de Madrid 44, 34004 Palencia, Spain.

Abstract

High nitrogen levels in sugar beet leaves detected in the growing final stage can be an indicator of late incorporations of nitrogen from organic matter from soils or fertilizers. These tardy uptakes are known to decrease sugar yields. Among the different ways to measure nitrogen status in crops, here chlorophyll content determination using vegetation indices is explored. In this study, pictures of sugar beet leaves taken with a commercial camera were used to calculate 25 RGB indices found in bibliographic review and to obtain two new indices. The performance of studied indices are examined to evaluate its ability to measure chlorophyll content and degradation for sugar beet leaves in different natural light conditions along 4 days at final cultivation stage.

Keywords: vegetation indices, chlorophyll content, sugar beet

5.1. INTRODUCTION

The main role of nitrogen (N) in sugar beet crops is its importance in the spreading of the leaves to capture sunlight, which is a decisive factor for the growth rate of both leaves and the storage root (Grzebisz et al., 2012).

Nitrogen concentration in the leaves increases in the first 70 days of a beet's growth, decreasing afterwards as the growth cycle progresses (Gordo-Ingelmo, 1994). It is known that in crops, leaf chlorophyll content is related to nitrogen status (Raymond Hunt et al., 2013). Indeed, in sugar beet crops it is often reported a decrease in chlorophyll content and an acceleration of canopy senescence towards the end of the vegetation (Manderscheid et al. 2010). Furthermore, it was found that a late N application increased chlorophyll concentration in the leaves (Malnou et al., 2008), and

that low levels of N give a pale green foliage due to low chlorophyll concentration (Draycott and Christenson, 2003).

The determination of leaf nitrogen levels in the last stage of beet crops becomes relevant since many authors have demonstrated that late nitrogen incorporations or releases from soil's organic substance decreases the sucrose content (Pocock et al., 1990). Draycott y Christenson (2003) and Malnou et al. (2008) proved that nitrogen quantity beyond an optimum level has a negative effect on sugar yield. This implies that soils which release a lot of N (normally, late in the summer) will suffer yield reductions, and therefore the polarization in that stage develops inversely to nitrogen availability. Gordo-Ingelmo (1994) also showed how sugar beet reacts to nitrogenous fertilization increases, with a larger development of leaves and roots, which in turn cause an excessive use of sucrose and an increase of non-sugars. This happens, mainly, in cases of excessive organic fertilization, because part of the nitrogen is released belatedly, causing a stop of the root ripeness.

This crucial importance of nitrogen to multiple aspects of beet crop growth have led to the development of different methods to determine nitrogen levels in crops, from destructive (and time consuming) chemical analyses (Bruinsma, 1963), to subjective leaf colour charts, or chlorophyll meters (Saberioon et al., 2014). Measurements with chlorophyll meters (Gholizadeh et al., 2011), while expensive, are demonstrated to be highly correlated with chemical analyses (Malnou et al., 2008).

Another accepted method for nitrogen determination is remote sensing image analysis (Meisinger et al., 2008). In this technique, images captured at different scales with different kinds of sensors can be used to calculate vegetation indices for many different aims: leaf chlorophyll content evaluation (Croft et al. 2015), yield prediction (Jaggard and Clark 1990; Clevers 1997), nutrient status estimation (Link and Reusch, 2006), disease (Mahlein et al. 2013; Hillnhütter et al., 2011) and weed detection (Woebbecke et al. 1995; Kazmi et al. 2015; García-Ruiz et al. 2015), or for monitoring crop growth (Sakamoto et al., 2011).

Recently, vegetation indices based on narrow-band imaging spectrometers (also called hyperspectral sensors) have been proposed, but they remain expensive and create very large data volumes (Raymond Hunt et al., 2011). However, farmers often require short-time, low-expense solutions to manage their fields. Along these lines, Kawashima and Nakatami (1998) have already proposed a low-cost diagnostic method to assess the

nutrient status of plants that is easy to use, based on the estimation of chlorophyll content of wheat and rye leaves, using a portable colour video camera and a personal computer. As a result, it was shown that chlorophyll content of leaves can be estimated with sufficient accuracy using such basic equipment. This research line has been continued in recent years, with the proposal of indices calculated from RGB bands of the visible light spectrum, using inexpensive, off-the-shelf cameras.

Li et al.'s (2010) cereal crop studies concluded that the estimations obtained from a digital camera or specialised sensors provided equivalent information about nitrogen fertilizer requirements. Vollmann et al. (2011) found a high correlation between the green value of an RGB image and chlorophyll content in soybean leaves. Lee and Lee (2013) calculated canopy cover based on rice canopy images, and significant correlations were found with LAI (Leaf area index), shoot dry weight and shoot N accumulation, all of them parameters related to growth and N nutrition. Saberioon et al. (2014) calculated a new index for rice leaves at leaf and canopy scale through PCA (Principal Component Analysis).

The main objective of the research presented here was, at leaf scale, to verify the validity of such methodologies based on index calculation from the RGB bands of leaves images (obtained using a non-scientific-grade camera) for chlorophyll content evaluation of sugar beet crop during the last growth stage.

Towards this aim, we have collected and photographed different size and colour sugar beet leaves from commercial farms and extracted RGB values. For this validation, we have used indices already proposed in the literature, and we propose novel ones based on the experimental data gathered during the study. Additionally, we have proposed a simple method to optimize the picture shooting conditions in order to improve the correlations of the different indices with the actual chlorophyll content measured.

5.2. METHODOLOGY

The experiment was conducted during the sugar beet harvest season in October, from 18th to 21st, 2013. Daily meteorological conditions (see Table 5.1) were collected during the experiment period from the automatic weather station belonging to the SIAR network (Agroclimatic Information System for Irrigation) of the MAGRAMA (Ministry of Agriculture, Food and Environment of Spain). The leaves were taken from two commercial fields at Magaz de Pisuerga (Latitude N41°58' 01.2'' Longitude W4° 26' 44.2'' Altitude 740m) and Tordesillas (Latitude N41° 31' 02.0''Longitude W5° 02' 52.4'' Altitude 710m). Five plants of the variety Fernanda KWS were randomly selected at each plot and brought to the laboratory within 40 minutes.

Table 5.1. Meteorological conditions during the experiment period

Date	Mean Temp. (°C)	Humidity (%)	Radiation (MJ m ⁻²)	Precipitation (mm)
18/10/2013	14.64	75.2	13.87	1.39
19/10/2013	14.02	86.2	11.29	6.57
20/10/2013	11.1	88.5	11.34	0
21/10/2013	13.23	81	6.65	0

Once at the laboratory, 7 leaves were selected from every single plant in order to obtain a representative sample in terms of sizes and colourings that can be naturally found in every sugar beet soil. Figure 5.1 shows some of the leaves used in the experiment. The leaves coming from Tordesillas had a powdery mildew foliar infection caused by *Erysiphe betae* fungus (AIMCRA, 2015). Since the manifestation of this disease -whitish cottony texture spots- could interfere in the results, these leaves were excluded from the study. Therefore, only the 35 leaves from Magaz were considered in the analyses.

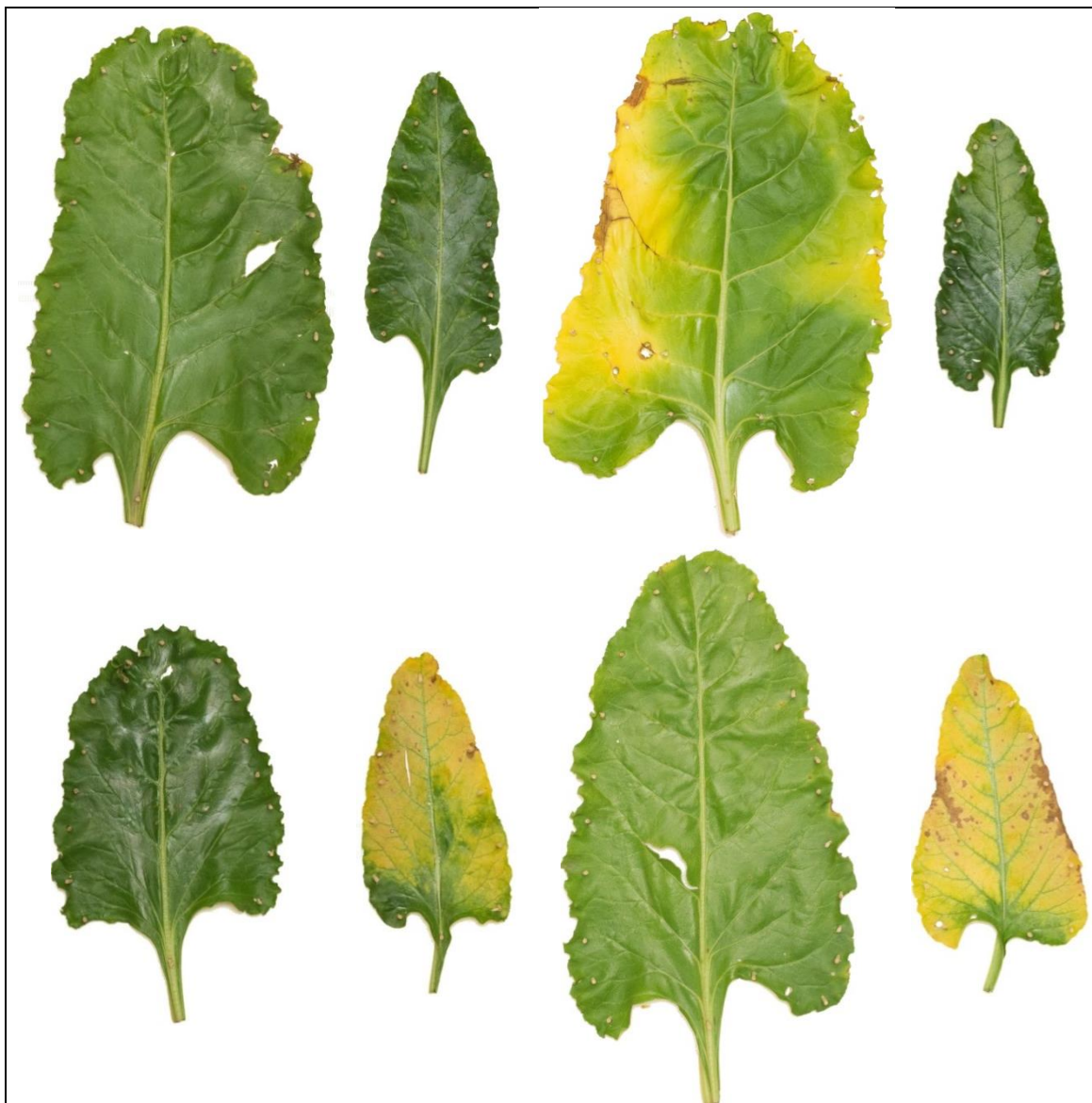


Figure 5.1. Some of the 35 leaves used in the experiment. The leaves were selected to provide a representative sample of the leaf size and colouring in commercial plots during the harvest season.

5.2.1. Chlorophyll measurement:

For each leaf, 10 instant and non-destructive measurements were taken with an area of 0,71 cm². Figure 5.2 shows the handheld chlorophyll content meter used: an Opti-Sciences² CCM-200 plus[®].



Figure 5.2. Optic chlorophyll meter CCM-200[®] from Opti-Sciences

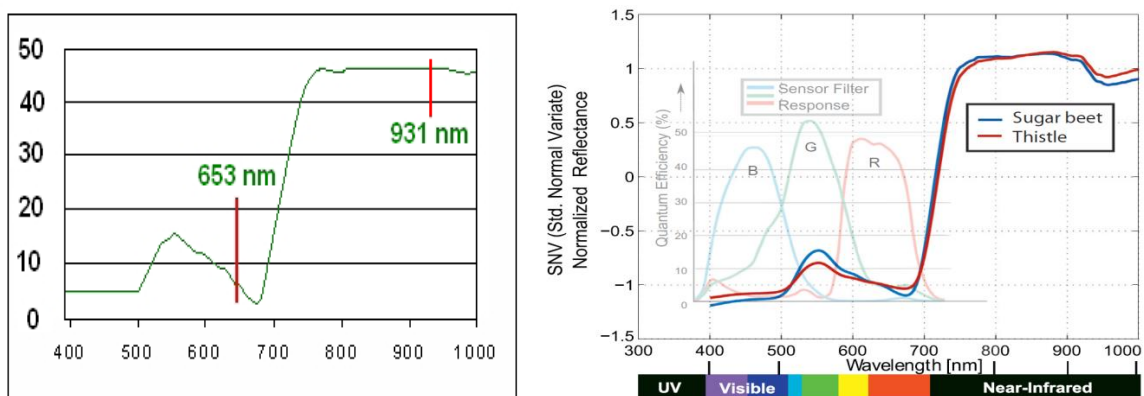


Figure 5.3. Left: optical absorbance in the two wavelengths measured by CCM-200. Right: spectral signature of sugar beet (blue) and creeping thistle (Kazmi et al. 2015)

² Opti-Sciences: www.optisci.com (last visit: 2015/10/17)

Chlorophyll has strong absorbance in the blue and red but not in the green or infrared bands. Thus, this characteristic can be used to determine relative chlorophyll concentration (CC). The CCM-200 plus uses two wavelengths for absorbance determinations (Figure 5.3). One wavelength falls within the chlorophyll absorbance range (653nm) while the other serves to compensate for mechanical differences such as tissue thickness (931nm, Near Infra-Red). The meter measures the absorbance of both wavelengths and calculates a Chlorophyll Concentration Index (CCI) value that is proportional to the amount of chlorophyll in the sample³.

The average of the 10 measurements was considered as the chlorophyll content of leaf in each moment.

5.2.2. Leaf data acquisition:

As Figure 5.4 shows, each leaf was vertically and independently placed on polyurethane sheets. Once that process was finished pictures were regularly taken during 4 days at different times (see Table 5.2) in a laboratory room, only with natural light coming from a single north-facing window covered with a thin translucent curtain. Photographs were taken in vertical position with a Sony α 55 (SLT-A55V) camera with an [APS-CCMOS](#) sensor of 16.2 mega pixel resolution and a Sony SAL 55-200mm lens.



Figure 5.4. The 35 leaves vertically arranged in individual polyurethane sheets for the photo shooting.

³ www.apogeeinstruments.com (last visit: 2015/10/17)

Table 5.2. Dates and time of the eight shoots of the experiment. On October 19th and 20th only one shoot could be carried out.

Date	Shoot		
	1	2	3
18	11:00 AM	1:30 PM	5:00 PM
19	10:00 AM	-	-
20	10:00 AM	-	-
21	10:00 AM	2:00 PM	4:00 PM

The camera was mounted on a tripod in a fixed position: 1-meter height and 2.5 meters far from the leaf (see Figure 5.5). Every picture was taken with 4912 x 3264 pixels resolution, 55mm focal distance, ISO-1600 sensitivity setting, using aperture-priority mode with white balance set to manual and punctual measurement of exposition.



Figure 5.5. LCD (Liquid Crystal Display) Sony α55 camera view with the leaf image about to photograph. The camera is mounted on a tripod to keep a fixed distance and height.

Before every single photograph was taken, a grey/white card Ezybalance[®] of Lastolite⁴ was placed in front of the leaf to be photographed and used for exposure and

⁴ www.lastolite.com (last visit: 2015/10/17)

colour correction. Ezybalance[®] works as a reflectance standard of 18% of brightness and, therefore, it will reflect 18% of the incident light under all lighting conditions (Murphy et al., 2009).

This methodology for leaf data acquisition was developed once and after the main problems in the image taking process were reviewed and considered how they might affect the final index values, as reported in the literature. Thus, Kawashima and Nakatani 1998 reported a difficulty in discriminating leaf colour under clear lighting conditions with direct solar radiation (Figure 5.6). Consequently, in their study they only used pictures taken in cloudy days. In the same line, El-Faki et al. (2000b) recommended to take the images under dim illumination, and Kazmi et al. (2015) concluded that shooting under a shade should be preferred.

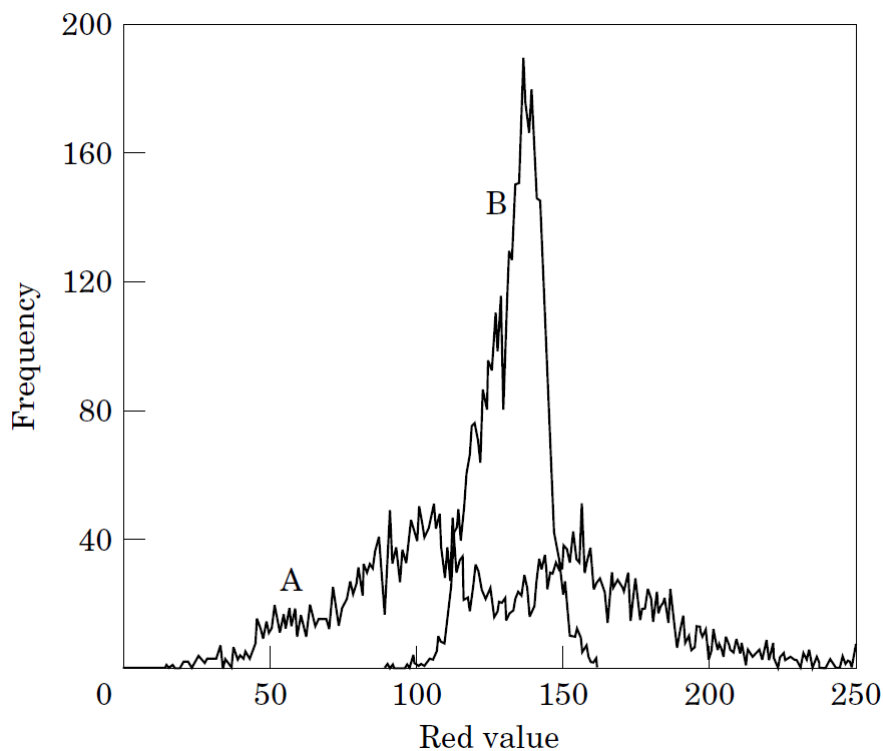


Figure 5.6: Frequency plot of red wavelength for leaves on a clear day (A) and a cloudy day (B) (taken from Kawashima and Nakatani 1998). Two peaks with large deviations can be seen in the clear day condition, in contrast to the single peak of the cloudy day image.

In order to avoid these problems related with the use of natural light, some authors photograph leaves from their study in laboratory using LED light (Saberioon et al. 2014) or incandescent light (Vollmann et al. 2011).

However, in this study it was decided to work with natural light, given our focus on its later applicability in the field (by farmers or researchers). Thus, we only reproduced in our laboratory the conditions of dim light typical of a cloudy day, with a single window facing north, through which no direct sunlight entered, with a translucent curtain to diffuse the incoming light.

Another issue observed in the literature is the directional reflectance effect caused by direct solar radiation as leaves orientate at different angles within the canopy (Kimes 1983; Pinter et al. 1990 cited in Kawashima and Nakatani 1998).

In this study, this effect has been minimized by photographing standing leaves with the same orientation in relation to the camera and the source of light, avoiding the influence of direct sunlight in the object.

Murphy et al. (2009) report that varying solar illumination and indirect reflections from surrounding objects may cause variable brightness, even when using identical camera settings. Thereby, when shooting in natural light with clear sky conditions, they performed a band-by-band calibration process using two standard reflectors of 15% and 18% brightness, to avoid the brightness differences caused by different lighting and camera-exposure times.

In our study we used a grey/whitecard that reflects 18% of the incoming light. Before each photograph, a point measurement was made on the card with the camera's own light measurement tool, in order to fix a precise shot exposure.

In the same study, and regarding the images' white balance, Murphy et al (2009) note that its purpose in digital cameras is that white objects in the image appear white to human eye, by modifying the relative contributions of red, green and blue in the photograph. Therefore, using a camera's automatic white balance may change relative contributions of red, green and blue depending on the lightning conditions and the colour of the target. Some authors addressed this problem by setting the white balance to a single setting (Goddijn and White 2006), but we can also find studies using white balance set to automatic mode (Vollmann et al. 2011).

In our study, we chose to use as reference a grey/white card in addition to white balancing manually to adjust the colour temperature in each photograph, so as to obtain colours closer to the real scene in every lightning condition.

5.2.3. Colour indices calculation:

Digital cameras record images as individual pixels recording the intensity of red (R), green (G) and Blue (B) (Li et al., 2010). The RGB colour component of digital camera images has 256 levels (0-256) being able to represent 256³ values with black as (0,0,0) and white (256,256,256) (Gonzalez and Wood, 1987 cited in Lee and Lee, 2013).

Photographs were saved as ARW (Sony's raw format). In total, 280 pictures were analyzed using Adobe® Photoshop® (Adobe Photoshop CC, version 14.1 x64, Adobe Systems Incorporated, U.S.). Besides RGB levels, this software offers a channel for the brightness scale in the histogram tool. A routine was designed to remove the background of each photograph, using several functionalities of the program to obtain exclusively the leaf pixels. The average RGB value for the total surface of each leaf was calculated by means of the histogram tool (Figure 5.7). Accordingly, each photographed leaf presented specific RGB coordinates per shoot, based on which the different colour indices were calculated.

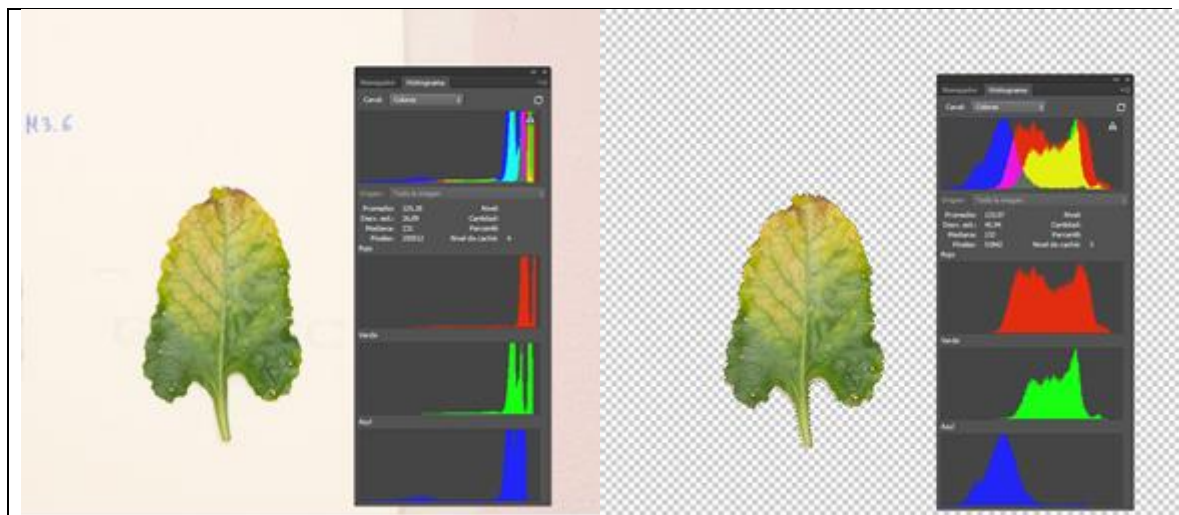


Figure 5.7. Left: image as was taken loaded in Adobe® Photoshop® 14.1. Histogram shows RGB levels of the entire photograph. Right: same image after background removal. The histogram only shows the leaf RGB levels.

Altogether, 280 pictures were analyzed based on three groups of vegetation indices: indices described and cited in the literature and new indices obtained by means of SLR (Stepwise Linear Regression) and PCA (Table 5.3).

The indices were calculated for different data sets: every shoot, all the shoots in a day, mean of daily shoots and three global data sets, all the eight shoots together, the means of every day together and finally, as well as the darkest shoot (day 18th, shoot 3) and the lightest one (21st, shoot 2) according to the mean value of the luminosity channel of the histogram tool in Adobe[®] Photoshop[®]. Besides this, entire dataset was divided into two subdatasets for validation process as is explained later.

5.2.3.1 Indices identified in bibliographic review:

A literature review was done to identify indices based on visible spectrum RGB levels. Table 5.3 lists the 25 indices that were selected and calculated. The results are grouped in two categories: indices studied by Kawashima and Nakatani (1998) and those found in several sources.

Table 5.3.List of the colour vegetation indices considered in study, including their equations and reference sources.

Index	Definition	Reference
R	red (0-255)	Kawashima and Nakatami (1998)
G	green (0-255)	Kawashima and Nakatami (1998)
B	blue (0-255)	Kawashima and Nakatami (1998)
r	$R/(R+G+B)$	Kawashima and Nakatami (1998)
g	$G/(R+G+B)$	Kawashima and Nakatami (1998)
b	$B/(R+G+B)$	Kawashima and Nakatami (1998)
R-G		Kawashima and Nakatami (1998)
R-B		Kawashima and Nakatami (1998)
G-B		Kawashima and Nakatami (1998)
$(R-G)/(R+G)$		Tucker (1979); Kawashima and Nakatami (1998)
$(R-B)/(R+B)$		Kawashima and Nakatami (1998)
$(G-B)/(G+B)$		Kawashima and Nakatami (1998)
$(R-G)/(R+G+B)$		Woebbecke et al. (1995); Kawashima and Nakatami (1998)
$(R-B)/(R+G+B)$		Kawashima and Nakatami (1998)
$(G-B)/(R+G+B)$		Woebbecke et al. (1995); Kawashima and Nakatami (1998)
RGRI	R/G	Saberioon et al. (2014)
GLI	$(2G-R-B)/(2G+R+B)$	Louhaichi et al. (2001)
VARI	$(G-R)/(G+R-B)$	Gitelson et al. (2002)
I_{PCA}	$0,994 R-B + 0,961 G-B + 0,914 G-R $	Saberioon et al. (2014)
ExR	1,4 r -g	Meyer et al. (1998a); Mao et al. (2003)
ExB	1,4 b -g	Mao et al. (2003)
ExG	2g -r -b	Woebbecke et al. (1995); Mao et al. (2003)
ExGR	ExG -ExR	Mao et al. (2003); Meyer and Neto (2008)
Gray	$0.2898 r + 0.5870 g + 0.1140 b$	Kazmi et al. (2015)
CIVE	$0.441 r - 0.811 g + 0.385 b + 18.78$	Kataoka et al. (2003)
PCA1	$-0.977 b + 0.916 (G-B/G+B) + 0.995 (R-B/R+B) + 0.771 (R-G/R+G)$	New calculated
PCA2	$0.999 R-B + 0.92 G-B + 0.886 R-G $	New calculated
I_1	$R+G-2B$	New calculated proposed
SLR1	$-60430 - 0.7316 B + 69680 b + 112800 g + 28270 (G-B/G+B) - 23890 (R-B/R+B) + 68380 (R-G/R+G)$	New calculated
SLR2	$-46240 - 2.678 B + 1.05 G + 52570 b + 87420 g + 20720 (G-B/G+B) - 18240 (R-B/R+B) + 52500 (R-G/R+G)$	New calculated
SLR3	$-25373 + 30106 b + 46539 g + 12776 (G-B/G+B) - 10507 (R-B/R+B) + 28821 (R-G/R+G)$	New calculated
SLR4	$-44312 + 51689 b + 81995 g + 21751 (G-B/G+B) - 18156 (R-B/R+B) + 50425 (R-G/R+G)$	New calculated
SLR5	$-41048 + 46964 b + 76841 g + 19998 (G-B/G+B) - 17173 (R-B/R+B) + 47162 (R-G/R+G)$	New calculated
I_2	$0.55 + 11.4 (G-B/G+B) - 12.5 (R-B/R+B) + 9 (R-G/R+G)$	New calculated proposed

5.2.3.2 New calculated indices methods and validation:

In order to explore the possibility of obtaining new indices, PCA and SLR methodologies were used. Previously, to ensure the validation of the calculated indices, dataset were divided into two subdatasets, the first one was used to generate the parameters of the new indices and the second was used to estimate the statistical error. Datasets were defined by choosing shoots alternately. Thus first subdataset was: shoot 1 and shoot 3 from day 18th, shoot 1 from day 20th and shoot 2 from day 21st. Second subdataset was shoot 2 from day 18th, shoot 1 from day 19th, and shoot 1 and shoot 3 from day 21st.

2.2.3.2.a PCA indices:

Multivariate procedure Principal Component Analysis (PCA) was conducted with IBM SPSS Statics 21 (IBM Corp., 2012). PCA reduces an initial set of observed correlated variables into a smaller number of principal components (uncorrelated variables) that account for most of the variance in the observed variables (O'Rourke and Hatcher, 2013). Each principal component is a linear weighted combination of the initial variables. Different indices found in the literature apply PCA to obtain new indices as a linear combination of the first ones. Indeed, Pagola et al. 2009 reported that PCA could be a useful tool to develop consistent index for chlorophyll determination of barley at leaf scale.

In this study, weights from correlation matrix were used as coefficients of the equations (Saberioon et al. 2014). Indices $PCA1$, $PCA2$ and I_1 were obtained by this methodology as it is shown in Table 5.3.

2.2.3.2.b SLR indices (Stepwise Linear Regression):

The SLR functionality from R software (version 2.15.3, R Development Core Team, 2008) was used as an alternative way to obtain new indices, As aforementioned, some literature indices were considered as inputs. Resultant indices were calculated by adding and removing variables one by one (Kazmi et al., 2015), using AIC (Akaike Information Criterion) method for variable selection (Yamashita et al., 2007). Indices from $SLR1$ to $SLR5$ and I_2 were obtained by means of this procedure (see Table 5.3).

5.2.4. Statistics:

STATISTICA 8.0 (StatSoft, Inc., 2007) was used for descriptive analysis, including maximum, minimum, mean, standard error and variation coefficient of the different CC measured with CCM-200 and for all the indices. Correlation matrixes that show Pearson correlation coefficients (R) and p-values of each index were also calculated for every shoot, all the shoots in a day, mean of daily shoots and finally for the three global subdata sets: all the eight shoots together, the means of every day together and finally one shoot of the first day and one shoot of the last day.

Graphs for comparison between several indices and CC are also plotted using Excel software (Microsoft Excel 2010) and including regression equations and coefficients of determination R^2 .

For validation of new indices RMSE was calculated as follows:

$$RMSE = \sqrt{\frac{1}{n} \sum_{i=1}^n (M_i - P_i)^2}$$

where A_i =Measurement with CCM-200, P_i =Predicted by index, and n =number of observations. Units are CCI.

5.3. RESULTS AND DISCUSSION

As described above in this study, 35 vegetation indices (based on the RGB bands of the visible spectrum) from 280 photographs have been calculated, in order to assess their correlation with the chlorophyll content results in the same leaves of spring sown sugar beet as measured at harvest with an optic chlorophyll meter CCM-200.

5.3.1. Chlorophyll content measurements

From the summary of descriptive statistics for the CCM-200 measurements shown in Table 5.4, we can see how chlorophyll content decreases over time (as reflected in the means column). The same can be said of the minimum and maximum values. Therefore, the chlorophyll deterioration in the leaves is evident as time goes by. The coefficient of variation's (CV) high values are clearly due to a very heterogeneous group of samples, since diverse colouring and a wide size range were purposefully part of our sampling process.

This fact is also illustrated by the vegetation indices calculated (Table 5.5) which, in a similar manner, show a wide variance of coefficients (again due to the heterogeneity of the starting samples).

Table 5.4. Summary of descriptive statistics for CCM-200 measurements: minimum, maximum, mean, standard error and coefficient of variation (CV).

Date	min	max	mean	Std. Error	CV
18/10/2013	2.76	55.82	24.49	2.55	61.60
19/10/2013	2.51	55.71	23.37	2.52	63.91
20/10/2013	2.00	55.48	21.78	2.64	71.80
21/10/2013	1.74	55.36	21.07	2.73	75.57
All	1.74	55.82	22.57	1.29	67.74

Table 5.5. Summary of descriptive statistics for some of the indices studied in this work using mean values from all shoots: minimum, maximum, mean, standard error and coefficient of variation.

Index	max	min	mean	std. Error	CV
$(R-B)/(R+B)$	0.51	0.13	0.33	0.01	26.06
$(R-B)/(R+G+B)$	0.31	0.08	0.20	0.00	26.18
I_{PCA}	268.47	65.51	165.90	2.79	28.10
ExR	0.25	0.09	0.14	0.00	28.76
I_1	248.00	56.00	158.86	2.82	29.69
I_2	0.51	0.01	0.21	0.01	58.62

It is worth noticing that, in a few cases, chlorophyll content (as measured with the CCM-200) was higher in the last day of the experiment (Figure 5.8), indicating an increase in chlorophyll. As this fact is incompatible with chlorophyll degradation, it is obvious that some element had affected the readings of the equipment (e.g., dehydration, extraneous factors not detected ...)

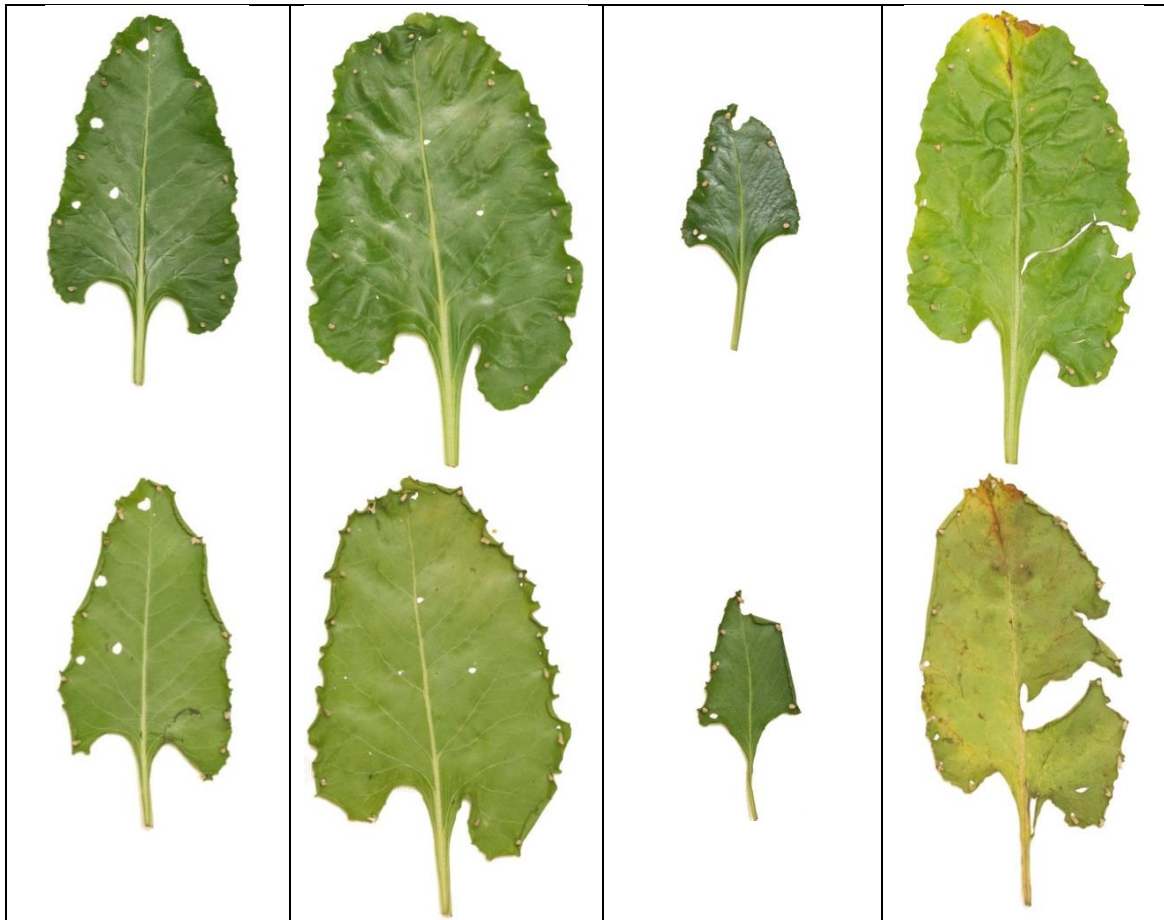


Figure 5.8. Some of the leaves in which measurements with CCM-200 resulted in an increment of chlorophyll content after 4 days. The degraded status of the leaves may have somewhat interfered the readings.

5.3.2. Correlation of CCM-200 measurements and color indices

Pearson correlation coefficients for each index will be shown in this section, according to each group of indices previously defined. We found in all the groups indices with high R values which are aligned with other studies in the literature that find close correlations between chlorophyll content and RGB values, e.g., for potato and soybean leaves (Yadav et al., 2010 and Vollmann et al., 2011).

5.3.2.1 Indices studied in Kawashima and Nakatani (1998)

The results obtained for this group of indices (Table 5.6) are consistent with Kawashima and Nakatani's 1998 description. Thus, $G-B$ and $R-B$ (i.e., corrected values for R and G based on B) show several of the highest values in different shoots although, overall, it is $(R-B)/(R+G+B)$ the index with the highest values evaluating every measure as a group (either the eight shoots are analyzed, or the average of the first and the last day, or the two shoots with the greatest difference of the brightness calculated with the camera). $G-B$ keeps high values above 0.90 in day 18, but in the rest of days the number noticeably decreases (except for one shoot in day 21), thus showing rather irregular behaviour. On the other hand, $R-B$ itself behaves more regularly, although its correlation indices decrease when the global data are analyzed.

Correlation coefficients for $R-B$ and $G-B$ are higher than those for R and G alone, since taking B as the basis decreases the bias noise in R , G and B . This observation is in accordance with the results given by Kawashima and Nakatani 1998 and Saberioon et al. 2013.

In this experiment $(R-B)/(R+G+B)$ would have a similar role to that of $(R-B)/(R+B)$ in Kawashima and Nakatani's research. This is consistent with the fact that both indices, in both studies, have very close results in their correlation indices with the chlorophyll content. Furthermore, we can see in figures 5.9 and 5.10 graphs illustrating the connection between the values of the $(R-B)/(R+B)$ and $(R-B)/(R+B+G)$ indices, and the chlorophyll content for the whole four days, along with linear regressions, determination coefficients and Pearson correlation coefficients.

Table 5.6. Correlation coefficients for indices studied by Kawashima et al. 1998. Results are given for individual shoot, daily (taking into account three shoots or mean values of three shoots in days 18th and 21st) and global datasets: data from all the days using the eight shoots, data from all the days using mean values for days 18th and 21st, and one shoot from day 18th and one shoot from day 21st. Bald figures denote highest R in a shoot. Significance levels: ** (p<0.01) and * (p<0.05).

Source	Index	18/10/2013					19/10/2013	20/10/2013	21/10/2013					Global		
		shoot 1	shoot 2	shoot 3	3 shoots together	mean of shoots	shoot 1	shoot 1	shoot 1	shoot 2	shoot 3	3 shoots together	mean of shoots	8 shoots together	means of shoots	extreme shoots
Kawashima and Nakami 1998	R	-0.8357**	-0.8079**	-0.8156**	-0.818**	-0.8705**	-0.8215**	-0.7431**	-0.8532**	-0.8536**	-0.9213**	-0.8613**	-0.9094**	-0.798**	-0.8449**	-0.7632**
	G	-0.8161**	-0.7823**	-0.8011**	-0.7969**	-0.9038**	-0.7662**	-0.6498**	-0.7764**	-0.7366**	-0.8744**	-0.7621**	-0.8815**	-0.7411**	-0.8471**	-0.6947**
	B	0.2616 ns	0.349*	0.2934 ns	0.2981**	0.4271**	0.0835 ns	-0.0296 ns	-0.119ns	-0.0249 ns	-0.4242*	-0.1592 ns	-0.2232 ns	-0.0036 ns	0.0079 ns	0.086**
	r	-0.9019**	-0.9007**	-0.8904**	-0.897**	-0.8969**	-0.8915**	-0.8678**	-0.9024**	-0.904**	-0.9062**	-0.8986**	-0.9086**	-0.8786**	-0.8824**	-0.8788**
	g	-0.4695 ns	-0.4684 ns	-0.4589**	-0.4632**	-0.4771**	-0.084 ns	0.1786 ns	0.4043**	0.4538**	0.507**	0.4528**	0.4651**	0.0611 ns	0.0539 ns	0.0501**
	b	0.9243**	0.9151**	0.9091**	0.914**	0.9205**	0.8997**	0.8463**	0.864**	0.8241**	0.8597**	0.8325**	0.868**	0.8535**	0.8696**	0.8496**
	R-G	-0.6707**	-0.6682**	-0.6603**	-0.6662**	-0.6645**	-0.749**	-0.7179**	-0.7934*	-0.8142**	-0.8**	-0.8016**	-0.8036**	-0.7227**	-0.7186**	-0.7236**
	R-B	-0.9102**	-0.9156**	-0.8963**	-0.9071**	-0.9114**	-0.8879**	-0.8648**	-0.9186**	-0.9188**	-0.932**	-0.918**	-0.9289**	-0.8879**	-0.8977**	-0.8802**
	G-B	-0.9151**	-0.9332**	-0.9082**	-0.9183**	-0.931**	-0.8824**	-0.8506**	-0.9043**	-0.8381**	-0.8813**	-0.8639**	-0.8905**	-0.8678**	-0.8858**	-0.8527**
	(R-G)/(R+G)	-0.7399**	-0.7353**	-0.7341**	-0.7362**	-0.7359**	-0.8034**	-0.7632**	-0.8376**	-0.8437**	-0.8482**	-0.8418**	-0.8449**	-0.7666**	-0.7609**	-0.7549**
	(R-B)/(R+B)	-0.9276**	-0.9201**	-0.9123**	-0.9183**	-0.9226**	-0.9068**	-0.8752**	-0.9004**	-0.8823**	-0.9037**	-0.8827**	-0.9081**	-0.8813**	-0.8941**	-0.8809**
	(G-B)/(G+B)	-0.9034**	-0.8891**	-0.8849**	-0.8895**	-0.8996**	-0.8699**	-0.7511**	-0.7438**	-0.6626**	-0.7164**	-0.6888**	-0.7334**	-0.7766**	-0.7957**	-0.765**
	(R-G)/(R+G+B)	-0.7167**	-0.711**	-0.7096**	-0.7122**	-0.7118**	-0.7899**	-0.753**	-0.8297**	-0.8369**	-0.8409**	-0.8344**	-0.8377**	-0.7549**	-0.7492**	-0.7435**
	(R-B)/(R+G+B)	-0.9288**	-0.9238**	-0.9151**	-0.9212**	-0.9241**	-0.909**	-0.8845**	-0.9088**	-0.8981**	-0.9125**	-0.8958**	-0.9165**	-0.8908**	-0.9015**	-0.8916**
	(G-B)/(R+G+B)	-0.8748**	-0.8604**	-0.8584**	-0.8614**	-0.8733**	-0.8223**	-0.6454**	-0.6046**	-0.4875**	-0.5178**	-0.5206**	-0.5603**	-0.6894**	-0.7075**	-0.6753**

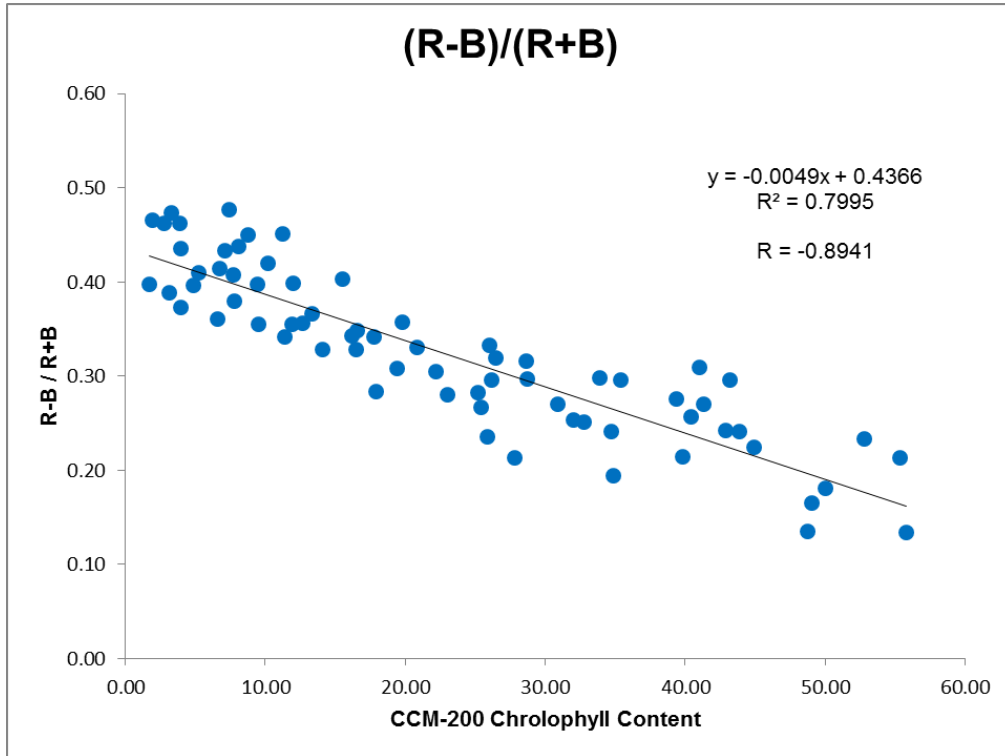


Figure 5.9. Relationship between (R-B)/(R+B) index and CC measured by CCM-200 for all days dataset (mean values of three shots are used for days 18th and 21st). Regression line, equation, R^2 and R-values are shown.

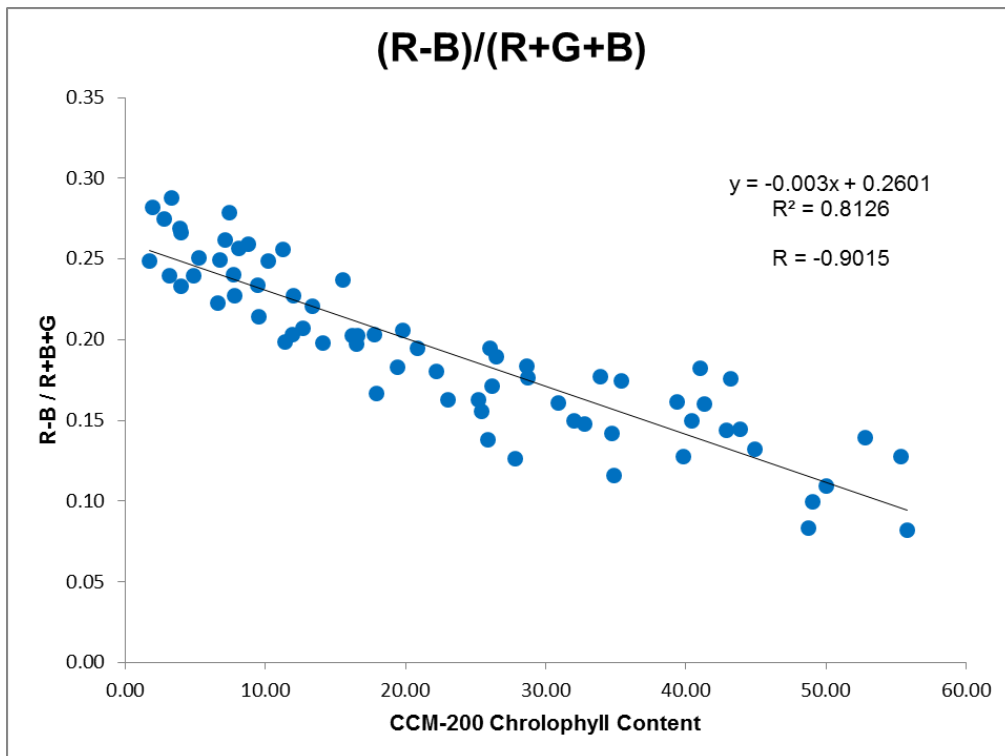


Figure 5.10. Relationship between (R-B)/(R+G+B) index and CC measured by CCM-200 for all days dataset (mean values of three shots are used for days 18th and 21st). Regression line, equation, R^2 and R-values are shown.

5.3.2.2 Indices from various sources:

In this group, can be observed how the I_{PCA} index developed by Saberioon et al. 2014 gets the best results (Table 5.7), behaving in a stable manner during all the experimentation period. $RGRI$ (Saberioon et al. 2014), $VARI$ (Gitelson et al. 2002), and ExR (Meyer et al. 1998a) indices all show high correlations (above 0.75). This last two indices are used for vegetation extraction and artificial vision in agriculture (Kazmi et al. 2015). The relationship of ExR and I_{PCA} with the measures calculated with the CCM-200 along the experimentation period are shown in figures 5.11 and 5.12. As can be shown I_{PCA} exhibits a better performance with higher R^2 and lower dispersion.

Table 5.7. Correlation coefficients for indices studied for different researchers. Results are given for individual shoot, daily (taking into account three shoots or mean values of three shoots in days 18th and 21st) and global datasets: data from all the days using the eight shoots, data from all the days using mean values for days 18th and 21st, and one shoot from day 18th and one shoot from day 21st. Bold figures denote highest R in a shoot. Significance levels: ** (p<0.01) and * (p<0.05).

Source	Index	18/10/2013					19/10/2013	20/10/2013	21/10/2013					Global		
		shoot 1	shoot 2	shoot 3	3 shoots together	mean of shoots	shoot 1	shoot 1	shoot 1	shoot 2	shoot 3	3 shoots together	mean of shoots	8 shoots together	means of shoots	extreme shoots
Various	<i>RGRl</i>	-0.7385**	-0.7324**	-0.732**	-0.7341**	-0.733**	-0.7981**	-0.7576**	-0.8288**	-0.8356**	-0.8377**	-0.8325**	-0.8358**	-0.7619**	-0.7563**	-0.7514**
	<i>GLI</i>	-0.4712*	-0.47**	-0.4598**	-0.4647**	-0.4788**	-0.0836 ns	0.1829 ns	0.4074*	0.4564**	0.5089**	0.4553**	0.465**	0.0646 ns	0.0563 ns	0.0541**
	<i>VARI</i>	0.781**	0.7776**	0.776**	0.7781**	0.7772**	0.8261**	0.7806**	0.851**	0.8549**	0.8599**	0.8539**	0.8569**	0.7867**	0.781**	0.7746**
	<i>I_{PCA}</i>	-0.9205**	-0.929**	-0.9058**	-0.9181**	-0.928**	-0.888**	-0.8607**	-0.9057**	-0.9001**	-0.9165**	-0.9008**	-0.9143**	-0.8907**	-0.9066**	-0.8855**
	<i>ExR</i>	-0.7866**	-0.7842**	-0.7784**	-0.7829**	-0.7814**	-0.8254**	-0.7896**	-0.853**	-0.8594**	-0.8611**	-0.8557**	-0.86**	-0.7969**	-0.7929**	-0.789**
	<i>ExB</i>	0.8913**	0.8779**	0.8751**	0.8785**	0.8883**	0.8497**	0.7106**	0.6938**	0.5945**	0.6364**	0.6232**	0.6642**	0.7411**	0.7587**	0.729**
	<i>ExG</i>	-0.4695**	-0.4684**	-0.4589**	-0.4632**	-0.4774**	-0.084 ns	0.1786 ns	0.4043*	0.4538**	0.507**	0.4528**	0.4624**	0.0611 ns	0.0525 ns	0.0501**
	<i>ExGR</i>	0.233 ns	0.2095 ns	0.2313 ns	0.2236*	0.2244*	0.547**	0.5606**	0.7027**	0.7169**	0.7382**	0.7184**	0.7227**	0.5188**	0.5093**	0.4966**
	<i>GREY</i>	-0.8345**	-0.8189**	-0.818**	-0.8204**	-0.8336**	-0.7501**	-0.4969**	-0.3947*	-0.2603 ns	-0.2537 ns	-0.294**	-0.3165 ns	-0.5713**	-0.5869**	-0.5921**
	<i>CIVE</i>	0.382*	0.386*	0.3732*	0.3786*	0.3909*	-0.0358 ns	-0.253 ns	-0.4693**	-0.5095**	-0.5577**	-0.5101**	-0.5191**	-0.145*	-0.1364 ns	-0.1679 ns

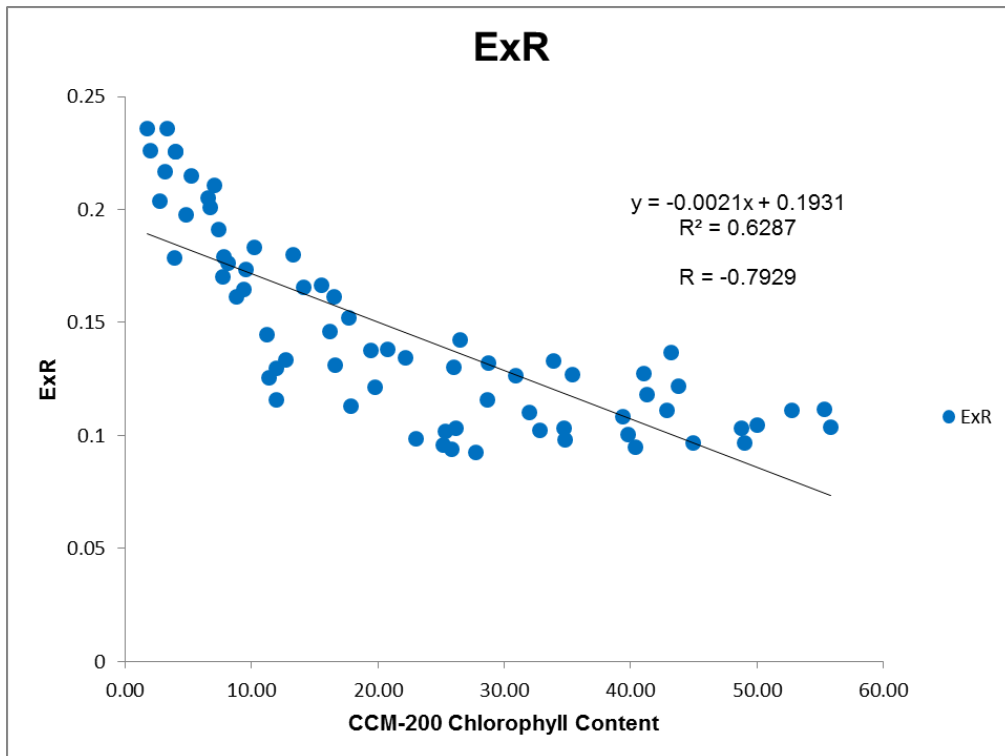


Figure 5.11. Relationship between ExR index and CC measured by CCM-200 for all days dataset (mean values of three shots are used for days 18th and 21st). Regression line, equation, R^2 and R-values are shown.

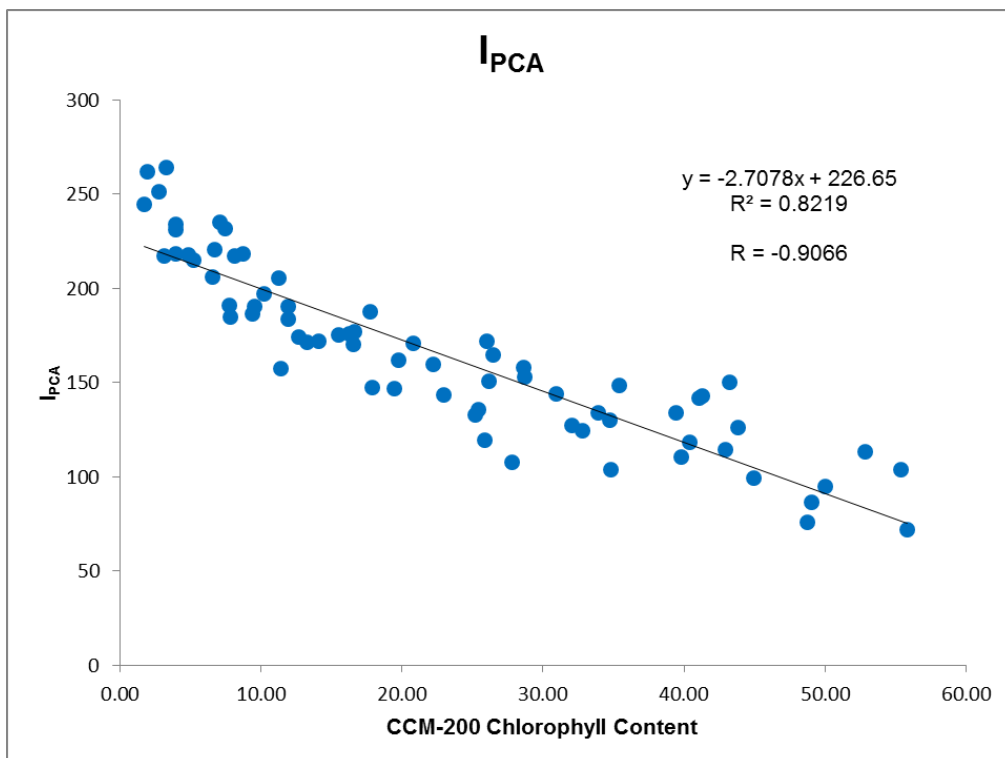


Figure 5.12. Relationship between IPCA index and CC measured by CCM-200 for all days dataset (mean values of three shots are used for days 18th and 21st). Regression line, equation, R^2 and R-values are shown.

5.3.2.3 Indices Calculated via PCA:

This group includes indices calculated *ex novo* with PCA. The three indices have similar behaviour to that of I_{PCA} (see Table 8). $PCA1$ uses the same bands that those in I_{PCA} but standardized by the addition of both channels adding the standardized blue. $PCA2$ uses three bands as I_{PCA} . Finally, I_I removes (R-G) difference and remains more simplified as $R+G-2B$.

Considering every value, $PCA2$ and I_I get better correlations which agree with Saberioon et al.'s 2014 research. However, the R-G inclusion does not provide a significant improvement. The relationship between $PCA2$ and chlorophyll content is shown in figure 5.13, and in a similar manner for the I_I index in figure 5.14. Both indices show good performances with high R and similar linear regressions which allows us to consider them as equivalent.

From the three indices we will choose the simplest I_I to examine later its performance.

Table 5.8. Correlation coefficients for new indices obtained by PCA process. Results are given for individual shoot, daily (taking into account three shoots or mean values of three shoots in days 18th and 21st) and global datasets: data from all the days using the eight shoots, data from all the days using mean values for days 18th and 21st, and one shoot from day 18th and one shoot from day 21st. Bold figures denote highest R in a shoot. Significance levels: ** (p<0.01) and * (p<0.05).

Source	Index	18/10/2013					19/10/2013	20/10/2013	21/10/2013					Global		
		shoot 1	shoot 2	shoot 3	3 shoots together	mean of shoots	shoot 1	shoot 1	shoot 1	shoot 2	shoot 3	3 shoots together	mean of shoots	8 shoots together	means of shoots	extreme shoots
Calculated via PCA	PCA1	-0.9277**	-0.9198**	-0.912**	-0.918**	-0.9227**	-0.906**	-0.8703**	-0.894**	-0.8724**	-0.8964**	-0.8742**	-0.9015**	-0.8775**	-0.8913**	-0.8768**
	PCA2	-0.9205**	-0.9289**	-0.9058**	-0.918**	-0.9278**	-0.8881**	-0.8608**	-0.9059**	-0.9006**	-0.9168**	-0.9011**	-0.9146**	-0.8908**	-0.9065**	-0.8855**
	I ₁	-0.9183**	-0.9291**	-0.9072**	-0.9178**	-0.9254**	-0.892**	-0.8729**	-0.929**	-0.9152**	-0.9328**	-0.9183**	-0.9346**	-0.8924**	-0.9061**	-0.8831**

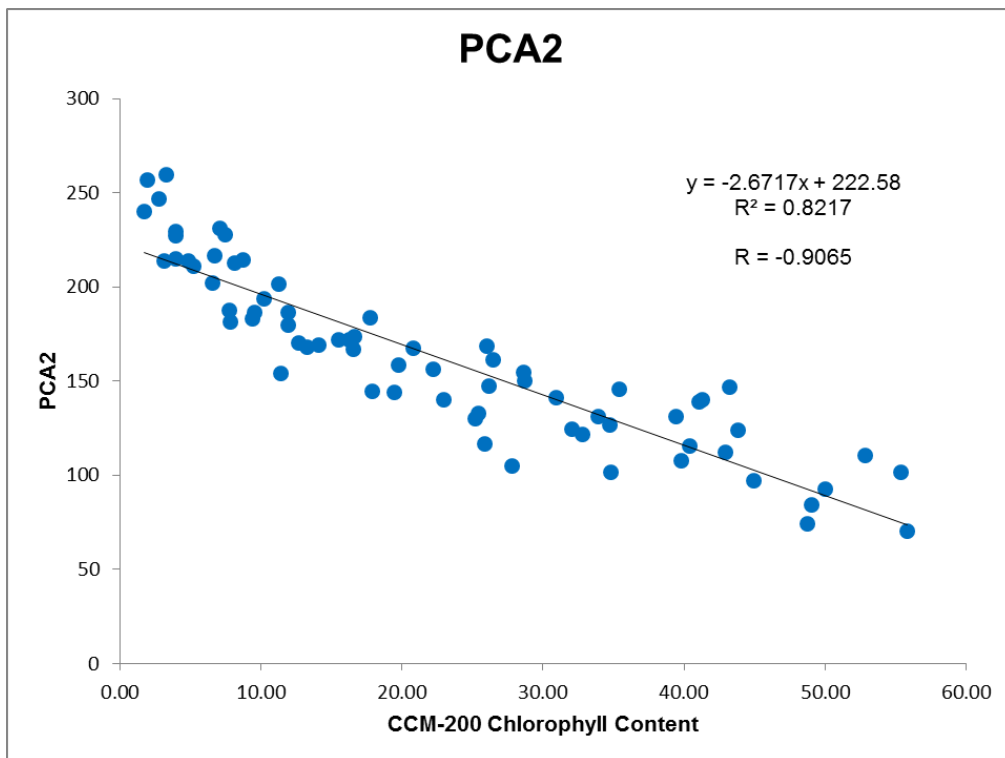


Figure 5.13. Relationship between PCA2 index and CC measured by CCM-200 for all days dataset (mean values of three shots are used for days 18 and 21). Regression line, equation, R^2 and R values are shown.

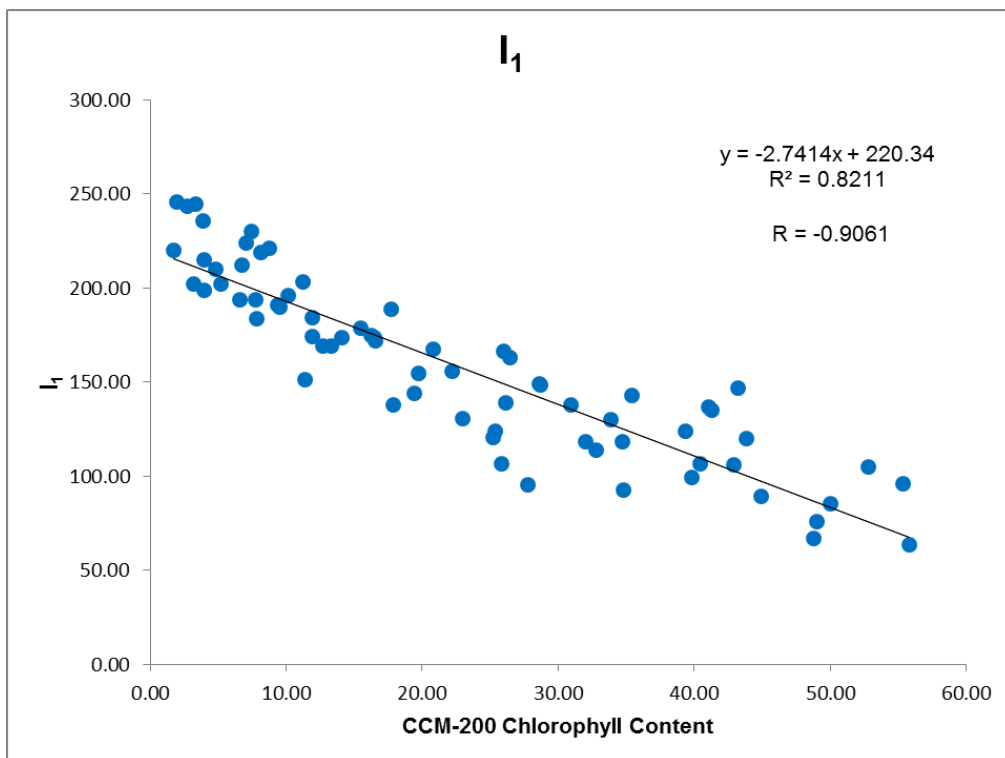


Figure 5.14. Relationship between I1 index and CC measured by CCM-200 for all days dataset (mean values of three shots are used for days 18 and 21). Regression line, equation, R^2 and R values are shown.

5.3.2.4 Indices calculated via SLR:

SLR1 and *SLR2* indices (Table 5.3) were calculated first, obtaining the highest correlation values for every single shoot, but also as a group (Table 5.9). In relation to this high correlation, they also have the highest variation coefficients (Table 5.5), similar to the chlorophyll measurements with the CCM-200, thus showing a behaviour more sensitive to chlorophyll content changes.

Nevertheless, many authors warn about the potential problems of this automatic process (Singer and Willett 2003), since this method will not necessarily produce the best model if there are redundant predictors (and it may frequently fail when applied to new datasets, see Judd et al., 2008). In the same way, Derksen and Keselman 1992 affirm that the degree of correlation between the predictor variables affect the final model.

Therefore, in order to avoid or minimise these problems (especially, the collinearity), *SLR3*, *SLR4*, *SLR5* y I_2 indices (Table 5.3) were developed. *SLR1* (Figure 5.15), for example, uses *B* bands and its *b* standardized value, among other elements. On the other hand, *SLR2* uses *B* and *G* channels, but also their corresponding standardized values. Considering that this could be a source of collinearity, the next step was to avoid the entrance of a band and its standardized value in the analysis, getting in this way *SLR3*, *SLR4* and *SLR5*. Finally, I_2 is the result of removing from the process single bands and only evaluating the G-B, R-B and R-G differences, in line with the I_{PCA} index, but in this case dividing each one by the addition of the corresponding channels ($G+B$), ($R+B$) and ($R + G$).

In this refinement process R-value and R^2 are diminished. Nevertheless, these indices keep very high correlation values (over 0.9, as a rule, see Table 5.9) with the chlorophyll content for each measure and for the global group, and R^2 keeps reasonably high (Figures 5.16 and 5.17).

In this group we select, therefore, $I_2 = 0.55 + 11.4 (G-B/G+B) - 12.5 (R-B/R+B) + 9 (R-G/R+G)$ which is the simplest and use the same bands that those in I_{PCA} but normalized.

Table 5.9. Correlation coefficients for new indices obtained by SLR process. Results are given for individual shoot, daily (taking into account three shoots or mean values of three shoots in days 18 and 21) and global datasets: data from all the days using the eight shoots, data from all the days using mean values for days 18 and 21, and one shoot from day 18 and one shoot from day 21. Bold figures denote highest R in a shoot. Significance levels: ** (p<0.01) and * (p<0.05).

Source	Index	18/10/2013					19/10/2013	20/10/2013	21/10/2013					Global		
		shoot 1	shoot 2	shoot 3	3 shoots together	mean of shoots	shoot 1	shoot 1	shoot 1	shoot 2	shoot 3	3 shoots together	mean of shoots	8 shoots together	means of shoots	extreme shoots
Calculated via SLR	SLR1	0.9349**	0.9391**	0.9191**	0.9304**	0.9478**	0.8823**	0.8406**	0.9365**	0.9221**	0.9416**	0.9269**	0.9517**	0.9084**	0.943**	0.9139**
	SLR2	0.9424**	0.9241**	0.9229**	0.929**	0.9458**	0.9008**	0.8892**	0.9403**	0.9319**	0.9511**	0.9334**	0.9513**	0.917**	0.9406**	0.9094**
	SLR3	0.9391**	0.935**	0.9334**	0.9347**	0.9375**	0.9207**	0.9165**	0.928**	0.9319**	0.9427**	0.9242**	0.9428**	0.9138**	0.9236**	0.9155**
	SLR4	0.9356**	0.927**	0.9234**	0.9267**	0.9341**	0.9086**	0.8955**	0.9132**	0.9187**	0.9291**	0.9087**	0.9364**	0.9079**	0.9276**	0.9146**
	SLR5	0.9301**	0.9204**	0.9154**	0.9204**	0.9266**	0.9099**	0.9019**	0.9061**	0.9088**	0.9308**	0.9032**	0.9312**	0.9061**	0.9238**	0.9091**
	I_2	0.9254**	0.9216**	0.9169**	0.9204**	0.9221**	0.9147**	0.9123**	0.9434**	0.9487**	0.9567**	0.9414**	0.9523**	0.9001**	0.9033**	0.897**

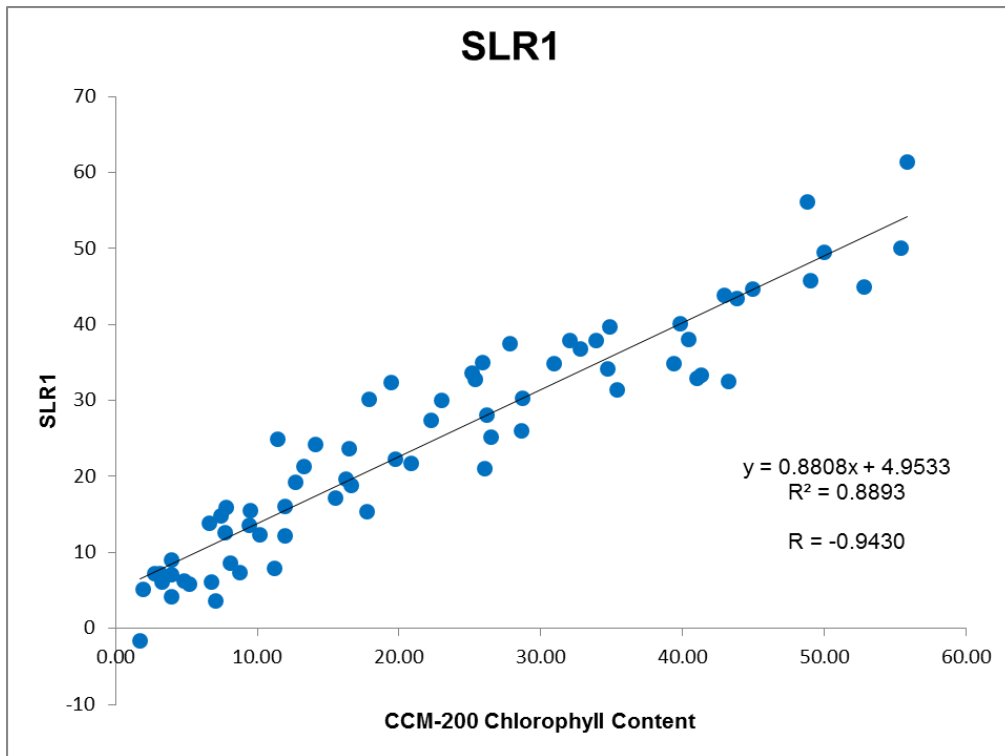


Figure 5.15. Relationship between SLR1 index and CC measured by CCM-200 for all days dataset (mean values of three shots are used for days 18 and 21). Regression line, equation, R^2 and R values are shown.

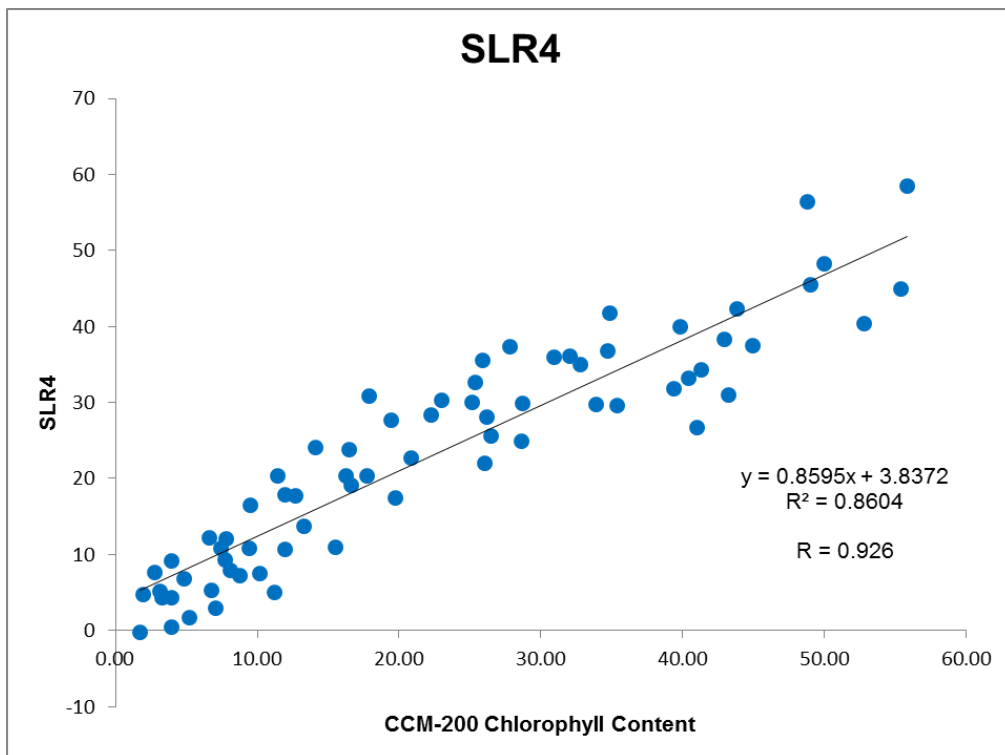


Figure 5.16. Relationship between SLR4 index and CC measured by CCM-200 for all days dataset (mean values of three shots are used for days 18 and 21). Regression line, equation, R^2 and R values are shown.

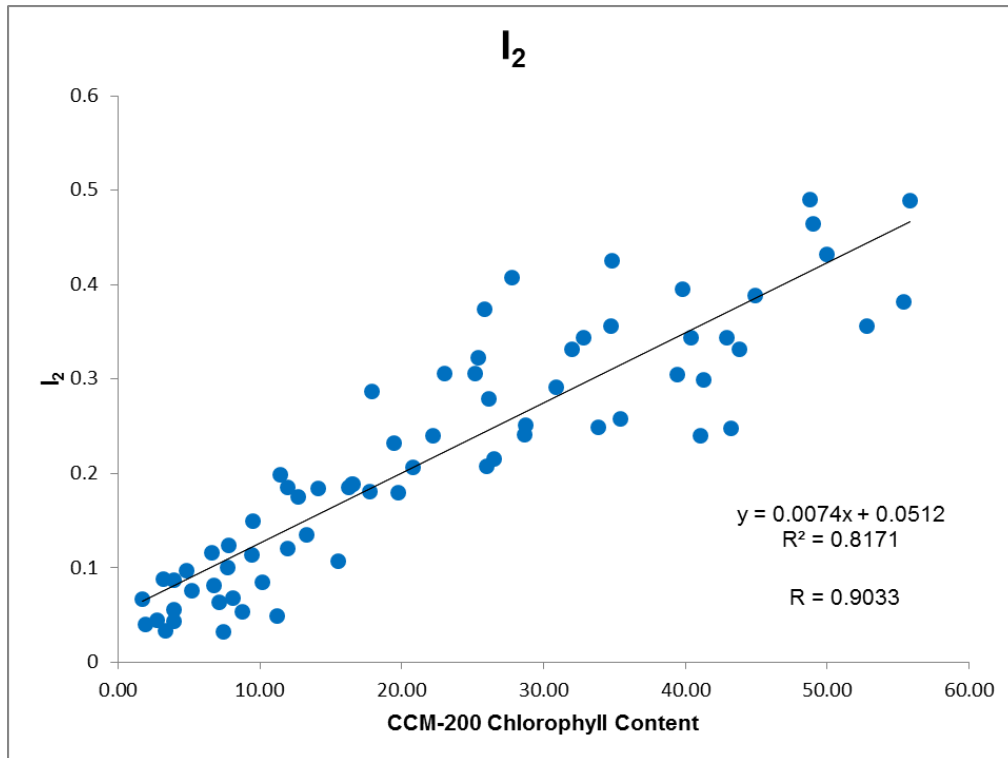


Figure 5.17. Relationship between I_2 index and CC measured by CCM-200 for all days dataset (mean values of three shots are used for days 18 and 21). Regression line, equation, R^2 and R-values are shown.

5.3.3. Validation of new indices:

Figure 5.18 and 5.19 show predicted and measured CCI for I_1 and I_2 . The graphics reflects only index validation subdataset. As it can be observed both indices predicted CCI with a good degree of reliability. Root mean square error for I_1 and I_2 applied to control subdataset was 6.23 CCI and 6.42 respectively.

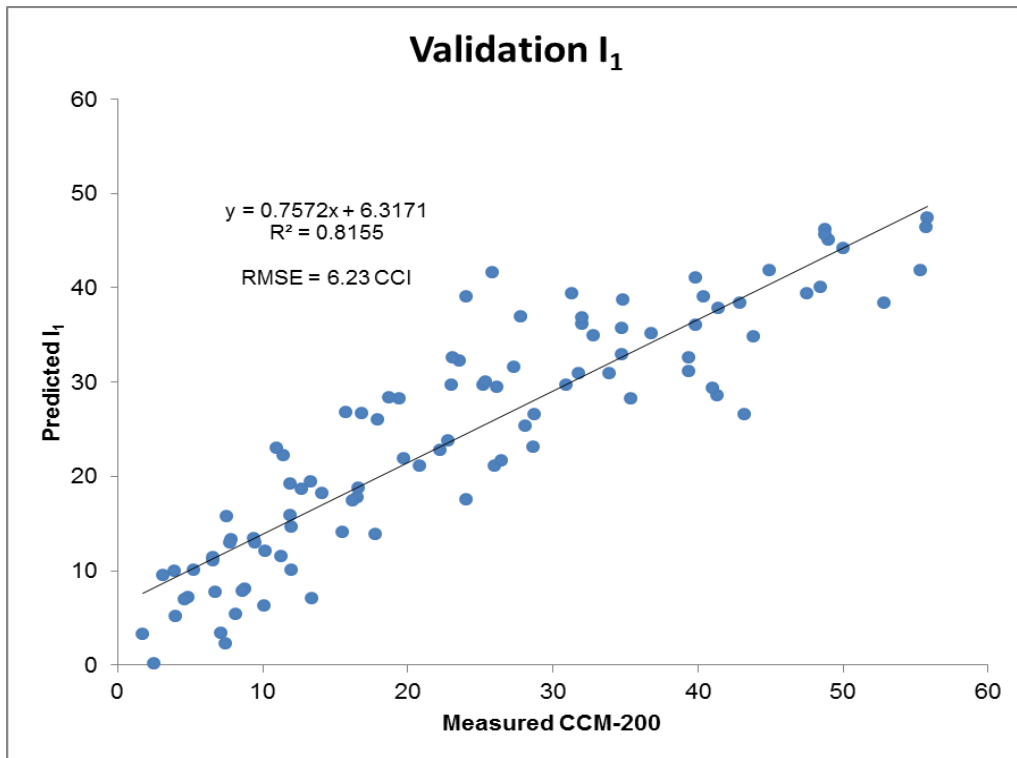


Figure 5.18. Measured CCI with CCM-200 vs. predicted with I₁ for validation subdataset

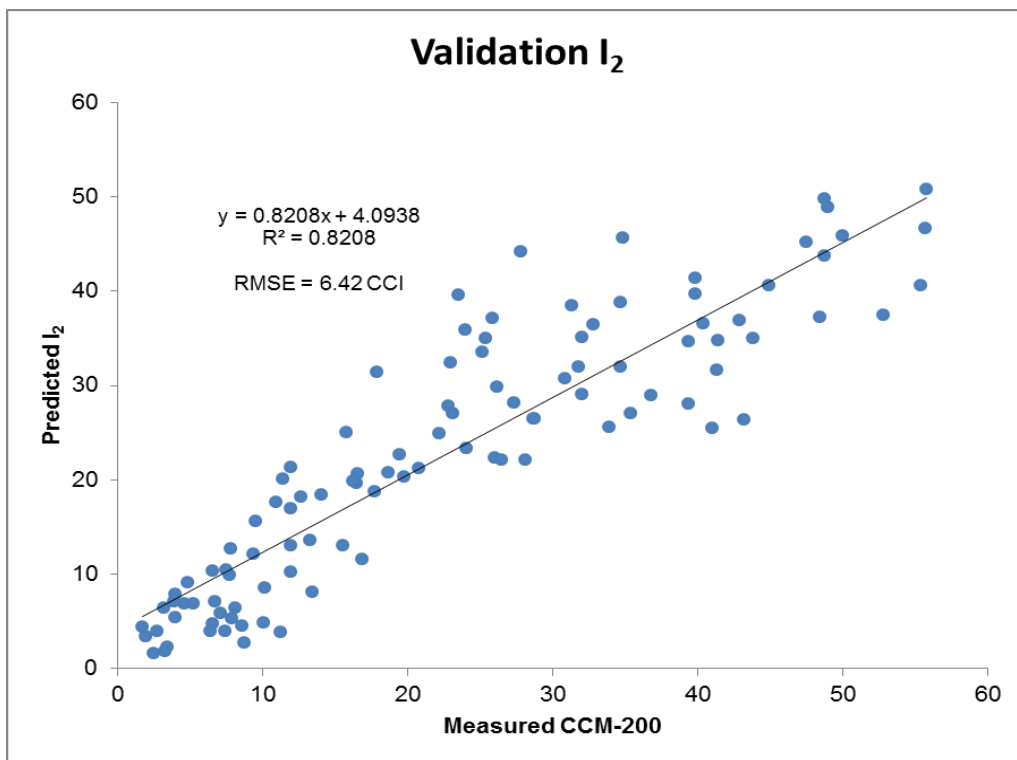


Figure 5.19. Measured CCI with CCM-200 vs. predicted with I₂ for validation subdataset

5.3.4. Analysis of indices performance:

5.3.4.1 Hourly evolution

In figures 5.20, 5.21, 5.22 and 5.23 we can observe the dispersion graphs of the $(R-B)/(R+G+B)$ (similar to $R-B/R+B$), I_{PCA} , I_1 and I_2 indices in the three shoots of the first and the last experimentation day, in addition to coefficient of determination for the average measurements. In general, in both days, the three shoots had very close values for every cited index, thus minimizing the differences produced by changes in solar elevation over time, and the changeable sky conditions during the day.

In day 18 (figures 5.20, 5.21, 5.22 and 5.23 on the left) we can observe minimal changes between shoots in every index, which present almost identical gradient values and intercepts.

In day 21 (figures 5.20, 5.21, 5.22 and 5.23 on the right), a slight variation in every index can be seen, greater in relation to day 18. However, the intercept variations do not exceed 5% in any case. As for gradients, $(R-B)/(R+G+B)$ and I_2 indices reveal almost parallel straight lines, while I_{PCA} and I_1 have slightly different straight lines for the second shot, different to the former two.

This small difference between shots in both days may be due to sky conditions, as day 18 was a cloudy, rainy day and (as reported in the literature) those are better conditions for shooting. However, the variations between shots during the apparently less favorable conditions in day 21 (a cloudless day) are minimal, in light of the results.

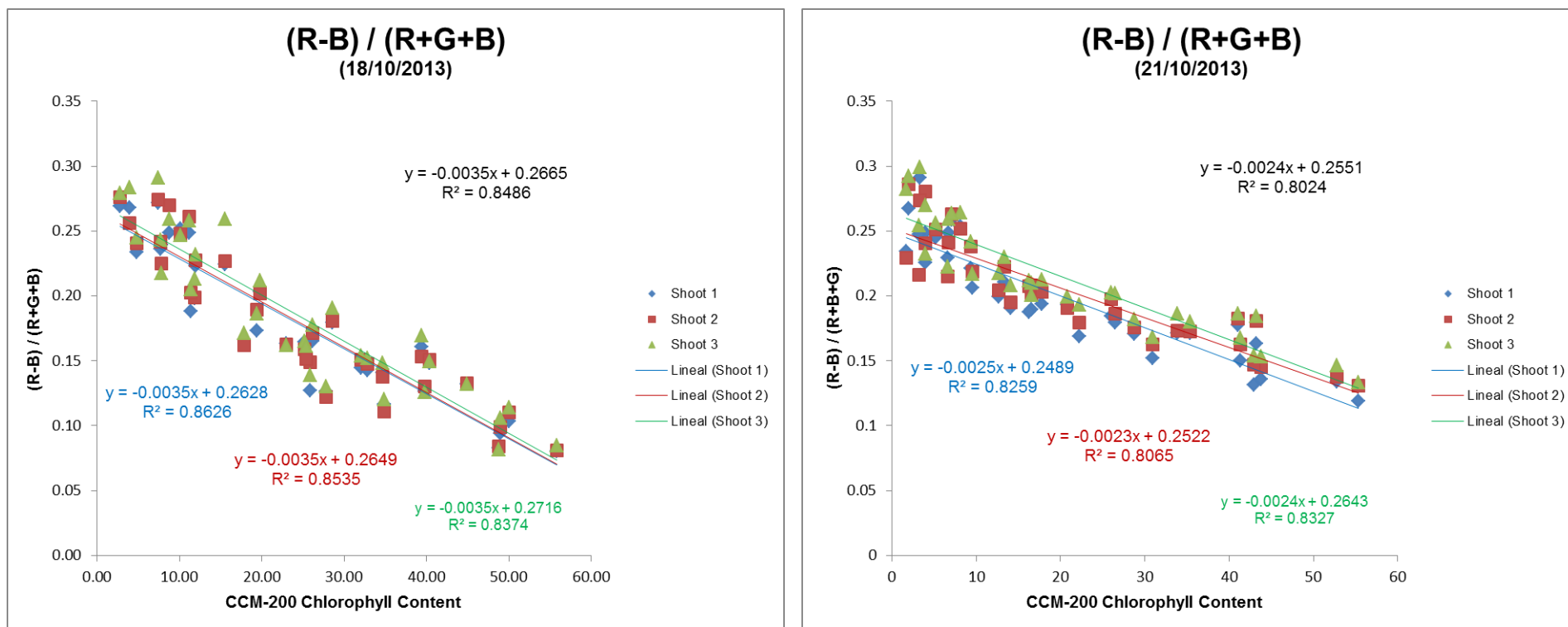


Figure 5.20. Relationship between $(R-B)/(R+G+B)$ index and CC measured by CCM-200 for three shoots on day 18th (left) and day 21st (right). Regression lines, equations and coefficient of determination are shown.

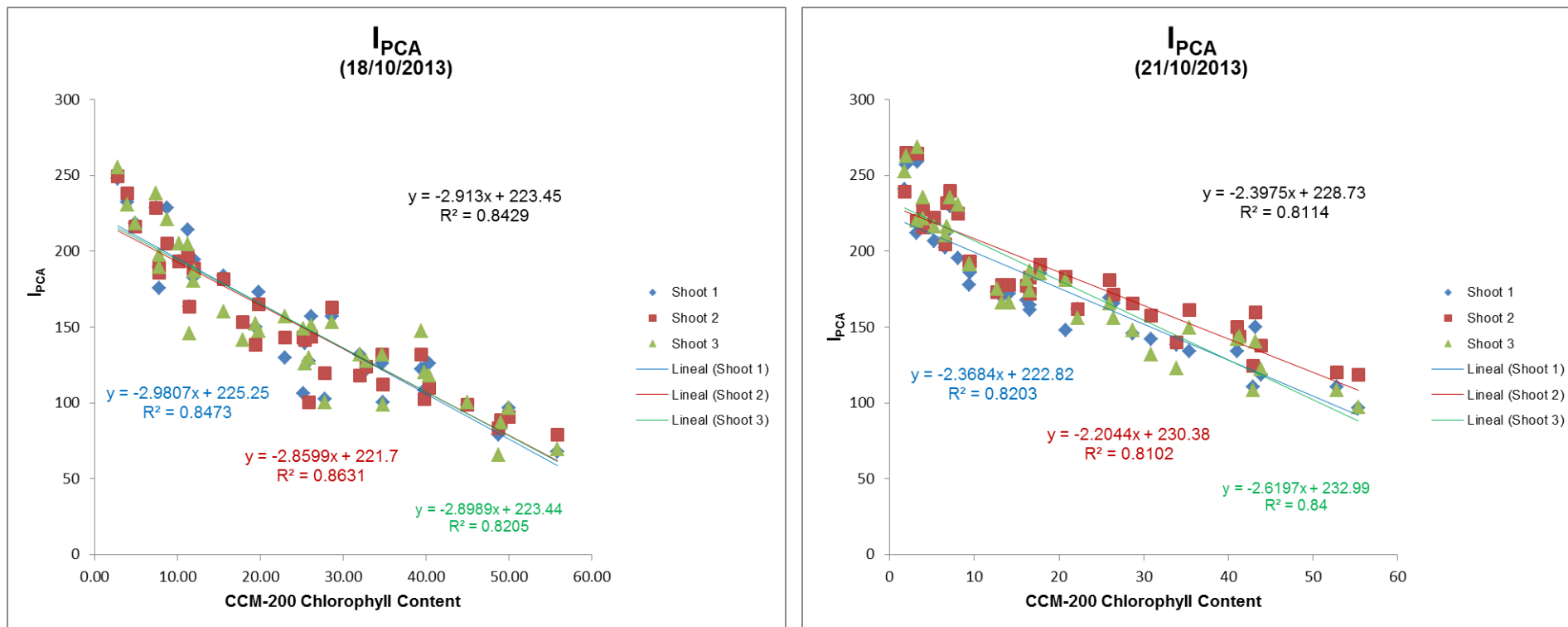


Figure 5.21. Relationship between IPCA index and CC measured by CCM-200 for three shoots on day 18th (left) and day 21st (right). Regression lines, equations and coefficient of determination are shown.

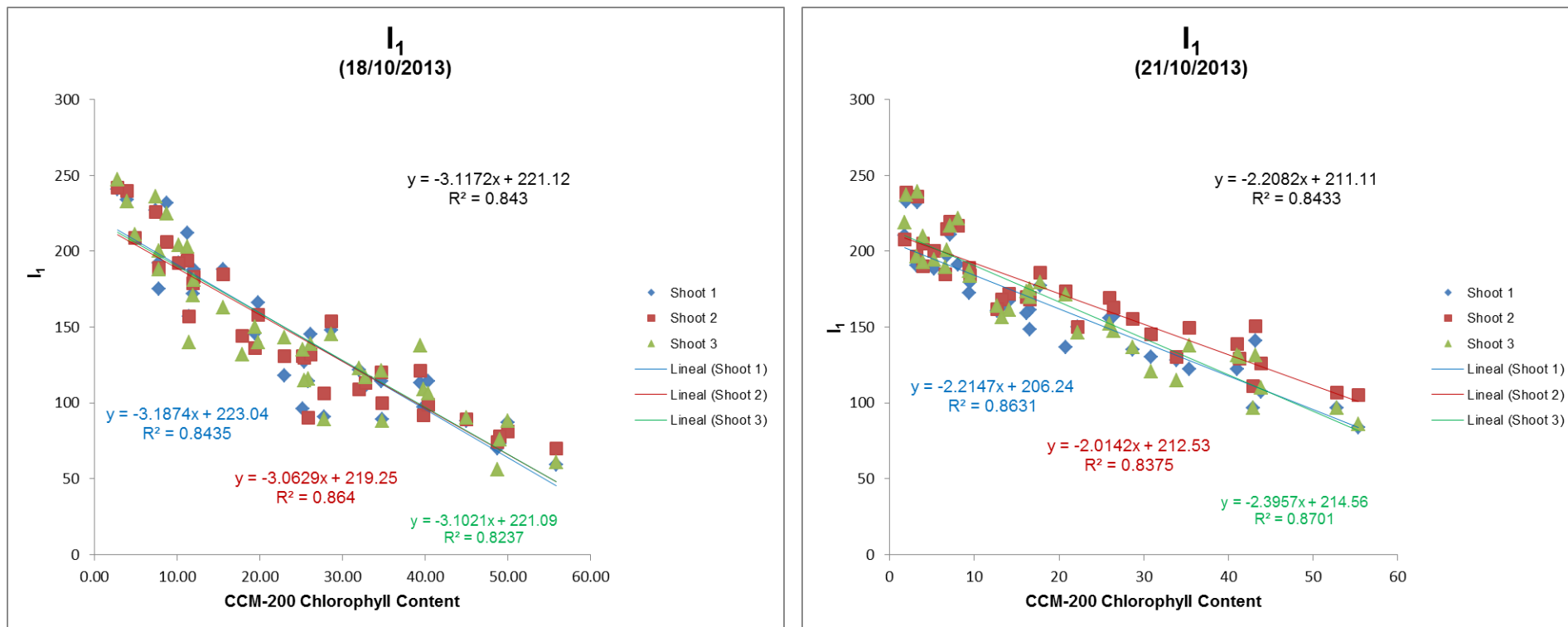


Figure 5.22. Relationship between I1 index and CC measured by CCM-200 for three shoots on day 18th (left) and day 21st (right). Regression lines, equations and coefficient of determination are shown.

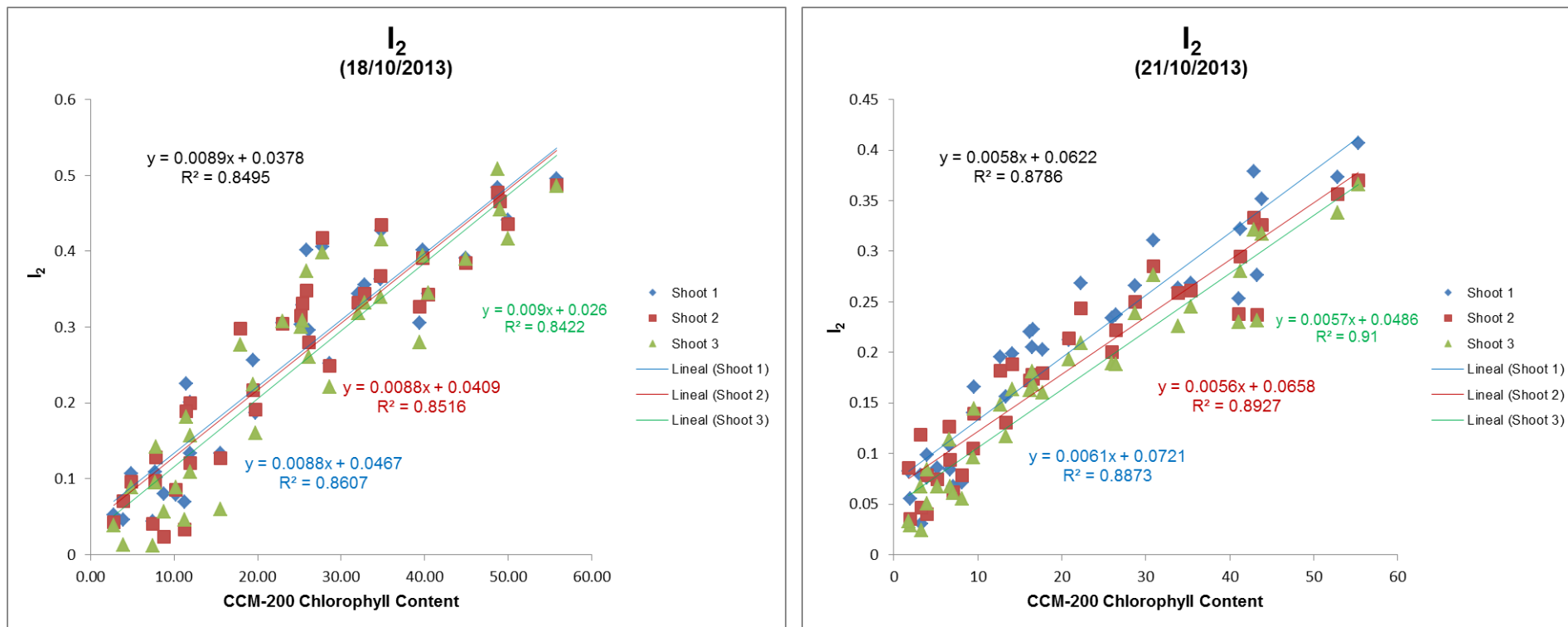


Figure 5.23. Relationship between SLR6 index and CC measured by CCM-200 for three shoots on day 18th (left) and day 21st (right). Regression lines, equations and coefficient of determination are shown.

5.3.4.2 Daily evolution

Figures 5.24 and 5.25 show the relationship between $(R-B)/(R+G+B)$ (similar to $R-B/R+B$), I_{PCA} , I_1 and I_2 indices and chlorophyll content for the validation subdataset. The graphs show how for the changeable conditions (cloudless, rainy, cloudy) during the experiment, these indices describe leaf chlorophyll content evolution measure with CCM-200, which is a decrease due to its own degradation in this case.

As it has been reported, chlorophyll content decreases each day (Table 5.4), and this trend is reflected on index values (Table 5.10). Then, analysing the evolution of the four indices, we obtain how it increases for $(R-B)/(R+G+B)$, I_{PCA} and I_1 (negative correlation) and decreases in case of I_2 (positive correlation). Figures 5.24 and 5.25 also illustrate this behaviour: on the one hand, for those indices presenting negative correlation with the chlorophyll content, the values of each day are higher than in the previous dates; on the other hand, for the SLR6 index, with positive correlation, the values are lower.

Therefore, it can be observed how the regression lines approximate to each other, even overlapping at low chlorophyll contents. This responds to the fact that leaves with initial low chlorophyll content are not going to deteriorate in the same grade than those which starting content was higher. In general, for all the indices the regression lines get separated, which reflects degradation day by day, greater between extrem days (18th and 21st) and lower between consecutive day (18th and 19th).

In this sense, $(R-B)/(R+G+B)$ index is apparently less accurate when analysing the evolution of those leaves which initial chlorophyll content is low. In this case, the lines of the different days would overlap till 20 CCI approximately. The same applies for I_2 but the range is limited to the first 10 CCI. This problem is almost eliminated in case of I_{PCA} and I_1 .

New calculated indices improve the already good performance of both indices found in bibliographic review which have the best results for this experiment data. This way, coefficient of determination of both new indices for the validation subdataset is slightly higher than the other indices. I_1 simplifies I_{PCA} and increases R^2 keeping its good

performance for low chlorophyll contents. Regarding to I_2 , it offers the highest global R^2 and improves $(R-B)/(R+G+B)$ performance in low chlorophyll content leaves.

Table 5.10. Summary of descriptive statistics for $(R-B)/(R+G+B)$, I_{PCA} , I_1 and I_2 indices for daily values: minimum, maximum, mean, standard error and coefficient of variation.

Index	Date	max	min	mean	std. Error	CV
$(R-B)/(R+G+B)$	18/10/2013	0.28	0.08	0.18	0.01	31.58
	19/10/2013	0.30	0.11	0.20	0.01	27.49
	20/10/2013	0.31	0.12	0.21	0.01	22.12
	21/10/2013	0.29	0.13	0.21	0.01	20.18
I_{PCA}	18/10/2013	250.89	72.08	151.88	7.99	31.11
	19/10/2013	246.64	82.54	157.64	8.15	30.59
	20/10/2013	255.08	90.17	175.74	7.38	24.86
	21/10/2013	263.98	104.01	179.17	7.03	23.21
I_1	18/10/2013	243.33	63.33	144.50	8.57	35.07
	19/10/2013	243.13	73.41	150.69	8.48	33.31
	20/10/2013	244.87	82.44	168.86	7.20	25.22
	21/10/2013	245.33	96.00	172.41	6.52	22.39
I_2	18/10/2013	0.49	0.03	0.26	0.02	56.42
	19/10/2013	0.44	0.02	0.22	0.02	60.60
	20/10/2013	0.40	0.01	0.19	0.02	56.40
	21/10/2013	0.38	0.03	0.18	0.02	53.31

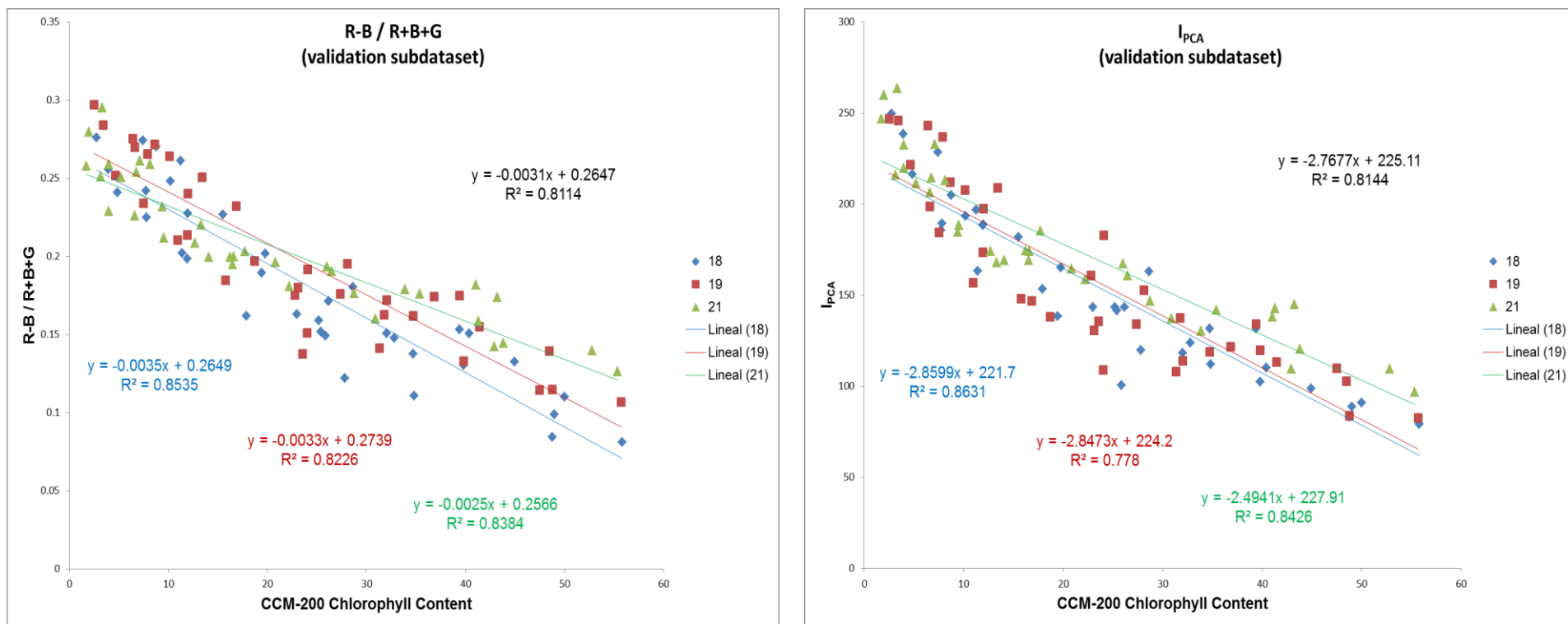


Figure 5.24. Relationship between (R-B)/(R+G+B) index (left), I_{PCA} index (right) and CC measured by CCM-200 validation subdataset. Regression lines, equations, daily and global R² values are shown.

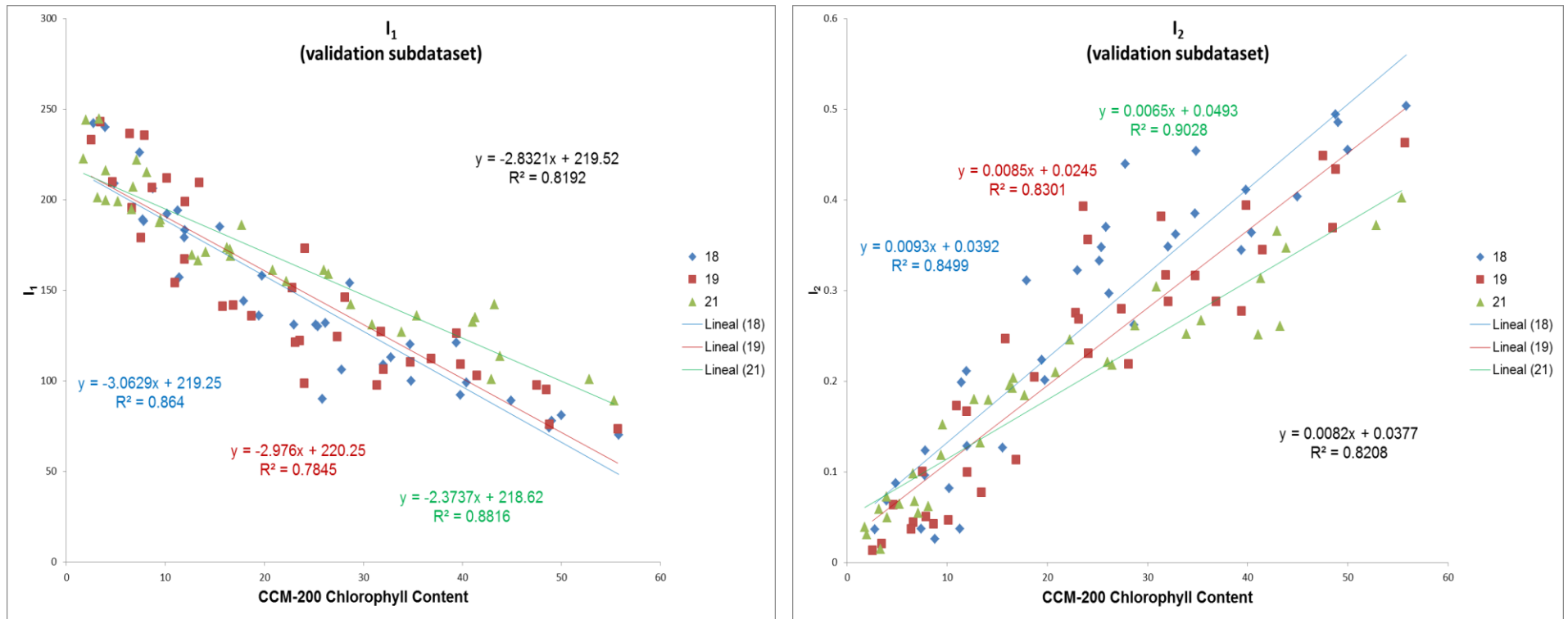


Figure 5.25. Relationship between I1 index (left), I2 index (right) and CC measured by CCM-200 for validation subdataset. Regression lines, equations, daily and global R² values are shown.

5.3.5. Analysis of Leaf data acquisition procedure

Results show that the procedure worked well to compare CC from leaves at different hours and days with different light conditions during harvest time. What is more, evolution of indices along the 4 days of study reproduces the chlorophyll degradation process even with different light conditions.

5.4. CONCLUSIONS

The main aim of this study was to test the vegetation indices based on visible spectrum for chlorophyll content determination in spring sown sugar beet leaves, at the final stage of the cultivation period. Furthermore, we intended to understand the feasibility of this kind of analysis using inexpensive, conventional off-the-shelf cameras and commonly used image-processing software. As a result in this research high correlations for sugar beet leaves have been found.

Based on the study, the selected indices from scientific literature ($R-B/R+B$), ($R-B/R+B+G$) and I_{PCA} , and novel ones I_1 and I_2 may be used for analyzing the chlorophyll content and, therefore, the nitrogen content in spring sowing sugar beet leaves for different natural light conditions in harvest season.

Shoots procedure to leaf data acquisition has been proved to work to compare measurements at different hours in a day and different days. Even in those cases where the optical meter has obtained wrong values, the indices show correctly the decrease of leaves chlorophyll content. Even so there is room for imagen calibration improvement.

Determination of leaves nitrogen status in the last stage of sugar beet crop is outstanding considering that high levels in that cultivation period have a negative effect on sugar yield. So this study is a first step to provide an easy and non-expensive tool to detect changes in nitrogen levels of sugar beet at final cultivation stage.

The results showed in this work allow us to go further through this line research and to start to investigate at canopy scale.

5.5. REFERENCES

- AIMCRA (Asociación de Investigación para la Mejora del Cultivo de la Remolacha Azucarera) 2015. <http://www.aimcra.es> [last visited 2015/09/26]
- Bruinsma, J., 1963. The quantitative analysis of chlorophylls a and b in plant extracts. *Photochem. Photobiol.* 2, 241–249.
- Clever-s, J. G. P. W (1997). A Simplified Approach for Yield Prediction of Sugar Beet Based on Optical Remote Sensing Data. *KEMOTE SENS. ENVIKON.* 61:221-228 (1997) OElsevier Science Inc., 1997.
- Croft, H., Chen, J.M, Zhang, Y., Simic, A., Noland, T.L., Nesbitt, N., Arabian, J. (2015) Evaluating leaf chlorophyll content prediction from multispectral remote sensing data within a physically-based modelling framework. *ISPRS Journal of Photogrammetry and Remote Sensing* 102 (2015) 85–95.
- Derksen, S. and H. J. Keselman. 1992. Backward, forward and stepwise automated subset selection algorithms: Frequency of obtaining authentic and noise variables. *British Journal of Mathematical and Statistical Psychology* 45: 265-282.
- Draycott, A.P., Christenson, D.R., 2003. *Nutrients for Sugar Beet Production: Soil–Plant Relationships.* CAB International, Wallingford, 242 pp.
- El-Faki, M., Zhang, N., Peterson, D., 2000b. Weed detection using color machine vision. *Trans. ASAE* 43 (6), 1969–1978.
- Garcia-Ruiz, F.J., Wulfsohn, D., Rasmussen, J.(2015) Sugar beet (*Beta vulgaris* L.) and thistle (*Cirsium arvensis* L.) discrimination based on field spectral data. *biosystems engineering* 139 (2015) 1-5.
- Gholizadeh, A., Amin, M.S.M., Anuar, A.R., Aimrun, W., Saberioon, M.M., 2011. Temporal variability of SPAD chlorophyll meter readings and its relationship to total nitrogen in leaves within a Malaysian paddy field. *Aust. J. Basic Appl. Sci.* 5 (5), 236–245.
- Gitelson, A. A., Kaufman, Y. J., Stark, R., & Rundquist, D. (2002). Novel algorithms for remote estimation of vegetation fraction. *Remote Sensing of Environment*, 80, 76–87.

- Goddijn, L.M., White, M., 2006. Using a digital camera for water quality measurements in Galway Bay. *Estuarine, Coastal and Shelf Science* 66, 429–436.
- Golzarian, M.R., Frick, R.a., 2011. Classification of images of wheat, ryegrass and brome grass species at early growth stages using principal component analysis. *Plant Meth.*7(1),28.
- Gordo-Ingelmo, L.F (1994). *Composición química y control agrícola de los no-azúcares en la remolacha azucarera*. Caja de Ahorros Municipal de Burgos. ISBN: 84-87152-25-2
- Grzebisz W., Pepliński K., Szczepaniak W., Barłóg P., Cyna K. (2012). Impact of nitrogen concentration variability in sugar beet plant organs throughout the growing season on dry matter accumulation patterns. *J. Elem.* 17(3): 389-407, DOI: 10.5601/jelem.2012.17.3.03.
- Hillnhütter, C., Mahlein, A. -K., Sikora, R., & Oerke, E. -C. (2011). Remote sensing to detect plant stress induced by *heterodera schachtii* and *rhizoctonia solani* in sugar beet fields. *Field Crops Research*, 122(1), 70–77.
- Hunt, E.R., Daughtry, C.S.T., Eitel, J.U.H., Long, D.S., 2011. Remote sensing leaf chlorophyll content using a visible band index. *Agronomy Journal* 103, 1090–1099.
- Hunt, E. R., Doraiswamy, P.C., McMurtrey, J. E., et al. (2013) A visible band index for remote sensing leaf chlorophyll content at the canopy scale. *International Journal of Applied Earth Observation and Geoinformation* 21 (2013) 103–112.
- Judd C. M., McClelland G. H., and Ryan C. S. *Data Analysis: A Model Comparison Approach* (2e). Published by Routledge, 2008. ISBN: 978-0-8058-3388-1.
- Kataoka, T., Kaneko, T., Okamoto, H., Hata, S., 2003. Crop growth estimation system using machine vision. In: *Proceedings of IEEE/ASME International Conference on Advanced Intelligent Mechatronics (AIM)*, vol. 2, pp. 1079–1083.
- Kawashima, S. and Nakatani, M. (1998). An Algorithm for Estimating Chlorophyll Content in Leaves Using a Video Camera. *Annals of Botany* 81: 49-54, 1998.
- Kazmi,W., Garcia-Ruiz, F.J., Nielsen, J., Rasmussen, J., Jørgen Andersen, H. (2015). Detecting creeping thistle in sugar beet fields using vegetation indices. *Computers and Electronics in Agriculture* 112 (2015) 10–19.

- Kimes, D.S., 1983. Dynamics of directional reflectance factor distributions for vegetation canopies. *Applied Optics* 22: 1364±1372.
- K.W. Jaggard and C.J.A. Clark (1990). Remote sensing to predict the yield of sugar beet in England. AFRC Institute of Arable Crops Research Broom's Barn, Higham, Bury St Edmunds, Suffolk IP28 6NP, U.K.
- Lee, K.J., Lee, B.W., 2013. Estimation of rice growth and nitrogen nutrition status using colour digital camera image analysis. *Eur. J. Agron.* 48, 57–65.
- Link, A., Reusch, S., 2006. Implementation of site-specific nitrogen application status and development of the YARA N-sensor. In: NJF Seminar 390, Precision Technology in Crop Production Implementation and Benefits, Lillehammer, Norway, November 7–8, 2006. Norsk Jernbaneforbund, Stockholm, Sweden, pp. 37–41.
- Li, Y., Chen, D., Walker, C.N., Angus, J.F., 2010. Estimating the nitrogen status of crops using a digital camera. *Field Crops Res.* 118, 221–227.
- Mahlein, A.K., Rumpf, T., Welke, P., Dehne, H.W., Plümer, L., Steiner, U., Oerke, E.C. (2013). Development of spectral indices for detecting and identifying plant diseases. *Remote Sensing of Environment* 128 (2013) 21–30.
- Malnou, C.S., Jaggard, K.W., Sparkes, D.L. Nitrogen fertilizer and the efficiency of the sugar beet crop in late summer, *European Journal of Agronomy*, Volume 28, Issue 1, January 2008, Pages 47-56, ISSN 1161-0301.
- Manderscheid, R., Pacholski, A., Weigel, H.-J., 2010. Effect of free air carbon dioxide enrichment combined with two nitrogen levels on growth, yield and yield quality of sugar beet: evidence for a sink limitation of beet growth under elevated CO₂. *Eur. J. Agron.* 32, 228–239.
- Mao, W., Wang, Y., Wang, Y., 2003. Real time detection of between-row weeds using machine vision. In: ASAE Annual Meeting, St. Joseph, MI, Paper No. 031004.
- Meisinger, J.J., Schepers, J.S., Raun, W.R., 2008. Crop nitrogen requirement and fertilization. In: Schepers, J.S., Raun, W.R. (Eds.), *Nitrogen in Agricultural Systems*. Agronomy Monograph, 49. ASA-CSSA-SSSAJ, Madison, WI, pp. 563–612.

- Meyer, G.E., Mehta, T., Kocher, M.F., Mortensen, D.A., Samal, A., 1998. Textural imaging and discriminant analysis for distinguishing weeds for spot spraying. *Trans. ASAE* 41 (4), 1189–1197.
- Microsoft. Microsoft Excel. Redmond, Washington: Microsoft, 2010. Computer Software.
- Murphy, R.J., Underwood, A.J., Jackson, A.C. (2009) Field-based remote sensing of intertidal epilithic chlorophyll: Techniques using specialized and conventional digital cameras. *Journal of Experimental Marine Biology and Ecology* 380 (2009) 68–76.
- O'Rourke, N., & Hatcher, L. (2013). *A Step-by-Step Approach to Using SAS for Factor Analysis and Structural Equation Modeling* (2nd Ed.). Cary, NC: SAS Press. Edition: 2nd, Publisher: SAS Press, ISBN: 978-1-59994-230-8.
- Pagola, M., Ortiz, R., Irigoyen, I., Bustince, H., Barrenechea, E., Aparicio-Tejo, P., Lamsfus, C., Lasa, B., 2009. New method to assess barley nitrogen nutrition status based on image colour analysis, comparison with SPAD-502. *Comput. Electron. Agric.* 65, 213–218.
- Pinter PJ Jr, Jackson RD, Moran MS. 1990. Bidirectional reflectance factors of agricultural targets : A comparison of ground-, aircraft-, and satellite-based observations. *Remote Sensing of Environment* 32: 215-228.
- Pocock, T.O., Milford, G.F.J., Armstrong, M.J., 1990. Storage root quality in sugar-beet in relation to nitrogen uptake. *J. Agric. Sci., Camb.* 115, 355–362.
- R Development Core Team (2008). *R: A language and environment for statistical computing*. R Foundation for Statistical Computing, Vienna, Austria. ISBN 3-900051-07-0, URL <http://www.R-project.org>.
- Saberioon, M.M., Amina, M.S.M, Anuar, A.R., Gholizadeh, A., Wayayok, A., Khairunniza-Bejo, S. (2014) Assessment of rice leaf chlorophyll content using visible bands at different growth stages at both the leaf and canopy scale. *International Journal of Applied Earth Observation and Geoinformation* 32 (2014) 35–45.

- Sakamoto, T., Shibayama, M., Kimura, A., Takada, E., 2011b. Assessment of digital camera-derived vegetation indices in quantitative monitoring of seasonal rice growth. *ISPRS. Journal of Photogrammetry and Remote Sensing* 66 (6), 872–882.
- Singer J.D, Willett J.B, 2003. *Applied Longitudinal Data Analysis: Modeling Change and Event Occurrence*. Oxford University Press, USA. ISBN-13: 978-0195152968.
- Tucker, C.J., 1979. Red and photographic infrared linear combinations for monitoring vegetation. *Remote Sens. Environ.* 8, 127–150.
- Vollmann, J., Waltera, H., Sato, T., Schweiger, P. (2011). Digital image analysis and chlorophyll metering for phenotyping the effects of nodulation in soybean. *Computers and Electronics in Agriculture* 75 (2011) 190–195.
- Woebbecke, D., Meyer, G.E., Von Bargen, K., Mortensen, D.A., 1995. Color indices for weed identification under various soil, residue, and lighting conditions. *Trans. ASAE* 38 (1), 259–269.
- Yadav, S.P., Ibaraki, Y., Gupta, S.D., 2010. Estimation of the chlorophyll content of micropropagated potato plants using RGB based image analysis. *Plant Cell Tissue Organ Cult.* 100, 183–188.
- Yamashita T., Yamashita K., Kamimura R. (2007). A Stepwise AIC Method for Variable Selection in Linear Regression. *Communications in Statistics - Theory and Methods*. Vol. 36, Iss. 13.

5.6. PRACTICAL APPLICATION OF DEVELOPED METHODOLOGY TO OTHER CASE STUDIES

Detection of *Sinapis arvensis* Weeds in Alfafa Crop by Using RGB Indices (short communication)

Luis Fernando Sánchez Sastre

Agriculture and Forestry Engineering Department, ETSIIAA, Universidad de Valladolid, Avenida de Madrid 44, 34004 Palencia, Spain.

INTRODUCTION

The current growth of the UAV (Unmanned Aerial Vehicle) has been increasingly used for farming applications as remote sensing platform. These aerial platforms allow to raise different data gathering sensors or devices (Eisenbeiss, 2009) as commercial digital cameras (Teoh et al., 2012) and even view these data in real time (Kerle et al., 2008). UAV as others low altitude remote sensing platforms can be used to obtain high resolution images below cloud cover and near the field (Saberioon et al., 2014) allowing to get data when it is required even in real time (Hunt et al., 2005). In addition, they have a relative low cost and allow to obtain measurements of continuous areas and to get to difficult access places.

Traditionally, remote sensors used in the canopy detection are active and passive type (Moorthy et al., 2011). Systems based on passive teledetection depend on the variability of spectral answers of vegetation in the region of the visible and NIR (near infrared). There are many indices related to vegetation cover and chlorophyll content that can be classified depending on the part of the spectrum that is worked with (Hunt et al., 2013) and which have applications such as detection of nitrogen deficiencies (Mercado-Luna et al., 2010), continuous monitoring of crop status (Sakamoto et al., 2012), disease detection (Hillnhütter et al., 2011), vegetation phenology and ecosystem indicators (Motohka et al., 2010), even weed detection (Kazmi et al. 2015; García-Ruiz et al. 2015).

However, expensive multispectral sensors are needed for most of these indices. Nevertheless, indices based on RGB bands of the visible spectrum from images captured with commercial cameras can have a good performance in some of those areas. In this way, Kawashima and Nakatani (1998) proposed a R-B / R+B index to calculate chlorophyll content in rice leaves using a video-camera.

Also, based on the good correlations shown by R-B/R+B and R-B/R+B+G at leaf scale for sugar beet leaves (see second research on this thesis document), considering that the colour rank in that study was from dark green to yellow, it was proposed to use these indices for checking its possible utility in detection of yellow weeds in fields of green crops. So in the frame of European LIFE Project Operation CO₂ yellow weeds (*Sinapis arvensis*) infection occurred in alfalfa crop (*Medicago sativa*) plots sited in the experimental parcel of Soto de Cerrato (Palencia, Spain) which belongs to University of Valladolid. Thus images from UAV were used to make a mosaic from which were calculated R-B/R+B, R-B/R+B+G and NDVI index (Tucker, 1979) for visual comparison.

METHODOLOGY

For picture captures there were used two commercial cameras set on a UAV Mikrokopter UfocamXXL8 V3 (Figure 5.26). An Olympus Pen EPM-1 (12.3 megapixels and 4/3" Live MOS sensor) were used for the RGB pictures and a commercial Olympus EP1 camera (also with a 12.3 megapixels Live MOS sensor) for NIR. In this camera it has been removed the low pass filter to block IR and it was installed a high pass IR filter which blocks in 720nm. This new filter blocks visible part of the spectre and it allows to capture NIR.



Figure 5.26. NIR and RGB cameras mounted in Mikrokopter Ufocam

Captured pictures were processed with Agisoft PhotoScan (PS) (Agisoft LLC, San Petersburgo, Russia). This software implements SFM-DMVR (Structure From Motion - Digital Multi-View 3D Reconstruction), which allows to produce 3D high precision and quality models based on a collection of disorganized pictures of an scene or an object, taken from different points of view with great accuracy and low deviation. Digital treatment of the pictures was also carried out with PCI-Geomatica 9.1.

Before the flights, it was need to mark 10 control points on the ground of known coordinates in order to correct geometrically and georeferer mosaics and the 3D model.

Flight height was set in 60 meters. Minimum longitudinal and transverse overlap, was 70% and 40% respectively, in order to guarantee the correct generation of the 3D model with Agisoft PhotoScan.

From each picture set, visible and NIR, a georefered orthophoto and a 3D model were produced in PhotoScan by different routines in a semiautomatic process in which the camera positions are calculated and control points are added. The process is repeated for each set, obtaining two georefered orthophotos (Visible and NIR) which should overlap perfectly sharing the same control points.

Both orthophotos are imported to PCI-Geomatic and the 4 channels are joined together (NIR-R-G-B)

RESULTS

Next figures successively show the comparison between the RGB generated orthophoto and the orthophotos in NIR, NDVI, $(R-B / R+B)$ and $(R-B / R+B+G)$

It can be observed in the figure 5.27 how the NIR picture allows to differentiate between vegetation and soil but weeds are not distinguished at all.

NDVI in figure 5.28 also differentiate soil from vegetation and also yellow weeds but those can be confused with soil as both are shown with dark hues.

In the cases of $(R-B/R+B)$ and $(R-B/R+B+G)$ (figures 5.29 and 5.30 respectively) seem to be more sensitive to yellow spots showing them clearly with whitish hues. Besides this, weeds are not confused with soil as it happens with NDVI. These indices seem to be also sensitive to light green, which apparently may introduce some noise in the picture.

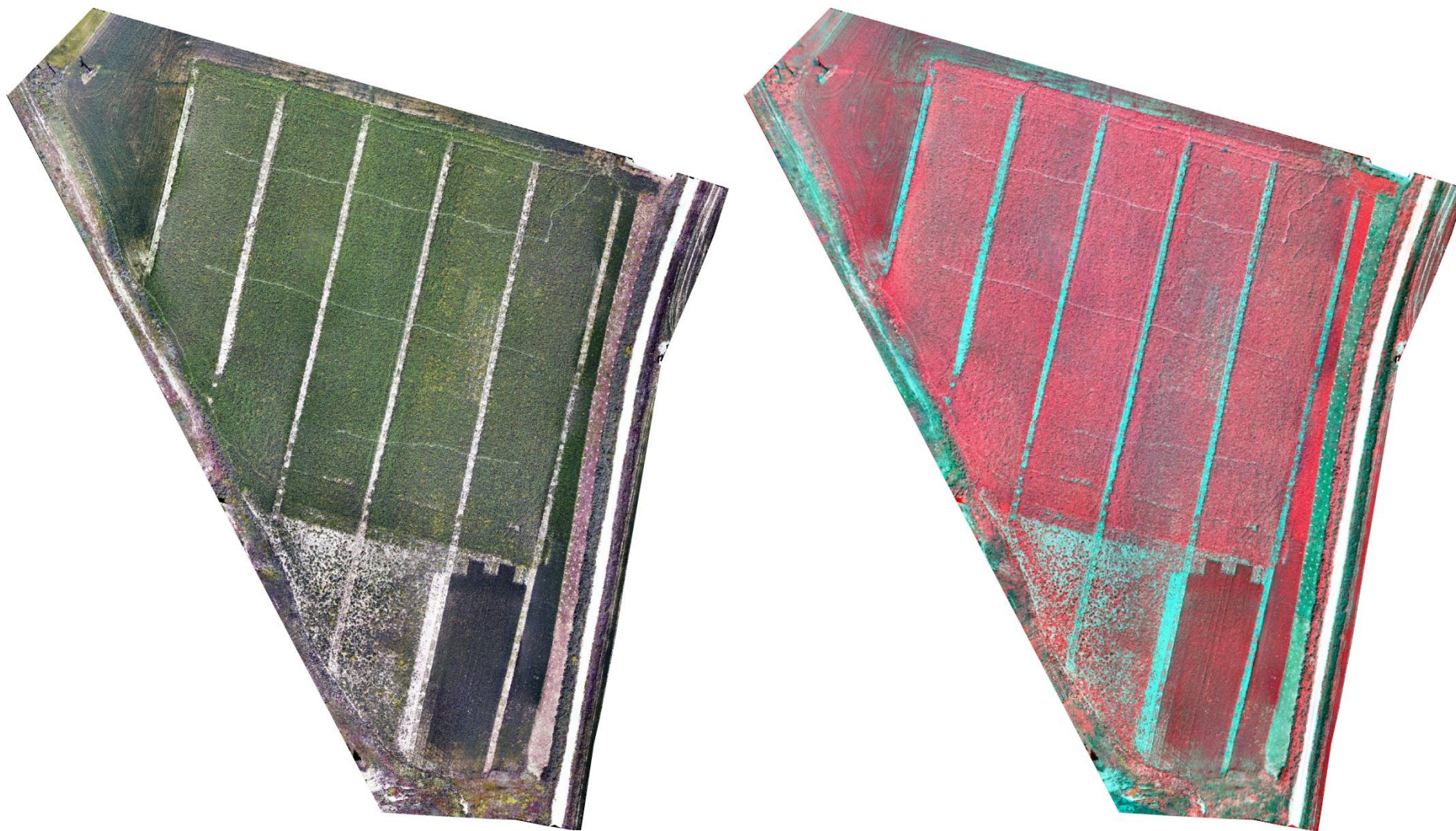


Figure 5.27. RGB vs. NIR-R-G composition

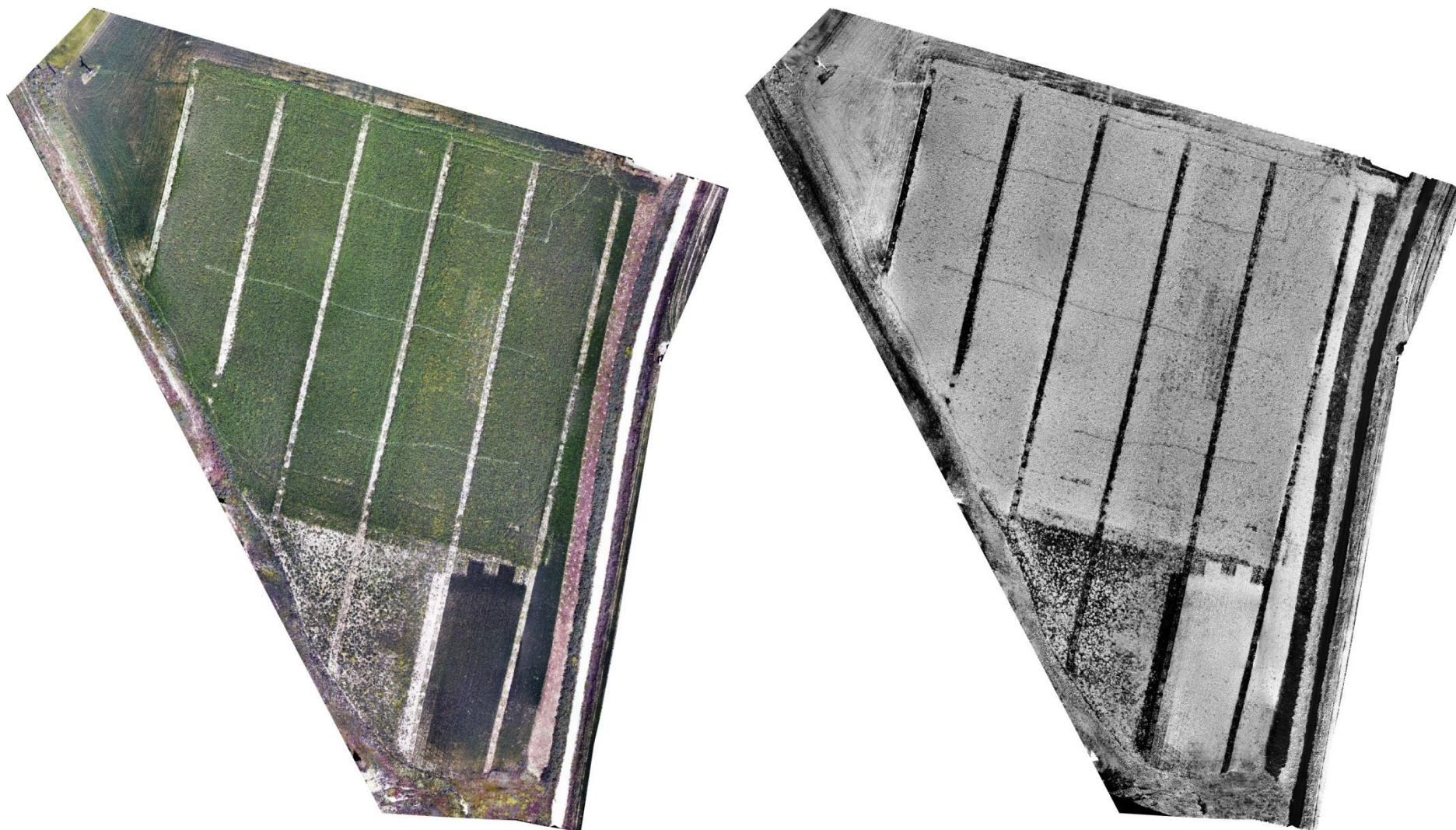


Figure 5.28. RGB vs. NDVI

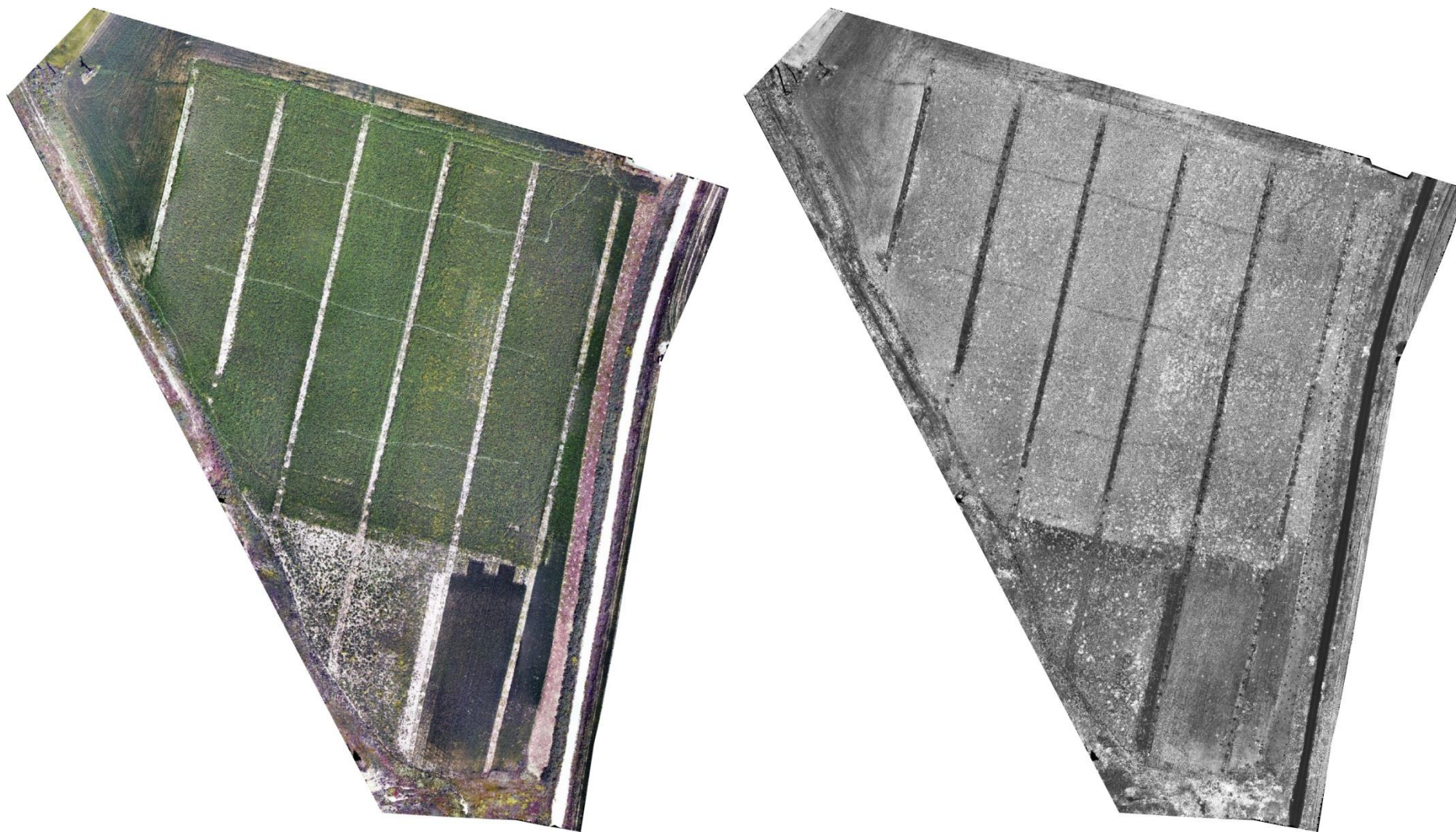


Figure 5.29. RGB vs. $(R-B)/(R+B)$

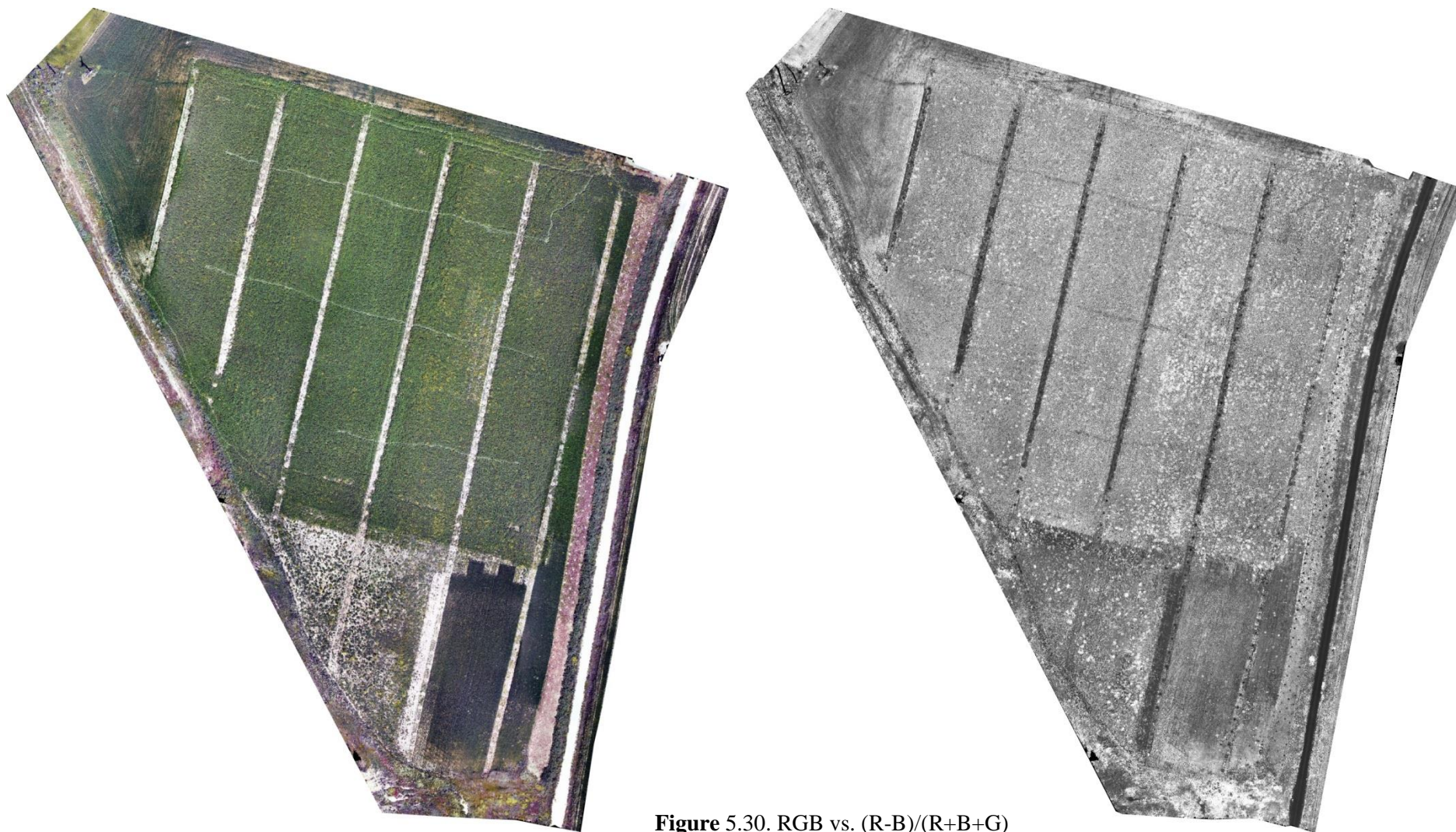


Figure 5.30. RGB vs. $(R-B)/(R+B+G)$

CONCLUSIONS

A combination of UAV with a conventional camera to get pictures, which allow to calculate vegetation indices based on RGB, can be a cheap and effective solution for weed detection.

In this work $(R-B / R+B)$ and $(R-B / R+B+G)$ indices were proved to be useful to detect yellow weeds (*Sinapis arvensis*) in an alfalfa crop (*Medicago sativa*).

Besides, $(R-B / R+B)$ and $(R-B / R+B+G)$ are more sensitive than NDVI in the detection of yellow weeds, with the advantage of not confusing weeds with soil.

As both indices seem to have great sensitivity to slight variations of colours from green to yellow, even overestimating them, they can be useful to the early detection of yellow weeds as soon as they show up.

REFERENCES

- Eisenbeiss, H.; 2009. UAV Photogrammetry. Thesis Diss. ETH No. 18515, Technische Wissenschaften ETH Zurich, IGP Mitteilung N. 105.
- Garcia-Ruiz, F.J., Wulfsohn, D., Rasmussen, J.(2015) Sugar beet (*Beta vulgaris* L.) and thistle (*Cirsium arvensis* L.) discrimination based on field spectral data. *biosystems engineering* 139 (2015) 1-5. <http://dx.doi.org/10.1016/j.biosystemseng.2015.07.012>
- Hillnhütter, C., Mahlein, A. -K., Sikora, R., & Oerke, E. -C. (2011). Remote sensing to detect plant stress induced by *heterodera schachtii* and *rhizoctonia solani* in sugar beet fields. *Field Crops Research*, 122(1), 70–77.
- Hunt, E. R.; M. Cavigelli, C.S.T.; Daugherty, J.; McMurtrey III; Walthall, C.L.; 2005. Evaluation of digital photography from model aircraft for remote sensing of crop biomass and nitrogen status. *Precis Agric*, 6: 359-378.
- Hunt, E. R., Doraiswamy, P.C., McMurtrey, J. E., et al. (2013) A visible band index for remote sensing leaf chlorophyll content at the canopy scale. *International Journal of Applied Earth Observation and Geoinformation* 21 (2013) 103–112
- Kawashima, S. and Nakatani, M. (1998). An Algorithm for Estimating Chlorophyll Content in Leaves Using a Video Camera. *Annals of Botany* 81: 49-54, 1998
- Kazmi,W., Garcia-Ruiz, F.J., Nielsen, J., Rasmussen, J., Jørgen Andersen, H. (2015). Detecting creeping thistle in sugar beet fields using vegetation indices. *Computers*

and Electronics in Agriculture 112 (2015) 10–19.
<http://dx.doi.org/10.1016/j.compag.2015.01.008>

- Kerle, N.; Huel, S.; Pfeiffer, N.; 2008. Real-time data collection and information generation using airborne sensors. En Zlatanova, S and Jonathan, L.; Geospatial Information Technology for Emergency Response. Pp 43-75. Ed. Taylor and Francis. London.
- Mercado-Luna, A., Rico-Garcia, E., Lara-Herrera, A., Soto-Zarazua, G., Ocampo-Velazquez, R., Guevara-Gonzalez, R., Herrera-Ruiz, G., 2010. Nitrogen determination on tomato (*Lycopersicon esculentum* Mill.) seedlings by colour imageanalysis (RGB). Afr. J. Biotechnol. 9 (33), 5326–5332.
- Moorthy, I., Miller, J. R., Jiménez Berni, J. A., Zarco-Tjeada, P., Hu, B., Chen, J. (2011) Field characterization of olive (*Olea europaea* L.) tree crown architecture using terrestrial laser scanning data. Agricultural and Forest Meteorology: volume 151, 204-214
- Motohka, T., Nasahara, K.N., Oguma, H., Tsuchida, S., 2010. Applicability of green-red vegetation index for remote sensing of vegetation phenology. Remote Sensing 2 (10), 2369–2387.
- Saberioon, M.M., Amina, M.S.M, Anuar, A.R., Gholizadeh, A., Wayayok, A., Khairunniza-Bejo, S. (2014) Assessment of rice leaf chlorophyll content using visible bands at different growth stages at both the leaf and canopy scale. International Journal of Applied Earth Observation and Geoinformation 32 (2014) 35–45. <http://dx.doi.org/10.1016/j.jag.2014.03.018>
- Sakamoto, T., Gitelson, A.A., Nguy-Robertson, A.L., Arkebauer, T.J., Wardlow, B.D., Suyker, A.E., 2012. An alternative method using digital cameras for continuous monitoring of crop status. Agric. For. Meteorol. 154–155, 113–126.
- Teoh, C.C., Hassan, D.A., Radzali, M.M., Jafnim, J.J., 2012. Prediction of SPAD chlorophyll meter readings using remote sensing technique. J. Trop. Agric. Food Sci. 40 (1), 127-136.
- Tucker, C.J., 1979. Red and photographic infrared linear combinations for monitoring vegetation. Remote Sens. Environ. 8, 127–150.

6. REGIONAL ANALYSIS OF SUGAR BEET CROP UNDER FUTURE SCENARIOS OF CLIMATE CHANGE

REGIONAL ANALYSIS OF SUGAR BEET CROP UNDER FUTURE SCENARIOS OF CLIMATE CHANGE

Luis Fernando Sánchez Sastre, Paula Carrión Prieto.

Agriculture and Forestry Engineering Department, ETSIIAA, Universidad de Valladolid, Avenida de Madrid 44, 34004 Palencia, Spain.

Abstract

Evapotranspiration (ET) is a main factor affecting crop yields which is related to water requirements of the plants. Because of changes predicted in future global climate it is necessary to assess the effects of different environmental conditions in crops such as sugar beet, which depend on irrigation to obtain high yields, in order to foresee measurements of adaptation. In the study presented herein future conditions extracted from RCP4.5 scenario of IPCC for 2050 and 2070, in Spanish region of Castilla y León, were used as inputs of FAO crop simulation model (Aquacrop). Thus, a regional analysis of future trends in yields, biomass and CO₂ assimilation of sugar beet crop are carried out and adaptation measurements are also proposed.

Keywords: sugar beet, climate change, AR5, evapotranspiration, Aquacrop, CO₂.

6.1. INTRODUCTION

Crop water requirements are the result of adding the crop transpiration and the evaporation produced in the soil. This addition is known as *evapotranspiration* (ET), and it basically depends on the local climate conditions: temperature, humidity, wind speed and solar radiation (Ding et al., 2013).

The essential role performed by this process in the hydrological cycle (Sellers et al., 1996, as cited in Gowda et al., 2008) is well known since long time ago, being a facet that affects crop growth fundamentally and, therefore, impacting on water demand and irrigation management (Nam et al., 2015).

An industrial crop of great importance in the Spanish region of Castilla y León is spring sown sugar beet. As many other crops, sugar beet requires more water than is provided by local precipitations, and thus irrigation is necessary to satisfy these hydrological requirements. Besides, irrigation is the most determining factor in

production, being an indispensable practice in sugar beet crop in Spain. (AIMCRA, Research Association for Sugar Beet Crop Improvement, 2005).

However, the availability of water for crop irrigation will probably decrease in the future due to increased demands from other sectors and the environment (Santos et al., 2010). Environmental changes are, in fact, a main source of uncertainty concerning future beet crop yields, especially considering the human influence on the climate system, which seems to be clear and accepted by most scientists (IPCC 2001). The latest work from the Intergovernmental Panel on Climate Change (IPCC), i.e., the Fifth Assessment Report (AR5, IPCC 2014), states that anthropogenic emissions of Green House Gases (GHG) are the highest in history and their effects are extremely likely to be the dominant cause of the observed warming since the mid-20th century (Figure 6.1).

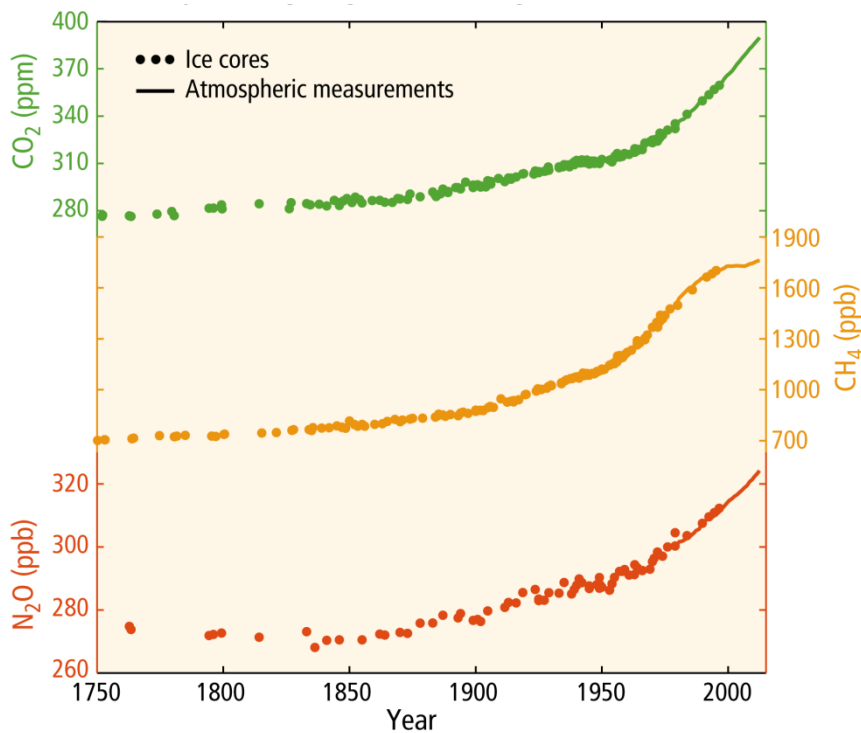


Figure 6.1. Globally averaged greenhouse gas concentration. Source: AR5 – Climate Change 2014: Synthesis Report (IPCC 2014).

Many works on historical data provide illustrative figures about climate changes occurred the last decades. Since 1900, global warming is between 0.3 and 0.6°C, and in most of Europe, the increase in annual average temperatures during the 20th century has been of about 0,8 °C (Ros, 1991).

Indeed, several studies have confirmed an increase in the ET_0 (Reference Evapotranspiration) under climate change conditions, in the Mediterranean area in general (Garcia-Garizabal et al., 2014), and especially in Spain (Espadafor et al. 2011 and Vicente-Serrano et al., 2014a).

For instance, Vicente Serrano et al. (2014a) reported a large increase in ET_0 at the monthly and annual scales, and obtained an average annual change throughout Spain of 29.4 mm each decade from 1961 to 2011. Besides this increase in ET_0 , precipitation observed in Spain between 1961 and 2011 decreased 218.7 mm per decade, (Vicente-Serrano et al., 2014b). In addition to this, it is noteworthy that the frequency and intensity of heavy precipitation events has increased in Europe in the last years (IPCC, 2014).

The 4 SRES (Special Reports on Emission Scenarios) scenarios of AR4 (IPCC 2007) are replaced in AR5 by 4 new scenarios of RCP (Representative Concentration Pathways) emission proposed by van Vuuren et al. (2011), which are defined by their total radiative forcing (2.6, 4.5, 6, and 8.5 $W m^{-2}$ in 2100: RCP2.6, RCP4.5, RCP6.0 and RCP8.5 respectively). The new scenarios can take into account the politics aimed at restricting climate change in 20th century. Each single RCP is based on an internally consistent set of socioeconomic assumptions and include: one scenario in which the mitigation efforts lead to a very low level of forcing that aims to keep global warming likely below 2°C above pre-industrial temperatures (RCP2.6); two stabilising scenarios (RCP4.5 and RCP6.0), and one scenario with a very high level of GHG (RCP8.5) emissions, Figure 6.2 and Figure 6.3.

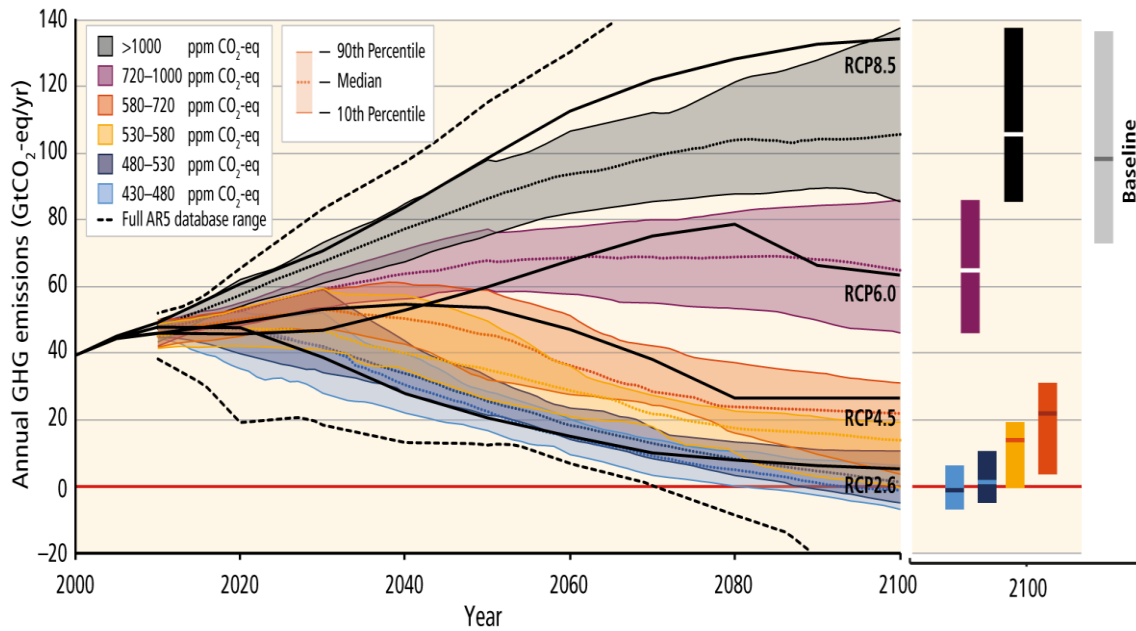


Figure 6.2.GHG emission pathways 2000-2100: All AR5 scenarios. Source: AR5 – Climate Change 2014: Synthesis Report (IPCC 2014).

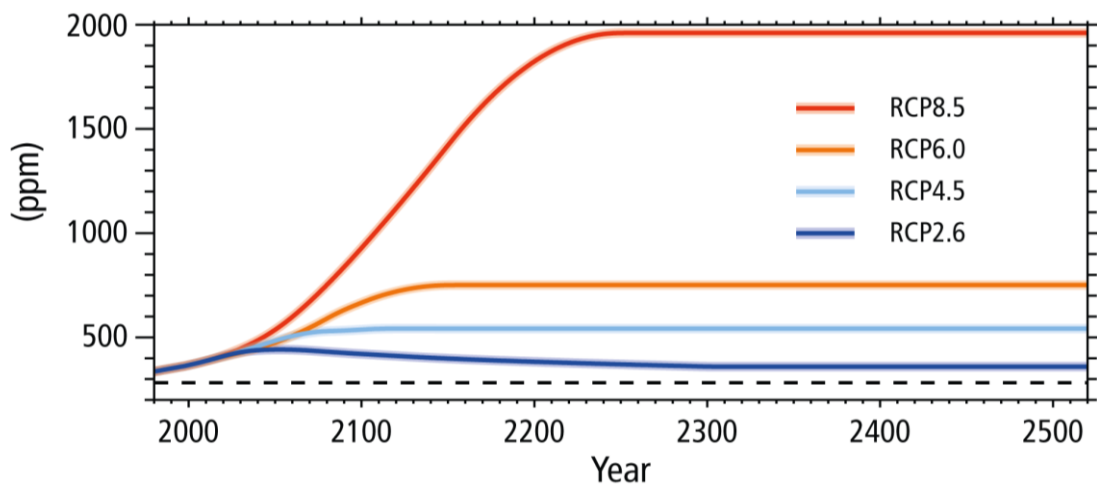


Figure 6.3. Up: Atmospheric CO₂ (ppm) for all AR5 scenarios. Source: AR5 – Climate Change 2014: Synthesis Report (IPCC 2014).

According to AR5 data -Climate Change Synthesis Report (IPCC, 2014), the global mean surface temperature change for mid-21st century relative to 1986–2005 is between 0.4°C and 2.6°C depending on RCPs. For the end of the century this range may likely be between 0.3°C and 4.8°C according to RCPs (see Table 6.1). Regarding precipitation, changes will not be uniform. Annual mean precipitations may experience an increase or a decrease at different latitudes. If there were a precipitations linear reduction in the time, hydrological resources for the crops would decrease significantly (Urbano, 2008).

Table 6.1. Global mean surface temperature change relative to 1986-2005 for the mid and the late 21st century for all AR5 scenarios. Source: AR5 – Climate Change 2014: Synthesis Report (IPCC 2014).

Global Mean Surface Temperature Change (°C)				
Scenario	2046–2065		2081–2100	
	Mean	Likely range	Mean	Likely range
RCP2.6	1	0.4 to 1.6	1	0.3 to 1.7
RCP4.5	1.4	0.9 to 2.0	1.8	1.1 to 2.6
RCP6.0	1.3	0.8 to 1.8	2.2	1.4 to 3.1
RCP8.5	2	1.4 to 2.6	3.7	2.6 to 4.8

Along with the future scenarios developed through the climate models, the crop growth/yield simulation models are essential tools to evaluate and predict the crops performance in climate conditions different to the current ones. Once validated, these models can be used to evaluate the effects of environmental changes on crop physiology (Southworth et al., 2000).

Numerous studies published during the last years use simulation models to assess the climate change impact on future crop yields (Grassini et al., 2015). Among several current growth models, the AquaCrop model developed by FAO is easy to use and targets different stakeholders such as farmers and researchers.

AquaCrop Model is an application for simulating crops efficiency under different water conditions (Raes et al. 2008; Steduto et al., 2008). It was developed as result of the FAO Irrigation and Drainage Division review (Steduto et al., 2012) based on the studies made by Doorenbos and Kassam (1979) about the impact of water in plant efficiency.

AquaCrop Model splits evapotranspiration (ET) into different components: yield evaporation (Es), crops transpiration (Ta), the final efficiency of any crops (Y) in produced biomass (B), and the harvest index (HI). In this way, the growth and simulation model calculates biomass as the product of water productivity (WP) and T, which multiplied by the harvest index defined to each crop, results in the harvest efficiency:

$$Y = HI \cdot B = HI \cdot (WP \cdot Ta)$$

FAO recommends the model application for multiple purposes such as harvest evaluation in different geographic locations and future climate scenes, irrigation

management, available water optimization, and water policies decision-support tools. Moreover, according to United Nations Marco Convention about Climate Change (UNFCCC 2010) AquaCrop is specifically useful to study the response of different crops under high carbon dioxide concentration and global warming conditions.

Specific characteristics which make a difference between AquaCrop and other models are: it considers water as a restricting factor; it uses canopy instead of the LAI (Leaf Area Index); it uses random productivity values for different requests of evaporation and CO₂ concentration, which leads to a big extrapolation ability based on location, season and weather including future climate scenarios, a relative low number of variables, balance between accuracy, simplicity and strength.

For example, it was used in the prediction of climate change impacts on cotton yields in Greece (Voloudakis et al., 2015), wheat in Sardinia (Soddu et al., 2013), of maize in Zimbabwe (Masanganiseet al., 2012). Also, for cotton irrigation optimization in Spain (García-Vila et al., 2009) and experiments about the crop response under elevated CO₂ (Vanuytrecht et al., 2011), and for assisting farmers in pre-season decision making on cropping patterns and on irrigation strategies for several crops in southern Spain (García-Vila and Fereres 2012).

The study of trends and spatial distribution of ET₀ is essential to assess future water requirements of crops, irrigation policies, and yields at regional scale (Tanasijevic et al., 2014). What is more, as climate change is heterogeneous, changes at the regional scale need to be better understood (Zhang et al., 2010). Therefore, the work presented in this study aims to assess and detect possible future trends in a very important industrial sugar beet crop located in Castilla y León, according to latest scientific knowledge about climate change using ET projections and water-driven simulation crop growth model AquaCrop. In addition, by estimating CO₂ uptake of this crop it is expected to supply information about sugar beet potential for mitigation policies or environmental impacts methodologies such as life cycle assessments or carbon footprints.

6.2. METHODOLOGY

6.2.1. Area of study:

The area of study includes most of sugar beet areas in Castilla y León (see Figure 6.4). This region is located inside the Spanish spring sown sugar beet area, known as sugar beet cultivation northern zone. Castilla y León accounts for 90% of Spanish production of spring sown sugar beet with 26573 ha (MAGRAMA, 2014) and the entire north zone is the area of UE that achieves the greatest yields per hectare with 33,7% of the farmers getting more than 120t/ha (AIMCRA, 2015).

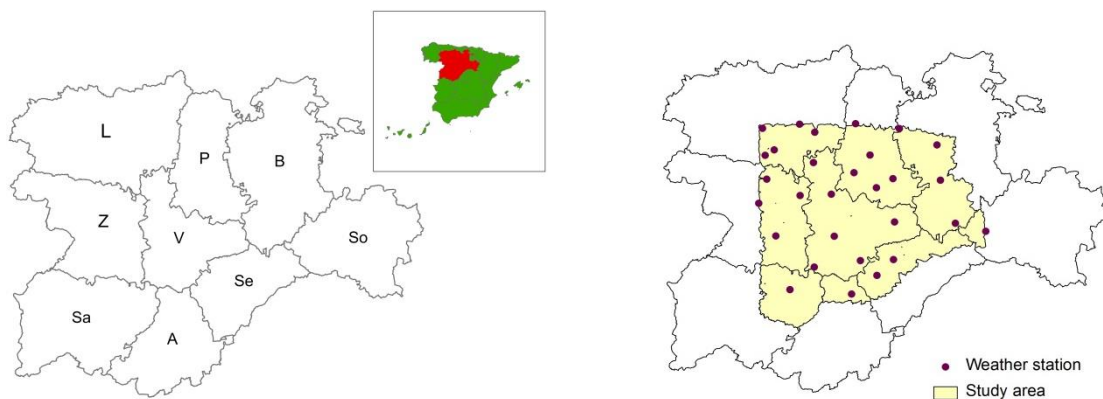


Figure 6.4. Left: situation of Castilla y León region in Spain. Province codes are as follows: L (León), P (Palencia), B (Burgos), Z (Zamora), V (Valladolid), So (Soria), Sa (Salamaca), A (Ávila) and Se (Segovia). Right: location of weather stations in the area of study.

This way, 3 of the 4 beet factories working in the region are into the studied area. The factory located in Miranda de Ebro has been excluded since 75% of the sugar beet processed come from bordering regions (Junta de Castilla y León, 2015). The 9 provinces of Castilla y León are represented to certain extent, being Valladolid the only province which surface is completely inside of the studied area.

6.2.2. Meteorological Data:

Daily weather data from 2001 to 2014 (when available) were collected from 31 automatic weather stations belonging to the SIAR network (Agroclimatic Information System for Irrigation) of the MAGRAMA (Ministry of Agriculture, Food and Environment of Spain). All the weather stations within the area of study described below (Table 6.2).

Table 6.2: Meteorological variables supplied by S.I.A.R stations from 2011 to 2014

Var	Description	Units
T_M	Mean temperature	$^{\circ}\text{C}$
T_{\min}	Minimum temperature	$^{\circ}\text{C}$
T_{\max}	Maximum temperature	$^{\circ}\text{C}$
H_M	Minimum humidity	%
H_{\min}	Mean humidity	%
H_{\max}	Maximum humidity	%
V_M	Mean wind speed	ms^{-1}
V_{\max}	Maximum wind speed	ms^{-1}
P	Precipitation	mm
ET_o	Reference Evapotranspiration	mm
R	Solar radiation	MJm^{-2}

Daily data from those years have been used to calculate a representative meteorological year for each season to build the baseline scenario of the study. Mann-Kendall tau test (Kendall, 1955) was conducted to detect decreasing or increasing trends in dataset.

6.2.3. Projected Meteorological Data for 2050 and 2070 (RCP4.5):

The most recent climate data projected for 2050 and 2070 in the locations of the SIAR stations that are currently used in AR5 were obtained through the WorldClim global climate layers (<http://www.worldclim.org>). In that project, different GCM (Global Climate Model) output data from CMIP5 (IPCC Coupled Model Intercomparison Project Phase 5, <http://cmip-pcmdi.llnl.gov/cmip5/>) have been downscaled and calibrated using WorlClim 1.4 as a reference baseline (Hijmans et al. 2005).

The layers selected in this study were 30-second resolution projections of the Earth system model MPI-ESM-LR developed by the Max Planck Institute for Meteorology (MPI-M) for RCP4.5. The MPI-ESM is composed of coupled general circulation models for the atmosphere and the ocean, as well as subsystem models for land and vegetation, and for the marine biogeochemistry. Thus, the carbon cycle has been added to the model system (Giorgetta et al. 2013).

RCP4.5 represents stabilization without overshoot pathway to 4.5 W m⁻² at stabilization after 2100 (Wise et al., 2009; Thomson et al., 2011). This RCP4.5 scenario is not as optimistic regarding GHG reduction as RCP2.6, but it does consider a reduction in greenhouse gases starting before 2050.

Using Geographical Information System (GIS) software ArcGIS® 10 (by Esri), annual mean temperature and annual precipitation were extracted for the coordinates of every weather station.

6.2.4. Calculated Reference Evapotranspiration (ET₀):

In this work, we used the Penman-Monteith simplified equation for hypothetical crop (Allen et al. 1998), which has been adopted by the FAO and is now known as the FAO-56 PM equation:

$$ET_0 = \frac{0.408\Delta(R_n - G) + \gamma \frac{900}{T+273} u_2 (e_s - e_a)}{\Delta + \gamma(1 + 0.34u_2)}$$

In this equation, ET₀ is the reference evapotranspiration (mm d⁻¹), R_n is the net radiation at the crop surface (MJ m⁻² d⁻¹), G is the soil heat flux density (MJ m⁻² d⁻¹), T is the mean air temperature at 2 m height (°C), u₂ is the wind speed at 2 m height (m s⁻¹), e_s is the saturation vapor pressure (kPa), e_a is the actual vapor pressure (kPa), e_s - e_a is the saturation vapor pressure deficit (kPa), Δ is the slope of the vapor pressure curve (kPa °C⁻¹), and γ is the psychrometric constant (kPa °C⁻¹).

Many studies have used this equation successfully, applying it to different climates and time scales (Allen et al., 2006). In Spain, it has been used, for example, by Espadafor et al. (2011) and Vicente-Serrano et al., (2014), in order to examine historical trends of ET₀.

Although there exists a FAO-specific FAO software to calculate ET₀ (ET₀ Calculator, see <http://www.fao.org/nr/water/eto.html>), in this study we chose to develop all the required calculations for the equation using commercial spreadsheet software (Microsoft Excel 2010), to ease the process of weather station data insertion. In this way, we only needed to insert the daily data related to the table variables in the spreadsheet (except ET₀), coming directly from the SIAR network stations, without any

unit/format conversion. Based on these daily data, monthly and yearly values have also been calculated.

ET₀ has been calculated for the baseline scenario using this method, both for 2050 and 2070. For these future 2050 and 2070 scenarios we have used the temperature and precipitation data obtained from the previous section. The rest of wind, humidity and radiation parameters were assumed stationary.

To validate this method, we have compared the graphs displaying real values coming from the stations with the values obtained with the aforementioned method, and calculating regression lines.

6.2.5. Crop Evapotranspiration (ET_c):

ET_c is calculated as the product of ET₀ and crop-specific coefficient K_c. Monthly values for sugar beet K_c were obtained from AIMCRA works (AIMCRA 2015).

6.2.6. AquaCrop:

A detailed description of the model can be found in Raes et al. (2009) and Steduto et al. (2009). A reference manual of the 4.0 version used in this work can be found in Raes et al., 2012. Briefly, AquaCrop develops a structure of sub-models (Figure 6.5) for the crop growth model, including: soil's water balance, crop development, crop growth and efficiency, climate factors (mainly, temperature, precipitation, evapotranspiration and atmosphere carbon dioxide concentration).

Furthermore, AquaCrop also includes several crop management aspects such as irrigation or fertilization, considering that these inputs influence directly the soil's water balance, as well as crop's development and final performance.

AquaCrop, however, does not include pests, diseases nor weed effects into the model.

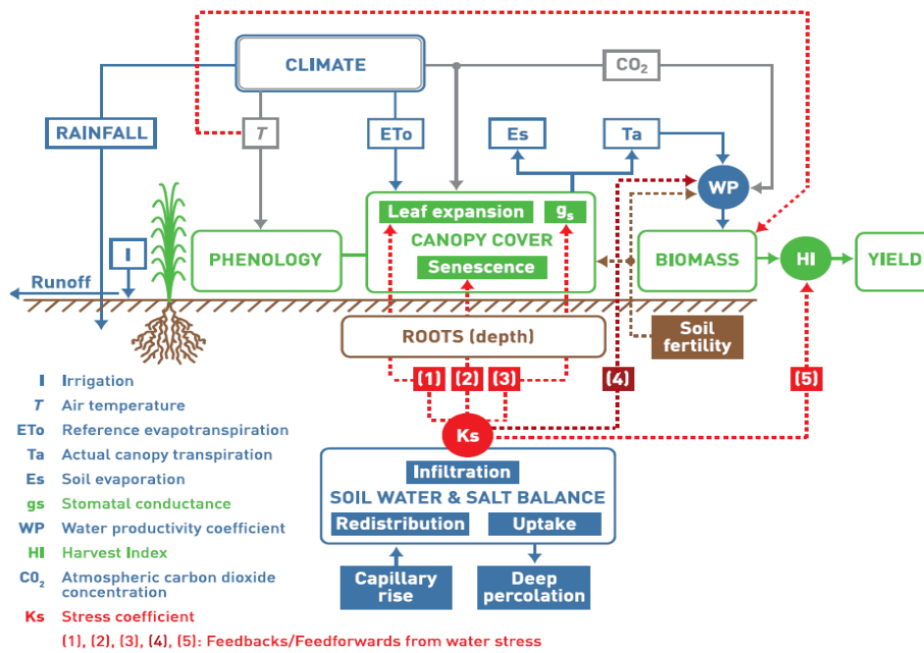


Figure 6.5. AquaCrop flow chart showing the main components of the soil-plant-atmosphere continuous (Steduto et al., 2008)

6.2.6.1 Climate Inputs:

- Temperature: file with minimum and maximum temperature, daily or monthly.
- Evapotranspiration: file with daily or monthly ET₀
- Precipitation: file with daily or monthly precipitation.
- CO₂ concentration: file with Mauna Loa Observatory (Hawaii) records and estimated values for the future.

6.2.6.2 Irrigation Schedule

The appropriate irrigation schedule for crops in this area was inserted, based on the AIMCRA recommendations (AIMCRA 2008), with a total of 553 mm during the whole cycle.

6.2.6.3 Crop Model Calibration

AquaCrop can be used to simulate crop growth with certainty after local calibration and validation (Hsiao et al., 2009).

By default, AquaCrop offers files for the simulation of different crops. In the case of the sugar beet, the model is automatically calibrated and validated to Foggia, Italy in 2000. In Spain there is an initiative for calibration and validation of the model (García-Vila, 2013) which was still not available as of this writing.

Stricevic et al. (2011) calibrated the model for the specific conditions of northern Serbia, although they conclude that this calibration only implied small changes of a few of the default model coefficients (which illustrates the resilience of the model).

Since the main goal of our work is not the model calibration itself (which would require an specific study, and is already in development by other authors), but rather to use the model as a tool to get future prediction trends, it was decided to adjust the model supplied by the program to get typical crops from the concerned area (i.e., one with average production above 100 t ha⁻¹).

In general, it is more suitable to study the different crop stages through the growing-degree days (GDD), to better reflect the plant physiology (Grassini et al., 2015). Thus, it was chosen to change the necessary GDD to achieve each growth stage based on recent research efforts and field data (Table 6.3) from a study made in 2011 and 2012, in different locations in the area of our study (see first research in this thesis document).

Table 6.3. Canopy development phases of growing cycle (GDD), adjusted for sugar beet

Site	GDD	Source
Emergence	190	Field data Hoffmann and Kluge-Severin 2011
85% Canopy	900	Malnou et al., 2006
100% Canopy	1200	Malnou et al., 2008
Senescence	not reached	Field data
Madurity	3600	Field data

In a similar manner, it was also decided to lightly increase the WP parameter from 18 to 19 gm⁻². This is supported by the conclusions of previous research which suggest that, although sugar beet is a C3 species, it is very efficient in water use, closer to C4 crops (Rinaldi and Vonella, 2006).

Plantation density in the model has been increased until 125000 plants ha⁻¹, which is the density used in the field plots.

Some of the other most representative parameters include the harvest index (HI), which has been maintained at 70%, coinciding with previous research work (Martínez-Quesada, 2008) and data previously obtained in the field samples.

Similar to Stricevic et al. (2011), soil fertility was not addressed, as field plot nutrient requirements were fully satisfied following the AIMCRA recommendations. We have not specified soil types either.

Adjustment validation was made by calculating the percentage of error between real production data from the field, available from experiments in 2011 and 2012, and those simulated with AquaCrop.

Also, the global Root Mean Square Error (RMSE) was calculated for all the cases:

$$\text{RMSE} = \sqrt{\frac{1}{n} \sum_{i=1}^n (A_i - S_i)^2}$$

In this equation, A_i =Actual yield, S_i =Simulated yield and n =number of observations. Units are t ha⁻¹ of yield dry matter. Hence, as RMSE gets close to zero, we can conclude that model adjustment is better.

6.2.6.4 Carbon uptake:

Carbon content data in different parts of the sugar beet were obtained from (see first research in this thesis document). As mean values, 43.5% C in roots and 37.5% C in leaves were obtained. Using the product of dry matter, carbon content and CO₂ conversion ratio (44/12) total amount of CO₂ assimilated by sugar beet crop is obtained.

6.2.6.5 Cartography and spatial interpolation:

Lorite et al., 2013 developed two software tools, known as AquaData and AquaGIS to facilitate AquaCrop simulation runs and the presentation and interpretation of simulation results, including spatial visualization. As both tools are only available under request for the moment, in this work the GIS software ArcGIS 10 (ArcGIS® software by Esri) was used to generate maps of Temperature, Reference Evapotranspiration,

Crop Evapotranspiration, Yield and CO₂ uptake. These are shown in the results section below.

As for spatial interpolation, there are several well-known methods such as IDW (Inverse Distance Weighting, Jones et al., 1986), Kriging and Splines (Laslett, 1994) which are widely used. It is possible to find works that choose different methods for interpolating the same variable. Thus, for ET₀ interpolation, Nam et al. (2015) used IDW in South Korea and Todorovic et al. (2013) used Spline in the Mediterranean area. In our work, IDW was rejected in order to minimize points isolated by bull's-eye effect, while Spline was not chosen either, since it is more appropriate for medium- and small-scale (New et al., 1999).

Hence, we used the ordinary kriging method, coupled with a spherical isotropic variogram (Raziei and Pereira 2013). The spatial analyst toolbox from ArcGIS 10 was used.

Interpolation validation was conducted by “leave one out” cross-validation, which consists on using one of the stations as the validation dataset, and using the rest of stations as the training set to calculate the error of the resulting model in that validation station; and then repeating this process for each and every station of our set

6.3. RESULTS

6.3.1. Evapotranspirationn Baseline:

The average of the obtained ET₀ values from the 29 weather stations, with daily data from 2011 to 2014, is shown in Figure 6. Monthly data are shown, using boxplots, in Figure 6.7.

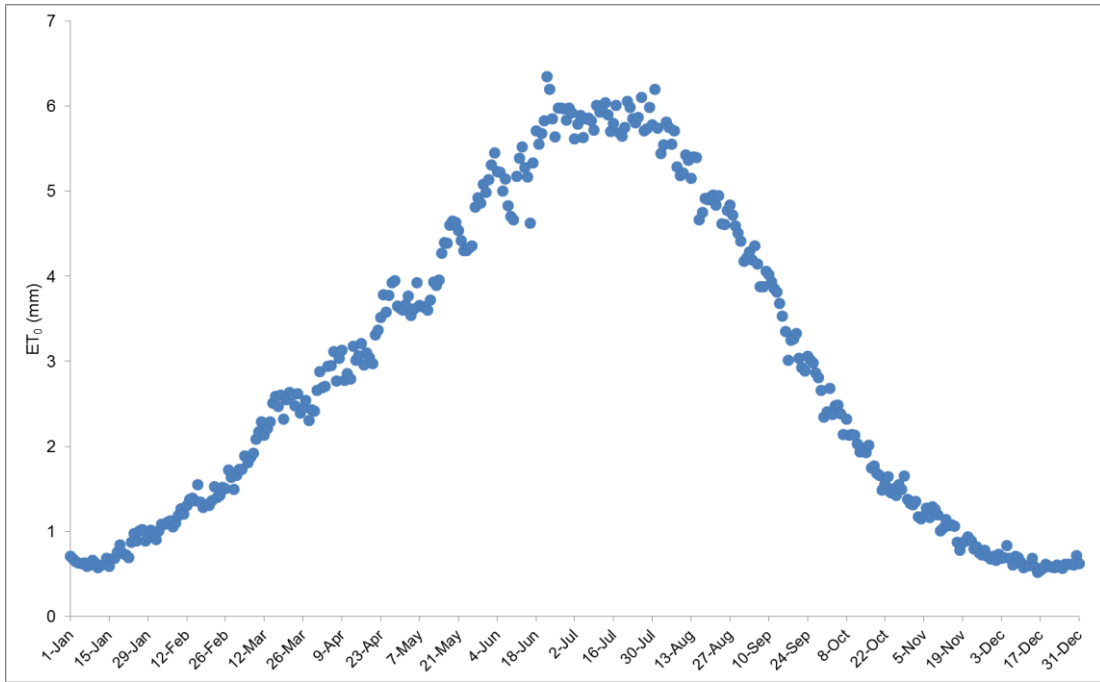


Figure 6.6. Actual daily ET_0 from the 29 stations in the area of our study, from 2001 to 2014 (Baseline scenario).

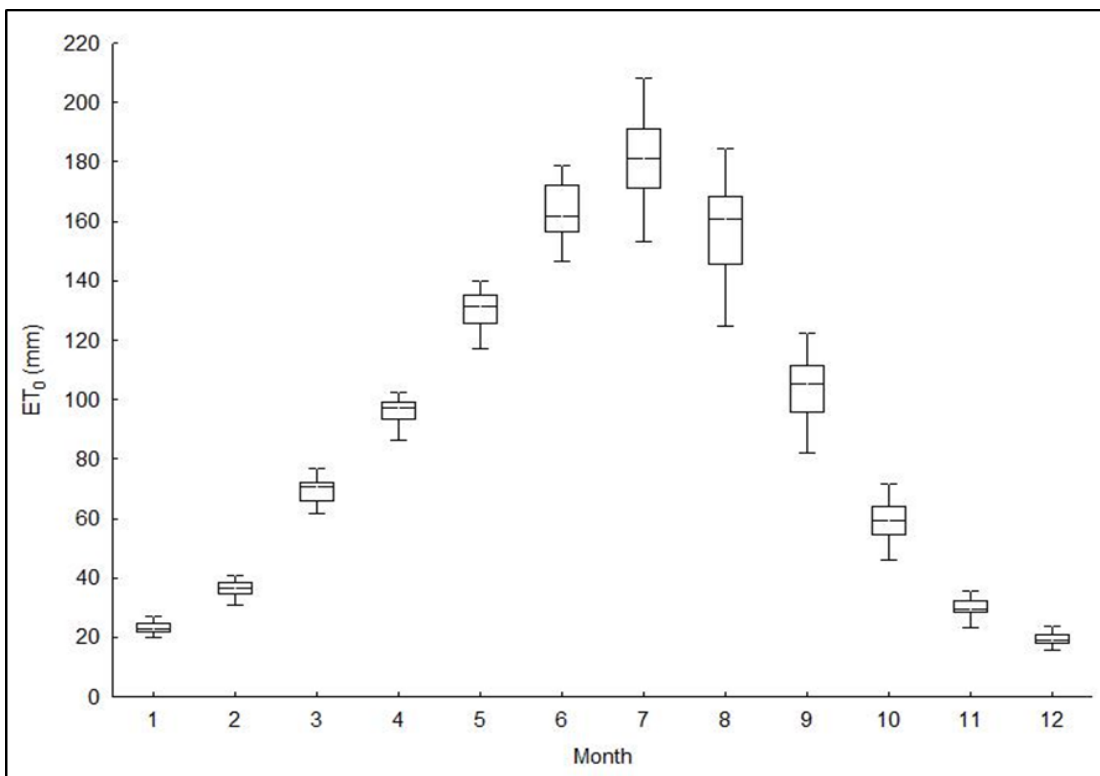


Figure 6.7. Monthly ET_0 at the 29 weather stations, from 2001 to 2014 (baseline scenario). Boxes indicate the 25th and 75th percentiles.

We can observe how the highest values are found between June and August, while the lowest are found from November to March, as it is expected in a continental Mediterranean climate.

As noted by some authors, using daily data can be more problematic than using monthly records, when assessing long-term trends (Vicente-Serrano et al., 2014). However, here we chose the higher accuracy provided by daily data, in order to minimize errors in the results obtained from the crop model.

The comparison between actual values measured in the stations and those calculated with the FAO-56 PM equation is shown in Figure 6.8.

A coefficient of determination R^2 practically equal to 1, which means that the method of calculating ET_0 with the FAO-56 PM equation is perfectly acceptable, generating results very close to those offered by the stations.

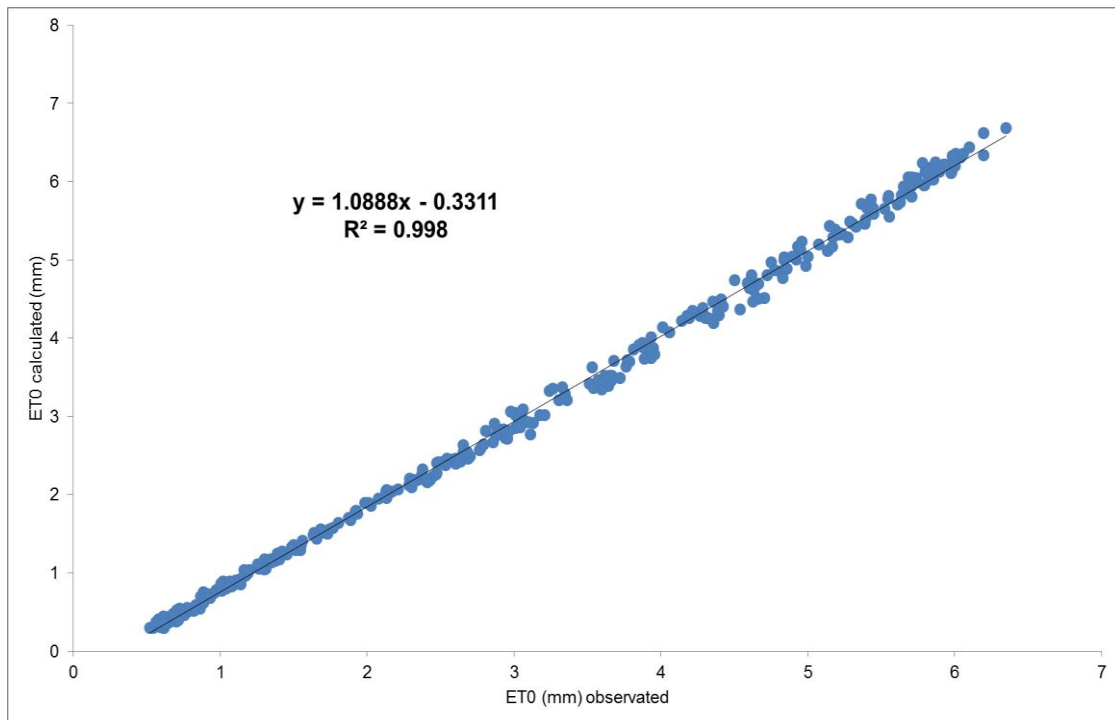


Figure 6.8. ET_0 values obtained from 29 weather stations within the concerned area from 2001 to 2014 against ET_0 values calculated through FAO-56 PM. Regression equation and R^2 are also shown.

Despite the fact that the general tendency in Spain in the last decades is towards an increase in ET_0 (Vicente-Serrano et al., 2014a), a Mann-Kendall test applied only to the years from where data have been compiled for this work (not shown), no clear ET_0 tendency can be perceived, which is beneficial when it comes to the creation of a “representative year” model.

6.3.2. Worldclim data

Below (Figure 6.9), yearly average temperatures for each station in the area of the study are shown. Data for the current situation (baseline scenario) are the average values obtained from 2011 to 2014 for each station. Data from 2050 to 2070 are the values obtained from the climate layers of Worldclim.

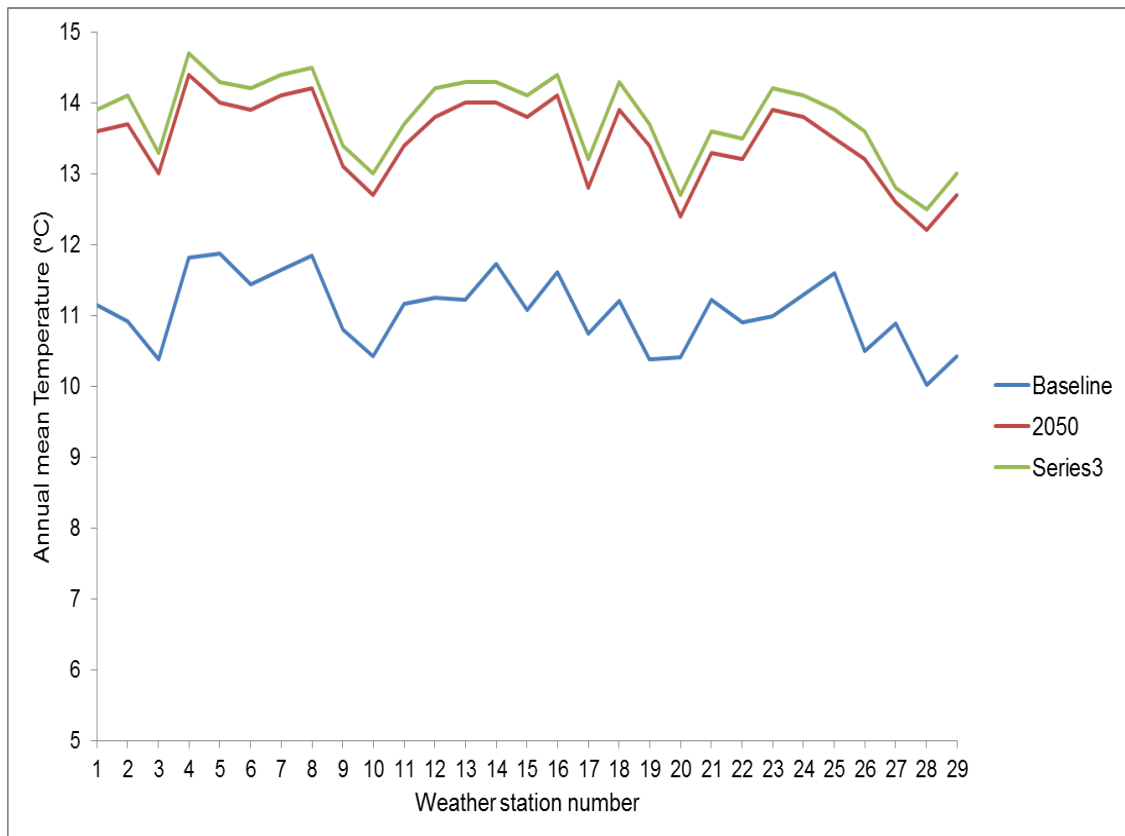


Figure 6.9. Annual mean Temperature at the 29 weather stations. Baseline data are mean observed values from 2011 to 2014. Annual mean Temperature for 2050 and 2070 for the location of each station, obtained from Worldclim, are also shown.

The average temperature increase of the whole set of stations is of 2.4°C and 2.7°C for 2050 and 2070, respectively. These values are beyond the global averages for the RCP4.5 scenario.

Ribalaygua et al. (2013), working with SRES scenarios, reported increases in maximum and minimum temperature averages between 1.5°C and 2.5°C (depending on the scenario), relative to the 1971–2000 period, for mid-21st century in Aragón (north-eastern Spanish region). In that study, regarding precipitation, authors explain that there was not a clear tendency, but rather greater uncertainties. However, all the scenarios suggested a moderate decrease in rainfall for the mid-century (2–4%).

In this work, the percentage of change of annual precipitations for 2050 and 2070 in the concerned area are minimum compared to the current scenario (not shown), and do not influence the final results.

6.3.3. Adjustment Crop Model Validation:

Although we were not able to perform a calibration of the model for the concerned area with the necessary requirements (see Heng et al., 2009), the adjustment made to the file automatically supplied by the program to the sugar beet crop shows an adequate performance when applied it to the plots of land in the study, in 2011 and 2012, with errors below 10% in all cases except the plot 1 in 2012 (14.72%) (Table 6.4). Until a perfectly calibrated and validated model for the Spanish spring sown sugar beet zone is finally available, a RMSE value below 2 t ha⁻¹ implies that our adjusted model is useful for our aims of analyzing spatial trends for the crop in future scenarios of climate change.

Table 6.4. Comparison between observed and simulated yields (t ha⁻¹ of dry biomass). Individual error (%) and RMSE (t ha⁻¹) for all the cases are shown.

Year	Site	Actual Yield (dry biomass: t ha ⁻¹)	Simulated Yield (dry biomass: t ha ⁻¹)	Error (%)
2011	1	18.50	20.10	8.62
2011	2	24.19	24.86	2.78
2012	1	19.28	22.12	14.72
2012	2	24.88	26.79	7.71
2012	3	23.94	22.58	5.68
				RMSE= 1.91 t ha ⁻¹

6.3.4. Interpolation validation:

As described above, we performed a “leave one out” cross-validation of ET₀ values, as a reference to assess the behavior of the spatial Kriging interpolation applied to the study variables. With a 5% mean error between observed and interpolated values, we can consider such interpolation method as a consistent tool for the creation of maps which are representative of the spatial distribution of the studied variables (Table 6.5).

Table 6.5. Comparison between observed and interpolated values for “leave one out” cross-validation. Individual and mean errors (%) are shown.

Station	ET ₀	Leave one out	% Error
1	993.77	1076.26	8.30
2	1081.99	1085.19	0.30
3	945.35	1058.88	12.01
4	1095.40	1133.92	3.52
5	1198.92	1099.38	8.30
6	1164.45	1092.29	6.20
7	1058.66	1080.05	2.02
8	1085.24	1102.77	1.62
9	1051.19	1029.12	2.10
10	996.70	1026.39	2.98
11	1113.70	1072.92	3.66
12	1151.62	1101.64	4.34
13	1120.09	1116.48	0.32
14	1188.99	1111.25	6.54
15	1083.24	1053.55	2.74
16	1142.07	1073.70	5.99
17	955.10	1057.94	10.77
18	1001.16	1145.97	14.46
19	1084.00	1046.83	3.43
20	1028.37	1020.63	0.75
21	1048.77	1058.58	0.94
23	1030.29	1124.94	9.19
26	990.65	1044.76	5.46
27	1151.77	1005.56	12.70
29	1010.51	1025.54	1.49
Average error=			5.20%

6.3.5. ET₀ y ETc

In the baseline scenario, the central and southern zones show higher ET₀ values, decreasing as we move towards the periphery, especially towards the north and northeast (Burgos province). In future scenarios, there is a clear annual ET₀ increase for all the area studied in 2050 as in 2070 (Figure 6.10), being greater for the latter, and even reaching 200 mm differences compared to the baseline scenario (Figure 6.11). This increase is, logically, a response to the temperature rise as it has been the only parameter modified in FAO-56 PM, keeping all the others unchanged. Furthermore, Vicente-Serrano et al. (2014a) reported that, in Spain, the FAO-56 PM equation is highly sensitive to changes in relative humidity and maximum temperatures, according to the range of variation of these variables.

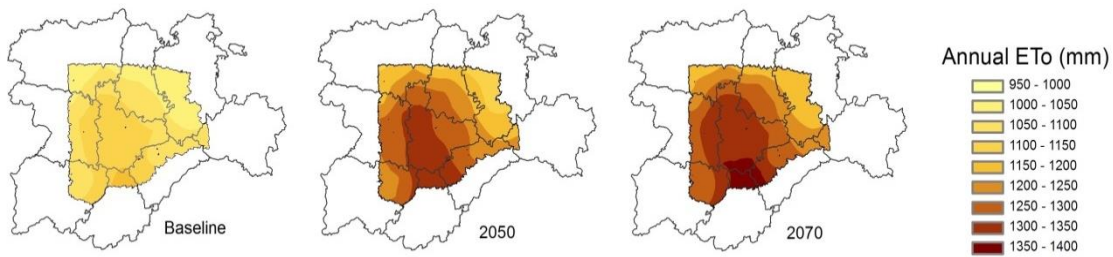


Figure 6.10. Spatial distribution of annual ET₀ (mm) in the area of study for baseline, 2050 and 2070 scenarios.

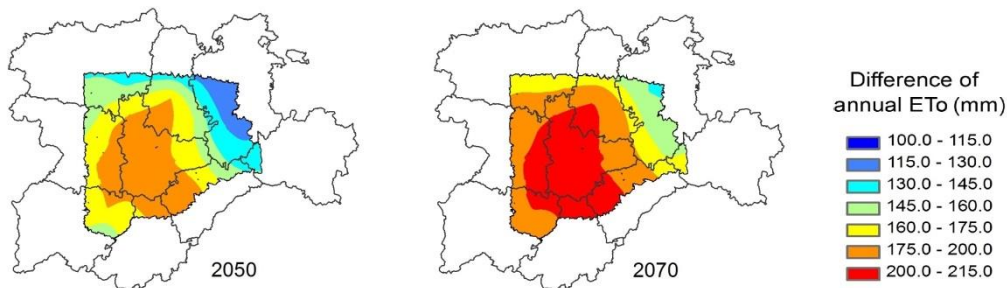


Figure 6.11. Spatial distribution of differences in yearly ET₀ (mm) in the area of the study, for the 2050 and 2070 scenarios, compared to those of the baseline scenario.

In the areas of our study, the areas most affected by the increase in ET₀ are the Valladolid province, southern Palencia, northern Salamanca and Ávila, northeastern Segovia, and eastern Zamora.

The ET₀ increase in future scenarios make the spatial distribution differences already existent in the baseline scenario more dramatic, with this increase being greater in the central zone, with a clear southwards direction (and slightly to the west). In other words, areas with lower ET move towards the north and northeast over time.

In Figure 6.12, monthly differences in ET_c values with respect to the baseline scenario are shown, calculated with the monthly K_c for the sugar beet crop. According to the results for ET₀, these differences turn into increases for the two future scenarios, being greater in 2070.

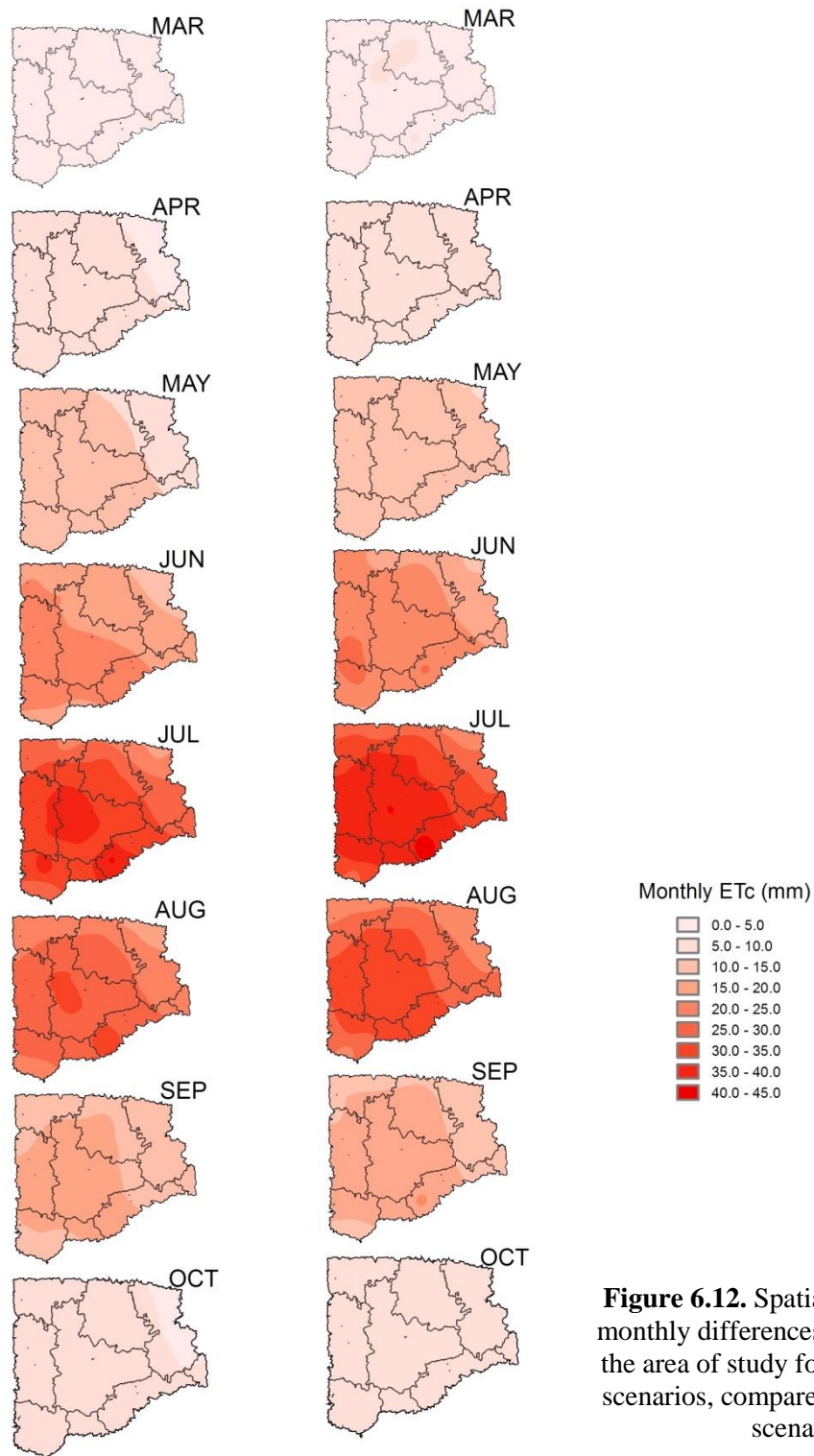


Figure 6.12. Spatial distribution of monthly differences of ET_c (mm) in the area of study for 2050 and 2070 scenarios, compared to the baseline scenario.

Between March and May ET_c increase go from 1.5 to 20mm in the future scenarios. July is the month when the increases reach the highest values, with zones around 40mm, and dropping slightly, then keeping high values in August and then dropping again in

September until October, when values are already near to those at the start of the crop period.

6.3.6. Yield

As expected, yield is affected by changes in ET_0 (Figure 6.13). Taking into consideration the pattern for ET_0 described above, we found how in the central zone our area of study, yield goes down for both 2050 and 2070, around 9%.

Therefore, as seen for other crops, future global warming may be beneficial in some regions, but could reduce productivity in zones where optimal temperatures already exist (Ortiz et al., 2008).

This decrease in yield is slightly larger in 2050, probably owing to a greater photosynthetic activity in 2070 thanks to larger CO_2 concentrations.

Hence, we can also see how the negative effect of higher temperatures and less precipitations can be partly compensated by larger photosynthetic rates due to the expected CO_2 increase (OECC, 2005).

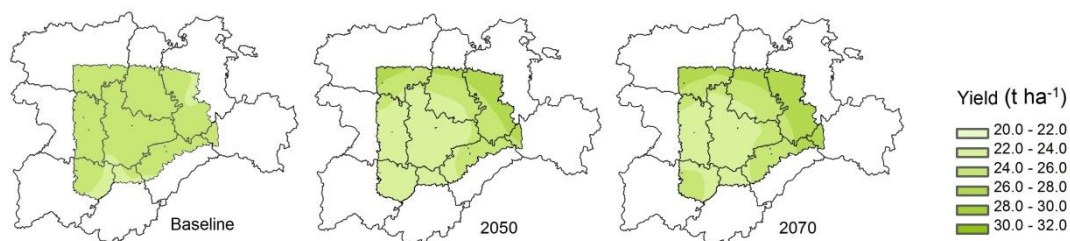


Figure 6.13. Spatial distribution of Yield (mm) in the concerned area, for the baseline, 2050 and 2070 scenarios with usual growing season.

These trends are consistent with studies that have carried out FACE (Free Air Carbon Enrichment) experiments to simulate future scenarios with larger CO_2 concentrations, like Manderscheid et al. (2010), who recorded an increase of yield between 7 and 16% with the CO_2 concentration levels provided for mid-21st century for the A1B IPCC scenario (SARS scenario).

On the other hand, in northwestern León, and northeastern Burgos, we actually observe predictions of an increase in yield for 2050, over a region which grows over to

northern Palencia in 2070, reaching a 10% yield increase. This can be explained by those being colder zones, where the change in ET_0 would cause a smaller absolute increase that is still tolerated by the plant, which benefits from the higher temperatures in that scenario.

However, it should be noted that yield simulations generated by the model in years 2050 and 2070 change the crop period: in the baseline, cultivation goes from March until November, while in future simulations the crop season comes earlier, to October or the end of September, depending on the area.

This responds to the fact that crops, with increasing temperatures, take less time to reach the necessary GDD in each growth stage.

These results show how certain rises in temperature can increase the developmental rate of the crop, resulting in an earlier harvest. However, we should be aware that such “heat stress” may result in negative effects on crop production (Southworth et al., 2000).

In this way, if the cultivation period were extended, bigger yields could be achieved, as long as the water requirements of the plant were met. In this sense, data about the positive influence of cycle extension on yield have been provided, based on field studies done in the concerned area (AIMCRA, 2007), suggesting yield increases of up to 20%. In Figure 6.14, the simulations have been extended until November, obtaining larger yields in general, both in 2050 and 2070 (up to 17%). These increases are more noticeable in the north and eastern zones than in the center and south. In 2070, as the result of higher CO_2 concentrations, the increase is emphasized, especially in the northern zone (Palencia and León) and in the east (Burgos).

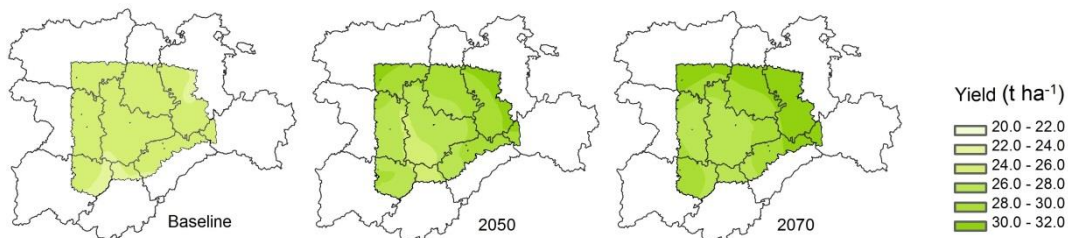


Figure 6.14. Spatial distribution of Yield (mm) in the area of study for baseline, 2050 and 2070 scenarios with extended growing season

Another positive aspect is that a future increase in temperatures could allow a lengthening of the cultivation period, allowing for earlier sowing. This would in turn allow an earlier development of the photosynthetic organ (the leaves), so as to make the most of the solar radiation: as certain authors have noted, due to the slow leaf development in spring, sugar beet crop achieves its highest canopy when the maximum solar radiation of the year has already passed (Scott and Jaggard, 1993; Kenter et al., 2006). By getting the largest field coverage in the least amount of time, and keeping this coverage for as long as possible, the plant can thus receive the most solar radiation (Van Heemst, 1986, as cited in Martínez-Quesada, 2008).

In this way, the softer winter temperatures can lead to higher productivity in that part of the year, somehow balancing the losses from the other seasons (OECC, 2005).

6.3.7. Biomass and CO₂

Besides offering yield data, AquaCrop also provides results about the total biomass achieved by the crop, including the leaves.

Predicted CO₂ capture results are linked to the results of the amount of generated biomass (Figure 6.15). As it occurred with the crop production, there exists a decrease of the average biomass production and the CO₂ assimilation for all the area, of around 7% in 2050, which is slightly mitigated in 2070 (at 5%) for the same reason outlined above (related to the increased levels of CO₂). In absolute terms, CO₂ assimilated goes from 49 t ha⁻¹ in baseline scenario to 46 t ha⁻¹ and 47 t ha⁻¹ in the 2050 and 2070 scenarios, respectively.

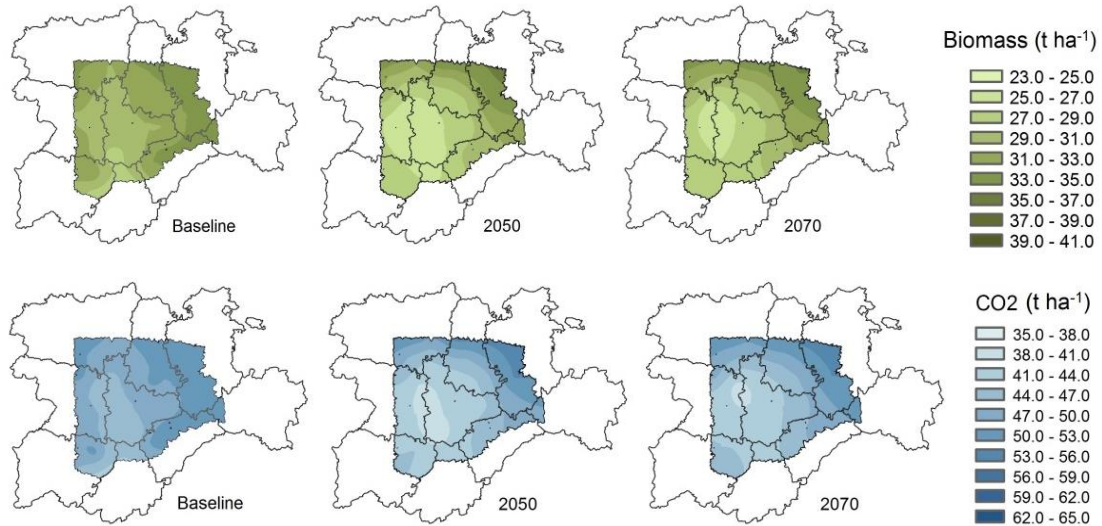


Figure 6.15. Spatial distribution of Biomass (t ha⁻¹) and CO₂ uptake (t ha⁻¹) in the area of our study, for the baseline, 2050 and 2070 scenarios with usual growing season.

As in the case of yield, if the cultivation cycle is expanded, larger average quantities of biomass and captured CO₂ will be achieved, throughout the area (8% and 12% in 2050 and 2070, respectively). In this case, data for the CO₂ captured (figure 6.16), go from 49 t ha⁻¹ in the baseline to 53 t ha⁻¹ and 55 t ha⁻¹ (on average) in 2050 and 2070, respectively (9% and 13% increases, approximately).

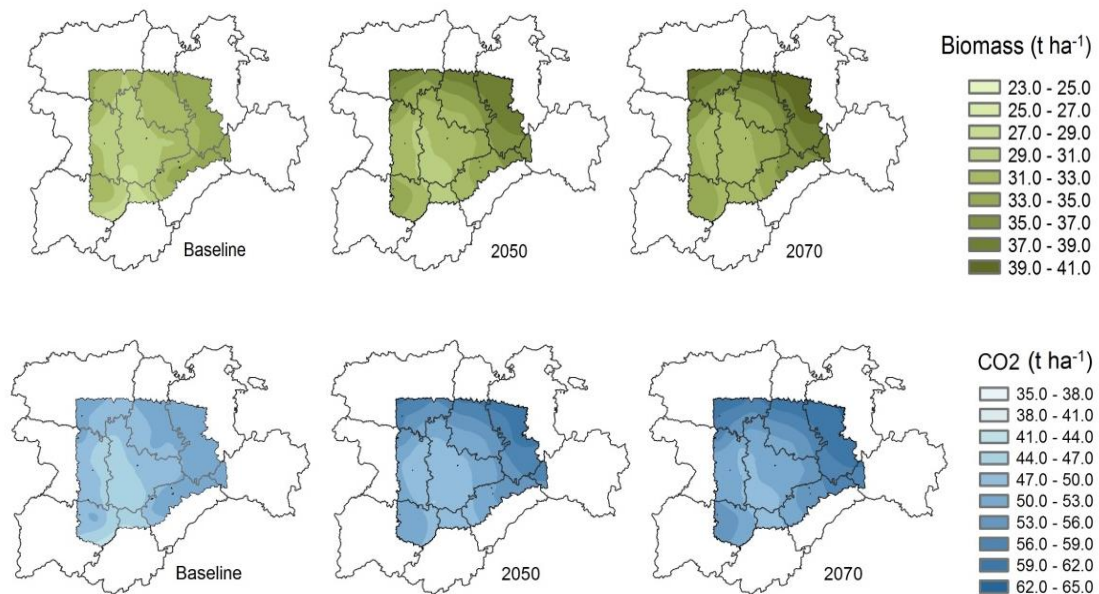


Figure 6.16. Spatial distribution of Biomass (t ha⁻¹) and CO₂ uptake (t ha⁻¹) in the area of study for baseline, 2050 and 2070 scenarios with extended growing season.

Summarizing, for the studied variables (ET₀, ET_c, Yield, Biomass and CO₂ assimilation), the predicted trends in this work, as described above, match in a regional scale what other studies that have observed on a smaller scale: a northward movement of crop suitability zones, as well as increased crop productivity in Northern Europe (Falloon and Betts, 2010).

Furthermore, the simulations carried out confirm that there is a greater potential for adaptation in northern, cooler zones, which compensate the reduction in yields by shifting the crop growing season to cooler months, in this case advancing sowing, and taking advantage of an extended growing period using suitable varieties (Osborne et al., 2013)

Although a regional approach is necessary to assess the effects of climate change in future yields and changes in crop suitability, it must be kept in mind that there are many uncertainties associated with this kind of yield simulations, including uncertainties in the GCM models and projections of future climate (Osborne et al., 2013), crop model errors, assumptions and observation errors (Saarikko, 2000). To these, we should add other likely factors such as an increase in extreme rainfall events and droughts, which should also be taken into account in future studies (Falloon and Betts, 2010).

6.4. CONCLUSION

This paper has studied the projected spatial distribution of evapotranspiration in 2050 and 2070 at a regional scale, in the crop area of the spring-sown sugar beet in the Castilla y León region. These projections were based mainly on the future impact of temperature and precipitation of the MPI-ESM-LR climate model, as well as the RCP4.5 emission scenario from the AR5. These results have served as inputs for the crop growth simulation software AquaCrop, which has been previously adjusted to model closely the weather conditions, agronomy and yield levels for sugar beet in the area of our study. In this way, we have been able to estimate and evaluate the consequences of future scenarios, as expected by the last IPCC report, regarding water requirements, yield, biomass and CO₂ assimilation.

Keeping in mind the uncertainty and errors associated to these methodologies (which are present both in climate models and crop simulation models, as well as on the assumptions made), the results coincide with the findings of other studies at different

scales and in different regions of Europe. On one side, in almost all the area studied, yield would decrease (at current irrigation levels), and the most suitable crop zones would move northwards, obtaining even higher yields. This overall yield decreases would be aggravated in the case of decreasing precipitation levels, or increased frequency of extreme events of drought. However, new opportunities for adaptation are opened by lengthening the cultivation cycle, delaying the harvest and advancing the sowing. This, along with more efficient irrigation, could lead to even higher yields and higher amounts of CO₂ captured.

6.5. REFERENCES

- AIMCRA. 2015. Memoria Campaña 2014/2015 (Siembra Primavera). Valladolid
- AIMCRA (2005). Revista AIMCRA 86, 6-10. Valladolid.
- AIMCRA (2007). Revista AIMCRA 96, 11-12. Valladolid.
- Allen, R.G., Pereira, L.S., Raes, D., Smith, M., 1998. Crop evapotranspiration. Guidelines for computing crop water requirements. In: FAO Irrigation and Drainage Paper No. 56. FAO.
- Allen, R.G., Pruitt, W.O., Wright, J.L., Howell, T.A., Ventura, F., Snyder, R., Itenfisu, D., Steduto, P., Berengena, J., Baselga, J., Smith, M., Pereira, L.S., Raes, D., Perrier, A., Alves, I., Walter, I., Elliott, R., 2006. A recommendation on standardized surface resistance for hourly calculation of reference ETo by the FAO56 Penman- Monteith method. *Agric. Water Manage.* 81, 1–22.
- Ding, R., Kang, S., Vargas, R., Zhang, Y., Hao, X., 2013. Multiscale spectral analysis of temporal variability in evapotranspiration over irrigated cropland in an arid region. *Agricultural Water Management* 130, 79–89.
- Doorenbos, J. and Kassam, A.H. (1979). Yield response to water. *Irrigation and Drainage Paper n.33*. FAO, Rome, Italy, 193 pp.
- Espadafor, M., Lorite, I.J., Gavilan, P., Berengena, J., 2011. An analysis of the tendency of reference evapotranspiration estimates and other climate variables during the last 45 years in Southern Spain. *Agricultural Water Management* 98, 1045–1061.

- Falloon, P., Betts, R. (2010). Climate impacts on European agriculture and water management in the context of adaptation and mitigation—The importance of an integrated approach. *Science of the Total Environment* 408 (2010) 5667–5687.
- Garcia-Garizabal, I., Causape, J., Abrahao, R., Merchan, D., 2014. Impact of climate change on Mediterranean irrigation demand: historical dynamics of climate and future projections. *Water Resources Management* 28, 1449–1462.
- Garcia-Vila, M. & Fereres, E. (2012). Combining the simulation crop model AquaCrop with an economic model for the optimization of irrigation management at farm level. *European Journal of Agronomy*. 36:21-31.
- García-Vila, M.; Fereres, E.; Mateos, L.; Orgaz, F.; Steduto, P.: 2009. Deficit irrigation optimization of cotton with AquaCrop. *Agron. J.*, 101:477-487.
- Garvía-Vila M. Aquacrop (FAO) para el cultivo de la remolacha. 2013. Seminario Internacional del Riego de Remolacha. Valladolid 5 de junio
- Garvía-Vila M. Aquacrop (FAO) para el cultivo de la remolacha. 2013. Revista AIMCRA 115, 26-29.
- Giorgetta, M. A., et al. (2013), Climate and carbon cycle changes from 1850 to 2100 in MPI-ESM simulations for the Coupled Model Intercomparison Project phase 5, *J. Adv. Model. Earth Syst.*, 5, 572–597, doi:10.1002/jame.20038.
- Gowda, P.H., Chavez J.L., Colaizzi P.D., Evett S.R., Hollew T.A., Tolck J. A.: 2008. ET mapping for agricultural water management: present status and challenges. *Irrigation Science*, March 2008, Volume 26, Issue 3, pp 223-237
- Grassini, P., Van Bussel, L.G.J., Van Wart, J. Wolf, J. Claessen, L., Yang, H., Boogaard, H., de Groot, H., Van Ittersum, M.K., Cassman, K.G. (2015) How good is good enough? Data requirements for reliable crop yield simulations and yield-gap analysis. *Field Crops Research* 177 (2015) 49–63.
- Heng, L.K.; Hsiao, T.C.; Evett, S.R.; Howell, T.A.; Steduto, P.: 2009. Testing of FAO AquaCrop model for rainfed and irrigated maize. *Agron. J.*, 101:488-498.
- Hijmans, R.J., S.E. Cameron, J.L. Parra, P.G. Jones and A. Jarvis, 2005. Very high resolution interpolated climate surfaces for global land areas. *International Journal of Climatology* 25: 1965-1978.

- Hsiao, T.C., Heng, L., Steduto, P., Roja-Lara, B., Raes, D., Fereres, E., 2009. AquaCrop—the FAO model to simulate yield response to water: parametrization and testing for maize. *Agron. J.* 101, 448–459.
- Intergovernmental Panel on Climate Change (IPCC), 2007. *Climate change: impacts, adaptation & vulnerability*. In: Contribution of Working Group II to the Fourth Assessment Report of the Intergovernmental Panel on Climate Change. Cambridge University Press.
- IPCC, 2001. *Climate Change 2001 — The Scientific Basis*. Cambridge University Press, Cambridge. 881 pp.
- IPCC, 2014: *Climate Change 2014: Synthesis Report*. Contribution of Working Groups I, II and III to the Fifth Assessment Report of the Intergovernmental Panel on Climate Change [Core Writing Team, R.K. Pachauri and L.A. Meyer (eds.)]. IPCC, Geneva, Switzerland, 151 pp.
- Kendall, M. G. (1955), *Rank Correlation Methods*, Charles Griffin, London, U. K.
- Kenter C., Hoffmann C. M. , Märländer B., Effects of weather variables on sugar beet yield development (*Beta vulgaris* L.), *European Journal of Agronomy*, Volume 24, Issue 1, January 2006, Pages 62-69, ISSN 1161-0301.
- Lamo de Espinosa; P. Urbano Terrón (eds.). *Asociación España-FAO Eumedia*, Madrid. pp. 115-128. ISBN: 978-84-936032-0-5.
- Laslett, G.M., 1994. Kriging and splines: an empirical comparison of their predictive performance in some applications. *Journal of American Statistical Association* 89 (426), 391–400.
- Lorite, I.J., García-Vila, M., Santos, C., Ruiz-Ramos, M., Ferere, E. *AquaData and AquaGIS: Two computer utilities for temporal and spatial simulations of water-limited yield with AquaCrop*. *Computers and Electronics in Agriculture*, Volume 96, August 2013, Pages 227-237.
- Manderscheid, R., Pacholski, A., Weigel, H.-J., 2010. Effect of free air carbon dioxide enrichment combined with two nitrogen levels on growth, yield and yield quality of sugar beet: evidence for a sink limitation of beet growth under elevated CO₂. *Eur. J. Agron.* 32, 228–239.

- Martínez-Quesada, J.J. (2008). Surbet. Modelo fisiológico de desarrollo de la remolacha azucarera de siembra otoñal. Tesis doctoral. Universidad de Sevilla.
- Masanganise, J., Chipindu, B., Mhizha, T., Mashonjowa, E., 2012. Model prediction of maize yield responses to climate change in North-Eastern Zimbabwe. *Afr. CropSci. J.* 20 (Supplement), 505–515.
- Nam, W.H., Hong, E.M., Choi, J.Y. (2015) Has climate change already affected the spatial distribution and temporal trends of reference evapotranspiration in South Korea?. *Agricultural Water Management* 150 (2015) 129–138. <http://dx.doi.org/10.1016/j.agwat.2014.11.019>
- New M, Hulme M, Jones P. 1999. Representing twentieth-century space-time climate variability. Part I: Development of a 1961–90 mean monthly terrestrial climatology. *Journal of Climate* 12: 829–856.
- OECC (Oficina Española de Cambio Climático) (2005) Principales Conclusiones de la Evaluación Preliminar de los Impactos en España por Efecto del Cambio Climático, Oficina Española de Cambio Climático, Ministerio de Medio Ambiente, Madrid.
- Ortiz, R., Sayre, K.D., Govaerts, B., Gupta, R., Subbarao, G.V., Ban, T., Hodson, D., Dixon, J.M., Reynolds, M. (2008). Climate change: Can wheat beat the heat?. *Agriculture, Ecosystems and Environment* 126 (2008) 46–58. [doi:10.1016/j.agee.2008.01.019](https://doi.org/10.1016/j.agee.2008.01.019)
- Osborne, T., Rose, G., Wheeler, T. (2013) Variation in the global-scale impacts of climate change on crop productivity due to climate model uncertainty and adaptation. *Agricultural and Forest Meteorology* 170 (2013) 183–194. <http://dx.doi.org/10.1016/j.agrformet.2012.07.006>
- Raes, D., Steduto, P., Hsiao, T.C., Fereres, E. and Heng L. (2008). AquaCrop Calculation Procedure, Prototype Version 2.3a. FAO, Rome, Italy, 64 p.
- Raes, D., Steduto, P., Hsiao, T.C., Fereres, E., 2009. AquaCrop—The FAO crop model to simulate yield response to water. II. Main algorithms and software description. *Agronomy J.* 101 (3), 438–477.
- Raes D., Steduto P., Hsiao T.H., and Fereres E. with contributions of the AquaCrop Network. 2012. Reference Manual Aquacrop software 4.0 version. FAO, Rome, Italy.

- Raziei, T., Pereira, L.S., 2013. Spatial variability of reference evapotranspiration in Iran utilizing fine resolution gridded datasets. *Agricultural Water Management* 126, 104–118.
- Ribalaygua, J., Pino, M.R., Pórtoles, J., Roldán, E., Gaitán, E., Chinarro, D., Torres, L. (2013). Climate change scenarios for temperature and precipitation in Aragón (Spain). *Science of the Total Environment* 463–464 (2013) 1015–1030.
- Rinaldi, M., Vittorio Vonella, A. 2006. The response of autumn and spring sown sugar beet (*Beta vulgaris L.*) to irrigation in Southern Italy: Water and radiation use efficiency. *Field Crops Research*. 95: 103-114.
- Ros, J. (1991). *El Cambio Climático y la Subida del Nivel del Mar*. Centro de Estudios y Experimentación de Obras Públicas, Madrid. 74 p. ISBN: 84-7790-097-3.
- Saarikko, R.A., 2000. Applying a site based crop model to estimate regional yields under current and changed climates. *Ecol. Modelling* 131, 191–206.
- Santos, C., Lorite, I.J., Tasumi, M., Allen, R.G., Fereres, E., 2010. Performance assessment of an irrigation scheme using indicators determined with remote sensing techniques. *Irrigation Science* 28, issue 6, 461-477.
- Scott, R.K., Jaggard K.W., 1993. Crop physiology and agronomy. In: Cooke, D.A., Scott, R.K. (Eds.), *The Sugar Beet Crop: Science into Practice*. Chapman & Hall, pp. 179±237.
- Sellers, P.J, L. Bounoua, G.J. Collatz, D.A. Randall, D.A. Dazlich, S.O. Los, J.A. Berry, I. Fung, C.J. Tucker, C.B. Field, and T.G. Jensen, 1996: Comparison of radiative and physiological effects of doubled atmospheric CO₂ on climate. *Science*, **271**, 1402-1406, doi:10.1126/science.271.5254.1402.
- Soddu, A., Deidda, R., Marrocu, M., Meloni, R., Paniconie, C., Ludwig, R., Sodde, M., Mascaro, G., Perrab, E., 2013. Climate variability and durum wheat adaptation using the AquaCrop model in southern Sardinia. *Proc. Environ. Sci.* 19, 830–835.
- Southworth, J. Randolph, J.C., Habeck, M., Doering, O.C., Pfeifer, R.A., Rao, D.G., Johnston, J.J. (2000). Consequences of future climate change and changing climate variability on maize yields in the midwestern United States. *Agriculture, Ecosystems and Environment* 82 (2000) 139–158

- Steduto P., Hsiao T.C, Fereres E., Raes D. 2012. Crop yield response to water. FAO Irrigation and Drainage paper 66.
- Steduto,P., Raes,D., Hsiao,T.C., Fereres, E., Heng,L., Izzi, G., Hoogeveen, J. (2008) AquaCrop: a new model for crop prediction under water deficit conditions. Options Méditerranéennes Series A, No.80, p 285-292
- Steduto, P., Hsiao, T.C., Raes, D., Fereres, E., 2009. AquaCrop—The FAO crop model to simulate yield response to water. I. Concepts and underlying principles. *Agronomy J.* 101 (3), 426–437.
- Stricevica, R.; Cosica, M.; Djurovica, N.; Pejicb, B.; Maksimovic, L.: 2011. Assessment of the FAO AquaCrop model in the simulation of rainfed and supplementally irrigated maize, sugar beet and sunflower. *Agricultural Water Management*, 98:1615-1621.
- Tanasijevic, L., Todorovic, M., Pereira, L.S., Pizzigalli, C., Lionello, P., 2014. Impacts of climate change on olive crop evapotranspiration and irrigation requirements in the Mediterranean region. *Agricultural Water Management* 144, 54–68.
- Thomson A, K Calvin, S Smith, P Kyle, A Volke, P Patel, S Delgado-Arias, B Bond Lamberty, M Wise, L Clarke, and J Edmonds. 2011. RCP4.5: a pathway for stabilization of radiative forcing by 2100. *Climatic Change*, 109:77-94
- Todorovic, M., Karic, B., Pereira, L.S. (2013). Reference evapotranspiration estimate with limited weather data across a range of Mediterranean climates. *Journal of Hydrology* 481 (2013) 166–176.
- UNFCCC (Convención Marco de las Naciones Unidas sobre el Cambio Climático). (2010) Compendium on methods and tools to evaluate impacts of, and vulnerability and adaptation to climate change
- Urbano, P. (2008). Impactos del Cambio Climático sobre la Producción Vegetal. In: *Repercusiones del Cambio Climático en la Agricultura y la Alimentación Mundial*; J.
- Vanuytrecht, E., Raes, D., Willems, P., 2011. Considering sink strength to model crop production under elevated atmospheric CO₂. *Agric. For. Meteorol.* 151,1753–1762.
- van Heemst, H.D.J., 1988. Plant data values required for simple crop growth simulation models: review and bibliography. In: *Simulation Report CABO-TT Nr.*

17.CABO and Department of Theoretical Production Ecology, Agricultural University, Wageningen University.

van Vuuren et al (2011) The Representative Concentration Pathways: An Overview. *Climatic Change*, 109 (1-2), 5-31

Vicente-Serrano, S. M., C. Azorin-Molina, A. Sanchez-Lorenzo, J. Revuelto, E. Morán-Tejeda, J. I. López-Moreno, and F. Espejo (2014a), Sensitivity of reference evapotranspiration to changes in meteorological parameters in Spain (1961–2011), *Water Resour. Res.*, 50, 8458–8480.

Vicente-Serrano, S. M., C. Azorin-Molina, A. Sanchez-Lorenzo, J. Revuelto, J. I. López-Moreno, J. C. González-Hidalgo, and F. Espejo (2014b), Reference evapotranspiration variability and trends in Spain (1961–2011), *Clim. Dyn.*, 42, 2655–2674.

Voloudakis, D., Karamanos, A., Economou, G., Kalivas, D., Vahamidis, P., Kotoulas, V., Kapsomenakis, J., Zerefos, C. (2015) Prediction of climate change impacts on cotton yields in Greece under eight climatic models using the AquaCrop crop simulation model and discriminant function analysis. *Agricultural Water Management* 147 (2015) 116–128.

Wise, MA, KV Calvin, AM Thomson, LE Clarke, B Bond-Lamberty, RD Sands, SJ Smith, AC Janetos, JA Edmonds. 2009. Implications of Limiting CO₂ Concentrations for Land Use and Energy. *Science*. 324:1183-1186.

Zhang, X., Kang, S., Zhang, L., Liu, J., 2010. Spatial variation of climatological monthly crop reference evapotranspiration and sensitivity coefficients in Shiyang river basin of northwest China. *Agricultural Water Management* 97,1506–1516.

7. RESUMEN DE RESULTADOS

RESUMEN DE RESULTADOS

En esta Tesis Doctoral se han estudiado los factores ambientales que influyen en el porcentaje de carbono asimilado por la planta de remolacha azucarera y se ha cuantificado el mismo. Además se ha desarrollado una herramienta para estimar el nivel de nitrógeno en hojas en época de cosecha, factor que está relacionado con la riqueza final de azúcar y por lo tanto con la cantidad de carbono total final asimilado por la planta. Por último se han estudiado los posibles efectos de escenarios futuros de cambio climático sobre el rendimiento, biomasa total y CO₂ asimilado por el cultivo.

En este capítulo se recoge un resumen de los resultados obtenidos en cada uno de los artículos científicos, presentados en relación a los objetivos programados.

Los resultados correspondientes a la primera parte de la Tesis Doctoral, recogidos en el artículo científico “**Identificación del Impacto de Variables Climáticas en el Contenido de Carbono en Raíz de Remolacha Azucarera**” son expuestos a continuación, en relación a los objetivos específicos establecidos:

En relación al objetivo 1.1 se ha confirmado que el contenido en carbono de la raíz de remolacha depende de las características climáticas y edafológicas de cada localización así como de las condiciones específicas de cada campaña de cultivo. Esto coincide con los resultados de Kenter et al. (2006) en cuanto a que el crecimiento de la planta y la composición de la raíz están influenciados por las condiciones ambientales de cada lugar de cultivo. Así, el factor localización es el que arroja las mayores diferencias significativas entre los tratamientos.

En cuanto al objetivo 1.2, la aplicación de una dosis de nitrógeno mayor que la recomendada tiene influencia en los parámetros relacionados con la cantidad de materia fresca, en particular en las hojas, mientras que la elección de la variedad lleva a diferencias en la concentración de nitrógeno en hojas y en el ratio entre contenido de carbono en la raíz y el contenido de nitrógeno en hojas. La influencia de la variedad en el contenido de carbono es relativa ya que una misma variedad puede presentar distintos valores de polarización en función de la localización, lo cual nos vuelve a señalar este último factor como decisivo.

Para el objetivo 1.3, el análisis comparativo entre el contenido de carbono (RC), el porcentaje de materia seca (RDM) y la polarización evidencian una relación positiva

entre los tres parámetros de tal forma que una mayor polarización lleva a un mayor contenido de materia seca (Kenter and Hoffmann, 2006) y esto también se traduce en un mayor contenido de carbono.

También se puede inferir que el porcentaje de carbono está relacionado con la composición relativa entre sacarosa, marco (celulosa, hemicelulosa, lignina...) y otros componentes. Los datos de las dos campañas muestran un mayor contenido en carbono (RC) en aquellas localizaciones donde se consiguieron mayores polarizaciones, mayor porcentaje de materia seca (RDM) y por lo tanto mayor cantidad de marco, y una relación positiva del ratio entre raíz y hojas con RC

A este respecto Hoffmann et al. (2005) sugiere que la correlación positiva entre concentración de sacarosa y marco podría ser explicada por unas paredes celulares menos gruesas, por células más pequeñas y/o mayor número de células lo cual puede tener influencia en la proporción de carbono presente en los tejidos radiculares. También cabe destacar que un compuesto como un compuesto como la betaína de alto contenido en carbono está relacionada con el contenido de sacarosa de tal forma que cuanto mayor concentración de sacarosa, mayor cantidad de betaína y por lo tanto, mayor contenido de carbono (Kenter et al. (2006) y Hoffmann et al. (2005)).

En relación al objetivo 1.4, se observa una relación negativa entre el contenido de nitrógeno en hojas con el contenido de carbono de la raíz (y en cierta medida con la polarización) en concordancia con lo observado con Shock et al. (2000), quienes encontraron una relación negativa entre la concentración de nitratos en peciolo y la polarización. En este sentido Pocock et al. (2009), concluyen que incrementos tardíos de la disponibilidad de nitrógeno en el cultivo bien por adiciones de fertilizantes o por su liberación por materia orgánica reducen el contenido de sacarosa, y tanto Draycott et al. (2003) como Malnou et al. (2008), indican que cantidades de nitrógeno por encima del óptimo tienen un efecto negativo en el rendimiento de azúcar de la raíz. Gordo-Ingelmo (1994) explica que la remolacha reacciona a los incrementos de nitrógeno con un mayor desarrollo de las hojas y las raíces, lo cual puede conducir a un consumo excesivo de sacarosa y un incremento de los no-azúcares. Esto ocurre, particularmente, con el aporte excesivo de abonos orgánicos en los cuales parte del nitrógeno es liberado tardíamente causando una parada de la maduración de la raíz. En consecuencia, la baja polarización y porcentaje de carbono de la raíz en Pampliega en 2012 que es donde existe una mayor cantidad de materia orgánica en suelo, podría estar asociado a una liberación retardada

de nitrógeno, lo cual explicaría también el hecho de que ese cultivo tuvo el mayor peso fresco de hojas y la mayor cantidad de nitrógeno absorbido por hectárea.

Para la consecución del objetivo 1.5, el análisis de componentes principales (PCA) de las variables climáticas calculadas para las distintas localizaciones y periodos de cultivo junto a los parámetros de las plantas medidos en cosecha mostraron una clara segregación por clusters o agregados lo cual indica la especificidad de cada zona y la influencia de los factores climáticos en el desarrollo del cultivo.

Se puede afirmar también que existe una relación positiva del contenido de carbono de la raíz con la temperatura media y la radiación acumulada en la primera fase del cultivo ya que las etapas tempranas del desarrollo del cultivo son decisivas en la formación y calidad de la remolacha Hoffmann (2005). Y por otra parte también se detecta una relación negativa entre el contenido de carbono en la raíz y la radiación acumulada en la última fase del cultivo. La explicación a este efecto está ligada al hecho de que la tasa de crecimiento de la remolacha decrece en otoño debido a la menor radiación solar junto a la senescencia de las hojas (Milford (1973) y Martínez-Quesada et al. (2003), lo cual provoca un movimiento de sustancias asimiladas hacia la raíz. En este proceso la disponibilidad de nitrógeno por la planta también tiene su influencia ya que su carencia evita el desarrollo de nuevos tejidos con el subsecuente aumento de la senescencia foliar, permitiendo la acumulación de asimilados en la raíz. Por lo tanto, una mayor radiación y/o disponibilidad de nitrógeno en la última fase del cultivo puede detener la senescencia y promover el surgimiento de nuevas hojas consumiendo productos asimilados desde la raíz.

Cabe destacar, paralelamente, como un resultado interesante, que la observación de los datos de emergencia de 2012 permiten concluir que cuanto mayor es el gradiente térmico diario, menor acumulación de GDD necesita la planta para emerger.

Finalmente, para el objetivo 1.6 se determina que el contenido medio en carbono de la materia seca de la raíz fue de 43.40 g/kg el primer año y 43.74 g/kg en la segunda campaña. El contenido medio de carbono en hojas durante los dos años fue de un 37.5%. Sin embargo, la cantidad total de CO₂ asimilado no solo depende del porcentaje de materia seca y de su contenido en carbono sino que depende en mayor medida de la cantidad total de materia seca que la planta haya acumulado y ésta se incrementa cuanto mayor es el peso fresco de la planta. Por lo tanto, se puede inferir, en términos

generales, que cuanto mayor peso fresco de la planta mayor cantidad de CO₂ absorbido. En el primer año Villavieja fue la parcela donde mayor captura de CO₂ hubo ya que fue la de mayor producción mientras que en el segundo año la mayor asimilación tuvo lugar en Pampliega por el mayor peso fresco de hojas y biomasa total a pesar de que el rendimiento no fue el mayor.

Los resultados correspondientes a la segunda parte de la Tesis Doctoral, recogidos en el artículo científico “**Evaluación del Uso de Índices de Vegetación RGB para Determinar el Contenido de Clorofila en Hojas de Remolacha Azucarera en Cosecha**” y de la comunicación “**Detección de malas hierbas (*Sinapis arvensis*) en un cultivo de alfalfa mediante el Uso de Índices RGB**” son expuestos a continuación, también en relación a los objetivos específicos establecidos:

Para alcanzar el objetivo 2.1, se consiguió, a partir de fotografías de hojas de remolacha tomadas con una cámara convencional, evaluar el contenido de clorofila de las mismas mediante la extracción de las bandas RGB y el cálculo de índices de vegetación.

El rango de tamaños y coloración de las hojas fue una muestra representativa de lo que se puede encontrar en cualquier campo de remolacha en la última fase del cultivo en época de cosecha.

Los resultados muestran la alta correlación de varios de esos índices de vegetación con el contenido en clorofila de las hojas, lo cual está en concordancia con diversos trabajos que encuentran altas correlaciones entre el contenido de clorofila en hojas y los valores RGB como por ejemplo para el cultivo de la patata y hojas de alubias (Yadav et al., 2010 and Vollmann et al., 2011).

Se testaron varios índices hallados en revisión bibliográfica seleccionando, en función de los mejores resultados, los siguientes: $(R-B)/(R+B+G)$ y $(R-B)/(R+ B)$ (Kawashima and Nakami, 1998) y IPCA (Saberioon et al, 2014).

En cuanto al objetivo 2.2 se exploró la posibilidad de desarrollar nuevos índices para lo que se dividieron los datos en un grupo para hallar los índices y otro de control. Las técnicas usadas fueron el análisis de componentes principales PCA (Pagola et al., 2009) y SLR (Regresión lineal paso a paso). Los índices obtenidos fueron $I_1 = R+G-2B$ e $I_2 = 0.55 +11.4 (G-B/G+B) -12.5 (R-B/R+B) +9 (R-G/R+G)$. Ambos con un alto

coeficiente de determinación (mayor de 0.80) y un bajo error cuadrático medio (de un 10%) al evaluarlos dentro del grupo de control.

En relación al objetivo 2.3, los gráficos de dispersión de los índices $(R-B)/(R+G+B)$ (similar a $R-B/R+B$), I_{PCA} , I_1 y I_2 muestran que las tres tomas del primer día de experimentación en diferentes horas del día y por lo tanto, con distintas condiciones de luz son prácticamente iguales. En el caso del último día se aprecian pequeñas variaciones entre tomas que no exceden de un 5%. Esto se puede achacar a diferencias entre las condiciones en un día claro y otro nublado.

En cuanto al análisis por días usando los datos del grupo de control, los cuatro índices funcionan de manera adecuada a la hora de representar la evolución del contenido de clorofila, esto es, un decremento producido por la degradación natural de la clorofila con el tiempo, es decir, las hojas van teniendo cada día menor contenido de clorofila. Esta evolución está previamente contrastada con los datos aportados con el medidor óptico de clorofila CCM-200 utilizado. Por lo tanto, los índices estudiados describen adecuadamente el proceso de degradación durante los 4 días en diferentes condiciones de iluminación incluso en aquellos casos donde el medidor óptico arrojó lecturas erróneas.

Se observa cómo las rectas de regresión de los índices para valores diarios se aproximan en el rango de valores bajos de clorofila, lo cual es lógico pues aquellos hojas que partieron con un bajo contenido de clorofila el primer día de experimento, no se van a seguir degradando en la misma medida de aquellas que partieron con valores más altos. En el caso de los índices $(R-B)/(R+B+G)$ y I_2 en ese rango de valores bajos se llegan a cruzar las rectas, hasta los 20 CCI en el primer caso y 10 CCI en el segundo. Los índices I_{PCA} y I_1 no presentan esa limitación.

Los nuevos índices llegan a mejorar el ya buen comportamiento de los índices ya existentes teniendo los coeficientes de determinación ligeramente superiores.

I_1 simplifica I_{PCA} pero incrementa su R^2 pero manteniendo su buen comportamiento con los valores bajos de clorofila. I_2 es el que presenta el coeficiente de determinación más alto y mejora el comportamiento del índice $(R-B)/(R+G+B)$ en el intervalo de valores bajos de clorofila.

Considerando el objetivo 2.4, a la vista de los resultados, la metodología propuesta fue la adecuada para comparar el contenido de clorofila en hojas de remolacha en diferentes horas y días solventando los problemas que implican las condiciones cambiantes que se producen al trabajar con luz natural, y por lo tanto amplía su futura aplicabilidad en campo. Este resultado ofrece una herramienta sencilla y de bajo coste para la determinación del contenido de clorofila y, por ende, de nitrógeno en hojas de remolacha en época de cosecha para detectar incorporaciones tardías que pueden llegar a reducir el rendimiento final de azúcar de la raíz.

Finalmente, examinando el objetivo 2.5, los resultados obtenidos demuestran como los índices RGB utilizados son apropiados para la detección de *Sinapis arvensis* en un cultivo de alfalfa (*Medicago sativa*) a partir de imágenes capturadas por un UAV (Vehículo Aéreo no Tripulado) o dron.

Ambos índices se muestran muy sensibles a las manchas amarillas originadas por la presencia de las malas hierbas representándolas con tonos claros que las diferencian del resto del cultivo y del suelo, mejorando el comportamiento del índice NDVI con el que no se puede discriminar entre malas hierbas y suelo. Estos índices también parecen ser sensibles a los tonos verdes claros lo cual parece introducir ruido en el mosaico originado.

Los resultados correspondientes a la tercera parte de la Tesis Doctoral, recogidos en el artículo científico “**Análisis Regional del Cultivo de Remolacha Azucarera Bajo Futuros Escenarios de Cambio Climático**” son descritos a continuación como en los casos anteriores, en relación a los objetivos específicos establecidos:

Para el objetivo específico 3.1, los resultados sobre la ET_0 en la zona remolachera estudiada de Castilla y León muestran que en el escenario actual, los mayores valores se dan en la zona centro y sur. Hacia las zonas periféricas decrece, en especial y significativamente hacia el norte y el noreste correspondiente con la provincia de Burgos. Para los futuros escenarios de 2050 y 2070 se observa un claro incremento de ET_0 en todas las zonas incluso llegando a diferencias de 200 mm comparando con el escenario actual. Este incremento es una respuesta lógica al aumento de temperatura que ha sido el parámetro utilizado como no estacionario en la fórmula FAO-56 PM para las estimaciones de ET_0 en 2050 y 2070 a partir de los datos obtenidos del modelo

climático MPI-ESM-LR en el escenario RCP4.5 del AR5 (IPCC, 2014). También coincide con Vicente-Serrano et al. (2014a) que encontraron que en España la ecuación FAO-56 PM es muy sensible a cambios en la humedad relativa y en las temperaturas máximas.

Las zonas más afectadas por el incremento de ET_0 son la provincia de Valladolid, el sur de Palencia, el norte de Salamanca y Ávila, el noreste de Segovia, y el este de Zamora. Este incremento de ET_0 agranda las diferencias de la distribución espacial actual, siendo este incremento mayor en la zona central, con una clara tendencia hacia el sur (y ligeramente hacia el oeste). En otras palabras, hay un movimiento hacia el norte y el noreste de la distribución de zonas con menor ET_0 con el tiempo.

Al igual que ET_0 , la ET_c mensual calculada con el coeficiente específico de cultivo (K_c) para la remolacha también aumenta con respecto a la situación actual, siendo este incremento mayor en 2070. Así entre marzo y mayo ET_c se incrementa desde 1.5 mm hasta 20 mm en los escenarios futuros. Julio es el mes donde los incrementos alcanzan los valores más altos, con zonas llegando a 40 mm de diferencia con respecto al escenario actual, aunque bajando ligeramente, manteniéndose valores altos en agosto para ya ir bajando desde septiembre hasta octubre, donde se vuelve a valores próximos a los del comienzo del ciclo.

En relación al objetivo 3.2, como cabía esperar, los rendimientos de las cosechas simulados con el modelo de crecimiento Aquacrop ajustado a las condiciones específicas de Castilla y León, se ven afectados por los cambios en ET_0 . Así, teniendo en cuenta el patrón de distribución espacial para la ET_0 se obtiene que en la zona central y sur del área de estudio, el rendimiento disminuye tanto para 2050 como para 2070 alrededor de 9%. Por lo tanto, al igual que lo observado para otros cultivos, un futuro calentamiento global puede ser beneficioso en algunas zonas pero reducir la productividad en aquellas regiones donde actualmente ya gozan de una temperatura óptima para un cultivo determinado (Ortiz et al., 2008).

Esta reducción de la producción es ligeramente mayor en 2050 debido seguramente a una mayor actividad fotosintética en 2070 por mayores concentraciones de CO_2 en la atmósfera. Por ello el efecto negativo de mayores temperaturas y menores precipitaciones pudieran ser en parte compensado por mayores tasas fotosintéticas debido a un probable incremento de la concentración de CO_2 (OECC, 2005).

Estas tendencias observadas son consistentes con experimentos realizados con técnicas FACE (fertilización carbónica al aire libre) para simular futuros escenarios con mayores concentraciones de CO₂ como los de Manderscheid et al. (2010) quienes registraron un incremento del rendimiento entre un 7 % y un 16% para los niveles de concentración estimados para la mitad del siglo XXI según el escenario A1B del IPCC.

Por otra parte, en el noroeste de León y noreste de Burgos se detectan incluso incrementos en la producción en 2050, lo cual se extiende al norte de Palencia en 2070 llegando a un 10% de incremento. Esto se puede explicar debido a que son zonas más frías en el escenario actual donde el cambio de la ET₀ causaría un menor incremento que en otras zonas que sería tolerado por la planta, la cual se beneficiaría paralelamente de mayores temperaturas en ese escenario futuro.

Sin embargo, hay que señalar que para las simulaciones generadas por el modelo para los años 2050 y 2070 el periodo de cultivo se acorta, es decir, de alcanzarse la época de cosecha en noviembre para el escenario actual, este momento se adelanta hasta octubre o finales de septiembre según zonas. Esto responde al hecho de que el cultivo con mayores temperaturas alcanza antes los grados día necesarios para cada fase de desarrollo.

Estos resultados muestran cómo ciertos aumentos de temperatura pueden incrementar la tasa de crecimiento del cultivo traduciéndose en una cosecha más temprana. Sin embargo, también se ha de tener en cuenta que el estrés térmico puede tener también efectos negativos sobre la producción (Southworth et al., 2000).

De este modo, si se extendiera el periodo de cultivo, se podrían alcanzar mayores cosechas mientras fueran satisfechos los requerimientos hídricos del cultivo. En este sentido, ya se han aportado datos sobre la influencia positiva del alargamiento del ciclo en base a datos de campo en la zona de estudio (AIMCRA, 2007), sugiriendo incrementos de hasta un 20%. En base a esto se alargaron las simulaciones de los años 2050 y 2070 hasta noviembre obteniendo mayores cosechas en general de hasta un 17%. Estos incrementos son mayores en el norte y este que en el centro y en el sur de la zona de trabajo. En 2070, debido a las mayores concentraciones de CO₂ el incremento se hace mayor sobre todo en la zona norte (Palencia y León) y el este (Burgos).

Otro aspecto positivo es que un futuro incremento de temperaturas podría permitir un alargamiento del cultivo a través de una siembra más temprana. Esto permitiría un desarrollo más temprano de las hojas como órgano fotosintético que a su vez haría que la planta pudiera aprovechar al máximo la radiación solar ya que como ciertos investigadores han resaltado, debido al lento desarrollo de las hojas de la remolacha en primavera, el cultivo alcanza la máxima cobertura del terreno cuando el máximo de radiación ya ha pasado (Scott and Jaggard, 1993; Kenter et al., 2006). El alcanzar la máxima cobertura del terreno en el menor tiempo posible y mantener dicha cobertura tanto como sea posible, se traduce en que el cultivo pueda así recibir la mayor cantidad de radiación solar posible (Van Heemst, 1986, as cited in Martínez-Quesada, 2008).

En base al objetivo 3.3, en cuanto a la biomasa total (incluyendo hojas) y el CO₂ capturado los resultados son similares a los de rendimiento o producción del cultivo. Existe un decremento en la cantidad de biomasa media y la asimilación de CO₂ para toda la zona de estudio de alrededor de un 7% en 2050 que es ligeramente mitigado en 2070 (5%) por la misma razón expuesta anteriormente relativa a la mayor concentración de CO₂ atmosférico. En términos absolutos el CO₂ asimilado medio por el cultivo para toda la zona cae desde las 49 t ha⁻¹ en el escenario actual a 46 t ha⁻¹ y 47 t ha⁻¹ en 2050 y 2070 respectivamente.

Al igual que en el caso de la producción, si el periodo de cultivo se alarga se consiguen mayores cantidades de biomasa total y de CO₂ capturado en el conjunto del área de estudio (8% y 12% en 2050 y 2070 respectivamente). En este caso, las cantidades medias de CO₂ absorbido van de las 49 t ha⁻¹ del escenario actual a las 53 t ha⁻¹ y 55 t ha⁻¹ en 2050 y 2070, lo que representan unos incrementos del 9% y del 13% respectivamente.

Para finalizar, en relación con el objetivo 3.4, las tendencias encontradas, a nivel regional, de los parámetros estudiados para futuros escenarios de cambio climático coinciden con las conclusiones de otros estudios aplicados a otras escalas: un desplazamiento hacia el norte de las zonas apropiadas para los cultivos y un incremento en la productividad de los mismos en el norte de Europa (Falloon and Betts, 2010).

Incluso las simulaciones llevadas a cabo confirman que existe un mayor potencial de adaptación en las zonas más fría del norte lo cual puede compensar la disminución de cosechas al desplazar el periodo de cultivo a meses más fríos, en este caso, adelantando

la siembra y aprovechando un alargamiento del ciclo con las variedades apropiadas (Osborne et al., 2013).

A pesar de la necesidad de realizar enfoques regionales para evaluar los efectos del cambio climático en las cosechas futuras y los cambios en la idoneidad de los cultivos, hay que tener en cuenta que existen múltiples incertidumbres inherentes a las simulaciones de crecimiento de cultivos que van desde los modelos climáticos y las proyecciones climáticas futuras (Osborne et al., 2013), pasando por los propios errores de los modelos de crecimiento, hasta suposiciones y errores de observación (Saarikko, 2000). A ello se une una mayor probabilidad de ocurrencia de fenómenos extremos de lluvias torrenciales y sequías, lo cual debería ser tenido en cuenta en futuros estudios (Falloon and Betts, 2010).

7.1. REFERENCIAS

AIMCRA (2007). Revista AIMCRA 96, 11-12. Valladolid.

Draycott, A.P., Christenson, D.R. (2003). Nutrients for sugarbeet production: soil-plant relationships, CABI Publishing, Wallingford, Oxfordshire, England, 2003

Falloon, P., Betts, R. (2010). Climate impacts on European agriculture and water management in the context of adaptation and mitigation—The importance of an integrated approach. *Science of the Total Environment* 408 (2010) 5667–5687.

Gordo-Ingelmo, L.F. (1994). Composición química y control agrícola de los no-azúcares en la remolacha azucarera, Caja de Ahorros Municipal de Burgos, Burgos, Spain, 1994.

Hoffmann, C.M. (2005). Changes in N Composition of Sugar Beet Varieties in Response to Increasing N Supply, *Journal of Agronomy and Crop Science*, 191 (2005) 138-145.

Hoffmann, C.M., Kenter, C., Bloch, D. (2005). Marc concentration of sugar beet (*Beta vulgaris* L) in relation to sucrose storage, *J. Sci. Food Agric.*, 85 (2005) 459-465.

IPCC, 2014: Climate Change 2014: Synthesis Report. Contribution of Working Groups I, II and III to the Fifth Assessment Report of the Intergovernmental Panel on

Climate Change [Core Writing Team, R.K. Pachauri and L.A. Meyer (eds.)]. IPCC, Geneva, Switzerland, 151 pp.

Kawashima, S. and Nakatani, M. (1998). An Algorithm for Estimating Chlorophyll Content in Leaves Using a Video Camera. *Annals of Botany* 81: 49-54, 1998.

Kenter, C., Hoffmann, C.M., Märländer, B. (2006). Effects of weather variables on sugar beet yield development (*Beta vulgaris* L.), *European Journal of Agronomy*, 24 (2006) 62-69.

Kenter C., Hoffmann C. M. , Märländer B., Effects of weather variables on sugar beet yield development (*Beta vulgaris* L.), *European Journal of Agronomy*, Volume 24, Issue 1, January 2006, Pages 62-69, ISSN 1161-0301.

Malnou, C.S., Jaggard, K.W., Sparkes, D.L. (2008). Nitrogen fertilizer and the efficiency of the sugar beet crop in late summer, *European Journal of Agronomy*, 28 (2008) 47-56.

Manderscheid, R., Pacholski, A., Weigel, H.-J., 2010. Effect of free air carbon dioxide enrichment combined with two nitrogen levels on growth, yield and yield quality of sugar beet: evidence for a sink limitation of beet growth under elevated CO₂. *Eur. J. Agron.* 32, 228–239.

Martínez-Quesada, J.J. (2008). Surbet. Modelo fisiológico de desarrollo de la remolacha azucarera de siembra otoñal. Tesis doctoral. Universidad de Sevilla.

Martínez Quesada, J.J., Morillo Velarde, R., Aguilera García, Y., Infante Vázquez, J.M. (2003). Growth of Sugar Beet Under Limited Nitrogen Conditions, in: *Sugar Beet Growth and Growth Modelling. Advances in Sugar Beet Research*, Institut International de Recherches Betteravieres, Brussels, Belgium, 2003, pp. 33-45.

Milford, G.F.J. (1973). The growth and development of the storage root of sugar beet, *Ann. Appl. Biol.*, 75 (1973) 427-438.

OECC (Oficina Española de Cambio Climático) (2005) Principales Conclusiones de la Evaluación Preliminar de los Impactos en España por Efecto del Cambio Climático, Oficina Española de Cambio Climático, Ministerio de Medio Ambiente, Madrid.

Ortiz, R., Sayre, K.D., Govaerts, B., Gupta, R., Subbarao, G.V., Ban, T., Hodson, D., Dixon, J.M., Reynolds, M. (2008). Climate change: Can wheat beat the heat?.

Agriculture, Ecosystems and Environment 126 (2008) 46–58.
doi:10.1016/j.agee.2008.01.019

Osborne, T., Rose, G., Wheeler, T. (2013) Variation in the global-scale impacts of climate change on crop productivity due to climate model uncertainty and adaptation. *Agricultural and Forest Meteorology* 170 (2013) 183–194.
<http://dx.doi.org/10.1016/j.agrformet.2012.07.006>

Pagola, M., Ortiz, R., Irigoyen, I., Bustince, H., Barrenechea, E., Aparicio-Tejo, P., Lamsfus, C., Lasa, B., 2009. New method to assess barley nitrogen nutrition status based on image colour analysis, comparison with SPAD-502. *Comput. Electron. Agric.* 65, 213–218.

Pocock, T.O., Milford, G.F.J., Armstrong, M.J. (2009). Storage root quality in sugarbeet in relation to nitrogen uptake, *The Journal of Agricultural Science*, 115 (2009) 355.

Saberioon, M.M., Amina, M.S.M, Anuar, A.R., Gholizadeh, A., Wayayok, A., Khairunniza-Bejo, S. (2014) Assessment of rice leaf chlorophyll content using visible bands at different growth stages at both the leaf and canopy scale. *International Journal of Applied Earth Observation and Geoinformation* 32 (2014) 35–45.

Saarikko, R.A., 2000. Applying a site based crop model to estimate regional yields under current and changed climates. *Ecol. Modelling* 131, 191–206

Scott, R.K., Jaggard K.W., 1993. Crop physiology and agronomy. In: Cooke, D.A., Scott, R.K. (Eds.), *The Sugar Beet Crop: Science into Practice*. Chapman & Hall, pp. 179±237

Shock, C.C., Seddigh, M., Saunders, L.D., Stieber, T.D. Miller, J.G. (2000). Sugarbeet nitrogen uptake and performance following heavily fertilized onion, *Agron. J.*, 92 (2000) 10-15.

Southworth, J. Randolph, J.C., Habeck, M., Doering, O.C., Pfeifer, R.A., Rao, D.G., Johnston, J.J. (2000). Consequences of future climate change and changing climate variability on maize yields in the midwestern United States. *Agriculture, Ecosystems and Environment* 82 (2000) 139–158

van Heemst, H.D.J., 1988. Plant data values required for simple crop growth simulation models: review and bibliography. In: *Simulation Report CABO-TT Nr. 17*. CABO

and Department of Theoretical Production Ecology, Agricultural University, Wageningen University.

Vicente-Serrano, S. M., C. Azorin-Molina, A. Sanchez-Lorenzo, J. Revuelto, J. I. López-Moreno, J. C. González-Hidalgo, and F. Espejo (2014), Reference evapotranspiration variability and trends in Spain (1961–2011), *Clim. Dyn.*, 42, 2655–2674.

Vollmann, J., Waltera, H., Sato, T., Schweiger, P. (2011). Digital image analysis and chlorophyll metering for phenotyping the effects of nodulation in soybean. *Computers and Electronics in Agriculture* 75 (2011) 190–195.

Yadav, S.P., Ibaraki, Y., Gupta, S.D., 2010. Estimation of the chlorophyll content of micropropagated potato plants using RGB based image analysis. *Plant Cell Tissue Organ Cult.* 100, 183–188.

8. CONCLUSIONES

CONCLUSIONES

A partir de los resultados obtenidos en el presente trabajo de Tesis Doctoral “*Análisis de la Influencia de Variables Ambientales sobre el Contenido de Carbono en el Cultivo de Remolacha Azucarera y Estimación del Contenido de Nitrógeno en Hojas Mediante Índices de Vegetación*” se han elaborado, por capítulos, las conclusiones siguientes:

En relación con el primer artículo científico “*Identificación del Impacto de Variables Climáticas en el Contenido de Carbono en Raíz de Remolacha Azucarera*”:

PRIMERA: se ha demostrado que el porcentaje de carbono en materia seca de raíz de remolacha azucarera está influenciado por las condiciones ambientales propias de cada lugar de cultivo, lo que incluye clima, suelo y condiciones específicas de cada campaña.

SEGUNDA: se ha identificado la relación positiva del contenido de carbono en raíz con la temperatura media y la radiación acumulada en la primera etapa del cultivo, y la relación negativa con la radiación acumulada en la última fase del mismo. Así mismo la emergencia se comprueba que está influenciada por el gradiente térmico diario.

TERCERA: se ha comprobado la relación directa entre riqueza en sacarosa o polarización con el porcentaje de materia seca y el contenido en carbono de la raíz que toma un valor medio de 43.57 g/kg en los dos años de estudio.

En relación con el segundo artículo científico “*Evaluación del Uso de Índices de Vegetación RGB para Determinar el Contenido de Clorofila en Hojas de Remolacha Azucarera en Cosecha*” y con la comunicación “*Detección de malas hierbas (Sinapis arvensis) en un cultivo de alfalfa mediante el Uso de Índices RGB*”:

CUARTA: se ha demostrado la viabilidad del uso de fotografías tomadas con una cámara convencional para estimar, mediante índices de vegetación, el contenido de clorofila/nitrógeno en hojas de remolacha en época de cosecha.

QUINTA: se han propuesto dos nuevos índices de vegetación, basados en la información del espectro visible, sensibles a los cambios en los niveles de

clorofila/nitrógeno y se ha desarrollado una metodología de calibración en la toma de imágenes para permitir su comparación en distintas condiciones de luz natural.

SEXTA: se ha demostrado la utilidad de dos índices de vegetación basados en el espectro visible para detectar la presencia de malas hierbas (*Sinapis arvensis*) en un cultivo de alfalfa (*Medicago sativa*) mediante la toma de fotografías desde un vehículo aéreo autónomo o dron.

En relación con el tercer artículo científico “***Análisis Regional del Cultivo de Remolacha Azucarera Bajo Futuros Escenarios de Cambio Climático***”

SÉPTIMA: se han estimado los efectos de escenarios futuros de cambio climático sobre la evapotranspiración, rendimiento, biomasa total y CO₂ capturado en el cultivo de la remolacha. Se produce un incremento general de la evapotranspiración y una disminución en el rendimiento, en la biomasa total producida y en el carbono asimilado, a la vez que se adelantan las cosechas.

OCTAVA: se ha detectado de manera general cómo en los futuros escenarios estudiados las zonas climáticamente más favorables para el cultivo de la remolacha se desplazan hacia el norte y el este del área de estudio, lo que coincide con las tendencias identificadas en otros estudios a distintas escalas.

NOVENA: se han identificado posibles medidas de adaptación que aprovechen las mayores temperaturas mediante el adelanto de la fecha de siembra o mediante el alargamiento del ciclo, posponiendo la cosecha. De esta manera se podría compensar e incluso mejorar las cosechas. Zonas actualmente más frías serán las que tengan mayor capacidad de adaptación.